CP COL 3.7(3)
CP COL 3.7(4)
CP COL 3.7(8)
CP COL 3.7(10)
CP COL 3.7(21)
CP COL 3.7(26)
CP COL 3.8(15)
CP COL 3.8(19)
CP COL 3.8(29)

APPENDIX 3LL

ESWPT SEISMIC MODELING, ANALYSIS, AND RESULTS

TABLE OF CONTENTS

LIST OF TABLES

LIST OF FIGURES

LIST OF FIGURES

ACRONYMS AND ABBREVIATIONS

Acronyms	Definitions
3D	three-dimensional
ATF	acceleration transfer function
EBE	embedded best estimate
EHB	embedded high bound
ELB	embedded lower bound
ESW	essential service water
ESWPT	essential service water pipe tunnel
EUB	embedded upper bound
FE	finite element
FIRS	foundation input response spectra
GWL	ground water level
ISRS	in-structure response spectra
MSM	modified subtraction method
OBE	operating-basis earthquake
PCCV	prestressed concrete containment vessel
PSFSV	power source fuel storage vault
R/B	reactor building
SRP	Standard Review Plan
SRSS	square root sum of the squares
SSI	soil-structure interaction
SSSI	structure-soil-structure interaction
UHS	ultimate heat sink
UHSRS	ultimate heat sink related structure
ZPA	zero period acceleration

3LL ESWPT SEISMIC MODELING, ANALYSIS, AND RESULTS

3LL.1 Introduction

This Appendix discusses the seismic analysis of the standalone segments of the essential service water pipe tunnel (ESWPT). The computer program, ACS SASSI (Reference 3LL-1), serves as the platform for the soil-structure interaction (SSI) analyses. The three-dimensional (3D) finite element (FE) ESWPT models used in the SSI analyses are initially developed using the ANSYS computer program (Reference 3LL-2). The models of the ESWPT structure are then translated from ANSYS models to SASSI models which include the subgrade layering and backfill properties. After verification of the translation from ANSYS to SASSI, the SASSI 3D FE models are dynamically analyzed in the frequency domain to obtain SSI seismic responses of the ESWPT standalone segments.

The SASSI model results for maximum accelerations and seismic soil pressures serve as basis for development of SSE loads. These loads are used as input to the ESWPT ANSYS models for performing the structural design, including loads and load combinations in accordance with the requirements of Section 3.8. Dead, live, and equipment loads applied to the components of each tunnel segment are footnoted in Table 3LL-1 through Table 3LL-3. The analysis cases performed for calculating seismic demands are outlined in Table 3LL-7. The SASSI analysis and results presented in this Appendix include site-specific SSI effects such as the layering of the subgrade, flexibility, embedment of the ESWPT structure, ground water level (GWL), and structure-soil-structure interaction (SSSI) of the large, heavy reactor building (R/B) complex and ultimate heat sink related structures (UHSRS) on the input ground motion.

3LL.2 Modeling Description and Analysis Approach

Modeling Description

The ESWPT includes four underground standalone segments running north-south on the east side and the west side of the R/B complex, which are separated by expansion joints (see Subsection 3.8.1.6 and Figure 3.8-201) that prevent interaction of segments at the interface. Three separate models provide the seismic response for the four standalone ESWPT segments. Tunnel Segment 1aN is representative of the two straight north-south tunnel segments, 1aN and 1bN, on both the east and west sides of the R/B complex, respectively, buried in backfill soil. These two segments are connected to the end of the UHS ESWPT, which is integrated with the UHSRS as described in Appendix 3KK. Tunnel Segment 1aS is the L-shaped tunnel segment on the east side of the R/B complex and is connected at its north end to Segment 1aN, and at its south end to the east end of the ESW pipe chase (ESWPC), which is the standard plant tunnel segment that runs in the east-west direction along the south side of the R/B complex, and is integrated with the R/B complex basemat. The FE model for Tunnel Segment 1bS is the L-shaped segment running west of the R/B complex and is connected at its north end to Segment 1bN, and at its south end to the west end of the standard plant ESWPC. The SSI analyses for all tunnel segments considered the standalone segments of the ESWPT as underground structures having the roof, the slab and the walls of the tunnel in full contact with soil. At the interfaces with the other ESWPT and ESWPC segments, the ESWPT structural model is disconnected from the model of the surrounding soil in order to accurately simulate the boundary conditions existing at the expansion joints.

The SSI models of both the structural components and the complete excavation volume for each of the three ESWPT segments are shown in Figures 3LL-1 through 3LL-6 as overall and cutaway views. Tables 3LL-1, 3LL-2, and 3LL-3 present the properties assigned to the structural components of the SASSI FE models for Segments 1aN, 1aS, and 1bS, respectively. Detailed descriptions and figures of the ESWPT including actual dimensions are contained in Section 3.8.

The ESWPT roof, interior and exterior walls, and basemat are modeled using four-node shell elements representing the gross section properties at the centerline of these reinforced concrete members. Densities that include the dynamic masses of self weight plus supplemental dead load and 25% of live load are assigned to these shell elements. Eight-node solid elements model the fill concrete below the ESWPT basemat in the SASSI structural model. A row of eight-node solid elements with backfill soil properties are added to the SASSI structural model on top of the tunnel and along the height of both the exterior walls and concrete fill to allow calculation of seismic earth pressures. Eight-node solid elements are also used for the SASSI excavated soil volume that serves to subtract the stiffness and mass of the excavated soil from the free-field soil model.

The SSI analyses consider the best estimate stiffness properties of the ESWPT reinforced concrete members and operating-basis earthquake (OBE) structural damping values of Chapter 3 Table 3.7.1-3(b), such as 4 percent damping for reinforced concrete. Based on estimates of in-plane and out-of-plane stresses, the ESWPT roof slabs are likely to develop cracks reducing their effective out-of-plane stiffness by about 50%. This 50% stiffness reduction is consistent with Table 2-1 of ASCE 43-05 (Reference 3LL-7).

The location of the lower boundary used in the SASSI analysis is greater than 710 feet below grade. The depth is greater than the embedment plus twice the depth of the largest base dimensions (i.e. 217.5’ x 2 + 31’ = 466’ for Tunnel Segment 1aN) as recommended by SRP 3.7.2. A ten layer half-space is used below the lower boundary in the SASSI analysis. The SASSI half-space simulation consists of additional layers with viscous dashpots added at the base of the half-space. The half-space layer has a thickness of 1.5 Vs/f, where Vs is the shear wave velocity of the half-space and f is the frequency of analysis. The half-space is sub-divided by the selected number of layers in the half-space.

Model Verification

The translation of the ESWPT structural models from ANSYS to SASSI is confirmed by comparing the results from the modal analysis of the fixed base structure in ANSYS and the SASSI analysis of the model resting on the surface of a half-space with high stiffness. An eigenvalue analysis was performed on the ANSYS models to obtain cumulative mass participation as a function of frequency and to identify the major modal frequencies and mode shapes. Transfer functions were computed at various node locations throughout the SASSI models and structural frequencies were obtained from the peaks of these transfer functions. The SSI analyses use refined mesh models of the ESWPT structures that have a sufficient number of degrees of freedom to accurately capture the seismic response of the standalone tunnel segments at frequencies up to 50 Hz. The FE mesh of the dynamic models used for SSI analyses is identical to the mesh of the models used for calculation of stress demands for design of the ESWPT structures. Therefore, 1g static analyses are not performed to verify that the models have a sufficient number of degrees of freedom.

Table 3LL-4 presents natural frequencies, associated modal responses, and the percentage of modal participating mass of the ANSYS and SASSI fixed-base ESWPT models. Figures 3LL-8 through 3LL-10, Figures 3LL-12 through 3LL-14, and Figures 3LL-16 through 3LL-18 present the transfer functions at various nodal locations obtained from the SASSI analyses ESWPT Segment 1aN, 1aS, and 1bS models, respectively, resting on the surface of a very stiff half-space. The frequencies of the ANSYS modes are plotted as solid vertical lines for comparison. The close correlation between the SASSI transfer function results with the ANSYS eigenvalue results verifies the accuracy of the three structural model translations. Table 3LL-4 also presents the percentage of modal participating mass obtained from the ANSYS model.

<u>Input Control Motion</u>

The safe-shutdown earthquake (SSE) ground motion for the seismic design of the ESWPT is defined by the envelope of the site-specific foundation input response spectra (FIRS) and the minimum design earthquake spectra as discussed in Subsection 3.7.1.1. The design ground motion is defined as the free-field outcrop motion at the bottom of the ESWPT foundation located at elevation 791.08 ft. The minimum earthquake spectra defined as the US-APWR certified seismic design response spectra (CSDRS) anchored to a zero period acceleration (ZPA) of 0.10 g envelops the ESWPT site-specific FIRS at all frequencies. Therefore, the CSDRS-compatible acceleration time histories used for the standard design of US-APWR plant were scaled to 1/3 and used as input outcrop motion for the ESWPT design. The input control motion for SASSI analysis is obtained by converting these outcrop motion acceleration time histories to within-layer motion. The three components of the input motion are applied to the SSI model separately by using vertically propagating shear and compression waves for the horizontal and vertical components, respectively.

The structural design includes accidental torsion loads to address uncertainties related to incoherency of the input ground motion in accordance with Section 3.1.1(e) of ASCE 4-98 (Reference 3LL-3). Incoherency typically lowers responses in the higher frequency range. Due to the low energy content of the input design ground motion at higher frequencies, the spatial variation of the input ground motion is deemed insignificant for the design of the ESWPT. Therefore, incoherence of the input control motion is not considered in the SSI and SSSI analysis of the ESWPT. Wave passage effects are considered small and do not impact the seismic design because the tunnel foundation is supported by a stiff limestone layer which will experience low strains under the low seismic motion at the site.

SSI Analysis Cases

Seismic design of the ESWPT is based on the envelope of responses obtained from SSI analyses of the ESWPT standalone models for the following site conditions:

a. Embedded lower bound (ELB), embedded best estimate (EBE), embedded upper bound (EUB), and embedded high bound (EHB) soil/rock dynamic properties reflecting engineered backfill that is saturated below the nominal GWL of 795 ft.

b. ELB, EBE, EUB and EHB full column profiles soil/rock dynamic properties reflecting engineered backfill that is saturated below high GWL located at the top of the ESWPT structure.

c. ELB full column profile reflecting dynamic properties of unsaturated engineered backfill when the GWL is located below the top of the limestone strata.

The frequency domain SSI analyses of ESWPT standalone segments are performed using a cutoff frequency of 50 Hz for all soil cases. The following frequencies of analysis are used:

- for frequency range 0 to 15 Hz, the spacing of analyzing frequency points is about 0.33 Hz, i.e. three frequency points per 1.0 Hz frequency interval,

- for frequency range 15 Hz to 40 Hz, three frequency points per 0.5 Hz interval

- for frequency range 40 Hz to 50 Hz, two frequency points per 1.0 Hz interval.

The strain-compatible rock and backfill properties for the SASSI analyses are developed as discussed in Subsection 3.7.2.4.5. SSI analyses of the ESWPT consider the site-specific stratigraphy and subgrade dynamic properties described in Subsection 2.5.4 as well as the backfill conditions around the ESWPT. The strain-compatible dynamic properties of supporting rock and engineered backfill used for the SASSI analysis of the ESWPT are presented in Table 3LL-8 and Tables 3LL-9 through 3LL-11, respectively.

The maximum shear wave passing frequency for the rock subgrade layers below the base slab and concrete fill, based on layer thicknesses of 1/5 wavelength, ranges from 54.8 Hz for ELB to 83.8 Hz for EUB and EHB profiles. The passing frequency for the engineered backfill ranges from 45.6 Hz for ELB to 118.5 Hz for EHB. The ELB maximum passing frequency is lower than the 50 Hz cutoff frequency, which is justified due to the three stiffer soil cases (ELB, EUB, and EHB) governing at frequencies above 17 Hz in the longitudinal direction of Tunnel Segment 1aN, 29 Hz in the longitudinal direction of Tunnel Segment 1aS, and 26 Hz in the transverse direction of Tunnel Segment 1bS as shown in Figure 3LL-26, Figure 3LL-27, and Figure 3LL-28, respectively.

The SASSI analyses produce results for maximum accelerations, in-structure response spectra (ISRS), seismic displacements, and seismic soil pressures. The seismic design is based on the envelope of responses obtained from SSI analyses of the three ESWPT models for the nine site conditions considered. The maximum accelerations and soil pressure results that serve as the basis for developing SSE loads for structural design are amplified to account for the SSSI effects on the design ground motion from the nearby structures and foundations. Amplification factors as a function of frequency are used to incorporate the SSSI effects in the design ISRS as described below.

<u>SSSI Effects</u>

The seismic design considers the effects of SSSI on the ESWPT free field ground motion from the adjacent R/B complex and UHSRS by using the results of the SSI analyses of the R/B complex and UHSRS models described in Appendix 3NN and 3KK, respectively. ESWPT standalone segments are underground structures whose response is governed by the response of the surrounding soil. Therefore, the consideration of the effects of the nearby large and heavy structures on the free field ground motion is an adequate approach for addressing the overall SSSI effects on ESWPT without performing explicit SSSI analyses.

Acceleration response spectra for the near field responses at locations along the centerline of the ESWPT segments are compared with the free-field motion acceleration response spectra. For every frequency of the response spectra, a SSSI spectral amplification factor is calculated, for both the roof and basemat elevations, as the ratio of the response of the near field nodes at ESWPT locations to free-field motion spectra to help determine the impact of the SSSI effects. For ratios less than 1, the amplification factor is assigned a value of 1. These spectral amplification factors are used to adjust responses of ESWPT roof, basemat and walls to account for SSSI effects. The adjustment of the design ISRS is performed by multiplying the acceleration response spectra with the corresponding amplification factor at each frequency. Spectral amplification factors obtained from the SSI analyses of the UHSRS are used to adjust responses obtained for the north straight ESWPT segments 1aN and 1bN. Spectral amplification factors obtained from the SSI analyses of the R/B complex are used to adjust responses obtained for Segments 1aS and 1bS. Amplification factors calculated for 100 Hz are used to include the SSSI effects in the maximum accelerations results that serve as basis for development of SSE loads for structural design. Table 3LL-12 shows the amplification factors used to adjust the ESWPT design basis ZPA.

Use of Modified Subtraction Method

The analyses are performed using the modified subtraction method (MSM). To verify the accuracy of the results using the MSM, a verification study is performed on Tunnel Segment 1aN. The verification SSI analyses are performed using both the MSM and the more computationally robust flexible volume method, also known as the direct method, for the EUB soil case using cut-off frequency of analysis of 50 Hz. The difference between these two methods resides in the definition of interaction nodes for which impedances are calculated for SSI analyses. For the MSM, the choice of interaction nodes includes all nodes on the outer face of the excavated soil volume. The direct method considers all nodes in the excavated volume as interaction nodes. A comparison of the transfer functions and ISRS at key locations resulting from the two methods demonstrates that the results using the MSM appropriately capture the ESWPT SSI responses. Figure 3LL-19 shows the key nodal locations of the Tunnel Segment 1aN MSM study. Figure 3LL-20 and Figure 3LL-21 present examples of transfer function and in-structure response spectra comparisons, respectively, of the MSM versus the flexible volume method for a key node of the ESWPT.

Effects of Groundwater Level Variation

The effects of GWL variations are studied by comparing responses of ESWPT straight segment 1aN for the four soil cases reflecting dynamic properties of the backfill (ELB, EBE, EUB and EHB) for three different ground water levels:

- Nominal- located at elevation of 795 ft
- High- located at approximately elevation 804 ft (top of the ESWPT)
- Unsaturated- when GWL is located below the rock subgrade top elevation of 782 ft

The ESWPT SSI response is mostly governed by the response of the surrounding soil, making it the most sensitive of all site-specific Category I structures to GWL changes. As a result, conclusions made in studying GWL effects on the ESWPT also indicate the overall GWL effects on the seismic response of other site-specific Category I structures.

The comparisons of SSI analyses results for the three different GWLs show that responses obtained from the SSI analyses with high GWL are usually bounding. The results of the study showed that the response of the ESWPT when embedded in saturated backfill envelops unsaturated backfill responses for all frequencies for all soil profiles. The results also showed that the SSI analysis of the unsaturated backfill LB profile yields high peaks in the in-structure response spectra (ISRS) at higher frequencies. As a result, the design basis for the ESWPT is developed as the envelope of responses obtained from the SSI analyses of saturated backfill profiles with nominal and high GWL and from the SSI analysis of the ELB unsaturated backfill profile of all three ESWPT segment FE models.

Dynamic Lateral Soil Pressures

Static equivalent loads representing dynamic lateral pressures and seismic inertia SSE loads obtained from the SASSI analysis are applied in the ANSYS analyses to calculate the demands on ESWPT structural members. A uniformly distributed dynamic lateral pressure load of 3.5 ksf is applied on the exterior walls of the tunnels that envelops the lateral dynamic soil pressures from the elastic solution provided in Subsection 3.5.3.2 of ASCE 4-98 (Reference 3LL-3), and numerically-calculated dynamic soil pressures from the SASSI results which are amplified to account for the SSSI effects of the UHSRS and R/B complex on the ESWPT free field motion. Figure 3LL-29 shows the comparison of the ASCE 4-98 and SSI analysis soil pressures versus the dynamic soil pressure used for design. The seismic inertia demands are calculated by applying equivalent quasi-static seismic accelerations in all three directions. The SSE earth loads are applied to the ESWPT structures as equivalent uniform pressure acting in the two horizontal directions, as lateral pressure loads acting normal to the roof slab and walls and as in-plane pressure loads transferred to the tunnel roof and walls by friction.

Application of SASSI Results in the Structural Design

Equivalent static analysis of the ANSYS model is used to calculate the structural demands on the ESWPT due to the seismic soil pressures and seismic inertia loads, which are combined as appropriate with other applicable design loads in accordance with the factored load combinations described in Subsection 3.8.4. Seismic inertia forces are applied to the ESWPT as mass accelerations at each node in each direction with a seismic coefficient of 0.25. The value of the seismic coefficient that is equal for all three directions of the design earthquake is determined conservatively based on the results of the SSI analyses for maximum acceleration and envelops effects of SSSI. Maximum nodal acceleration and lateral earth pressures obtained from the SSI analyses of segments 1aN, 1aS and 1bS for all saturated backfill profiles (nominal and high GWL) and unsaturated ELB profile, due to all three directions of the earthquake are combined using the Square Root Sum of Square (SRSS) method to produce the maximum demands for each direction of motion. Results are then enveloped for each of the soil cases and GWL. SSSI amplification factors are then applied and design maximum acceleration and dynamic soil pressures are determined as an envelope of maximum computed demands for all three segments.

Demands calculated from the ANSYS analyses for Segments 1aN, 1aS and 1bS are combined on an absolute basis to produce the maximum demands for each structural component of the ESWPT. Loads applied on the tunnel ANSYS models are combined spatially by the Newmark 100%-40%-40% combination rule of RG 1.92 (Reference 3LL-5). Load combinations use the 100%-40%-40% combination rule because the design of concrete elements includes the effects of the interaction of different components, such as interaction of axial forces with the moments or axial forces with shear. Since the direction of input motion that results in the maximum axial force may be different from that producing the maximum moment or shear, the 100%-40%-40% method produces more accurate design demands.

With the exception of the extreme flooding cases, design load combinations include static soil pressure demands on the ESWPT that consider differential water elevations with a high GWL (approximately 804 ft) inside of the ESWPT loop and an unsaturated GWL (below 782 ft) outside of the ESWPT loop. The asymmetry of hydrostatic loads in this case results in the most conservative demand and design of the ESWPT structure.

Accidental torsion is included in the structural design demands by considering an accidental eccentricity of ± 5 percent of the maximum structure dimension for both horizontal directions, consistent with Acceptance Criterion 11 of SRP 3.7.2.11. The accidental torsion is included by applying angular accelerations in combination with the seismic inertia accelerations, the soil pressures, and other applicable loads. The angular accelerations are computed as the product of the total base shear multiplied by ±5 percent of the maximum structure dimension for both horizontal directions, and divided by the structure's mass moment of inertia about the vertical axis of its center of gravity.

Table 3LL-17 compares results of the ANSYS quasi-static analyses for the displacements of the ESWPT structures under SSE design loads with the relative displacements results obtained from the SSI analyses of the different ESWPT segments. The comparison demonstrates that the ANSYS analyses yield seismic demands that envelop the results of the seismic response SSI analyses.

3LL.3 Seismic Analysis Results

Table 3LL-4 presents the natural frequencies and descriptions of the associated modal responses obtained from the fixed-base ANSYS analysis of the straight portion of the ESWPT (Segment 1aN Model). These frequencies were compared to the frequencies obtained from the transfer functions for the SASSI model to confirm adequacy of the translation of the FE models from ANSYS to SASSI. Table 3LL-5 presents a summary of SSI effects on the seismic response of the ESWPT segments and Table 3LL-6 presents a summary of the analyses performed on the ESWPT.

The maximum absolute nodal accelerations obtained from the SASSI SSI analyses of the ESWPT models are presented in Tables 3LL-12 to 3LL-14. The results are presented for each of the major ESWPT components and envelop all backfill conditions described above. The maximum accelerations have been obtained by combining cross-directional contributions (i.e. X-response due to X-input, X-response due to Y-input, and X-response due to Z-input) in accordance with RG 1.92 (Reference 3LL-5) using the square root sum of the squares (SRSS) method.

The forces and moments in Table 3LL-16 represent the enveloping maximum absolute values of seismic demands produced from ANSYS seismic analyses and used for seismic design of the ESWPT structural components. These results include the combined demands from seismic inertia, seismic soil pressure, and the combinations of all directions of input motion. For structural design, the accidental torsion load case results in increased shear in the outer walls, which is included in the values reported in Table 3LL-16. Note that addition of the torsion by load case results in shear demand in the outer walls that meets or exceeds the accidental torsion requirements for design.

Maximum relative displacements provided in Table 3LL-17 are the maximum displacements of the nodes calculated in the SASSI seismic analyses relative to the center of the mat bottom. Maximum relative displacements were then compared to those obtained from SASSI to demonstrate that the structural design considers SSE loads that envelop responses obtained from SASSI analyses.

3LL.4 In-Structure Response Spectra

The enveloped broadened ISRS calculated in SASSI are presented in Figures 3LL-22, 3LL-23, 3LL-24, and 3LL-25 for the ESWPT basemat, exterior walls, interior walls, and roof, respectively, for all ESWPT segments. The spectra are presented for the horizontal and vertical directions for 0.5 percent, 2 percent, 3 percent, 4 percent, 5 percent, 7 percent, 10 percent, and 20 percent damping. Groups of nodes are used to generate the ISRS for the different structure components. The groups of nodes are selected to represent the key locations, including edges and centers, of the structure's components (i.e. walls, slabs, roof, and basemat). The number of nodes and locations are selected to provide design basis ISRS that envelop the responses at different locations within the component. The ISRS are resultant spectra, which have been combined using SRSS to account for cross-directional coupling effects in accordance with RG 1.122 (Reference 3LL-6). The ISRS envelop the results of all SSI analyses of the three ESWPT models for nine soil cases and capture the effects of flexibility and concrete cracking in the walls, roof slab, and basemat as well as SSSI effects. The ISRS have been broadened by 15 percent and all valleys removed. The spectra are used for the design of seismic category I and II subsystems and components housed within or mounted to the ESWPT. For the design of seismic category I and II subsystems and components mounted to the ESWPT walls and slabs, it is required to account for the effects of any seismic anchor motions associated with the seismic displacements of the structure.

3LL.5 References

3LL-1 *An Advanced Computational Software for 3D Dynamic Analysis Including Soil Structure Interaction,* ACS SASSI Version 3.0

including “Option A” & NQA “Option FS,” User Manuals Revision 7.0, Ghiocel Predictive Technologies, Inc., September 26, 2012.

3LL-2 ANSYS Release 13.0, SAS IP, Inc. 2010.

3LL-3 *Seismic Analysis of Safety-Related Nuclear Structures,* American Society of Civil Engineers, ASCE 4-98, Reston, Virginia, 2000.

3LL-4 *Damping Values for Seismic Design of Nuclear Power Plants*, Regulatory Guide 1.61, Rev. 1, U.S. Nuclear Regulatory Commission, Washington, DC, March 2007.

3LL-5 *Combining Responses and Spatial Components in Seismic Response Analysi*s, Regulatory Guide 1.92, Rev. 2, U.S. Nuclear Regulatory Commission, Washington, DC, July 2006.

3LL-6 *Development of Floor Design Response Spectra for Seismic Design of Floor-supported Equipment or Components*, Regulatory Guide 1.122, Rev. 1, U.S. Nuclear Regulatory Commission, Washington, DC, February 1978.

3LL-7 *Seismic Design Criteria for Structures, Systems and Components in Nuclear Facilities*, American Society of Civil Engineers, ASCE 43-05, Reston, Virginia, 2005.

Table 3LL-1

ESWPT Segment 1aN FE Model Component Properties

Components	Material	E (ksi)	Poisson's Ratio	Unit Weight (kcf)	Damping Ratio	Width or Height x Thickness(2) (ft)	Element type
Roof(4)	5,000 psi concrete	5,700	0.17	0.20(1)	0.04	25 x 1.41	Shell
Base slab	5,000 psi concrete	4,030	0.17	0.163(1)(3)	0.04	25 x 2	Shell
Exterior Walls	5,000 psi concrete	4,030	0.17	0.175(1)	0.04	12.67 x 2	Shell
Interior Walls	5,000 psi concrete	4,030	0.17	0.20(1)	0.04	12.67 x 1	Shell
Fill Concrete	3,000 psi concrete	3,122	0.17	0.15	0.04	25 x 9.08	Brick

Notes:

1) The unit weight includes equivalent dead loads due to piping and other supported components, and 25% of the applicable 50 psf live load on the base slab for dynamic analysis purposes. A pipe load of 50 psf is considered on the roof slab and 25 psf is considered on wall inside surfaces (inside surface of exterior walls and both sides of the interior wall).
2) The width or height of the component is adjusted from actual dimensions to suit the mesh pattern used for the FE model. The adjustments are minor and do not affect the accuracy of the analysis results. Actual component dimensions are shown in Section 3.8 Figure 3.8-203 and 3.8-205.
3) A 2 klf dead load representing the four ESW pipes is applied to the base slab.
4) Modulus of Elasticity, thickness and unit weight of roof slab are adjusted for cracking.

Table 3LL-2

ESWPT Segment 1aS FE Model Component Properties

Components	Material	E (ksi)	Poisson's Ratio	Unit Weight (kcf)	Damping Ratio	Width or Height x Thickness (ft) (2)	Element type
Roof(4) (N-S Leg)	5,000 psi concrete	5,700	0.17	0.21(1)	0.04	25 x 1.41	Shell
Roof(4) (E-W Leg)	5,000 psi concrete	5,700	0.17	0.21(1)	0.04	27 x 1.41	Shell
Base slab (N-S Leg)	5,000 psi concrete	4,030	0.17	0.163(1)(3)	0.04	25 x 2	Shell
Base slab (E-W Leg)	5,000 psi concrete	4,030	0.17	0.163(1)(3)	0.04	27 x 2	Shell
Exterior Walls (N-S Leg)	5,000 psi concrete	4,030	0.17	0.175(1)	0.04	12.67 x 2	Shell
Exterior Walls (E-W Leg)	5,000 psi concrete	4,030	0.17	0.175(1)	0.04	12.67 x 3	Shell
Interior Walls	5,000 psi concrete	4,030	0.17	0.20(1)	0.04	12.67 x 1	Shell
Fill Concrete (N-S Leg)	3,000 psi concrete	3,122	0.17	0.15	0.04	25 x 9.08	Brick
Fill Concrete (E-W Leg)	3,000 psi concrete	3,122	0.17	0.15	0.04	27 x 9.08	Brick

Notes:

1) The unit weight includes equivalent dead loads due to piping and other supported components, and 25% of the applicable 50 psf live load on the base slab for dynamic analysis purposes. A pipe load of 50 psf is considered on the roof slab and 25 psf is considered on wall inside surfaces (inside surface of exterior walls and both sides of the interior wall).
2) The width or height of the component is adjusted from actual dimensions to suit the mesh pattern used for the FE model. The adjustments are minor and do not affect the accuracy of the analysis results. Actual component dimensions are shown in Section 3.8 Figure 3.8-202.
3) A 2 klf dead load representing the four ESW pipes is applied to the base slab.
4) Modulus of Elasticity, thickness and unit weight of roof slab are adjusted for cracking.

Table 3LL-3

ESWPT Segment 1bS FE Model Component Properties

Components	Material	E (ksi)	Poisson's Ratio	Unit Weight (kcf)	Damping Ratio	Width or Height x Thickness (ft) (2)	Element type
Roof(4) (N-S Leg)	5,000 psi concrete	5,700	0.17	0.20(1)	0.04	25 x 1.41	Shell
Roof(4) (E-W Leg)	5,000 psi concrete	5,700	0.17	0.20(1)	0.04	25 x 1.41	Shell
Base slab (N-S Leg)	5,000 psi concrete	4,030	0.17	0.163(1)(3)	0.04	25 x 2	Shell
Base slab (E-W Leg)	5,000 psi concrete	4,030	0.17	0.163(1)(3)	0.04	25 x 2	Shell
Exterior Walls (N-S Leg)	5,000 psi concrete	4,030	0.17	0.175(1)	0.04	12.67 x 2	Shell
Exterior Walls (E-W Leg)	5,000 psi concrete	4,030	0.17	0.175(1)	0.04	12.67 x 2	Shell
Fill Concrete	3,000 psi concrete	3,122	0.17	0.15	0.04	23 x 10.08	Brick
Fill Concrete	3,000 psi concrete	3,122	0.17	0.15	0.04	25 x 9.08	Brick

Notes:

1) The unit weight includes equivalent dead loads due to piping and other supported components, and 25% of the applicable 50 psf live load on the base slab for dynamic analysis purposes. A pipe load of 50 psf is considered on the roof slab, and 25 psf is considered on wall inside surfaces (inside surface of exterior walls and both sides of the interior wall).
2) The width of the component is adjusted from actual dimensions to suit the mesh pattern used for the FE model. The adjustments are minor and do not affect the accuracy of the analysis results. Actual component dimensions are shown in Section 3.8 Figures 3.8-203 and 3.8-204.
3) A 2 klf dead load representing the four ESW pipes is applied to the base slab.
4) Modulus of Elasticity, thickness and unit weight of roof slab are adjusted for cracking.

Table 3LL-4

ESWPT Structural Frequencies

ESWPT Segment	Direction	ANSYS Model Frequency (Hz)(1)	SASSI Model Frequency (Hz)(1)	Difference (%)	Percent Effective Mass (%)(2)	Comments
1aN	Transverse	14.9	15.1	03	30.8	Vibrations at middle of roof slab and tunnel length
	Longitudinal	62.4	63.8	0.6	52.7	
	Vertical	70.0	71.5	0.5	41.0	
1aS	Transverse	16.2	15.8	0.6	20.4	Vibrations of longer arm of tunnel at middle of roof slab and tunnel length
	Longitudinal	64.8	64.0	0.3	12.9	
	Vertical	74.0	71.8	0.8	18.8	
1bS	Transverse	16.2	15.8	0.6	17.7	Vibrations of longer arm of tunnel at middle of roof slab and tunnel length
	Longitudinal	64.8	64.0	0.3	12.3	
	Vertical	74.1	71.0	1.1	24.7	

Notes:

1) Natural frequencies of ESWPT structural models include fill concrete below the ESWPT foundation.
2) Percent effective mass are from ANSYS modal analyses.

Table 3LL-5

SASSI Results for ESWPT Seismic Response

SSI Effect	Observed Response
Rock Subgrade	The rock subgrade has little to no effect on the ESWPT seismic response.
Backfill Embedment	The seismic response of the surrounding backfill soil determines the overall response of the buried ESWPT structure. The backfill soil frequencies that are in the range from 5 Hz for lower bound to 13 Hz for high bound, characterize the ESWPT horizontal response for all three segments. Frequencies of 11 Hz for lower bound, to 29 Hz for high bound characterize the vertical response of the ESWPT. The different ESWPT segments exhibit almost identical seismic behavior that is characterized by plane-strain racking response of the tunnel in its transverse direction.
Ground Water Level (GWL)	ESWPT standalone segments as light underground structures are the most sensitive to GWL changes among all of CPNPP 3 & 4 Category I structures. The results of an elaborate GWL sensitivity study performed on ESWPT Segment 1aN show that the high GWL results in amplified SSI responses bound the seismic design, and responses obtained from the EHB soil case with high GWL envelops the ESWPT response at almost all frequencies. Since the responses of the four ESWPT segments are the same, the conclusions of the GWL study performed on Tunnel Segment 1aN are applicable to all segments.
Structure-Soil-Structure Interaction (SSSI)	The seismic response of the R/B complex and UHSRS have considerable effect on the free field motions at ESWPT locations. Amplification factors are applied to the results of the SSI analyses to include SSSI effects in the ESWPT seismic design basis.

Table 3LL-6

Summary of Analyses Performed

Model	Loading Case	Analysis Method	Program	Input	Output	Three Components Combination	Modal Combination (for Dynamic Analyses)
Three-dimensional ESWPT FE Model	Seismic motion	Time history soil-structure interaction analysis in frequency domain using sub-structuring technique	SASSI	Time history input matching site-specific design response spectra from site-response analysis, site-specific soil profiles	Peak accelerations, in-structure response spectra, element forces, soil pressure.	SRSS	N/A
Three-dimensional ESWPT FE Model	Seismic inertia and soil pressure in addition to other loads	Static	ANSYS	Design loads per Subsection 3.8.4, peak seismic inertia and peak soil pressures based on the envelope of SSI results and pressures per ASCE 4-98, static hydrostatic and soil pressures, separate analysis for each direction of pressure.	Element and section demands for design	Newmark 100%-40%-40% combination rule	N/A

Table 3LL-7

SSI Analysis Cases for ESWPT

Straight Segment 1aN				
Analysis Case	No. Freq.	Cut-off Freq.	House File	Site File
ELB - Nominal	103	50 Hz	CPNPP34_ESWPT_1aN_ELB_NGWL.hou	ESWPT-ELB-NGWL_X.sit
EBE - Nominal	103	50 Hz	CPNPP34_ESWPT_1aN_EBE_NGWL.hou	ESWPT-EBE-NGWL_X.sit
EUB - Nominal	103	50 Hz	CPNPP34_ESWPT_1aN_EUB_NGWL.hou	ESWPT-EUB-NGWL_X.sit
EHB - Nominal	103	50 Hz	CPNPP34_ESWPT_1aN_EHB_NGWL.hou	ESWPT-EHB-NGWL_X.sit
ELB - High GWL	103	50 Hz	CPNPP34_ESWPT_1aN_ELB_HGWL.hou	ESWPT-ELB-HGWL_X.sit
EBE - High GWL	103	50 Hz	CPNPP34_ESWPT_1aN_EBE_HGWL.hou	ESWPT-EBE-HGWL_X.sit
EUB - High GWL	103	50 Hz	CPNPP34_ESWPT_1aN_EUB_HGWL.hou	ESWPT-EUB-HGWL_X.sit
EHB - High GWL	103	50 Hz	CPNPP34_ESWPT_1aN_EHB_HGWL.hou	ESWPT-EHB-HGWL_X.sit
ELB - Unsaturated	103	50 Hz	CPNPP34_ESWPT_1aN_ELB_DRY.hou	ESWPT-ELB-DRY_X.sit
EBE - Unsaturated (*)	103	50 Hz	CPNPP34_ESWPT_1aN_EBE_DRY.hou	ESWPT-EBE-DRY_X.sit
EUB - Unsaturated (*)	103	50 Hz	CPNPP34_ESWPT_1aN_EUB_DRY.hou	ESWPT-EUB-DRY_X.sit
EHB - Unsaturated (*)	103	50 Hz	CPNPP34_ESWPT_1aN_EHB_DRY.hou	ESWPT-EHB-DRY_X.sit

L-Shaped Segment 1aS				
Analysis Case	No. Freq.	Cut-off Freq.	House File	Site File
ELB - Nominal	103	50 Hz	CPNPP34_ESWPT_1aS_ELB_NGWL.hou	ESWPT-ELB-NGWL_X.sit
EBE - Nominal	103	50 Hz	CPNPP34_ESWPT_1aS_EBE_NGWL.hou	ESWPT-EBE-NGWL_X.sit
EUB - Nominal	103	50 Hz	CPNPP34_ESWPT_1aS_EUB_NGWL.hou	ESWPT-EUB-NGWL_X.sit
EHB - Nominal	103	50 Hz	CPNPP34_ESWPT_1aS_EHB_NGWL.hou	ESWPT-EHB-NGWL_X.sit
ELB - High GWL	103	50 Hz	CPNPP34_ESWPT_1aS_ELB_HGWL.hou	ESWPT-ELB-HGWL_X.sit
EBE - High GWL	103	50 Hz	CPNPP34_ESWPT_1aS_EBE_HGWL.hou	ESWPT-ELB-HGWL_X.sit
EUB - High GWL	103	50 Hz	CPNPP34_ESWPT_1aS_EUB_HGWL.hou	ESWPT-ELB-HGWL_X.sit
EHB - High GWL	103	50 Hz	CPNPP34_ESWPT_1aS_EHB_HGWL.hou	ESWPT-ELB-HGWL_X.sit
ELB - Unsaturated	103	50 Hz	CPNPP34_ESWPT_1aS_ELB_DRY.hou	ESWPT-ELB-DRY_X.sit

L-Shaped Segment 1bS				
Analysis Case	**No. Freq.**	**Cut-off Freq.**	**House File**	**Site File**
ELB - Nominal	103	50 Hz	CPNPP34_ESWPT_1bS_ELB_NGWL.hou	ESWPT-ELB-NGWL_X.sit
EBE - Nominal	103	50 Hz	CPNPP34_ESWPT_1bS_EBE_NGWL.hou	ESWPT-EBE-NGWL_X.sit
EUB - Nominal	103	50 Hz	CPNPP34_ESWPT_1bS_EUB_NGWL.hou	ESWPT-EUB-NGWL_X.sit
EHB - Nominal	103	50 Hz	CPNPP34_ESWPT_1bS_EHB_NGWL.hou	ESWPT-EHB-NGWL_X.sit
ELB - High GWL	103	50 Hz	CPNPP34_ESWPT_1bS_ELB_HGWL.hou	ESWPT-ELB-HGWL_X.sit
EBE - High GWL	103	50 Hz	CPNPP34_ESWPT_1bS_EBE_HGWL.hou	ESWPT-ELB-HGWL_X.sit
EUB - High GWL	103	50 Hz	CPNPP34_ESWPT_1bS_EUB_HGWL.hou	ESWPT-ELB-HGWL_X.sit
EHB - High GWL	103	50 Hz	CPNPP34_ESWPT_1bS_EHB_HGWL.hou	ESWPT-ELB-HGWL_X.sit
ELB - Unsaturated	103	50 Hz	CPNPP34_ESWPT_1bS_ELB_DRY.hou	ESWPT-ELB-DRY_X.sit

(*) Analysis is used in GWL study only

Table 3LL-8

ESWPT Rock Subgrade Profile and Passing Frequencies (Sheet 1 of 5)

CPNPP 3 & 4 Rock Subgrade Properties													
Elev. (ft)	Unit Weight (lb/ft^3)	Vs (ft/sec)			Vp (ft/sec)			Damping			Passing Frequency (Hz)		
		ELB	EBE	EUB	ELB	EBE	EUB	ELB	EBE	EUB	ELB	EBE	EUB
782.0	0.155	4603	5720	7108	9138	11356	14112	2.76%	1.88%	1.29%	410.7	510.4	634.3
779.8	0.155	4603	5720	7108	9138	11356	14112	2.76%	1.88%	1.29%	102.7	127.6	158.6
770.8	0.155	4603	5720	7108	9138	11356	14112	2.76%	1.88%	1.29%	82.1	102.1	126.9
759.6	0.155	4603	5720	7108	9138	11356	14112	2.76%	1.88%	1.29%	102.7	127.6	158.6
750.6	0.155	4603	5720	7108	9138	11356	14112	2.76%	1.88%	1.29%	82.1	102.1	126.9
739.4	0.155	4603	5720	7108	9138	11356	14112	2.76%	1.88%	1.29%	102.7	127.6	158.6
730.5	0.155	4603	5720	7108	9138	11356	14112	2.76%	1.88%	1.29%	136.9	170.1	211.4
723.7	0.155	4603	5720	7108	9138	11356	14112	2.76%	1.88%	1.29%	136.9	170.1	211.4
717.0	0.135	2355	3019	3870	6341	8129	10421	5.49%	3.65%	2.42%	157.0	201.3	258.0
714.0	0.155	4173	5113	6265	8922	10932	13395	2.50%	1.71%	1.17%	69.5	85.2	104.4
702.0	0.155	4173	5113	6265	8922	10932	13395	2.50%	1.71%	1.17%	69.5	85.2	104.4
690.0	0.155	5280	6467	7920	10063	12324	15094	2.50%	1.71%	1.17%	62.1	76.1	93.2
673.0	0.155	5280	6467	7920	10063	12324	15094	2.50%	1.71%	1.17%	62.1	76.1	93.2
656.0	0.15	3220	4046	5084	7319	9197	11556	2.59%	1.78%	1.22%	75.8	95.2	119.6
647.5	0.15	3220	4046	5084	7319	9197	11556	2.59%	1.78%	1.22%	75.8	95.2	119.6
639.0	0.15	3219	4045	5083	7316	9194	11555	2.60%	1.79%	1.23%	75.7	95.2	119.6
630.5	0.15	3219	4045	5083	7316	9194	11555	2.60%	1.79%	1.23%	75.7	95.2	119.6
622.0	0.13	2357	2950	3693	6034	7553	9454	2.54%	1.74%	1.19%	65.0	81.4	101.9
614.8	0.13	2357	2950	3693	6034	7553	9454	2.54%	1.74%	1.19%	65.0	81.4	101.9

Table 3LL-8

ESWPT Rock Subgrade Profile and Passing Frequencies (Sheet 2 of 5)

CPNPP 3 & 4 Rock Subgrade Properties														
Elev. (ft)	Unit Weight (lb/ft^3)	Vs (ft/sec)			Vp (ft/sec)			Damping			Passing Frequency (Hz)		
		ELB	EBE	EUB	ELB	EBE	EUB	ELB	EBE	EUB	ELB	EBE	EUB
607.5	0.13	2357	2950	3693	6034	7553	9454	2.55%	1.75%	1.20%	65.0	81.4	101.9
600.3	0.13	2357	2950	3693	6034	7553	9454	2.55%	1.75%	1.20%	65.0	81.4	101.9
593.0	0.135	2362	3153	4208	5370	7167	9566	4.62%	3.13%	2.12%	59.1	78.8	105.2
585.0	0.135	2362	3153	4208	5370	7167	9566	4.62%	3.13%	2.12%	59.1	78.8	105.2
577.0	0.135	2359	3150	4206	5362	7160	9560	4.64%	3.15%	2.13%	59.0	78.8	105.2
569.0	0.135	2359	3150	4206	5362	7160	9560	4.64%	3.15%	2.13%	59.0	78.8	105.2
561.0	0.135	2356	3147	4203	5356	7153	9553	4.66%	3.16%	2.14%	58.9	78.7	105.1
553.0	0.135	2356	3147	4203	5356	7153	9553	4.66%	3.16%	2.14%	58.9	78.7	105.1
545.0	0.135	2354	3144	4200	5350	7146	9547	4.68%	3.17%	2.15%	58.8	78.6	105.0
537.0	0.135	2354	3144	4200	5350	7146	9547	4.68%	3.17%	2.15%	58.8	78.6	105.0
529.0	0.135	2351	3141	4197	5344	7140	9539	4.69%	3.19%	2.16%	58.8	78.5	104.9
521.0	0.135	2351	3141	4197	5344	7140	9539	4.69%	3.19%	2.16%	58.8	78.5	104.9
513.0	0.14	2549	3305	4286	6002	7783	10092	6.67%	4.54%	3.09%	65.8	85.3	110.6
505.3	0.14	2549	3305	4286	6002	7783	10092	6.67%	4.54%	3.09%	65.8	85.3	110.6
497.5	0.14	2544	3300	4280	5991	7771	10080	6.70%	4.57%	3.11%	65.7	85.2	110.5
489.8	0.14	2544	3300	4280	5991	7771	10080	6.70%	4.57%	3.11%	65.7	85.2	110.5
482.0	0.14	2540	3296	4276	5982	7762	10070	6.74%	4.59%	3.13%	65.6	85.1	110.4
474.3	0.14	2540	3296	4276	5982	7762	10070	6.74%	4.59%	3.13%	65.6	85.1	110.4
466.5	0.14	2537	3292	4272	5974	7752	10060	6.77%	4.61%	3.14%	65.5	85.0	110.2
458.8	0.14	2537	3292	4272	5974	7752	10060	6.77%	4.61%	3.14%	65.5	85.0	110.2
451.0	0.145	2440	3079	3885	5977	7542	9516	2.85%	1.97%	1.36%	62.0	78.2	98.7

Table 3LL-8

ESWPT Rock Subgrade Profile and Passing Frequencies (Sheet 3 of 5)

CPNPP 3 & 4 Rock Subgrade Properties													
Elev. (ft)	Unit Weight (lb/ft^3)	Vs (ft/sec)			Vp (ft/sec)			Damping			Passing Frequency (Hz)		
		ELB	EBE	EUB	ELB	EBE	EUB	ELB	EBE	EUB	ELB	EBE	EUB
443.1	0.145	2440	3079	3885	5977	7542	9516	2.85%	1.97%	1.36%	62.0	78.2	98.7
435.3	0.145	2440	3079	3885	5977	7542	9516	2.85%	1.97%	1.36%	62.0	78.2	98.7
427.4	0.145	2440	3079	3885	5977	7542	9516	2.85%	1.97%	1.36%	62.0	78.2	98.7
419.5	0.145	2439	3078	3884	5975	7540	9514	2.86%	1.98%	1.36%	61.9	78.2	98.6
411.6	0.145	2439	3078	3884	5975	7540	9514	2.86%	1.98%	1.36%	61.9	78.2	98.6
403.8	0.145	2439	3078	3884	5975	7540	9514	2.87%	1.98%	1.37%	61.9	78.2	98.6
395.9	0.145	2439	3078	3884	5975	7540	9514	2.87%	1.98%	1.37%	61.9	78.2	98.6
388.0	0.15	4320	5344	6611	8396	10387	12850	2.83%	2.10%	1.55%	54.9	68.0	84.1
372.3	0.15	4320	5344	6611	8396	10387	12850	2.83%	2.10%	1.55%	54.9	68.0	84.1
356.5	0.15	4320	5344	6611	8396	10387	12850	2.83%	2.10%	1.55%	54.9	68.0	84.1
340.8	0.15	4320	5344	6611	8396	10387	12850	2.83%	2.10%	1.55%	54.9	68.0	84.1
325.1	0.15	4320	5344	6611	8396	10387	12850	2.83%	2.10%	1.55%	54.9	68.0	84.1
309.4	0.15	4320	5344	6611	8396	10387	12850	2.83%	2.10%	1.55%	54.9	68.0	84.1
293.6	0.15	4320	5344	6611	8396	10387	12850	2.83%	2.10%	1.55%	54.9	68.0	84.1
277.9	0.15	4317	5341	6608	8391	10381	12843	2.86%	2.12%	1.57%	54.9	67.9	84.0
262.2	0.15	4317	5341	6608	8391	10381	12843	2.86%	2.12%	1.57%	54.9	67.9	84.0
246.4	0.15	4317	5341	6608	8391	10381	12843	2.86%	2.12%	1.57%	54.9	67.9	84.0
230.7	0.15	4317	5341	6608	8391	10381	12843	2.86%	2.12%	1.57%	54.9	67.9	84.0
215.0	0.15	4317	5341	6608	8391	10381	12843	2.86%	2.12%	1.57%	54.9	67.9	84.0
199.3	0.15	4317	5341	6608	8391	10381	12843	2.86%	2.12%	1.57%	54.9	67.9	84.0
183.5	0.15	4317	5341	6608	8391	10381	12843	2.86%	2.12%	1.57%	54.9	67.9	84.0

Table 3LL-8

ESWPT Rock Subgrade Profile and Passing Frequencies (Sheet 4 of 5)

CPNPP 3 & 4 Rock Subgrade Properties													
Elev. (ft)	Unit Weight (lb/ft^3)	Vs (ft/sec)			Vp (ft/sec)			Damping			Passing Frequency (Hz)		
		ELB	EBE	EUB	ELB	EBE	EUB	ELB	EBE	EUB	ELB	EBE	EUB
167.8	0.15	4315	5338	6603	8387	10375	12834	2.88%	2.13%	1.58%	54.9	67.9	84.0
152.1	0.15	4315	5338	6603	8387	10375	12834	2.88%	2.13%	1.58%	54.9	67.9	84.0
136.3	0.15	4315	5338	6603	8387	10375	12834	2.88%	2.13%	1.58%	54.9	67.9	84.0
120.6	0.15	4315	5338	6603	8387	10375	12834	2.88%	2.13%	1.58%	54.9	67.9	84.0
104.9	0.15	4315	5338	6603	8387	10375	12834	2.88%	2.13%	1.58%	54.9	67.9	84.0
89.2	0.15	4315	5338	6603	8387	10375	12834	2.88%	2.13%	1.58%	54.9	67.9	84.0
73.4	0.15	4315	5338	6603	8387	10375	12834	2.88%	2.13%	1.58%	54.9	67.9	84.0
57.7	0.15	4313	5335	6599	8383	10369	12826	2.89%	2.15%	1.59%	54.8	67.8	83.9
42.0	0.15	4313	5335	6599	8383	10369	12826	2.89%	2.15%	1.59%	54.8	67.8	83.9
26.2	0.15	4313	5335	6599	8383	10369	12826	2.89%	2.15%	1.59%	54.8	67.8	83.9
10.5	0.15	4313	5335	6599	8383	10369	12826	2.89%	2.15%	1.59%	54.8	67.8	83.9
-5.2	0.15	4313	5335	6599	8383	10369	12826	2.89%	2.15%	1.59%	54.8	67.8	83.9
-21.0	0.15	4313	5335	6599	8383	10369	12826	2.89%	2.15%	1.59%	54.8	67.8	83.9
-36.7	0.15	4313	5335	6599	8383	10369	12826	2.89%	2.15%	1.59%	54.8	67.8	83.9
-52.4	0.15	4312	5333	6596	8381	10366	12820	2.91%	2.16%	1.60%	54.8	67.8	83.9
-68.1	0.15	4312	5333	6596	8381	10366	12820	2.91%	2.16%	1.60%	54.8	67.8	83.9
-83.9	0.15	4312	5333	6596	8381	10366	12820	2.91%	2.16%	1.60%	54.8	67.8	83.9
-99.6	0.15	4312	5333	6596	8381	10366	12820	2.91%	2.16%	1.60%	54.8	67.8	83.9
-115.3	0.15	4312	5333	6596	8381	10366	12820	2.91%	2.16%	1.60%	54.8	67.8	83.9
-131.1	0.15	4312	5333	6596	8381	10366	12820	2.91%	2.16%	1.60%	54.8	67.8	83.9
-146.8	0.15	4312	5333	6596	8381	10366	12820	2.91%	2.16%	1.60%	54.8	67.8	83.9

Table 3LL-8

ESWPT Rock Subgrade Profile and Passing Frequencies (Sheet 5 of 5)

CPNPP 3 & 4 Rock Subgrade Properties													
Elev. (ft)	Unit Weight (lb/ft^3)	Vs (ft/sec)			Vp (ft/sec)			Damping			Passing Frequency (Hz)		
		ELB	EBE	EUB	ELB	EBE	EUB	ELB	EBE	EUB	ELB	EBE	EUB
-162.5	0.15	4311	5331	6592	8380	10362	12812	2.93%	2.17%	1.61%	54.8	67.8	83.8
-178.2	0.15	4311	5331	6592	8380	10362	12812	2.93%	2.17%	1.61%	54.8	67.8	83.8
-194.0	0.15	4311	5331	6592	8380	10362	12812	2.93%	2.17%	1.61%	54.8	67.8	83.8
-209.7	0.15	4311	5331	6592	8380	10362	12812	2.93%	2.17%	1.61%	54.8	67.8	83.8
-225.4	0.15	4311	5331	6592	8380	10362	12812	2.93%	2.17%	1.61%	54.8	67.8	83.8
-241.2	0.15	4311	5331	6592	8380	10362	12812	2.93%	2.17%	1.61%	54.8	67.8	83.8
-256.9	0.15	4311	5331	6592	8380	10362	12812	2.93%	2.17%	1.61%	54.8	67.8	83.8

Table 3LL-9

ESWPT Backfill Soil Profile and Passing Frequencies- Nominal GWL

CPNPP 3 & 4 Backfill Properties with Nominal GWL EL. 795'																		
Layer	Thick. (ft)	Unit Weight (lb/ft^3)	Vs (ft/sec)				Vp (ft/sec)				Damping				Passing Frequency (Hz)			
			ELB	EBE	EUB	EHB	ELB	EBE	EUB	EHB	ELB	EBE	EUB	EHB	ELB	EBE	EUB	EHB
1	1.5	0.125	503	653	846	1098	1047	1358	1762	2286	2.82%	1.68%	1.00%	0.59%	67.1	87.0	112.9	146.4
2	1.5	0.125	503	653	846	1098	1047	1358	1762	2286	2.82%	1.68%	1.00%	0.59%	67.1	87.0	112.9	146.4
3	2.125	0.125	571	763	1020	1363	1189	1589	2123	2836	3.48%	2.07%	1.23%	0.73%	53.8	71.8	96.0	128.2
4	2.125	0.125	571	763	1020	1363	1189	1589	2123	2836	3.48%	2.07%	1.23%	0.73%	53.8	71.8	96.0	128.2
5	2.125	0.125	551	747	1012	1372	1147	1555	2107	2855	4.36%	2.56%	1.50%	0.88%	51.9	70.3	95.3	129.1
6	2.125	0.125	551	747	1012	1372	1147	1555	2107	2855	4.36%	2.56%	1.50%	0.88%	51.9	70.3	95.3	129.1
7	1.4167	0.125	533	732	1004	1379	1109	1523	2091	2870	5.14%	2.98%	1.72%	1.00%	75.2	103.3	141.8	194.6
8	1.4167	0.125	533	732	1004	1379	1109	1523	2091	2870	5.14%	2.98%	1.72%	1.00%	75.2	103.3	141.8	194.6
9	1.4167	0.125	533	732	1004	1379	1109	1523	2091	2870	5.14%	2.98%	1.72%	1.00%	75.2	103.3	141.8	194.6
10	1.224	0.125	518	719	997	1382	1079	1496	2075	2878	5.78%	3.33%	1.91%	1.10%	84.7	117.4	162.9	225.9
11	2.274	0.125	518	719	997	1382	1079	1496	2075	2878	5.78%	3.33%	1.91%	1.10%	45.6	63.2	87.7	121.6
12	2.6675	0.125	628	860	1178	1614	1306	1790	2452	3360	4.50%	2.59%	1.49%	0.86%	47.0	64.5	88.3	121.0
13	2.6675	0.125	684	932	1269	1727	1424	1939	2641	3596	3.99%	2.30%	1.33%	0.77%	51.3	69.8	95.1	129.5
14	2.4175	0.125	678	926	1265	1728	1411	1928	2634	3599	4.23%	2.44%	1.41%	0.81%	56.0	76.6	104.6	142.9
15	2.9175	0.125	676	924	1264	1728	3448	4714	6445	8811	4.29%	2.47%	1.42%	0.82%	46.3	63.4	86.6	118.5
16	2.52	0.125	669	918	1260	1729	3411	4681	6424	8815	4.56%	2.61%	1.50%	0.86%	53.1	72.9	100.0	137.2
17	2.52	0.125	669	918	1260	1729	3410	4680	6423	8815	4.57%	2.62%	1.50%	0.86%	53.1	72.8	100.0	137.2
18	2.52	0.125	663	912	1256	1729	3379	4652	6405	8817	4.80%	2.74%	1.57%	0.89%	52.6	72.4	99.7	137.2
19	2.52	0.125	663	912	1256	1729	3379	4652	6404	8817	4.80%	2.74%	1.57%	0.89%	52.6	72.4	99.7	137.2

Table 3LL-10

ESWPT Backfill Soil Profile- High GWL

CPNPP 3 & 4 Backfill Properties with High GWL EL. 804'														
Layer	Thick. (ft)	Unit Weight (lb/ft^3)	Vs (ft/sec)				Vp (ft/sec)				Damping			
			ELB	EBE	EUB	EHB	ELB	EBE	EUB	EHB	ELB	EBE	EUB	EHB
1	1.5	0.125	503	653	846	1098	1047	1358	1762	2286	2.82%	1.68%	1.00%	0.59%
2	1.5	0.125	503	653	846	1098	1047	1358	1762	2286	2.82%	1.68%	1.00%	0.59%
3	2.125	0.125	571	763	1020	1363	1189	1589	2123	2836	3.48%	2.07%	1.23%	0.73%
4	2.125	0.125	571	763	1020	1363	1189	1589	2123	2836	3.48%	2.07%	1.23%	0.73%
5	2.125	0.125	551	747	1012	1372	1147	1555	2107	2855	4.36%	2.56%	1.50%	0.88%
6	2.125	0.125	551	747	1012	1372	1147	1555	2107	2855	4.36%	2.56%	1.50%	0.88%
7	1.4167	0.125	533	732	1004	1379	1109	1523	2091	2870	5.14%	2.98%	1.72%	1.00%
8	1.4167	0.125	533	732	1004	1379	1109	1523	2091	2870	5.14%	2.98%	1.72%	1.00%
9	1.4167	0.125	533	732	1004	1379	1109	1523	2091	2870	5.14%	2.98%	1.72%	1.00%
10	1.225	0.125	518	719	997	1382	1079	1496	2075	2878	5.78%	3.33%	1.91%	1.10%
11	2.274	0.125	518	719	997	1382	1079	1496	2075	2878	5.78%	3.33%	1.91%	1.10%
12	2.6675	0.125	628	860	1178	1614	3199	4384	6007	8230	4.50%	2.59%	1.49%	0.86%
13	2.6675	0.125	684	932	1269	1727	3488	4750	6468	8808	3.99%	2.30%	1.33%	0.77%
14	2.4175	0.125	678	926	1265	1728	3454	4720	6449	8811	4.23%	2.44%	1.41%	0.81%
15	2.9175	0.125	676	924	1264	1728	3448	4714	6445	8811	4.29%	2.47%	1.42%	0.82%
16	2.52	0.125	669	918	1260	1729	3411	4681	6424	8815	4.56%	2.61%	1.50%	0.86%
17	2.52	0.125	669	918	1260	1729	3410	4680	6423	8815	4.57%	2.62%	1.50%	0.86%
18	2.52	0.125	663	912	1256	1729	3379	4652	6405	8817	4.80%	2.74%	1.57%	0.89%
19	2.52	0.125	663	912	1256	1729	3379	4652	6404	8817	4.80%	2.74%	1.57%	0.89%

Table 3LL-11

ESWPT Backfill Soil Profile- Unsaturated

CPNPP 3 & 4 Unsaturated Backfill Properties														
Layer	Thick. (ft)	Unit Weight	Vs (ft/sec)				Vp (ft/sec)				Damping			
		(lb/ft^3)	ELB	EBE	EUB	EHB	ELB	EBE	EUB	EHB	ELB	EBE	EUB	EHB
1	1.5	0.125	503	653	846	1098	1047	1358	1762	2286	2.82%	1.68%	1.00%	0.59%
2	1.5	0.125	503	653	846	1098	1047	1358	1762	2286	2.82%	1.68%	1.00%	0.59%
3	2.125	0.125	571	763	1020	1363	1189	1589	2123	2836	3.48%	2.07%	1.23%	0.73%
4	2.125	0.125	571	763	1020	1363	1189	1589	2123	2836	3.48%	2.07%	1.23%	0.73%
5	2.125	0.125	551	747	1012	1372	1147	1555	2107	2855	4.36%	2.56%	1.50%	0.88%
6	2.125	0.125	551	747	1012	1372	1147	1555	2107	2855	4.36%	2.56%	1.50%	0.88%
7	1.4167	0.125	533	732	1004	1379	1109	1523	2091	2870	5.14%	2.98%	1.72%	1.00%
8	1.4167	0.125	533	732	1004	1379	1109	1523	2091	2870	5.14%	2.98%	1.72%	1.00%
9	1.4167	0.125	533	732	1004	1379	1109	1523	2091	2870	5.14%	2.98%	1.72%	1.00%
10	1.225	0.125	518	719	997	1382	1079	1496	2075	2878	5.78%	3.33%	1.91%	1.10%
11	2.274	0.125	518	719	997	1382	1079	1496	2075	2878	5.78%	3.33%	1.91%	1.10%
12	2.6675	0.125	628	860	1178	1614	1306	1790	2452	3360	4.50%	2.59%	1.49%	0.86%
13	2.6675	0.125	684	932	1269	1727	1424	1939	2641	3596	3.99%	2.30%	1.33%	0.77%
14	2.4175	0.125	678	926	1265	1728	1410	1927	2633	3597	4.23%	2.44%	1.41%	0.81%
15	2.9175	0.125	676	924	1264	1728	1407	1924	2631	3597	4.29%	2.47%	1.42%	0.82%
16	2.52	0.125	669	918	1260	1729	1393	1911	2622	3599	4.56%	2.61%	1.50%	0.86%
17	2.52	0.125	669	918	1260	1729	1392	1911	2622	3599	4.57%	2.62%	1.50%	0.86%
18	2.52	0.125	663	912	1256	1729	1380	1899	2615	3599	4.80%	2.74%	1.57%	0.89%
19	2.52	0.125	663	912	1256	1729	1379	1899	2615	3600	4.80%	2.74%	1.57%	0.89%

Table 3LL-12

ESWPT SASSI FE Model Maximum Nodal Accelerations[1][2] in the N-S Direction (Y) (g)

Component	Nominal GWL				High GWL				Unsaturated	Max Accel.
	ELB	EBE	EUB	EHB	ELB	EBE	EUB	EHB		(g)
Roof	0.12	0.11	0.12	0.12	0.10	0.11	0.11	0.13	0.13	0.13
Basemat	0.09	0.10	0.11	0.10	0.09	0.10	0.11	0.11	0.09	0.11
Interior Wall	0.12	0.11	0.12	0.12	0.10	0.11	0.11	0.12	0.13	0.13
Exterior Walls	0.10	0.11	0.12	0.12	0.10	0.11	0.11	0.13	0.13	0.13

Notes:

1) Maximum accelerations are taken as the envelope of Tunnel Segment 1aN, 1aS, and 1bS nodal accelerations (ZPA).

2) For structural design using the loads and load combinations in Section 3.8, the seismic demands are calculated in ANSYS using the maximum accelerations as quasi-static gravity loads and combining them with the demands calculated in ANSYS by applying an equivalent static seismic soil pressure.

3) Values presented in this table are not adjusted for SSSI effects.

Table 3LL-13

ESWPT SASSI FE Model Maximum Nodal Accelerations[(1)(2)] in the E-W Direction (X) (g)

Component	Nominal GWL				High GWL				Unsaturated	Max Accel.
	ELB	EBE	EUB	EHB	ELB	EBE	EUB	EHB		(g)
Roof	0.11	0.12	0.13	0.14	0.11	0.12	0.14	0.14	0.11	0.14
Basemat	0.10	0.11	0.10	0.12	0.10	0.11	0.10	0.12	0.10	0.12
Interior Wall	0.11	0.12	0.13	0.14	0.11	0.12	0.14	0.14	0.11	0.14
Exterior Walls	0.11	0.12	0.13	0.14	0.11	0.12	0.14	0.14	0.11	0.14

Notes:

1. Maximum accelerations are taken as the envelope of Tunnel Segment 1aN, 1aS, and 1bS nodal accelerations (ZPA).

2. For structural design using the loads and load combinations in Section 3.8, the seismic demands are calculated in ANSYS using the maximum accelerations as quasi-static gravity loads and combining them with the demands calculated in ANSYS by applying an equivalent static seismic soil pressure.

3. Values presented in this table are not adjusted for SSSI effects.

Table 3LL-14

ESWPT SASSI FE Model Maximum Nodal Accelerations(1)(2) in the Vertical Direction (Z) (g)

Component	Nominal GWL				High GWL				Unsaturated	Max Accel.
	ELB	EBE	EUB	EHB	ELB	EBE	EUB	EHB		(g)
Roof	0.11	0.12	0.13	0.13	0.11	0.13	0.15	0.19	0.10	0.19
Basemat	0.10	0.11	0.12	0.12	0.10	0.11	0.12	0.13	0.10	0.13
Interior Wall	0.10	0.11	0.12	0.13	0.11	0.11	0.13	0.15	0.10	0.15
Exterior Walls	0.10	0.11	0.12	0.12	0.10	0.11	0.12	0.14	0.10	0.14

Notes:

1) Maximum accelerations are taken as the envelope of Tunnel Segment 1aN, 1aS, and 1bS nodal accelerations (ZPA).

2) For structural design using the loads and load combinations in Section 3.8, the seismic demands are calculated in ANSYS using the maximum accelerations as quasi-static gravity loads and combining them with the demands calculated in ANSYS by applying an equivalent static seismic soil pressure.

3) Values presented in this table are not adjusted for SSSI effects.

Table 3LL-15

Amplification Factors for Design Basis Maximum Accelerations (ZPA)

Tunnel Segment	Roof			Basement		
	NS	EW	V	NS	EW	V
ESWPT 1aN	1.2	1.2	1.1	1.2	1.1	1.0
ESWPT 1aS and 1bS	1.2	1.0	1.3	1.1	1.0	1.0

Table 3LL-16

Detailed ANSYS FE Model Maximum Seismic Design Forces and Moments

Tunnel Component	Design Demand	M (kip-ft/ft)	V (kip/ft)	T (kip/ft)
Roof Slab	Maximum Moment for NS and EW Rebar (both faces) – Compression not considered	62.5	-	-
	Maximum Tension and Corresponding Moment in EW dir.	16	-	113
	Maximum Out-of-Plane Shear	-	25	-
Basemat Slab	Maximum Moment for NS and EW Bottom Rebar – Compression not considered	65	-	-
	Maximum Moment for NS and EW Top Rebar – Tension is considered	44	-	22
	Maximum Out-of-Plane Shear	-	7	-
Exterior Walls	Maximum Moment for Vertical Rebar – Compression not considered	71	-	-
	Maximum Moment for Horizontal Rebar - Tension is considered	43.5	-	105
	Maximum Out-of-Plane Shear	-	20	-
	Maximum In-Plane Shear - NS dir.	-	13.3	-
	Maximum In-Plane Shear - EW dir. (1aS)	-	21.4	-
	Maximum In-Plane Shear - EW dir. (1bS)	-	18.2	-
Interior Wall	Maximum Moment for Vertical Rebar – Compression not considered	19	-	-
	Maximum Moment for Horizontal Rebar – Tension is considered	4	-	5
	Maximum Out-of-Plane Shear	-	7	-
	Maximum In-Plane Shear - NS dir.	-	6.4	-
	Maximum In-Plane Shear - EW dir. (1aS)	-	10.3	-
	Maximum In-Plane Shear - EW dir. (1bS)	-	8.5	-

Notes:

1) The forces and moments shown above include maximum absolute values of forces and moments due to seismic soil pressure that envelop all four subgrade shear wave velocity conditions (ELB, EBE, EUB, and EHB) for Tunnel Segments 1aN, 1bN, and 1bS. The forces and moments are used for structural design as described in Section 3.8.

Table 3LL-17

ESWPT Maximum Seismic Displacements for All Enveloped Conditions(1)

Tunnel	Nominal GWL				High GWL				Unsaturated	Max. Rel.
Segment	ELB	EBE	EUB	EHB	ELB	EBE	EUB	EHB	ELB	Displ. (in)
1aN	0.003564	0.003304	0.003194	0.002942	0.003539	0.003294	0.003185	0.002949	0.003645	0.003645
1aS	0.003829	0.003709	0.003483	0.002819	0.003910	0.003723	0.003522	0.002872	0.003818	0.003910
1bS	0.003273	0.003474	0.003342	0.002745	0.003273	0.003462	0.003332	0.002756	0.003312	0.003474

Notes:

1) The reported values are maximum relative displacements obtained from the SSI analyses of the ESWPT along the height of typical sections of Tunnel Segments 1aN, 1aS and 1bS. The SRSS method was used to combine the relative displacements from all three directions of earthquake for determination of maximum nodal displacements.

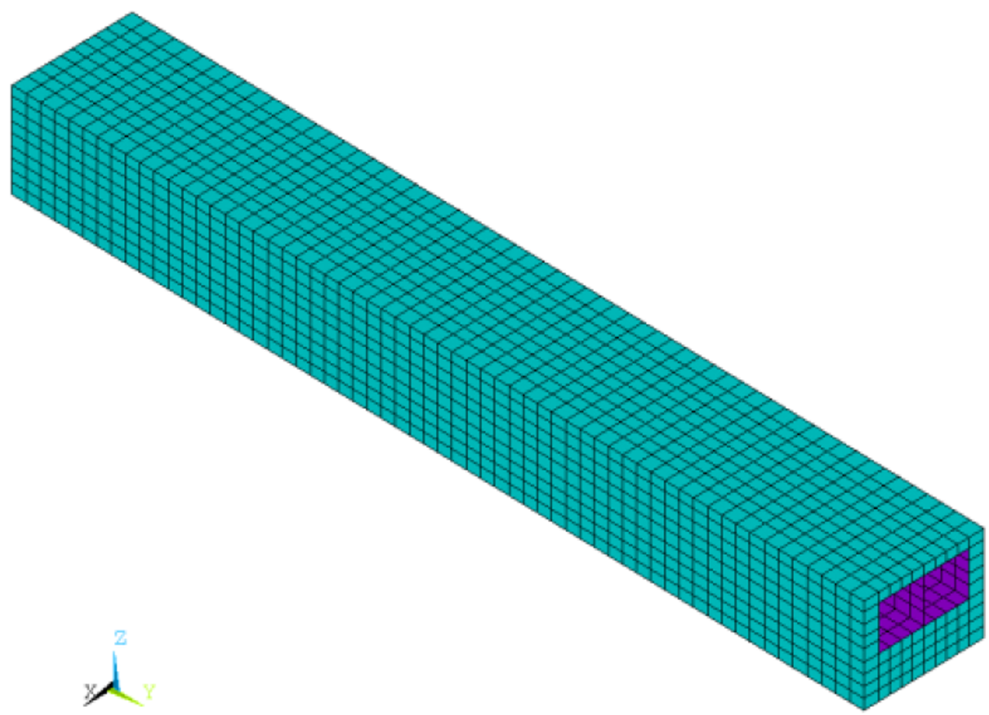

Figure 3LL-1 SASSI Model of ESWPT Segment 1aN- Structural Component

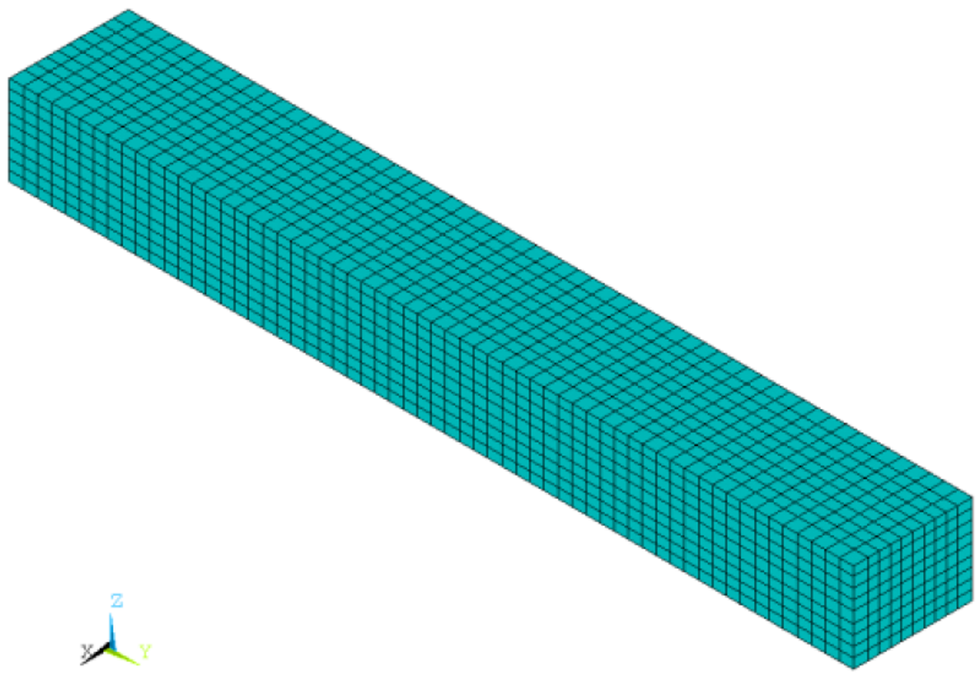

Figure 3LL-2 SASSI Model of ESWPT Segment 1aN- Excavated Volume

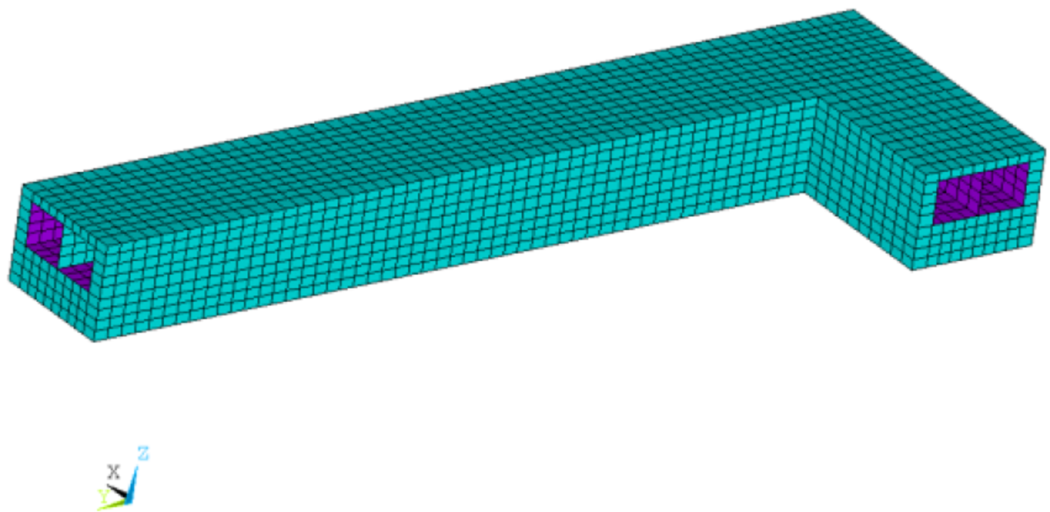

Figure 3LL-3 SASSI Model of ESWPT Segment 1aS- Structural Component

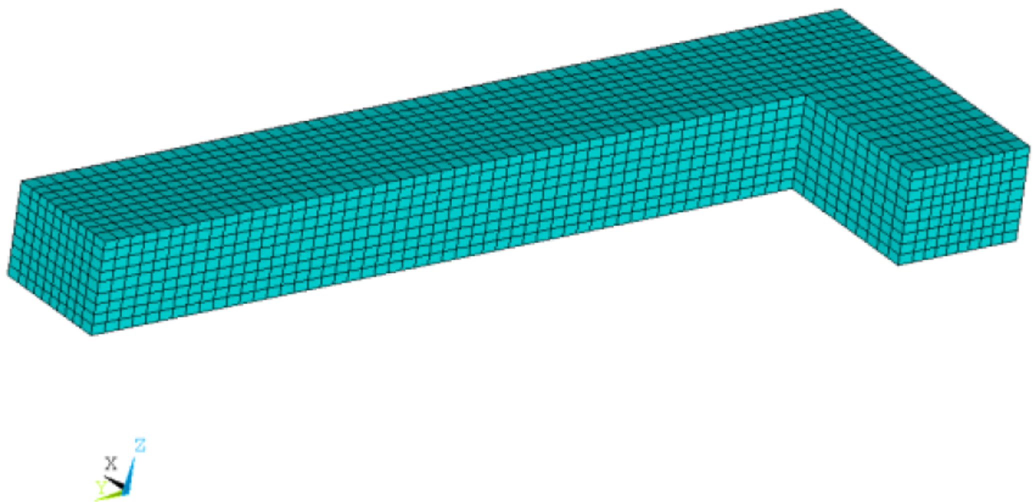

Figure 3LL-4 SASSI Model of ESWPT Segment 1aS Excavated Volume

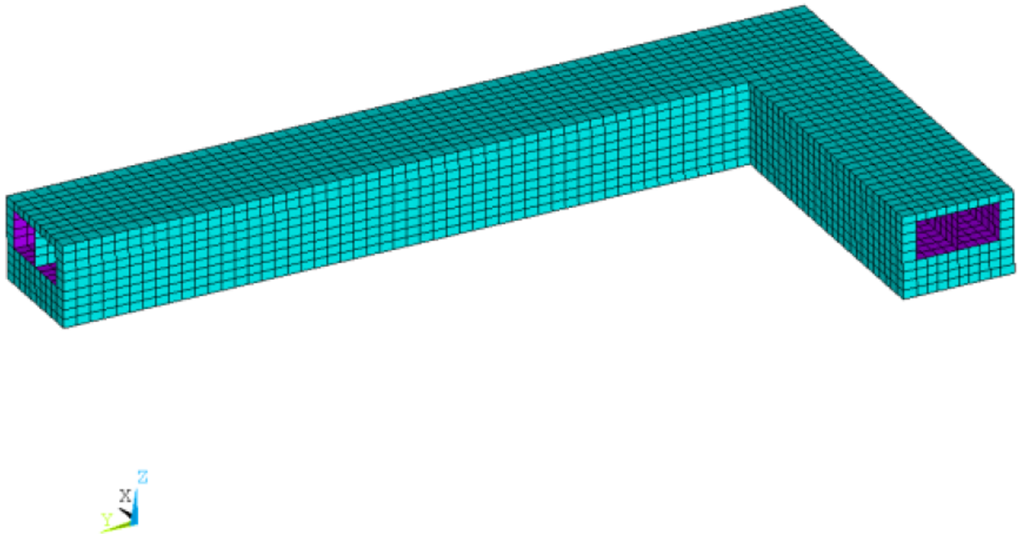

Figure 3LL-5 SASSI Model of ESWPT Segment 1bS- Structural Component

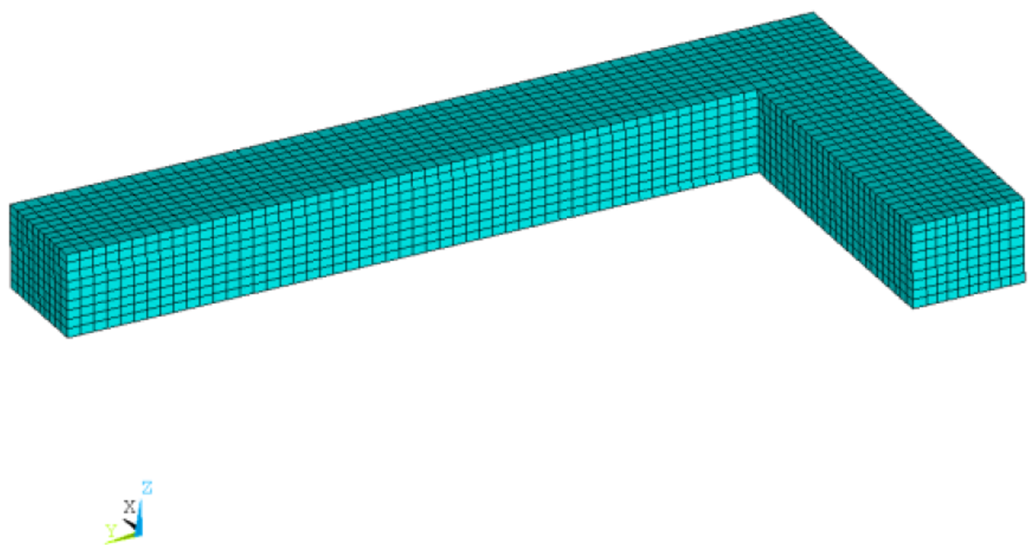

Figure 3LL-6 SASSI Model of ESWPT Segment 1bS Excavated Volume

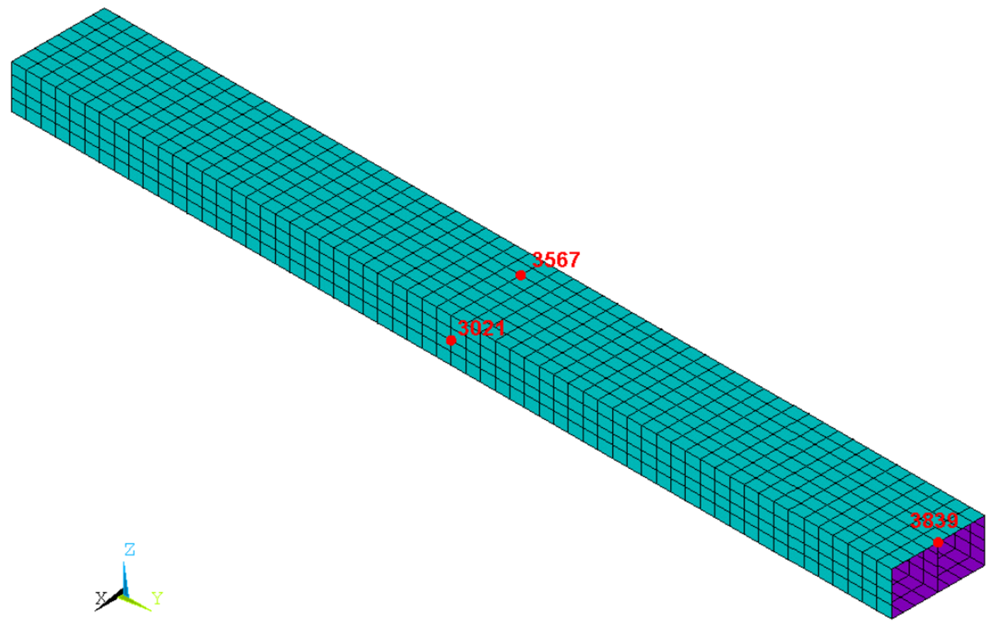

Figure 3LL-7 SASSI Model of ESWPT Segment 1aN- Validation Node Locations

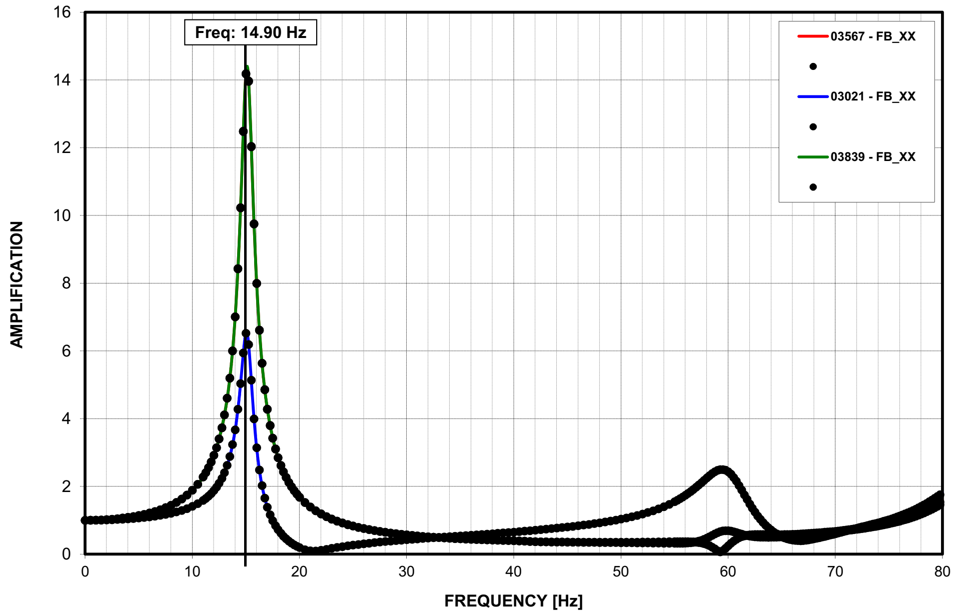

Figure 3LL-8 SASSI ATF Plot of Tunnel Segment 1aN-Longitudinal (X) Response

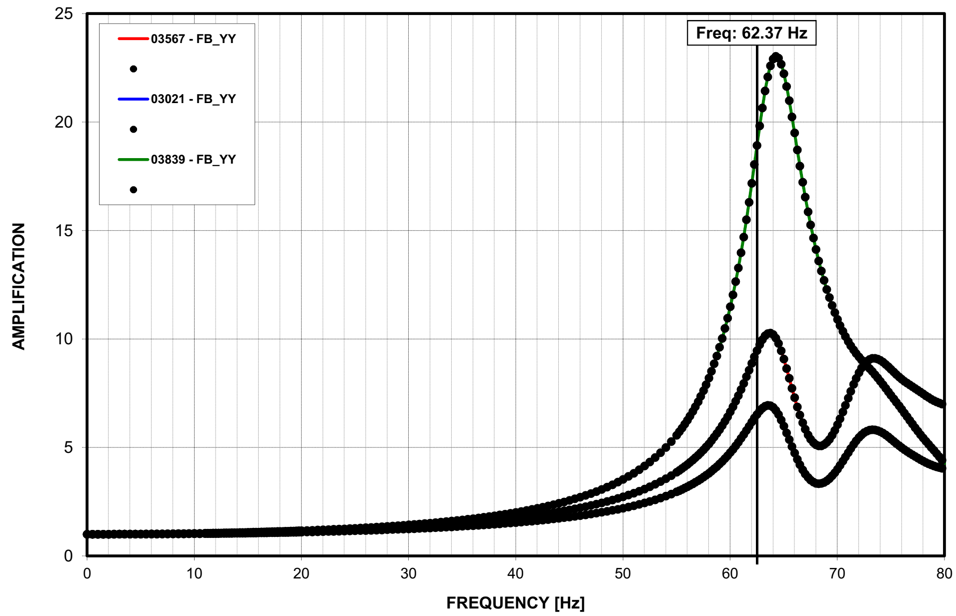

Figure 3LL-9 SASSI ATF Plot of Tunnel Segment 1aN- Longitudinal (Y) Response

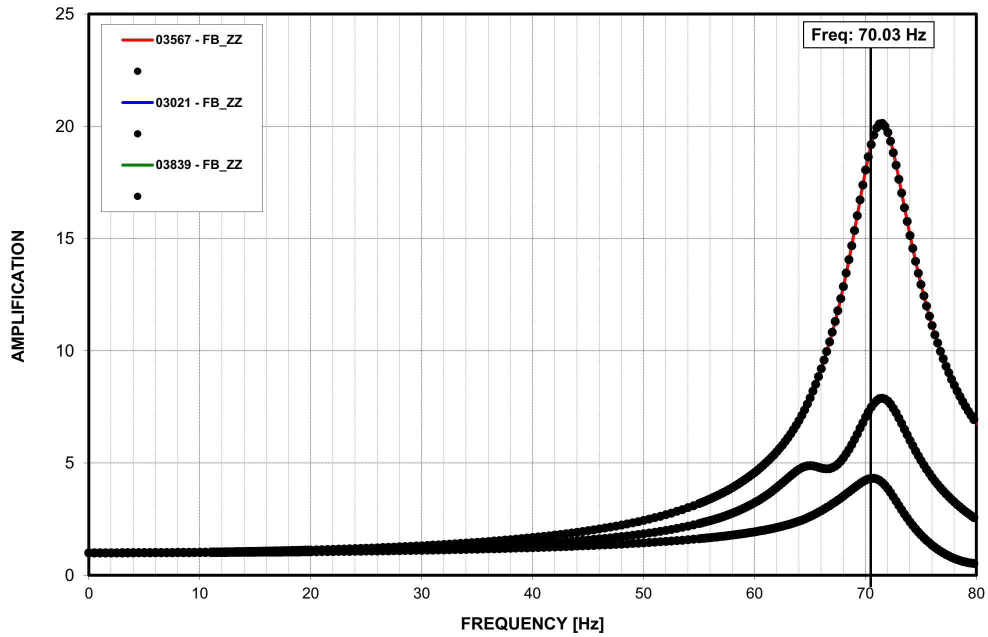

Figure 3LL-10 SASSI ATF Plot of Tunnel Segment 1aN- Vertical (Z) Response

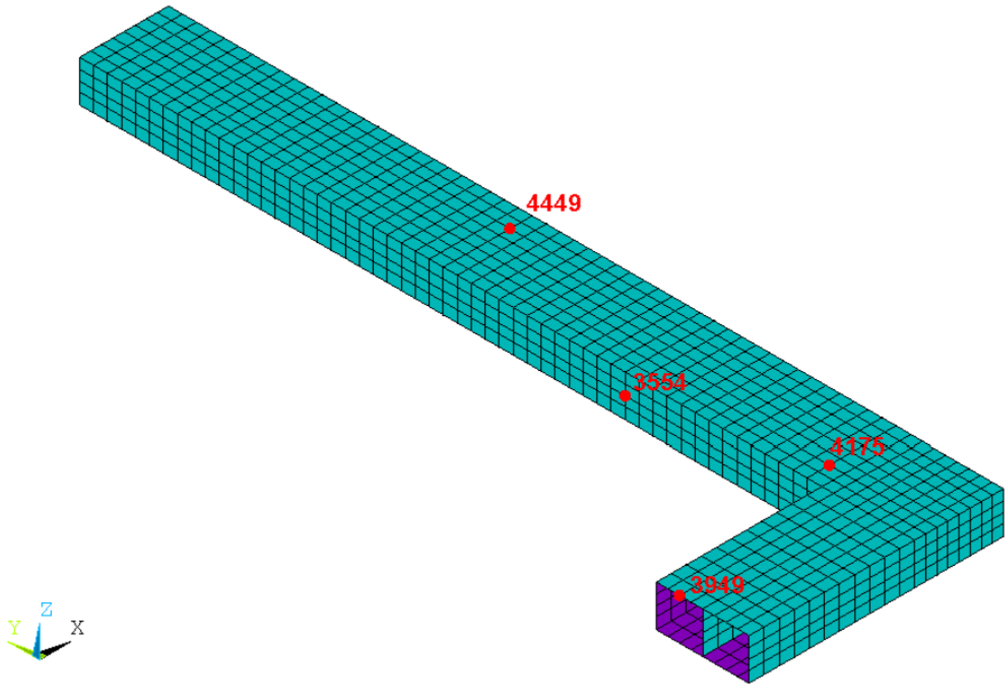

Figure 3LL-11 SASSI Model of ESWPT Segment 1aS-Validation Node Locations

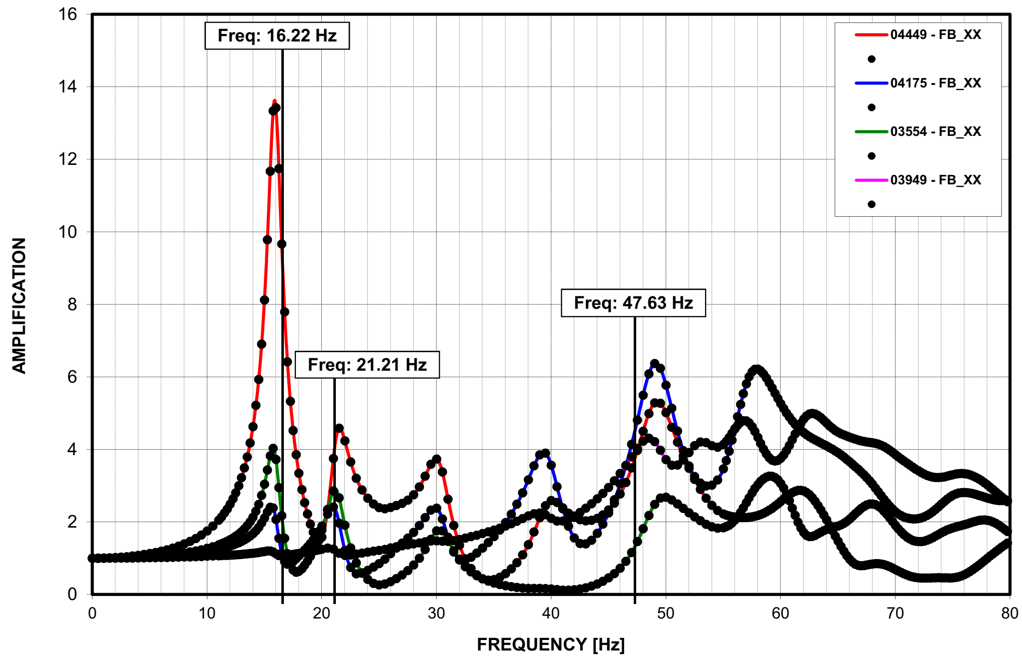

Figure 3LL-12 SASSI ATF Plot of Tunnel Segment 1aS-Transverse Response

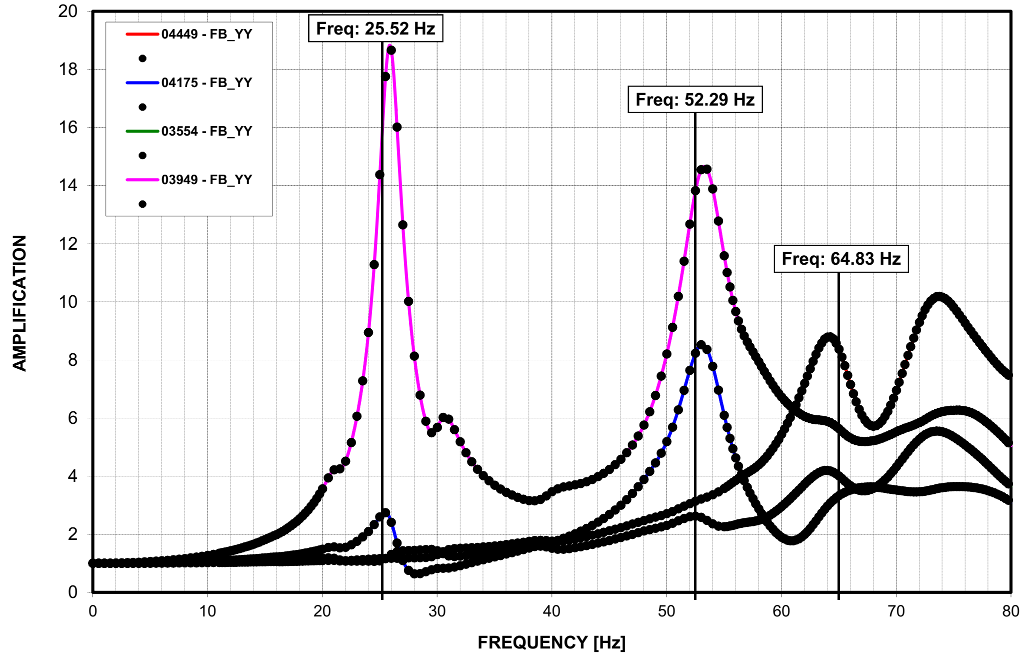

Figure 3LL-13 SASSI ATF Plot of Tunnel Segment 1aS-Longitudinal Response

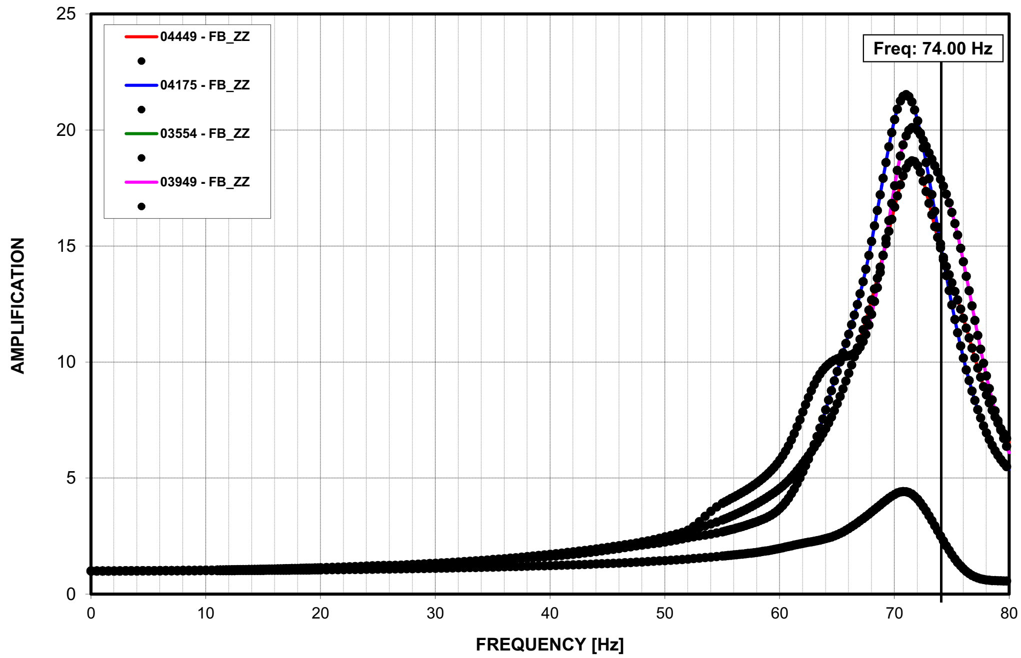

Figure 3LL-14 SASSI ATF Plot of Tunnel Segment 1aS-Vertical Response

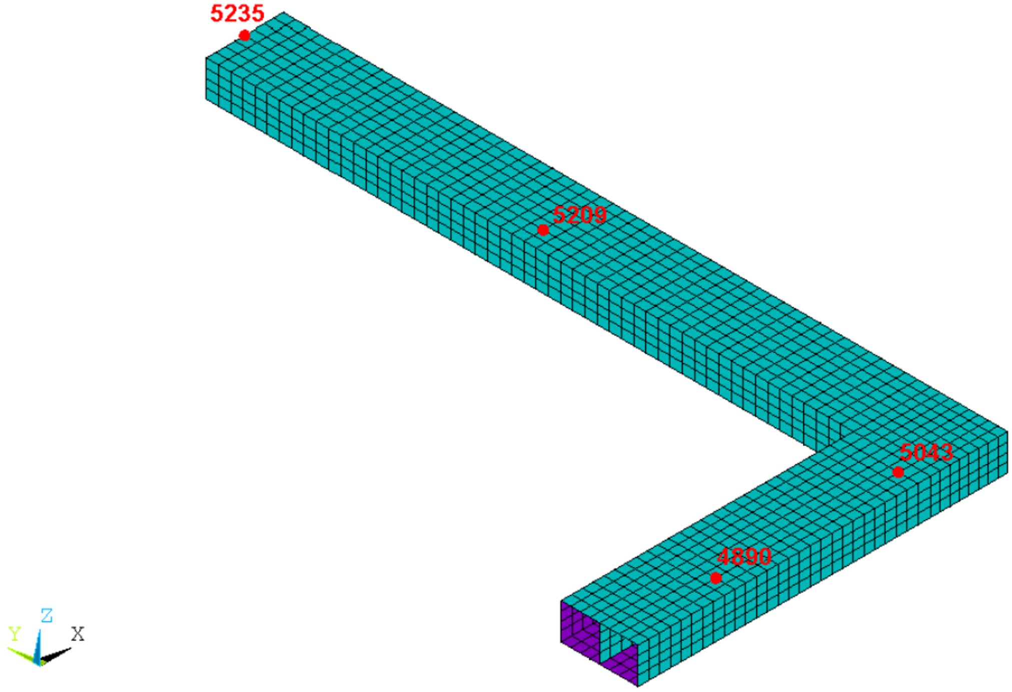

Figure 3LL-15 SASSI Model of ESWPT Segment 1bS-Validation Node Locations

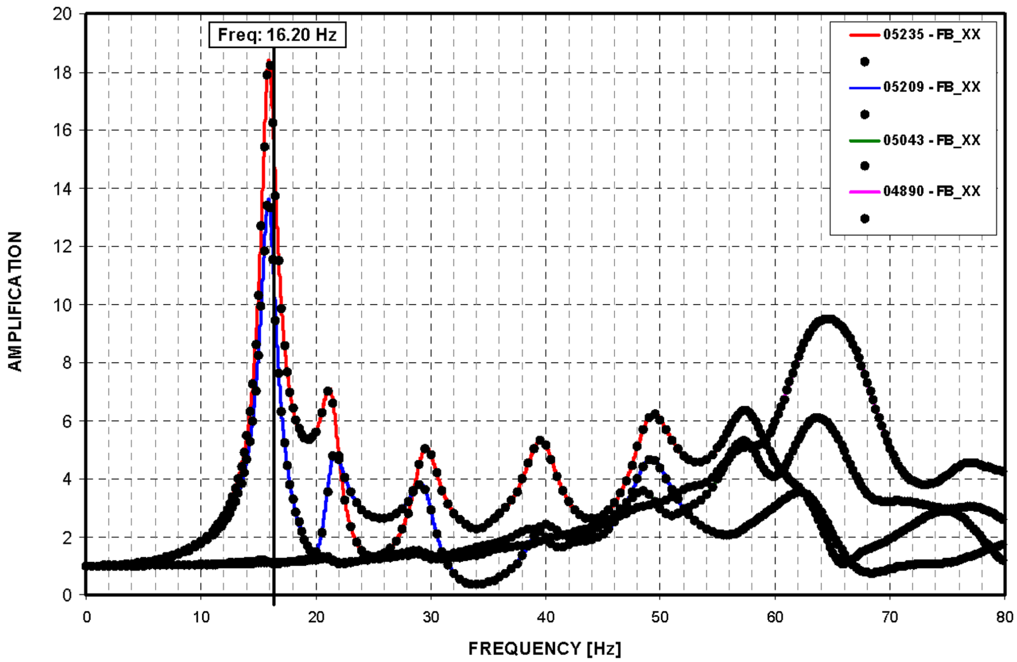

Figure 3LL-16 SASSI ATF Plot of Tunnel Segment 1bS-Transverse Response

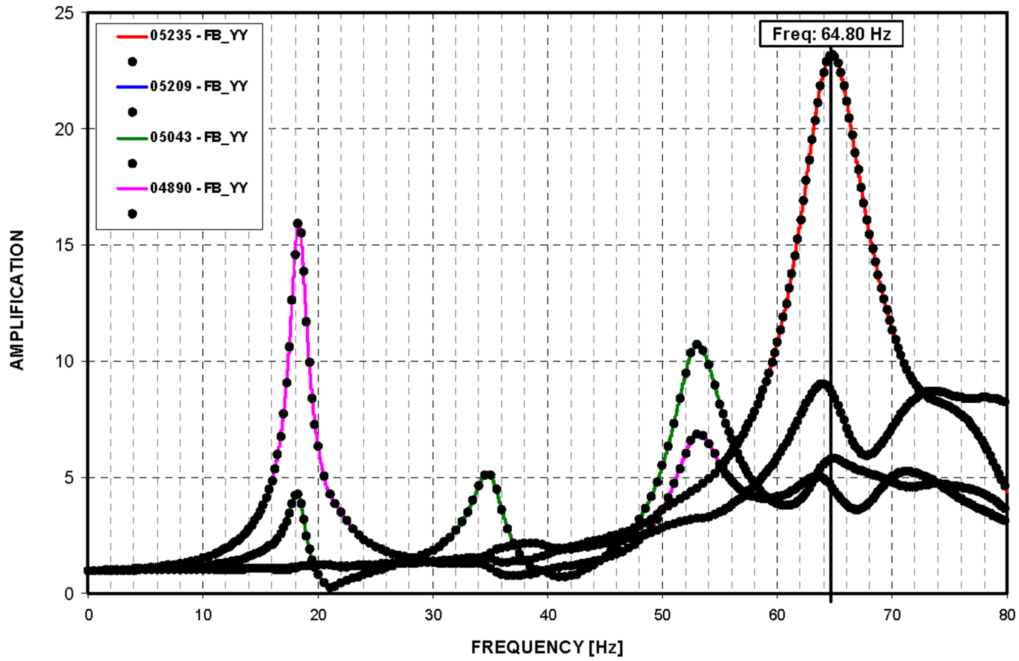

Figure 3LL-17 SASSI ATF Plot of Tunnel Segment 1bS-Longitudinal Response

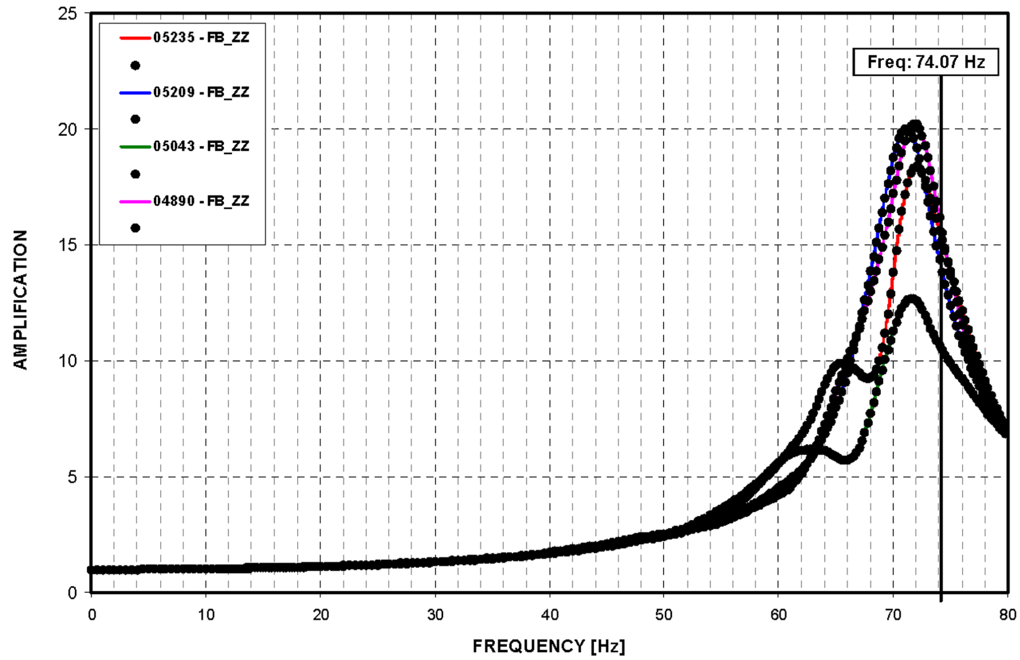

Figure 3LL-18 SASSI ATF Plot of Tunnel Segment 1bS-Vertical Response

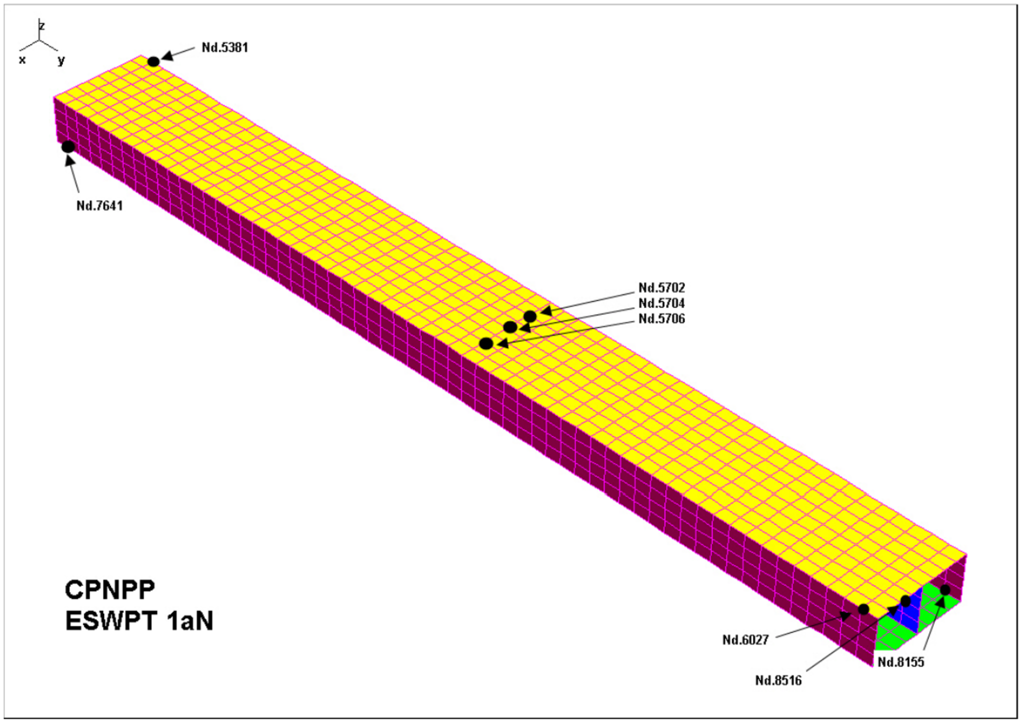

Figure 3LL-19 Key Nodes for Transfer Functions and Acceleration Response Spectra

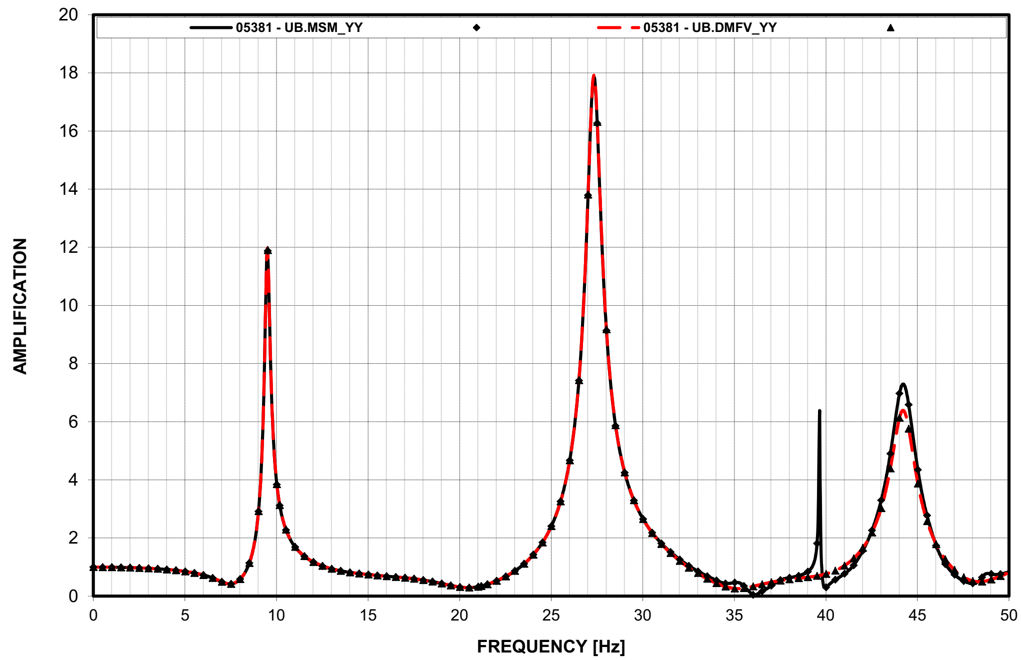

Figure 3LL-20 Transfer Function Comparison @ Node 5381 Y Direction; Y-Response

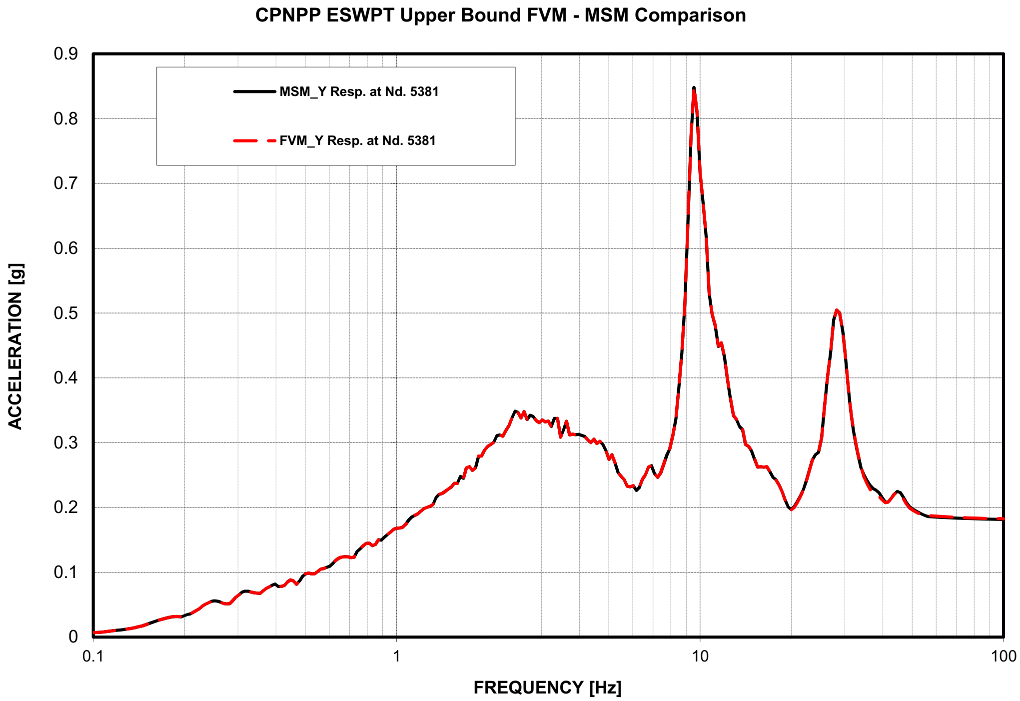

Figure 3LL-21 Acceleration Response Spectra Comparison @ Node 5381 Y Direction; Y-Response

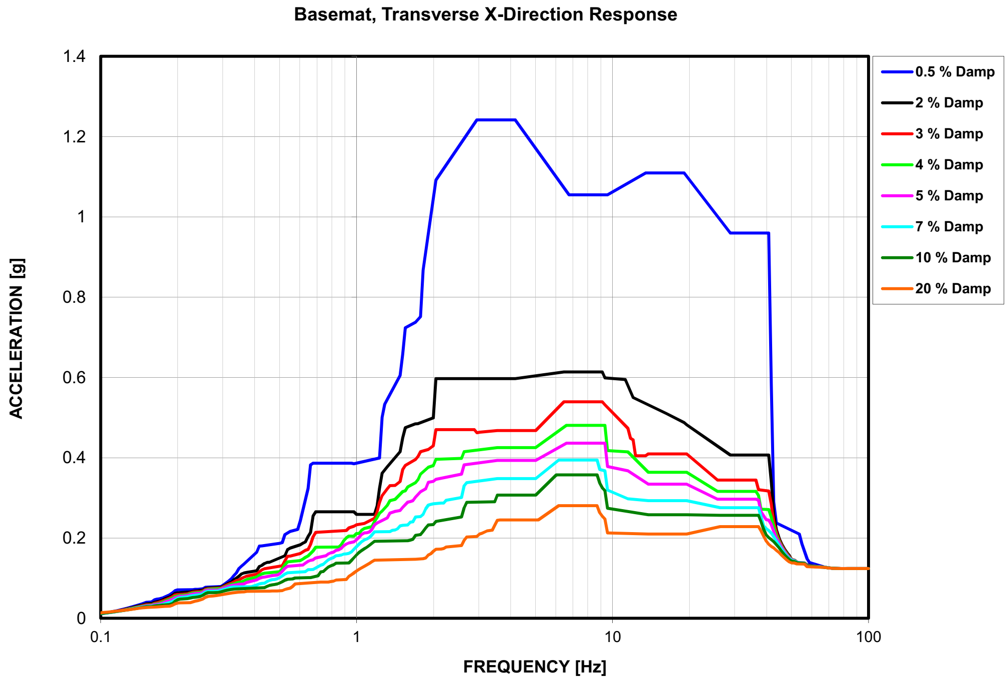

Figure 3LL-22 ISRS for ESWPT Basemat (Sheet 1 of 3)

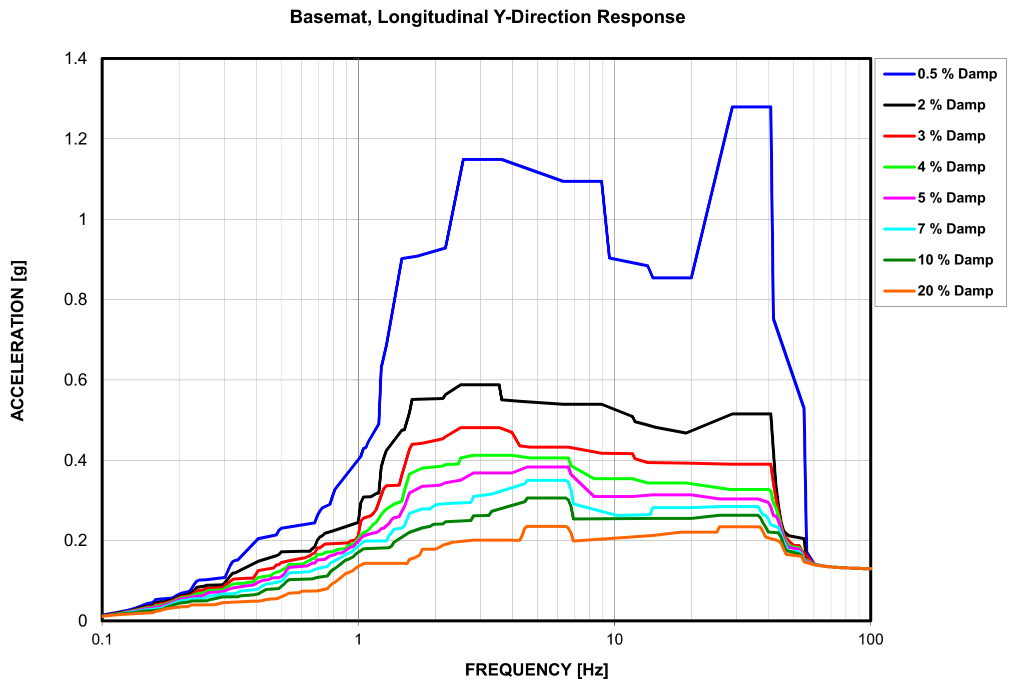

Figure 3LL-22 ISRS for ESWPT Basemat (Sheet 2 of 3)

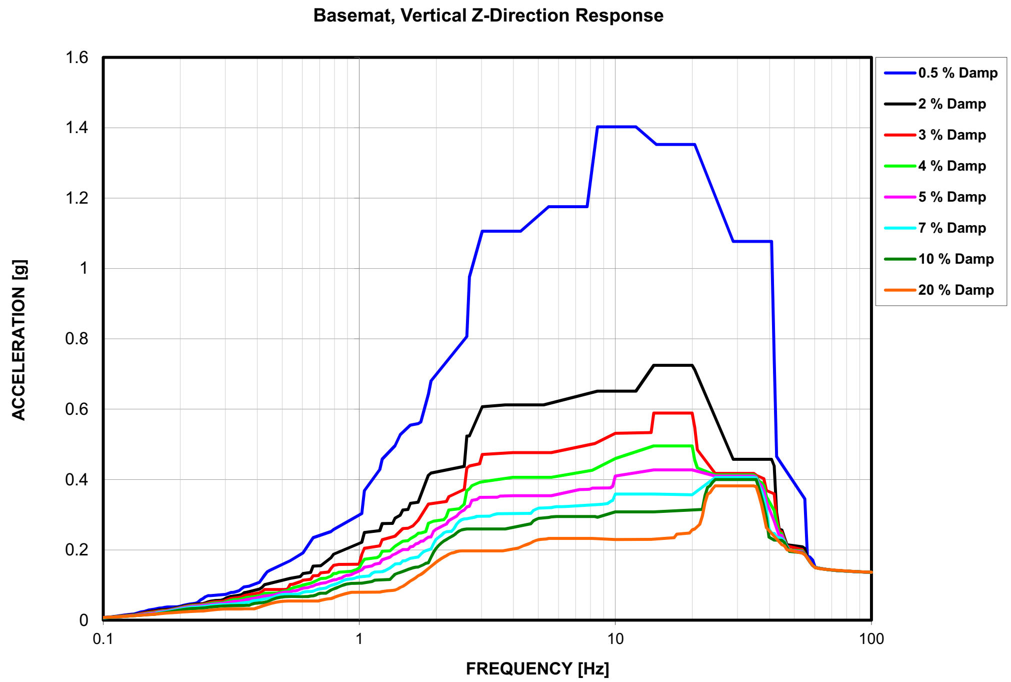

Figure 3LL-22 ISRS for ESWPT Basemat (Sheet 3 of 3)

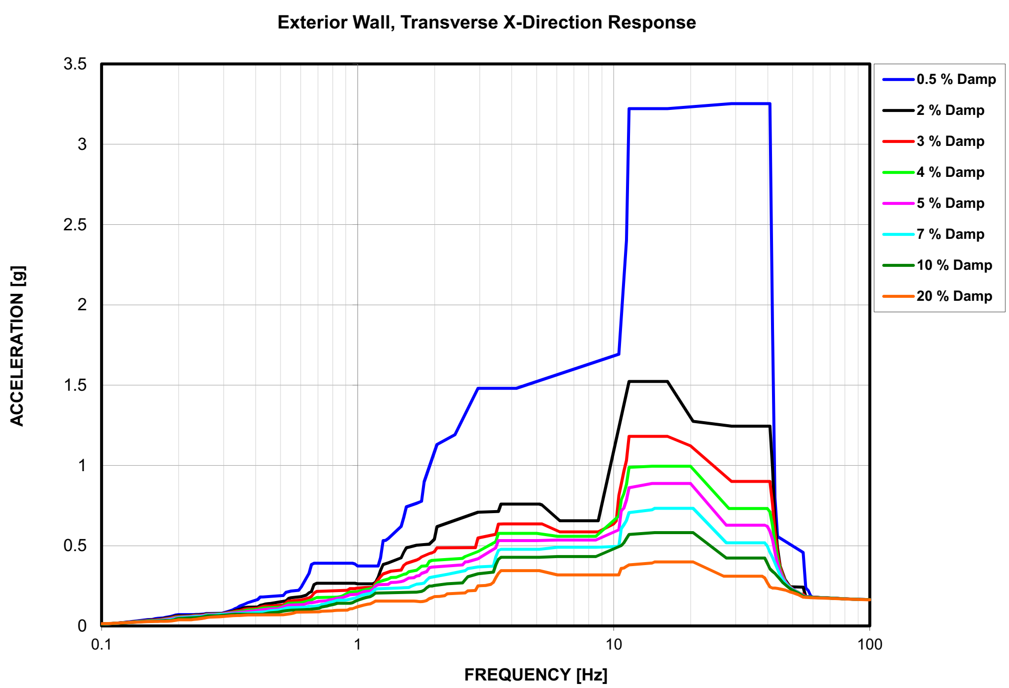

Figure 3LL-23 ISRS for ESWPT Exterior Walls (Sheet 1 of 3)

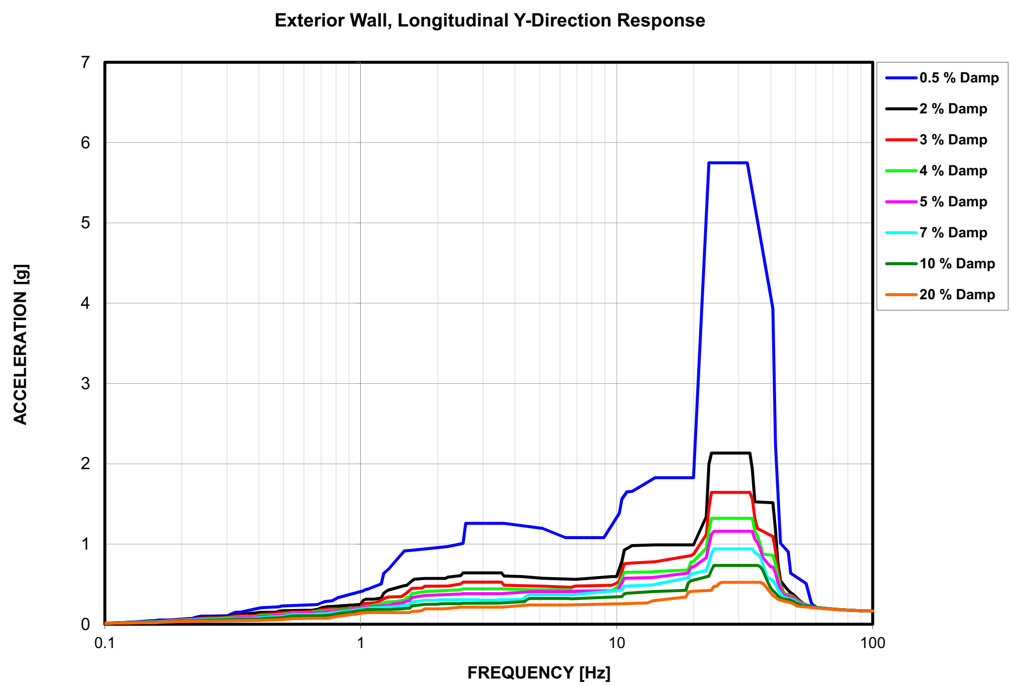

Figure 3LL-23 ISRS for ESWPT Exterior Walls (Sheet 2 of 3)

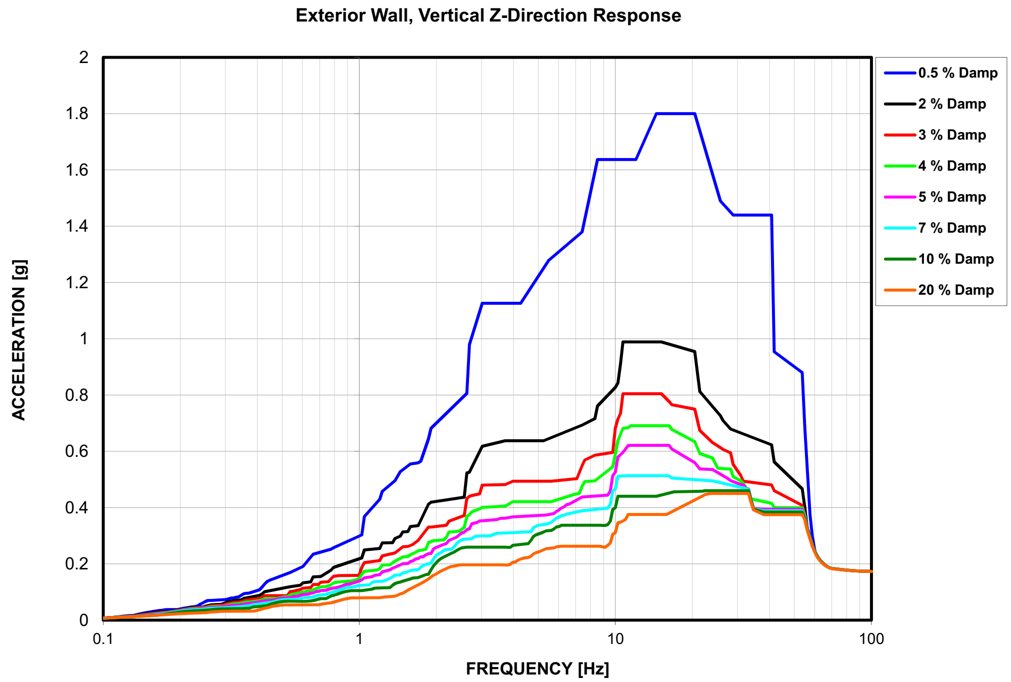

Figure 3LL-23 ISRS for ESWPT Exterior Walls (Sheet 3 of 3)

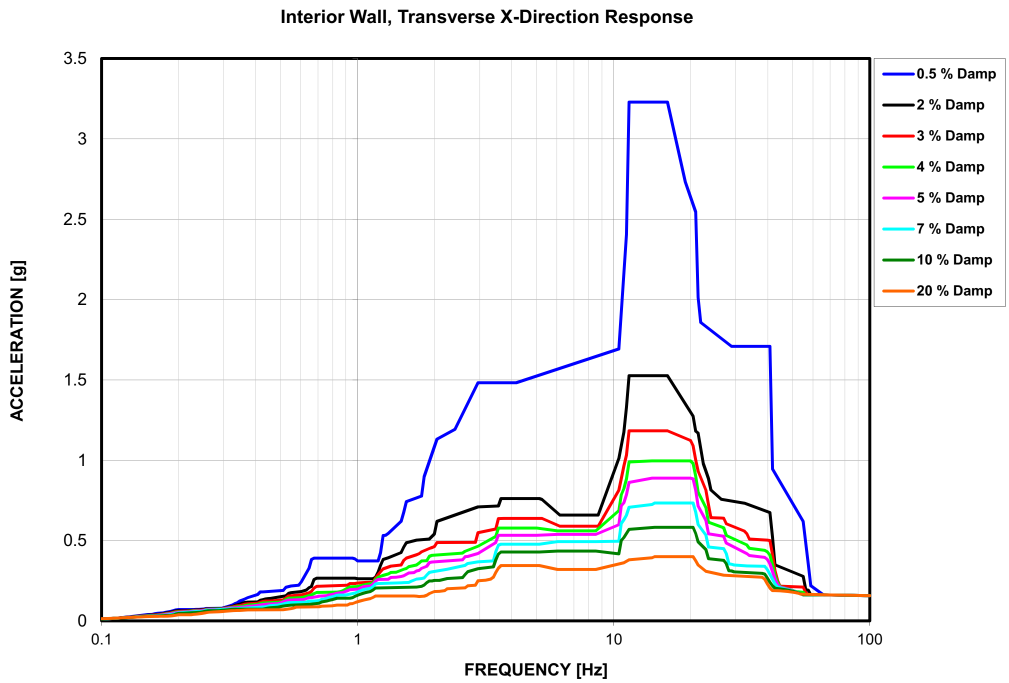

Figure 3LL-24 ISRS for ESWPT Interior Walls (Sheet 1 of 3)

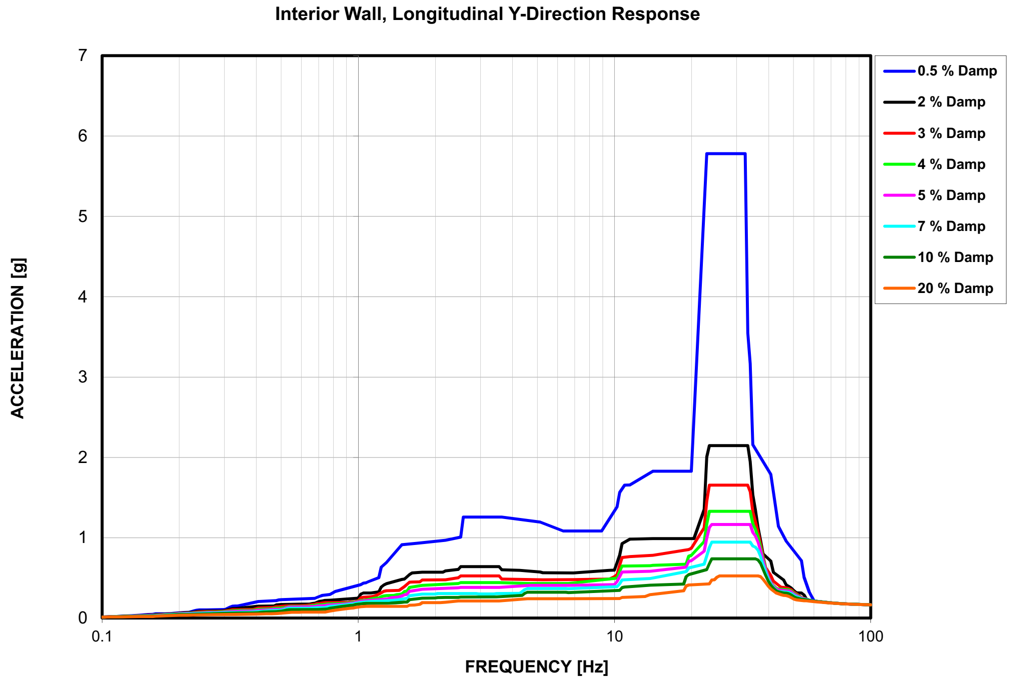

Figure 3LL-24 ISRS for ESWPT Interior Walls (Sheet 2 of 3)

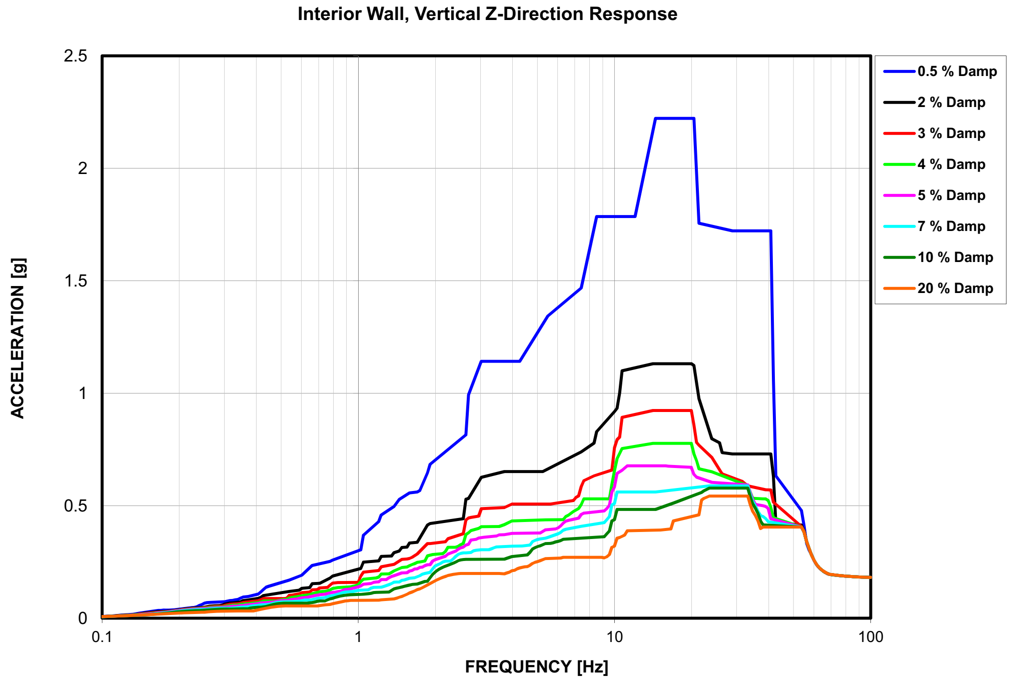

Figure 3LL-24 ISRS for ESWPT Interior Walls (Sheet 3 of 3)

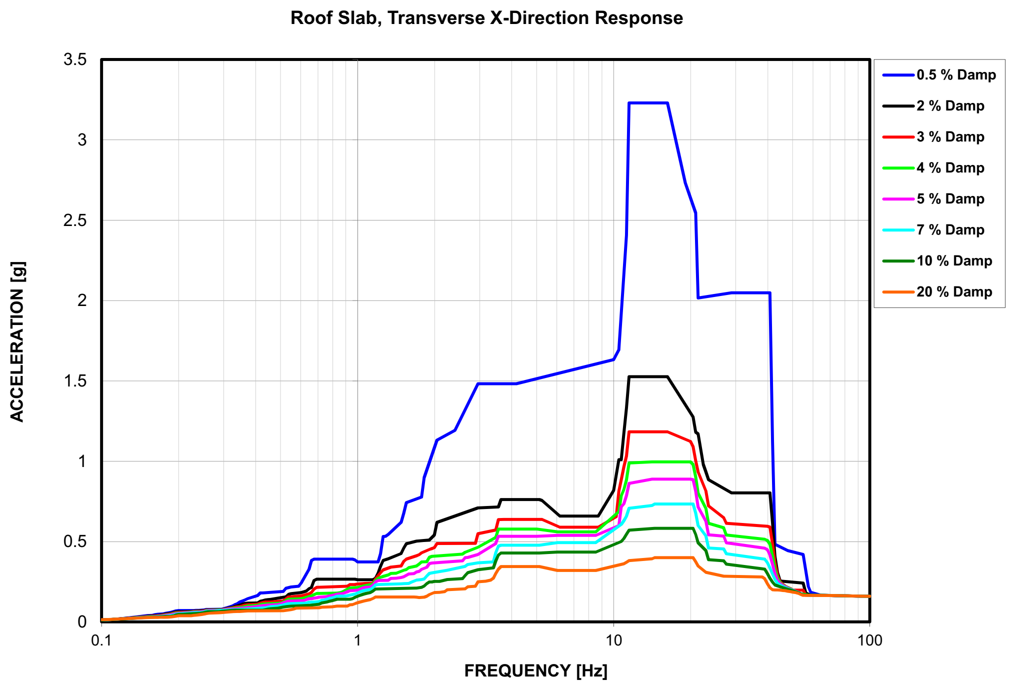

Figure 3LL-25 ISRS for ESWPT Roof (Sheet 1 of 3)

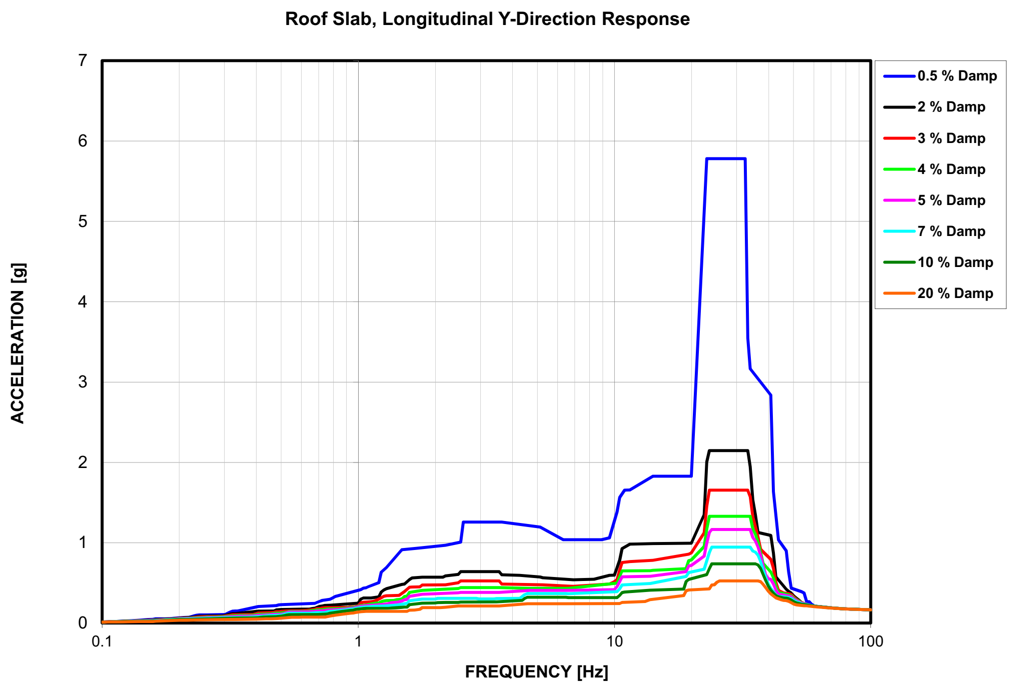

Figure 3LL-25 ISRS for ESWPT Roof (Sheet 2 of 3)

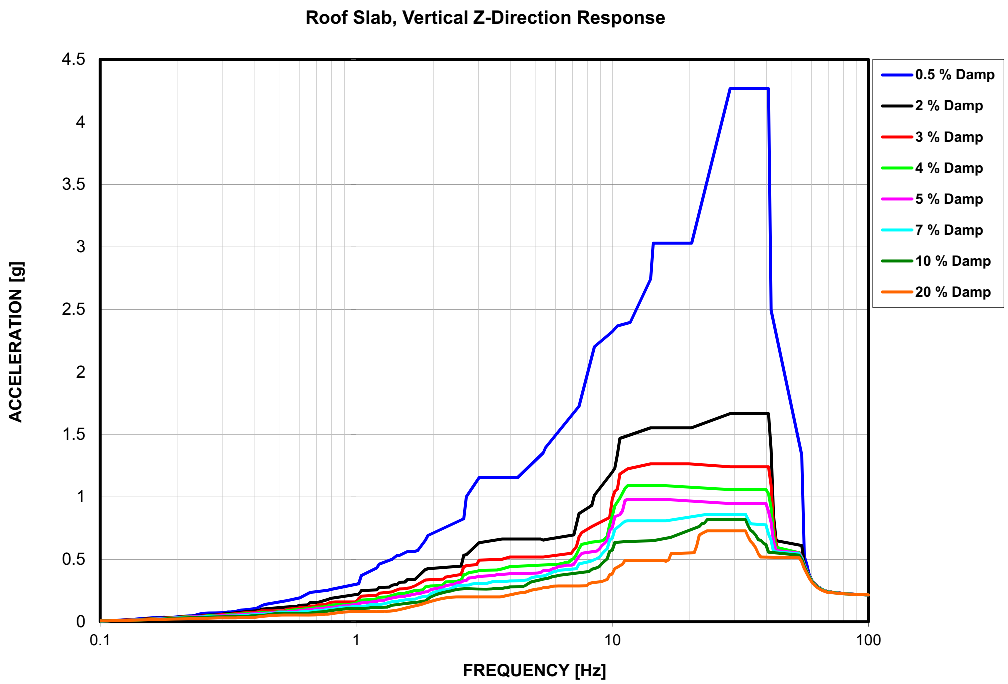

Figure 3LL-25 ISRS for ESWPT Roof (Sheet 3 of 3)

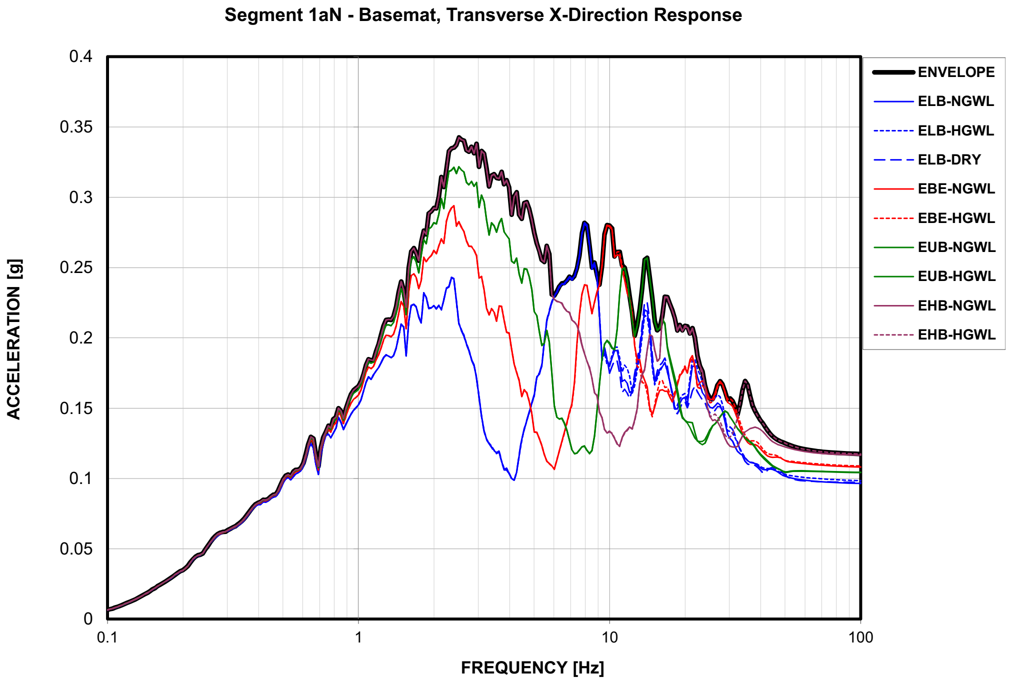

Figure 3LL-26 Envelope of Soil Cases – Segment 1aN – Transverse Response (Sheet 1 of 3)

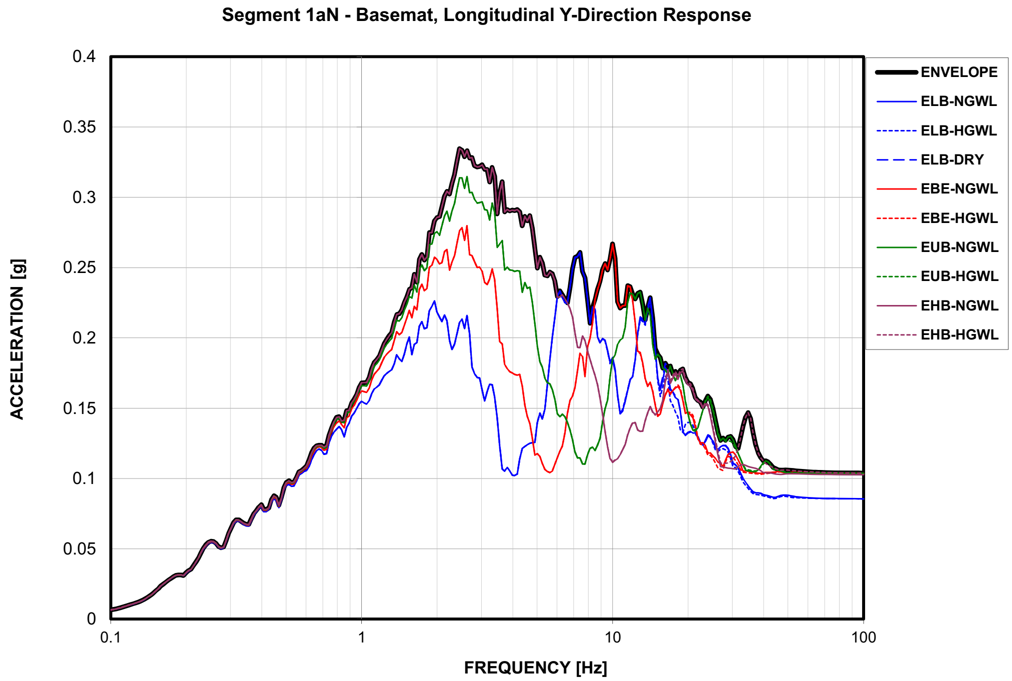

Figure 3LL-26 Envelope of Soil Cases – Segment 1aN – Transverse Response (Sheet 2 of 3)

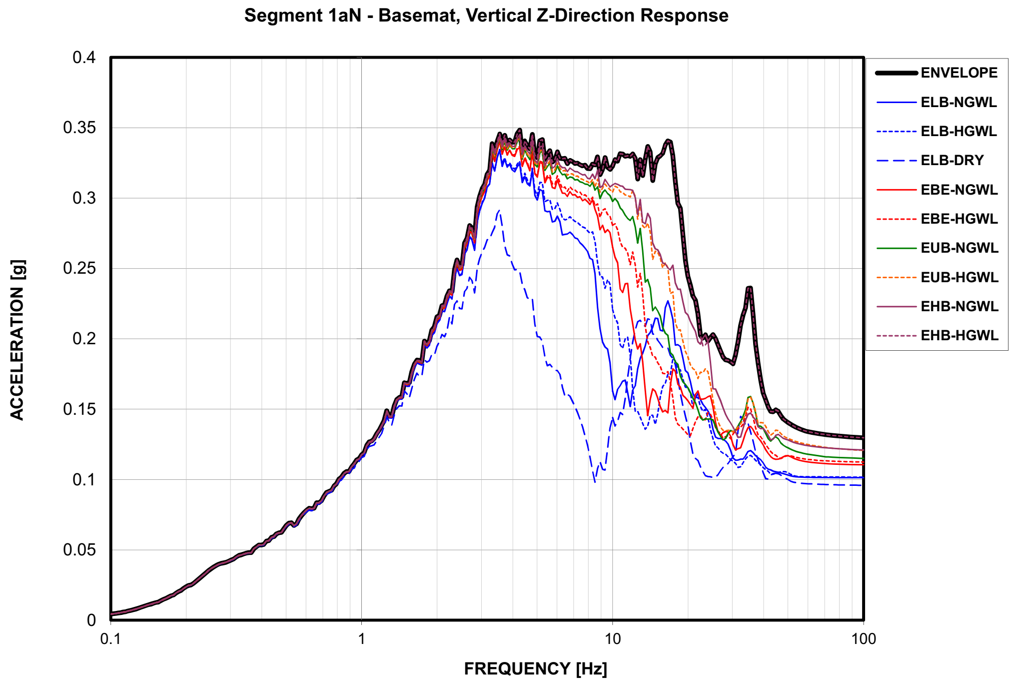

Figure 3LL-26 Envelope of Soil Cases – Segment 1aN – Transverse Response (Sheet 3 of 3)

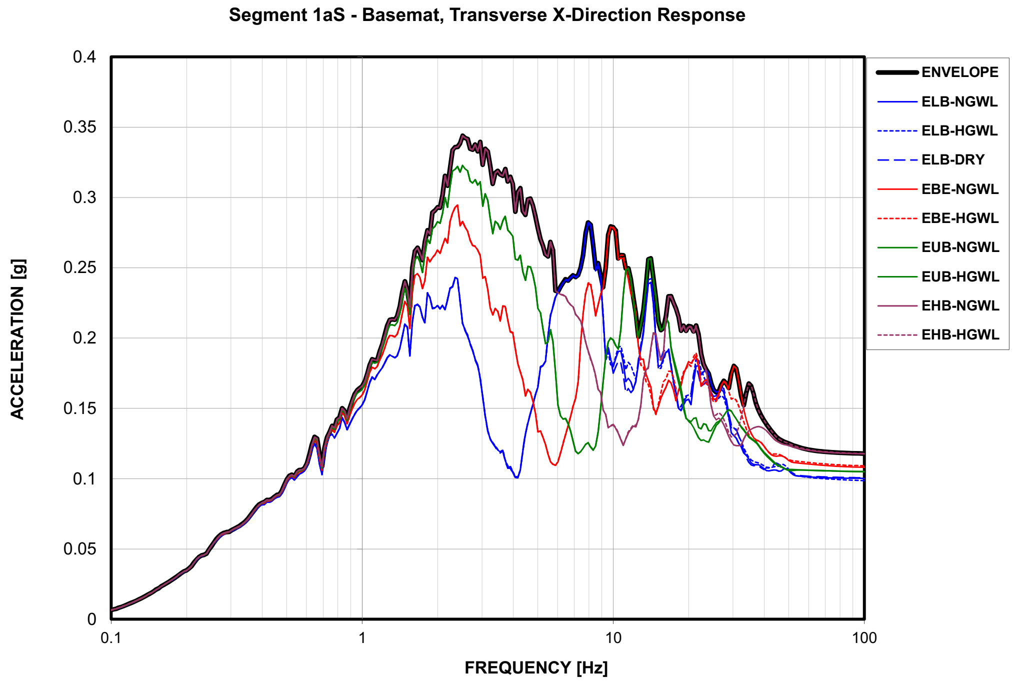

Figure 3LL-27 Envelope of Soil Cases – Segment 1aS – Transverse Response (Sheet 1 of 3)

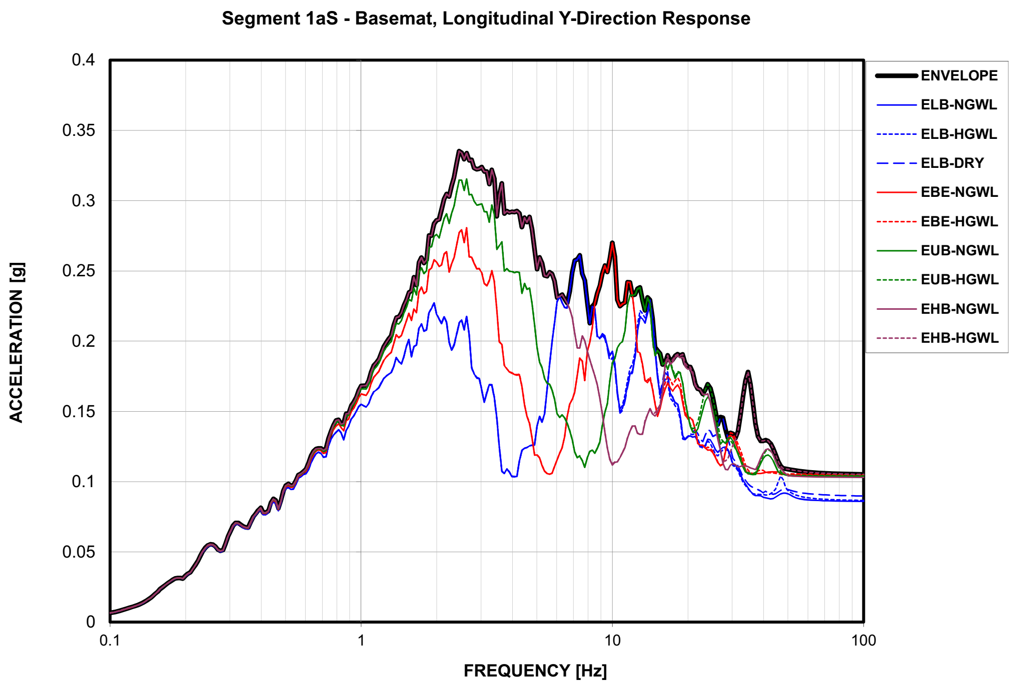

Figure 3LL-27 Envelope of Soil Cases – Segment 1aS – Transverse Response (Sheet 2 of 3)

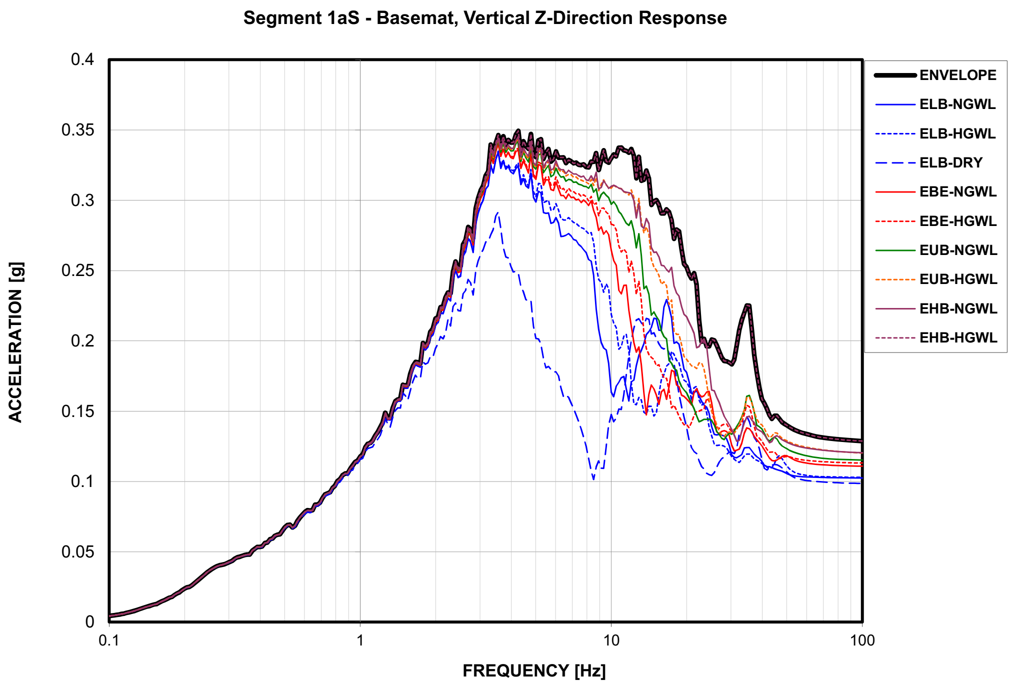

Figure 3LL-27 Envelope of Soil Cases – Segment 1aS – Transverse Response (Sheet 3 of 3)

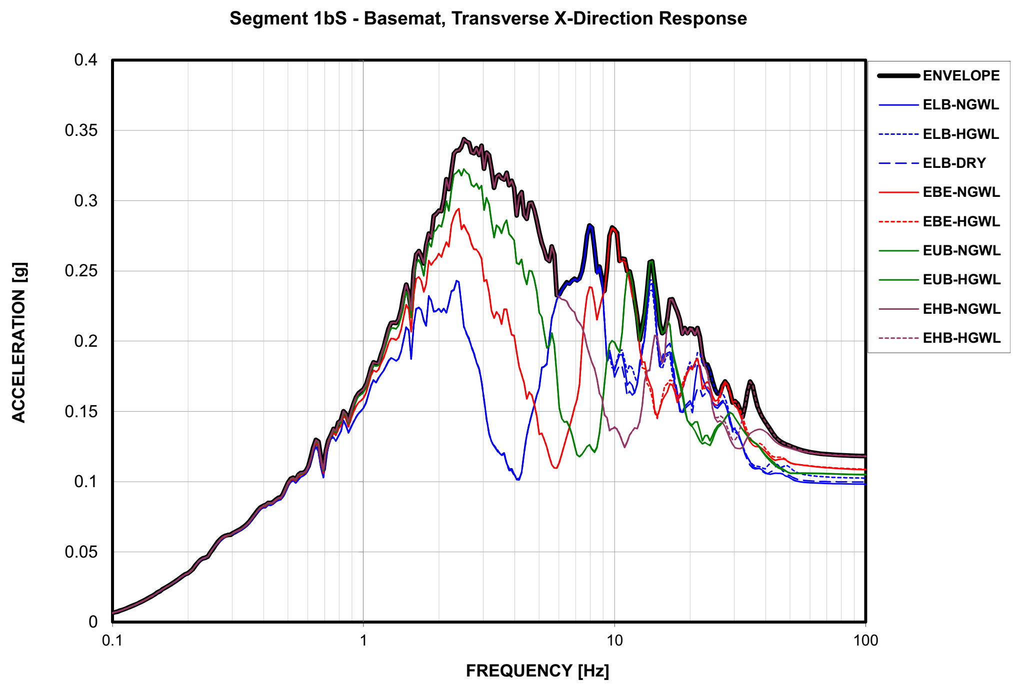

Figure 3LL-28 Envelope of Soil Cases – Segment 1bS – Transverse Response (Sheet 1 of 3)

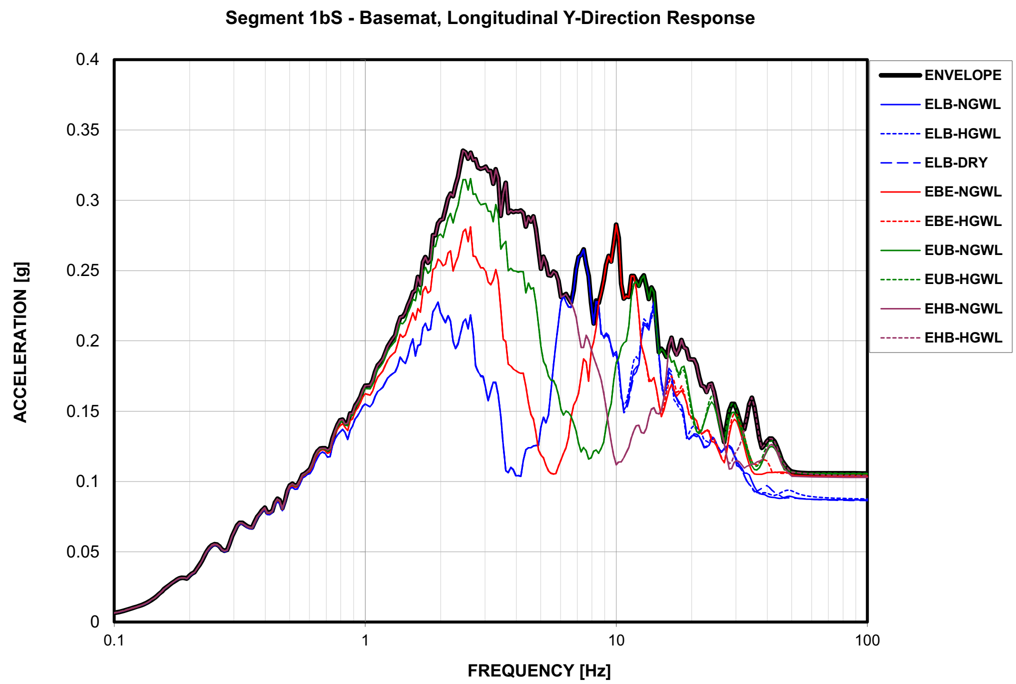

Figure 3LL-28 Envelope of Soil Cases – Segment 1bS – Transverse Response (Sheet 2 of 3)

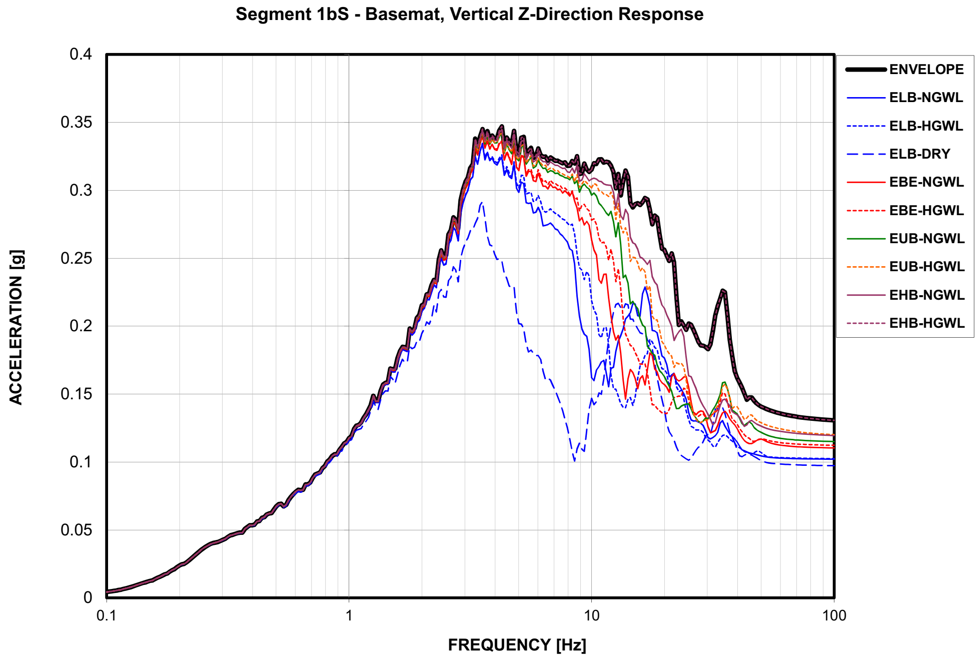

Figure 3LL-28 Envelope of Soil Cases – Segment 1bS – Transverse Response (Sheet 3 of 3)

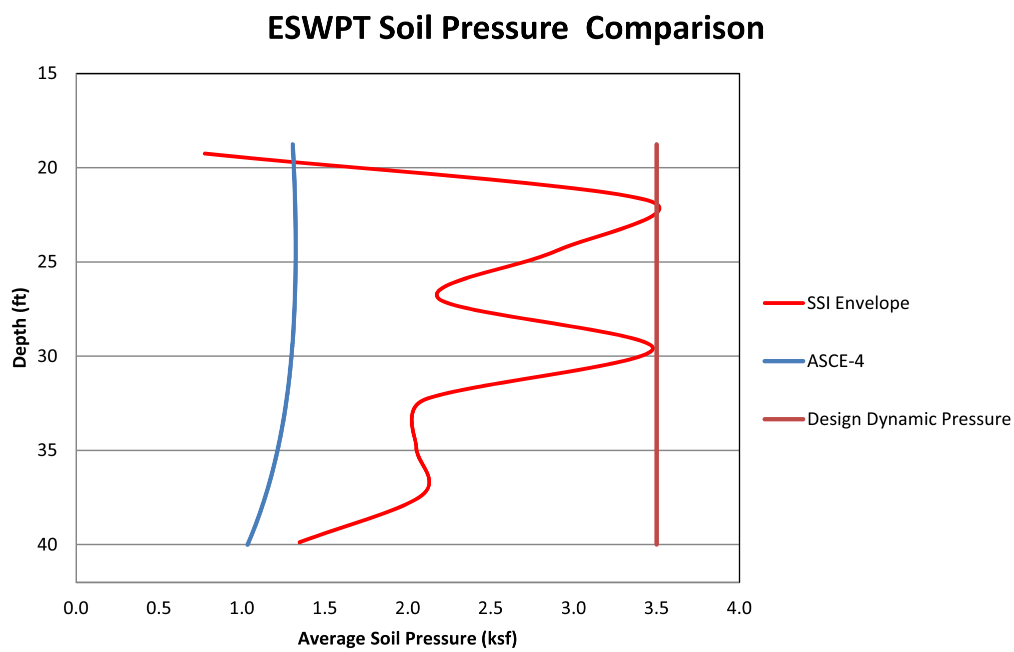

Figure 3LL-29 Lateral Soil Pressure Comparison

CP COL 3.7(3)
CP COL 3.7(4)
CP COL 3.7(8)
CP COL 3.7(8)
CP COL 3.7(12)
CP COL 3.7(21)
CP COL 3.7(26)
CP COL 3.8(15)
CP COL 3.8(19)
CP COL 3.8(29)

APPENDIX 3MM

PSFSV SEISMIC MODELING, ANALYSIS, AND RESULTS

TABLE OF CONTENTS

LIST OF TABLES

LIST OF FIGURES

ACRONYMS AND ABBREVIATIONS

Acronyms	Definitions
3D	three-dimensional
ARS	acceleration response spectra
ATF	acceleration transfer function
BE	best estimate
EBE	embedded best estimate
EHB	embedded high bound
ELB	embedded lower bound
EUB	embedded upper bound
FE	finite element
FIRS	foundation input response spectra
GWL	ground water level
HB	high bound
ISRS	in-structure response spectra
LB	lower bound
OBE	operating-basis earthquake
PSFSV	power source fuel storage vault
SBE	surface best estimate
SHB	surface high bound
SLB	surface lower bound
SUB	surface upper bound
SRSS	square root sum of the squares
SSI	soil-structure interaction
SSSI	structure-soil-structure interaction
UB	upper bound
ZPA	zero period acceleration

3MM PSFSV SEISMIC MODELING, ANALYSIS, AND RESULTS

3MM.1 Introduction

This Appendix discusses the seismic analysis of the power source fuel storage vaults (PSFSVs). The computer program SASSI (Reference 3MM-1 and 3MM-7) serves as the platform for the soil-structure interaction (SSI) analyses and structure-soil-structure interaction (SSSI) analyses. SSI analyses (Reference 3MM-7) are performed on a standalone model of the east PSFSV. The SSI analyses are performed on embedded and surface-mounted models which include the subgrade layering and rock/backfill soil dynamic properties that are compatible with the strains generated by the site-specific safe-shutdown earthquake (SSE) motion. SSSI analyses (Reference 3MM-1) are performed using two combined SASSI models, one which includes the R/B complex, T/B, and the west PSFSV, and one which includes the T/B and east and west PSFSVs. The SSI and SSSI results including nodal maximum accelerations and seismic soil pressures are used to develop input to the ANSYS model of the PSFSV for performing the structural design documented in Section 3.8. Table 3MM-9 summarizes the analyses performed for calculating seismic demands and in-structure response spectra (ISRS).

The SASSI analysis and results presented in this Appendix include site-specific effects such as the layering of the subgrade, embedment of the PSFSVs, flexibility of the basemat and subgrade, and interaction with adjacent structures (SSSI). The analyses results are also investigated to ensure that they envelop the site-specific effects of ground water level (GWL) variation and the potential for backfill soil separation at exterior side walls.

3MM.2 Modeling Description and Analysis Approach

<u>Modeling Description</u>

The PSFSV is a fully-embedded simple shear wall structure with four exterior walls plus two interior shear walls. The walls must resist the out-of-plane flexure and shear due to transverse accelerations, soil pressures (for exterior walls) and flexure imparted on the wall from flexure in the roof slab. The roof slab resists vertical seismic demands as a continuous three span plate in the east-west direction with two-way action in each span. Steel shoring beams, which are left in-place after the roof slab is cast, are not assumed to carry any slab loads after construction. This is a conservative assumption for calculating seismic demands because the vertical frequency of the roof slab is higher than the frequency of the peak of SSE spectra. The presence of beams increases the stiffness, and hence the frequency of the slab. Also, a conservative design of the reinforced concrete roof slab is achieved by not accounting for the presence of steel beams, because more positive flexure demand is induced in the mid-spans of the roof slab, and higher negative moment demands at the edges, as well as shear demands.

The three-dimensional (3D) finite element (FE) PSFSV models used in the SSI analyses are initially developed using the ANSYS computer program (Reference 3MM-2) before being translated into SASSI. The SASSI structural model used for the standalone seismic response SSI analyses and the ANSYS model used for computation of demands for structural design utilize the same mesh size. The east and west PSFSVs are nearly symmetric with the exception of the access tunnels. Due to the symmetry, SSI analysis is performed only on the standalone model of the east vault, and the SSI responses are deemed applicable to the west vault. The comparison of responses obtained from SSSI analyses of the east and west PSFSVs, discussed further below in “Model Verification”, demonstrates the similarity of responses for the two structures. Two types of SSI analysis, described further below, are performed: an analysis with SASSI considering a surface-mounted SSI model, and an analysis with SASSI considering the SSI model embedded in the surrounding backfill soil.

The FE model of the east PSFSV structure used for standalone SSI analysis is shown in Figure 3MM-1, Sheets 1 and 2, using three orthogonal axes: an x-axis pointing north, a y-axis pointing west, and a z-axis pointing up. Shell elements are used for the roof, interior and exterior walls, brick elements are used for the base mat, and stiff beam elements are used to model the fuel tanks and their supports, which are connected to the basemat. The fuel tank masses are represented by lumped mass elements. Brick elements are used to model the excavated soil elements in embedded models of the PSFSVs required for SSI and SSSI analyses. Stiff springs (1 x 10^8 k/ft) are used to connect the excavated soil elements to the coincident interaction nodes. The springs normal to the exterior walls are used to determine dynamic soil pressures. The spring stiffnesses simulate a “fully welded” condition in which the backfill is in full contact with the embedded soil. Table 3MM-1 presents the properties assigned to the structural components of the SASSI FE models used for SSI analysis. Table 3MM-2 summarizes the SASSI FE model structural component dimensions and weights (SSI model). Detailed descriptions and figures of the PSFSV are contained in Section 3.8.

SSSI analyses are performed using two combined SASSI models, a surface SSSI model which includes the R/B complex, T/B, and the west PSFSV, and an embedded SSSI model which includes the T/B and east and west PSFSVs. The structural models used in the SSSI analyses are shown in Figure 3MM-1, Sheets 3 through 6. The SSSI analyses utilize models of the PSFSV structures that consist of the same FE types as the model used for standalone SSI analyses, but utilize a coarser mesh which is verified as described further below. The SSSI analyses use structural models of the R/B complex and T/B that, besides minor modifications in the FE mesh to accommodate site-specific conditions, are identical to the design basis models used for standard design seismic response analyses. In the combined model used for the surface-mounted foundation SSSI analysis, massless solid elements are placed between the walls of the west PSFSV, R/B Complex and T/B with stiffness properties equivalent to the strain-compatible properties of the backfill soil. These elements are used to introduce the stiffness of the fill between the walls into the surface-mounted SSSI analyses and provide results for assessing the effects of SSSI on the earth pressures.

Consistent with recommendations in Section C3.1.3.1 of ASCE 4-98 (Reference 3MM-3), best estimate (BE) stiffness values are assigned to the reinforced concrete members in the SASSI analyses, considering the amount of cracking due to the expected stress levels present in the members. Based on stress results, the PSFSV roof slab does not experience flexural or shear cracking and is therefore modeled as un-cracked, using its gross section properties. The PSFSV walls are designed to resist all lateral loads due to seismic demands by in-plane shear action. The in-plane shear demand-to-capacity ratios are low (less than 0.5), indicating that the walls remain un-cracked for in-plane shear behavior. The out-of-plane seismic demand on the walls is controlled by free-field soil displacement, and using un-cracked flexure properties results in larger seismic flexure demands. Therefore, the walls of the PSFSV are also modeled as un-cracked in the out-of-plane and in-plane directions. The bending moments calculated in the basemat all produce demand-to-capacity ratios of less than 0.5 (not including local effects due to tank overturning loads). The out-of-plane displacements of the slab are controlled by the vertical displacements of the rock, which are negligible. Therefore the PSFSV basemat is also modeled as un-cracked. Operating-basis earthquake (OBE) structural damping values of Table 3.7.3-1(b), such as 4 percent damping for reinforced concrete, are used in the site-specific SASSI analyses. This is consistent with the requirements of Section 1.2 of RG 1.61 (Reference 3MM-4) for structures on sites with low seismic responses where the analyses consider a relatively narrow range of site-specific subgrade conditions.

The lower boundary of the soil layering used in the SSI analysis is 277 feet below grade. The depth is more than the embedment depth plus twice the depth of the largest base dimension (40’ + 2 x 98’ = 236’) recommended by SRP 3.7.2. Below the soil layering, a ten-layer half-space is used in accordance with the SASSI Manual recommendations. The site models used for the SSSI analyses have soil layers extending to a depth of 1079 feet below grade with an additional ten layers used to model the half-space. That depth below grade is more than twice the embedment depth plus twice the largest foundation base dimension of the largest foundation included in the SSSI combined models. The SASSI half-space simulation consists of additional layers with viscous dashpots added at the base of the half-space. The half-space layers have a thickness of 1.5 Vs/f where Vs is the shear wave velocity of the half-space and f is the frequency of analysis. The half-space is sub-divided by the selected number of layers in the half-space.

<u>Model Verification</u>

The translation of the PSFSV SSI model from ANSYS to SASSI is confirmed by comparing the results from the modal analysis of the fixed base structure in ANSYS and the SASSI analysis of the model resting on the surface of a half-space with high stiffness. An eigenvalue analysis was performed on the ANSYS model to obtain cumulative mass participation as a function of frequency and to identify the major modal frequencies and mode shapes. Transfer functions were computed for the SASSI model and structural frequencies were obtained from the transfer functions. Table 3MM-3 presents the first few natural frequencies and descriptions of the associated modal responses of the ANSYS and SASSI fixed-base PSFSV models. Figure 3MM-4 presents example plots of the SASSI fixed-base model transfer functions for the midspans of the three PSFSV roof panels. The frequencies of the ANSYS modes are plotted in Figure 3MM-4 as solid vertical lines for comparison. The close correlation between the SASSI transfer function results with the ANSYS eigenvalues results, as shown in Table 3MM-3, verifies the accuracy of the model translation. Table 3MM-3 also presents the percentage of modal participating mass obtained from the ANSYS model. Figure 3MM-5 shows a plot of the cumulative effective mass versus the frequency for the ANSYS model. Approximately 60% of the mass is captured below 100 Hz for both the north-south and east-west directions. Since the basemat comprises approximately 40% of the structure mass, and it has a frequency above 100 Hz, it is concluded that the cumulative effective mass captured in the horizontal direction satisfactorily reflects the active mass participation behavior of the PSFSV. Approximately 40% of the mass is captured in the vertical direction below 100 Hz. In addition to the basemat, the structure walls are very stiff in the vertical direction, and therefore the percentage of mass captured in the vertical direction is considered acceptable.

Besides the modal comparisons, a 1g static acceleration was applied to the ANSYS model in each of the three directions and a slowly varying input motion with a 1g maximum amplitude was applied to the SASSI model in each of the three directions (x, y, and z). For each direction, the difference between the resulting reactions in ANSYS and SASSI was less than 0.01%, indicating sufficient correlation between the models.

For SSI model verification, and for the SSI analysis cases (described further below), transfer functions are examined to verify that the interpolation was reasonable and that the expected structural responses are observed. For the SSI analysis cases, transfer functions, spectra, accelerations, and soil pressures are compared between the various soil profiles used in analyses to verify that the responses were reasonably similar between these cases except for the expected trends due to soil frequency changes.

The SSI analysis frequencies were selected to cover the range between the initial frequency of analysis (approximately 0.1 Hz) and the cutoff frequency. This frequency range captures the SSI resonance frequencies and the primary structural frequencies. It was verified that as the transfer functions approached the zero frequency (static input), the co-directional transfer function approached unity while the cross-directional terms approached zero. The frequencies were selected evenly spaced, typically at 0.5 Hz spacing. The resulting transfer functions were smooth and accurately captured peaks without needing to add frequencies for additional interpolation.

For SSSI analyses, the east PSFSV coarse mesh model is verified by comparing the acceleration transfer function (ATF) peak frequencies, obtained from the SASSI analysis of the coarse mesh east PSFSV model resting on the surface of a half-space with high stiffness, to the natural frequencies obtained from the modal analysis of the refined mesh fixed base structure in ANSYS. The results of this comparison are shown in Table 3MM-3, which demonstrates that there is no significant change in the overall dynamic response when using the coarser mesh for SSSI analyses. Figure 3MM-12 presents example plots of the SASSI fixed-base model transfer functions at the east PSFSV roof locations. The frequencies of the ANSYS modes are plotted in Figure 3MM-12 as solid vertical lines for comparison, showing the close correlation between the SASSI transfer function results with the ANSYS eigenvalues results for a typical node. The comparison of acceleration response spectra (ARS) of the east and west PSFSVs obtained from SSI verification analyses of the standalone coarse meshed models, embedded in the profile with best estimate properties (EBE), demonstrates that SSI results obtained from the analyses of the east PSFSV model are also applicable for the west PSFSV. Figure 3MM-10 provides example plots of the ARS obtained from these verification analyses at matching nodal locations of the east and west PSFSV models.

For the R/B, the standard plant model used for the site-specific SSSI analyses is adjusted to use a finer mesh on the south side to interface with the mesh used for the west PSFSV model. The re-meshed R/B model was verified by confirming that differences between the ATF for the standard plant model versus the re-meshed R/B model are negligible. The standard plant T/B dynamic model basement elements were also adjusted to use a finer mesh to be consistent with the mesh used for the PSFSV models. ARS comparisons were performed to verify that there is no significant difference in dynamic characteristics of the T/B due to the re-meshing.

Input Control Motion

The input motion for the PSFSV SSI analysis is defined by the envelope of the site-specific foundation input response spectra (FIRS) and the minimum design earthquake spectra as discussed in Subsection 3.7.1.1. Since the minimum design earthquake envelops the PSFSV FIRS at all frequencies, the design ground motion is defined by scaling to 1/3 of the certified seismic design response spectra (CSDRS), representing the outcrop motion at El. 782 ft. Therefore, the standard plant design basis time histories scaled by 1/3 are used as input motion for the SSI analyses of the surface-mounted foundation models. Site response analyses are performed to convert the time histories of the outcrop motion to within-column motion at El. 782 ft for use as input motion for the embedded foundation models. The three components of the input motion are applied to the SSI model separately by using vertically propagating shear and compression waves for the horizontal and vertical components, respectively. The input motion for the SASSI analyses is discussed further in Subsection 3.7.1.1.

The structural design includes accidental torsion loads to address uncertainties related to incoherency of the input ground motion in accordance with Section 3.1.1(e) of ASCE 4-98 (Reference 3MM-3). Incoherency typically lowers responses in the higher frequency range. Due to the low energy content of the input design ground motion at higher frequencies, the spatial variation of the input ground motion is deemed not significant for the design of the PSFSVs. Therefore, the SSI and SSSI analysis of the PSFSVs does not consider incoherency of the input ground motion.

SSI Analysis Cases

As stated previously, two types of SSI analysis are performed: analyses with SASSI considering a model mounted on the surface of truncated rock profiles, and analyses considering the model of the PSFSV structure embedded in full column profiles which include the engineered backfill on top of the rock subgrade. The results of the two types of SSI analyses are enveloped to provide a structural design that captures the effects of variations of site-specific parameters, such as backfill separation, in an efficient and conservative manner.

The strain-compatible rock and backfill properties for the SASSI analyses are developed as discussed in Subsection 3.7.2.4.5. The SASSI analyses account for the site-specific stratigraphy and subgrade conditions described in Subsection 2.5.4, as well as the backfill conditions around the embedded PSFSVs. The profiles used for the embedded analyses are presented in Table 3MM-10 and include the site-specific strain-compatible properties of the supporting media (rock)and engineered backfill. The surface SSI analysis cases use the same profiles as the embedded cases, with the layering truncated at elevation 782 ft. To account for uncertainty in the site-specific subgrade properties, three sets of dynamic properties of the rock are considered, including best estimate (BE), lower bound (LB), and upper bound (UB) properties. An additional high bound (HB) set of properties is also used for the engineered backfill materials to account for expected uncertainty in the backfill properties. Table 3MM-11 summarizes the SSI analysis cases for the PSFSV, the number of frequencies analyzed, cut-off frequency of the analysis, and maximum passing frequency for each analysis case. From Table 3MM-11, the maximum passing frequency exceeds the cutoff frequency, and the cutoff frequency is 50 Hz for all HB and UB analysis cases. The cutoff frequency and maximum passing frequency are below 50 Hz for only the EBE and ELB analysis cases. Based on the characteristics of the observed PSFSV responses discussed in Table 3MM-4, it can be concluded that the cut-off frequencies of analyses enable a seismic design of PSFSV that covers responses up to 50 Hz: The most significant SSI effects are due to the backfill, rather than the rock subgrade. The SSI backfill resonances for the ELB and EBE conditions occur up to approximately 15 Hz , which is well below the cutoff frequencies and maximum passing frequencies for the ELB and EBE analyses cases shown in Table 3MM-11. The cut-off frequency of 35 Hz and 45 Hz for ELB and EBE soil cases respectively is acceptable since the response beyond 35 Hz is controlled by the UB and/or HB soil cases, for which the passing frequency is at least 50 Hz. This behavior is consistent with SSI behavior as most of the energy of input motion is below 15 Hz. Figure 3MM-11 shows the in-structure response spectra for a basemat node, demonstrating this typical behavior.

A verification study was carried out to evaluate the effects of the cut-off frequency for lower bound and best estimate embedded analyses. The passing frequency of these analyses was less than 50 Hz based on Vs/5d. The actual cut-off frequency was taken closer to Vs/4d. The study compared the ISRS obtained by using the cut-off frequency as exactly Vs/5d and also the ISRS obtained when cut-off frequency was closer to Vs/4d. The ISRS results from using a higher cut-off frequency were always bounded by ISRS obtained for upper bound soil. Therefore it was concluded that the use of the cut-off frequency closer to Vs/4d for lower bound and best estimate analyses has no impact on final enveloped ISRS.

SSSI Effects

SSSI analyses are performed on two combined SASSI models: a surface model which includes the R/B complex, T/B and west PSFSV resting on the surface of the truncated surface lower bound (SLB), surface best estimate (SBE), and surface upper bound (SUB) soil profiles and an embedded model which includes the east PSFSV, west PSFSV and T/B. The west PSFSV model is included in the SSSI analyses to ensure comprehensive results. For the surface SSSI model, massless solid elements are used to represent the LB, BE, UB, and HB dynamic properties of the backfill between the buildings. GWL is considered at its nominal level of elevation 795 ft in the SSSI analyses because its results are bounding (see the detailed discussion of the effects of GWL variation below).

The SSSI effects were assessed by comparing the ARS and earth pressures obtained from the SSSI analyses of the combined models to the responses obtained from the standalone coarse mesh PSFSV models. The ARS comparisons showed that SSSI can amplify the PSFSV response. Amplifications are captured in the seismic soil pressures and seismic inertia loads as discussed further below. For developing the ISRS, SSSI effects are accounted for by taking the envelope of the ARS responses obtained from the SSSI analyses of the coarse mesh models, and SSI analyses of the refined mesh model.

Table 3MM-12 summarizes the SSSI analysis cases for the PSFSV, the number of frequencies analyzed, cut-off frequency of the analysis and maximum passing frequency for each analysis case. Based on the observed responses of the PSFSV as identified in Table 3MM-4, the cut-off frequencies used for SSSI analyses are adequate to capture effects of SSSI on the response of PSFSV up to 50 Hz. The most significant SSSI effects are due to the backfill and occur below 20 Hz, which is below the cutoff frequencies and maximum passing frequencies for the EBE and ELB analyses cases.

Use of Modified Subtraction Method

The embedded analyses are performed using the modified subtraction method (MSM). To verify the accuracy of the results using the MSM, a study is performed on the half-model of the standalone east PSFSV model (making use of the structure symmetry) for the UB embedded condition. The study is performed using both the MSM and the more computationally robust flexible volume method (also known as the direct method). The difference between these two methods resides in the definition of interaction nodes for which impedances are calculated for SSI analyses. For the MSM, the choice of interaction nodes includes all nodes on the outer face of the excavation volume, including the top surface. The direct method considers all nodes in the excavated volume as interaction nodes. A comparison of the transfer functions and in-structure response spectra at key locations resulting from the two methods for the UB embedded condition demonstrates that the results using the MSM appropriately capture the SSI responses. The results show that differences obtained from the two methods are negligible. Figure 3MM-6 presents typical examples of transfer function and ISRS comparisons of the MSM versus the flexible volume method at two locations of the PSFSV.

Effects of Ground Water Level Variation

The SSI analysis cases in Table 3MM-11 consider the site-specific ground water elevation of 795 ft (nominal GWL). Besides the SSI analysis cases in Table 3MM-11, an additional embedded best estimate (EBE) SSI analysis is used to investigate GWL effects representative of a case when backfill is unsaturated, i.e. when the GWL is located below the rock surface. The investigation confirmed the findings of a separate GWL variation effects study performed for the ESWPT, which found that the SSI analysis of saturated backfill profiles envelops the responses obtained from SSI analyses of unsaturated backfill everywhere, except for a few nodes in the structure. The SSI ISRS for the PSFSV saturated embedded and surface cases generally envelop the unsaturated case. There are a small number of ISRS frequencies where the unsaturated ISRS locally exceed the saturated ISRS, but these exceedances are small and occur across a narrow frequency band. The zero period accelerations (ZPAs) of the PSFSV saturated embedded and surface cases envelop the corresponding unsaturated ZPAs for all nodes. Figure 3MM-7 shows comparisons of the ISRS corresponding to the EBE and surface best estimate (SBE) saturated cases versus the ISRS for the unsaturated EBE cases, showing typical results of the study. Using the envelope of the responses obtained from SSI analyses of embedded and surface foundation effectively captures effects of GWL variations in the PSFSV seismic design.

Backfill Separation Effects

The SSI analyses of embedded conditions assume that the backfill soil is in full contact with the structure along the total height of the embedment. To justify this assumption, a backfill separation study was performed on the PSFSV model for the EBE condition where the top portion of the backfill soil is separated from the PSFSV exterior walls. For these cases, the SSI responses are calculated for the bounding nominal GWL of 795 ft. The depth of the separation is calculated based on PSFSV results for backfill pressures obtained from SSI analyses of the fully welded embedded model for the best estimate soil case. The connection between the backfill and the structure is separated for the portions of exterior walls where amplitudes of the dynamic soil pressures exceed the static at rest pressure. The backfill separation is modeled by taking the fully welded embedded case and removing the soil springs that are within the estimated depth of separation so that there is no contact. The effects of backfill separation are assessed by comparing the ISRS SSI results for the EBE separated case to the results for the SSI analysis cases for the fully welded EBE and SBE cases. The resulting ISRS are generally controlled by the fully embedded and surface SSI analysis cases. At a few locations, the ISRS obtained from the separated backfill analysis exceed the broadened and enveloped spectra obtained from fully embedded and surface analyses, but always by less than 5% and across a narrow frequency range. Based on these study results, use of the enveloped results of the SSI analysis cases in Table 3MM-11 in the seismic design is sufficient to effectively capture potential effects of soil separation. Figure 3MM-8 presents typical ISRS comparison results for two PSFSV roof and wall locations for separated conditions versus the fully welded EBE and SBE conditions.

Effects of Fuel Oil Tank Subsystem on SSI Response

In the SSI analyses, the three emergency power fuel oil tanks in the PSFSV are considered to be full with a total weight of 1155 kips each, which corresponds to the normal operating fuel level. The tanks are modeled with very high stiffnesses to simulate rigidity. Similarly, very stiff beam elements are used to represent the tank support connections to the basemat. Although the fuel oil tank subsystem is simulated as rigid in the SSI analyses, the effects of the fuel tank subsystem flexibility are accounted for in the design of the base slab. The flexibility is accounted for by conservatively applying, to the tank and support masses, the peak accelerations obtained from the 0.5% damping ISRS for the PSFSV basemat shown in Figure 3MM-3 for each orthogonal direction. Using the peak acceleration from the 0.5% damping ISRS is appropriate for tank sloshing modes and is conservative for the dominant impulsive mode of vibration, which is typically taken as 2% for OBE damping in accordance with RG 1.61 (Reference 3MM-4). Figure 3MM-3 Sheets 16 to 18 show that the ratio between the peak accelerations for 0.5% damping versus 2% damping is 2 or more. The mass and stiffness properties of the tank, and seismic behavior including hydrodynamic effects, will be accounted for in the detailed design of the tank, tank supports, tank support attachments to the basemat, and local reinforcement in the basemat at the tank support attachment points.

Dynamic Lateral Soil Pressures

The static equivalent loads representing dynamic lateral soil pressures are hand calculated based on Wood’s dynamic soil pressures as given in ASCE 4-98 (Reference 3MM-3), considering 0.2g for the horizontal earthquake acceleration αh and total saturated unit weight of the backfill soil. The responses of the PSFSV due to the static equivalent pressures calculated using ASCE 4-98 methodology were confirmed to envelop the responses due to the earth pressures calculated from the enveloped SSI analyses results for soil spring forces. This was confirmed by using ANSYS to perform static analysis of the PSFSV walls using both the SSI soil pressures and the ASCE 4-98 soil pressures applied to the external walls. The analysis showed that the resulting shear and moment demands on the external PSFSV walls are always controlled by the soil pressures calculated using ASCE 4-98, because the ASCE 4-98 pressures control over the majority of the height of the walls and therefore produce higher demands.

Potential increases in dynamic pressure due to site-specific SSSI effects were also considered based on the earth pressure results obtained from the SSSI analyses of the combined models. The comparisons showed that the site-specific SSSI effects do not change the conclusion that dynamic lateral pressures computed using the methodology in Section ASCE 4-98 control the design.

Figure 3MM-9 provides a typical example comparison of dynamic soil pressures derived from ASCE 4-98 versus site-specific SSI and SSSI analyses, at the east wall of the west PSFSV. Figure 3MM-9 shows how ASCE 4-98 pressures are larger than pressures obtained from SSI and SSSI analysis over the majority of the height of the wall. Based on the results of the dynamic soil pressure comparisons, which show that ASCE 4-98 methodology governs, the seismic soil pressures calculated using ASCE 4-98 are applied as equivalent static pressures on the structural elements of the ANSYS model for purposes of structural design.

Application of SASSI Results in the Structural Design

The enveloped results for all the SSI analysis cases listed in Table 3MM-11 are used to determine the maximum SSI nodal accelerations. The enveloped results for both SSSI models and all the SSSI analysis cases as listed in Table 3MM-12 are used to determine amplifications in the maximum SSI nodal accelerations due to SSSI effects.

From the enveloped SSI analyses results of the refined mesh model of the PSFSV, the maximum nodal acceleration for each node is computed as the SRSS of all cross-directional contributions. From the enveloped SSSI analyses results, maximum nodal accelerations are also computed as the SRSS of the cross-directional contributions. The SSSI nodal accelerations are compared to the SSI nodal accelerations. If maximum acceleration values obtained from SSSI analyses are higher than those obtained from the SSI analyses, for any component (i.e. exterior wall, roof slab, etc), the SSI computed acceleration values for that component are scaled by the largest scaling factor calculated for each orthogonal direction. Conservatively, the largest scaling factor for any node within a component is applied to all nodes within that component. The resulting enveloped, scaled nodal accelerations are applied to the ANSYS model to obtain the seismic inertia loads on the PSFSV.

Equivalent static analysis of the ANSYS model is used to calculate the structural demands on the PSFSV due to seismic soil pressures and seismic inertia loads, which are combined as appropriate with all other applicable design loads, in accordance with the factored load combinations described in Subsection 3.8.4.

The directional combination rule for the seismic inertia loads and seismic soil pressures is 100%-40%-40% for purposes of structural design. Load combinations use the 100%-40%-40% combination rule described in RG 1.92 (Reference 3MM-5) because the design of elements includes the effects of the interaction of different components, such as interaction of axial forces with the moments or axial forces with shear. Since the direction of input motion that results in the maximum axial force may be different from that producing the maximum moment or shear, the 100%-40%-40% method produces more accurate design demands. The combination method for seismic inertia loads and seismic soil pressures for stability considerations is conservatively based on 100%-100%-100%, as discussed separately in Subsection 3.8.5.

Accidental torsion is included in the structural design demands by considering an accidental eccentricity of ± 5 percent of the maximum structure dimension for both horizontal directions, consistent with Acceptance Criterion 11 of SRP 3.7.2.11. The accidental torsion is included by applying angular accelerations in combination with the seismic inertia accelerations, the soil pressures, and other applicable loads. The angular accelerations are computed as the product of the total base shear multiplied by ±5 percent of the maximum structure dimension for both horizontal directions, and divided by the structure's mass moment of inertia about the vertical axis of its center of gravity.

3MM.3 Seismic Analysis Results

Table 3MM-4 presents a summary of SSI and SSSI effects on the seismic response of the PSFSV. The maximum absolute nodal accelerations obtained from the SASSI analyses of the PSFSV models, including any increases due to SSSI effects, are presented in Table 3MM-5. The results are presented for each of the PSFSV components and envelop all site conditions described Table 3MM-11 and Table 3MM-12. The maximum accelerations have been obtained by combining cross-directional contributions in accordance with RG 1.92 (Reference 3MM-5) using the square root sum of the squares (SRSS) method. Table 3MM-6 presents the scaling factor used to amplify the maximum accelerations of each component of the PSFSV due to SSSI effects.

Maximum seismic design forces and moments for each of the PSFSV components are presented in Table 3MM-7, based on ANSYS analysis of the factored load combinations in Subsection 3.8.4. These results are calculated from ANSYS design model subjected to the enveloped SSI accelerations, which have been scaled up for SSSI effects, and include dynamic and static lateral soil pressures. The forces and moments also include the effects of accidental torsion, computed as described in Section 3MM.2.

The PSFSV shear walls are designed such that their in-plane shear forces add up to the horizontal load applied to the whole structure. The PSFSV shear wall base in-plane shear forces used for design are presented in Figure 3MM-2 . The magnitude of the in-plane design shear forces shown in Figure 3MM-2 have been conservatively increased to include the portion of the horizontal load, obtained from the ANSYS results, that would otherwise be taken by the out-of-plane walls. The forces presented in the figure are re-distributed based on the in-plane stiffnesses of the shear walls and are not symmetrical, due to model non-symmetry such as different wall thicknesses and openings in the PSFSV north wall.

The PSFSV displacements due to seismic loading are less than 0.30 inch. Table 3MM-8 summarizes the resulting maximum displacements for enveloped seismic loading conditions.

3MM.4 In-Structure Response Spectra

The enveloped broadened ISRS calculated in SASSI are presented in Figure 3MM-3 for the PSFSV components for each of the three orthogonal directions (east-west, north-south, vertical) for 0.5 percent, 2 percent, 3 percent, 4 percent, 5 percent, 7 percent, 10 percent and 20 percent damping. Groups of nodes are used to generate the ISRS for the different structure components. The groups of nodes are selected to represent the key locations, including edges and centers, of the structure's components (i.e. walls, slabs, roof, and basemat). The number of nodes and locations are selected to provide design basis ISRS that envelop the responses at different locations within the component. The ISRS for each orthogonal direction are resultant spectra which have been combined using SRSS to account for cross-directional coupling effects in accordance with RG 1.122 (Reference 3MM-6). The ISRS envelop the results of all SSI and SSSI analysis cases. The ISRS capture the effects of flexibility and concrete cracking in the walls, roof slab, and basemat. The ISRS have been broadened by 15 percent and any sharp valleys are filled so that the valley width is at least broad enough to cover ± 20 percent of the corresponding frequency. The spectra are used for the design of seismic category I and II subsystems and components housed within or mounted to the PSFSV. For the design of seismic category I and II subsystems and components mounted to the PSFSV walls and slabs, it is required to account for the effects of any seismic anchor motions associated with the structure seismic displacements.

3MM.5 References

3MM-1 *An Advanced Computational Software for 3D Dynamic Analysis Including Soil Structure Interaction,* ACS SASSI Version 2.3.0 including "Option A" & NQA "Option FS," Installation Kit Revision 5 (IKR5) and User Manuals Revision 7.0, Ghiocel Predictive Technologies, Inc., September 26, 2012.

3MM-2 ANSYS, Advance Analysis Techniques Guide, Release 11.0 SP1, ANSYS, Inc., 2007.

3MM-3 *Seismic Analysis of Safety-Related Nuclear Structures*. American Society of Civil Engineers, ASCE 4-98, Reston, Virginia, 2000.

3MM-4 *Damping Values for Seismic Design of Nuclear Power Plants*, Regulatory Guide 1.61, Rev. 1, U.S. Nuclear Regulatory Commission, Washington, DC, March 2007.

3MM-5 *Combining Responses and Spatial Components in Seismic Response Analysis,* Regulatory Guide 1.92, Rev. 2, U.S. Nuclear Regulatory Commission, Washington, DC, July 2006.

3MM-6 *Development of Floor Design Response Spectra for Seismic Design of Floor-supported Equipment or Components*, Regulatory Guide 1.122, Rev. 1, U.S. Nuclear Regulatory Commission, Washington, DC, February 1978.

3MM-7 *A System for Analysis of Soil-Structure Interaction*, SASSI2000 Version 3 Including User's Manual Version 3, Ostadan, F., University of California, Berkeley, April 2007.

Table 3MM-1

SSI FE Model Component Properties

Components	Material	E (ksi)	Poisson's Ratio	Unit Weight (kcf)	Damping Ratio	FE Thickness (ft)[4]	Element type
Exterior Walls	5,000 psi concrete	4,030	0.17	0.160[1]	0.04	2.5	Shell
Exterior Thickened Wall	5,000 psi concrete	4,030	0.17	0.1555[1]	0.04	4.50	Shell
Interior Walls	5,000 psi concrete	4,030	0.17	0.1833[1]	0.04	1.5	Shell
Roof (vault and tunnel connector)	5,000 psi concrete	4,030	0.17	0.1875[1]	0.04	2.0	Shell
Basemat	5,000 psi concrete	4,030	0.17	0.1615[1]	0.04	6.5	Brick
Basemat exterior extensions	5,000 psi concrete	4,030	0.17	0.150[1]	0.04	6.5	Brick
Exterior Fuel Access Tunnel Walls	5,000 psi concrete	4,030	0.17	0.1625[1]	0.04	2.0	Shell
Interior Fuel Access Tunnel Walls (2 ft)	5,000 psi concrete	4,030	0.17	0.175[1]	0.04	2.0	Shell
Fuel Access Tunnel Floor	5,000 psi concrete	4,030	0.17	0.1875[1]	0.04	2.0	Shell
Emergency Fuel Oil Tanks	Steel	4.176E+10[2]	0.3	1155 kips[2][3]	0[2]	N/A	Beam
Tank Supports	Steel	4.176E+10[2]	0.3	28.8 kips[2]	0[2]	N/A	Beam

Notes:

1) In addition to self weight, the unit weight includes uniform equivalent dead loads of 50 psf on all internal horizontal mat/slab surfaces, 25 psf on all internal vertical surfaces (both sides of interior walls), and 25% of a 100 psf live load on horizontal surfaces (except the basemat exterior extensions).
2) The tanks and tank supports are modeled as stiff beams and have an E value much higher than normal steel and zero damping for this reason. The beam elements representing the stiffness of the tanks and tank supports are modeled as massless. The weights of the tanks and tank supports are represented using lumped nodal masses.
3) The emergency fuel oil tanks and the oil stored within are given as the total mass in kips, for each tank. The tank supports are given as the total mass in kips for supporting all three fuel oil tanks.
4) Uncracked thicknesses are provided in this table.

Table 3MM-2

SSI FE Model Component Dimensions and Weights(1)

FE Component	Slab Width or Wall Height (ft)	Slab or Wall Length (ft)	Slab or Wall Thickness (ft)	Weight (kips)
North Exterior Wall	33.5	84.5	2.5	1,330
South Exterior Wall	33.5	84.5	2.5	1,420
West Exterior Wall	33.5	75.5	2.5	1,284
East Exterior Wall	33.5	75.5	4.5	1,926
West Interior Wall	33.5	75.5	1.5	695
East Interior Wall	33.5	75.5	1.5	695
Roof Slab	84.5 (east-west)	75.5 (north-south)	2(	2,392
Base mat including extensions	96.75 (east-west)	95 (north – south)	6.5	9,440
Fuel Access Tunnel	Varies	Varies	Varies	583
Tanks including full fuel oil content	N/A	N/A	N/A	1,155 x 3 tanks= 3,465
Tank supports	N/A	N/A	N/A	9.6 x 3 tanks= 28.8
Total Weight (kips)				22,290

Notes:

1) The FE model uses centerline modeling and therefore the width and length dimensions in the table have been adjusted from actual dimensions. The adjustments are minor and do not affect the accuracy of the analysis results. Actual component dimensions are shown in Section 3.8 Figures 3.8-201, 3.8-204, 3.8-205, 3.8-212, 3.8-213, and 3.8-214.
2) The North Exterior Wall has cutout sections and therefore weighs less than the South Exterior Wall.

Table 3MM-3

Summary of Modal Frequencies of Fixed-Base FE Model

ANSYS Model Frequency (Hz)	Percent Effective Mass (%) For ANSYS Model	SASSI Refined Mesh East PSFSV SSI Model Frequency (Hz)	Difference (%) Between SASSI SSI Model and ANSYS Model	SASSI Coarse Mesh East PSFSV SSSI Model Frequency (Hz)	Difference (%) Between SASSI SSSI Model and ANSYS Model	Comments
13.00	9.83	13.00	0.00	12.99	0.08	Overall east-west response, and local out-of-plane response of interior walls
16.09	12.36	16.00	0.56	16.50	2.50	Overall east-west response, and local out-of-plane responses of east interior wall and west exterior wall
18.03	8.99	18.25	1.21	18.51	2.66	Overall east-west response, and local out-of-plane response of west interior wall
21.70	1.47	22.00	1.37	22.34	2.95	Vertical response, roof slab
22.44	30.65	22.39	0.22	22.62	0.80	North-south response, overall structure
24.23	6.34	25.00	3.13	25.00	3.18	Vertical response
33.81	1.89	34.50	2.02	35.50	5.00	Vertical direction
27.40	1.73	28.50	3.94	22.70	18.76	Overall north-south response, and local out-of-plane response of north exterior wall

Table 3MM-4

SSI and SSSI Results for PSFSV Seismic Response

SSI and SSSI Effect	Observed Response
Rock Subgrade	The rock subgrade has insignificant SSI effect on the PSFSV seismic response. Instead, the structural natural frequencies obtained from SASSI analyses of the surface foundation characterize the response, due to the high stiffness of the rock and the small weight of the foundation.
Backfill Embedment	The properties of the backfill embedment affect the overall response of PSFSV structure. SSI horizontal response frequencies are observed at approximately 4 Hz, 5.5 Hz, 7 Hz, and 10 Hz, for the LB, BE, UB, and HB embedded conditions, respectively. SSI vertical response frequencies are observed at approximately 11 Hz, 15 Hz, 20 Hz, and 28 Hz, for the LB, BE, UB, and HB embedded conditions, respectively. The horizontal and vertical SSI response frequencies match closely with calculated soil column frequencies. The peaks of the SSI response increase in magnitude as the frequency of the backfill approaches that of the PSFSV structure.
Ground Water Effects	The SSI ISRS for the saturated embedded and surface cases generally envelop the unsaturated case. There are a small number of ISRS locations where the unsaturated ISRS locally exceeds the saturated ISRS, but these exceedances are small and occur across a narrow frequency band. Small frequency shifts in the response can be observed for some responses. The ZPAs of the PSFSV saturated embedded and surface cases envelop the corresponding unsaturated ZPAs for all nodes. Using the envelope of the responses obtained from SSI analyses of embedded and surface foundation is sufficient to address the effects of GWL variations in the PSFSV seismic design.
Backfill soil separation	The effects of backfill soil separation on the PSFSV response are small. The consideration of enveloped results from surface-mounted and embedded SSI analysis conditions as listed in Table 3MM-11 produces SSI results that effectively envelop the effects of backfill soil separation in the structural design.
SSSI Effects	SSSI with the large standard plant R/B Complex and T/B structures influences the PSFSV response in the mid and high frequency ranges, depending on the selected location and soil conditions. Increases in the ARS amplitudes up to 30% in the mid frequency range (5-15 Hz) for the horizontal directions and in the high frequency range (15-20 Hz) for the vertical direction, are observed. As expected, in most of the cases the governing SSI response in the horizontal directions, with the highest ARS peak amplitude in the 15-20 Hz range, is the surface standalone SSI PSFSV model. However, in some locations SSSI effects produced larger coupled SSI responses in the 5-15 Hz range. The SSSI effects, as expected, also differ significantly from soil to soil. SSSI effects did not result in significant changes to dynamic soil pressures computed from SSI analyses.

Table 3MM-5

SSI FE Model Component Peak Accelerations(1)(2)

Component	N-S SRSS Acceleration (g) (+/- X Direction)	E-W SRSS Acceleration (g) (+/- Y Direction)	Vertical SRSS Acceleration (g) (+/- Z Direction)
North/South Exterior Walls	0.374	0.204	0.145
West Exterior Wall	0.212	0.653	0.161
East Exterior Wall	0.185	0.327	0.140
Interior Walls	0.244	1.046	0.150
Fuel Access Tunnel	0.295	0.250	0.239
Roof Slab	0.244	0.406	0.706
Basemat	0.147	0.130	0.126

Notes:

1) The peak accelerations presented above are the envelope of all nodal values for the listed component, for all embedded and surface SSI analysis cases presented in Table 3MM-11, and include increases derived from the SSSI effects scaling factors. Because the values shown above are the envelope of all nodes for each PSFSV component, the peak acceleration values for individual nodes within a component may be smaller. Table 3MM-6 shows the SSSI effects scaling factors, which are applied uniformly to all nodal accelerations within a component.

2) For structural design using the loads and load combinations in Section 3.8, the peak acceleration for each node is multiplied by the nodal mass, and the scaling factor derived from the SSSI analyses, to obtain the seismic inertia loads.

Table 3MM-6

SSSI Effects Scaling Factors Applied to PSFSV Nodal Accelerations

Component	N-S (+/- X Direction)	E-W (+/- Y Direction)	Vertical (+/- Z Direction)
North/South Exterior Walls	1.296	1.025	1.02
West Exterior Wall	1.043	1.23	1.153
East Exterior Wall	1.064	1.359	1.045
Interior Walls	1.017	1.142	1.026
Fuel Access Tunnel	1.000	1.239	1.126
Roof Slab	1.000	1.679	1.286
Basemat	1.079	1.012	1.000

Table 3MM-7

Maximum Component Seismic Forces and Moments(1),(2)

Component	Component Key Forces and Moments		
	In-Plane Shear	Out-of-Plane Bending Moment (Maximum of Moment about either In-plane Axis)	Out-of Plane Shear
	(k/ft)	(k-ft/ft)	(k/ft)
South Exterior Wall	34.3	126.0	32.2
North Exterior Wall	48.5	125.8	46.2
West Exterior Wall	25.4	192.8	45.9
East Exterior Wall	24.3	212.5	49.5
West Interior Wall	39.4	19.2	7.9
East Interior Wall	36.6	17.6	8.9
Fuel Access Tunnel Walls	20.6	43.1	25.4
Fuel Access Tunnel Floor	11.1	22.7	14.9
Fuel Access Tunnel Roof	43.7	37.5	18.0
Roof Slab	22.1	103.7	12.4
Basemat	-	90.3	37.9

Notes:

1) The forces and moments are the maximum and minimum over all load combinations and include the combination of three orthogonal directions using the 100%-40%-40% method. The forces and moments are used for structural design as described in Section 3.8.
2) The force and moment values are the maximum/minimum finite element forces for walls and slabs and may be a result of force concentrations due to openings or corners.

Table 3MM-8

PSFSV Maximum Displacements(1),(2)

Component	Maximum Displacement (inches)	Description
Roof slab	0.121	Vertical displacement at midspan of west roof panel
Roof slab	0.044	Horizontal displacement equivalent to story drift
East exterior wall	0.083	Horizontal (out-of-plane) displacement near center of wall
West exterior wall	0.287	Horizontal (out-of-plane) displacement near center of wall

Notes:

1) The displacements are maximum relative displacements calculated in ANSYS.
2) Maximum displacements are due to seismic load combinations.

Table 3MM-9

Summary of Analyses Performed

Model	Loading Case	Analysis Method	Program	Input	Output	Three Components Combination
Three-dimensional east PSFSV FE Model for SSI analysis	Seismic motion	Time history soil-structure interaction analysis in frequency domain using sub-structuring technique	SASSI	Time history input motion scaled to 1/3 CSDRS, site-specific soil profiles.	Nodal accelerations, in-structure response spectra	SRSS
Three-dimensional R/B, T/B, and west PSFSV FE model for SSSI analysis	Seismic motion	Time history structure-soil-structure interaction analysis in frequency domain using sub-structuring technique, to obtain SSSI results	SASSI	Time history input motion scaled to 1/3 CSDRS, site-specific soil profiles	In-structure acceleration response spectra for determining ISRS spectral amplification factors and for determining nodal accelerations scaling factors for element and section demands	SRSS
Three-dimensional T/B and east and west PSFSV model for SSSI analysis	Seismic motion	Time history structure-soil-structure interaction analysis in frequency domain using sub-structuring technique, to obtain SSSI results	SASSI	Time history input motion scaled to 1/3 CSDRS, site-specific soil profiles	In-structure acceleration response spectra for determining ISRS spectral amplification factors and for determining nodal accelerations scaling factors for element and section demands	SRSS
Three-dimensional PSFSVs FE Model	Seismic soil pressure	Static	ANSYS	Soil pressures based on ASCE 4-98 (Reference 3MM-3), separate analysis for each direction of pressure.	Element and section demands, displacements	Added to seismic demands in same direction and combined by Newmark 100%-40%-40% Combination rule
Three-dimensional PSFSVs FE Model	Seismic inertia	Static	ANSYS	Nodal accelerations that envelop results of SSI analyses cases and have been scaled up by comparing enveloped SSSI analyses nodal accelerations to enveloped SSI analyses nodal accelerations.	Element and section demands, displacements	Combined by Newmark 100%-40%-40% Combination rule

Table 3MM-10 (Sheet 1 of 2)

Dynamic Soil and Rock Properties

Layer No.	Layer Thickness	Elevation of Top (ft)	Unit Weight (kcf)	Shear Wave Velocity, Vs (ft/s)				Compression Wave Velocity, Vp (ft/s)				Damping Ratio, Ds & Dp			
				LB	BE	UB	HB	LB	BE	UB	HB				
1	1.7417	822.00	0.125	503.01	652.50	846.42	1098.00	1047.10	1358.30	1762.00	2285.60	0.0282	0.0168	0.0100	0.0059
2	1.7416	820.26	0.125	520.27	679.89	888.33	1160.50	1083.00	1415.30	1849.20	2415.70	0.0300	0.0179	0.0106	0.0063
3	3.4667	818.52	0.125	571.32	763.30	1019.80	1362.50	1189.30	1588.90	2122.90	2836.20	0.0348	0.0207	0.0123	0.0073
4	3.4500	815.05	0.125	552.86	748.30	1012.80	1370.80	1150.90	1557.70	2108.30	2853.50	0.0429	0.0251	0.0147	0.0087
5	3.4500	811.60	0.125	538.62	736.41	1006.80	1376.40	1121.20	1533.00	2095.80	2865.10	0.0489	0.0284	0.0165	0.0096
6	3.4500	808.15	0.125	526.18	725.70	1000.80	1380.30	1095.30	1510.70	2083.40	2873.30	0.0543	0.0313	0.0181	0.0104
7	3.4500	804.70	0.125	546.96	756.17	1045.40	1445.10	1138.60	1574.10	2176.10	3008.10	0.0539	0.0310	0.0179	0.0103
8	3.0625	801.25	0.125	684.03	931.50	1268.50	1727.40	1423.90	1939.10	2640.60	3595.90	0.0399	0.0230	0.0133	0.0077
9	3.0625	798.19	0.125	679.15	927.14	1265.70	1727.80	1413.80	1930.00	2634.70	3596.70	0.0417	0.0241	0.0139	0.0080
10	3.1250	795.13	0.125	676.10	924.40	1263.90	1728.00	3258.50	4455.20	6091.40	8328.40	0.0429	0.0247	0.0143	0.0082
11	3.5000	792.00	0.125	668.73	917.80	1259.60	1728.80	3409.90	4679.90	6422.90	8815.20	0.0457	0.0262	0.0150	0.0086
12	3.2500	788.50	0.125	665.45	914.83	1257.70	1729.00	3393.10	4664.70	6412.90	8816.10	0.0470	0.0269	0.0154	0.0088
13	3.2500	785.25	0.125	662.66	912.30	1256.00	1729.10	3378.90	4651.80	6404.30	8816.80	0.0481	0.0274	0.0157	0.0090
14	15.0000	782.00	0.155	4602.80	5720.00	7108.30	7108.30	9137.70	11356.00	14112.00	14112.00	0.0276	0.0188	0.0129	0.0129
15	15.0000	767.00	0.155	4602.80	5720.00	7108.30	7108.30	9137.70	11356.00	14112.00	14112.00	0.0276	0.0188	0.0129	0.0129
16	15.0000	752.00	0.155	4602.80	5720.00	7108.30	7108.30	9137.70	11356.00	14112.00	14112.00	0.0276	0.0188	0.0129	0.0129
17	10.0000	737.00	0.155	4602.80	5720.00	7108.30	7108.30	9137.70	11356.00	14112.00	14112.00	0.0276	0.0188	0.0129	0.0129
18	10.0000	727.00	0.155	4602.80	5720.00	7108.30	7108.30	9137.70	11356.00	14112.00	14112.00	0.0276	0.0188	0.0129	0.0129
19	3.0000	717.00	0.155	2355.00	3019.00	3870.30	3870.30	6340.90	8128.90	10421.00	10421.00	0.0549	0.0365	0.0242	0.0242
20	12.0000	714.00	0.155	4172.80	5113.00	6265.10	6265.10	8921.80	10932.00	13395.00	13395.00	0.0250	0.0171	0.0117	0.0117
21	12.0000	702.00	0.155	4172.80	5113.00	6265.10	6265.10	8921.80	10932.00	13395.00	13395.00	0.0250	0.0171	0.0117	0.0117
22	17.0000	690.00	0.155	5280.30	6467.00	7920.40	7920.40	10062.00	12324.00	15094.00	15094.00	0.0250	0.0171	0.0117	0.0117
23	17.0000	673.00	0.155	5280.30	6467.00	7920.40	7920.40	10062.00	12324.00	15094.00	15094.00	0.0250	0.0171	0.0117	0.0117
24	10.0000	656.00	0.15	3219.80	4046.00	5084.10	5084.10	7318.80	9196.70	11556.00	11556.00	0.0259	0.0178	0.0122	0.0122

Table 3MM-10 (Sheet 2 of 2)

Dynamic Soil and Rock Properties

Layer No.	Layer Thickness	Elevation of Top (ft)	Unit Weight (kcf)	Shear Wave Velocity, Vs (ft/s)				Compression Wave Velocity, Vp (ft/s)				Damping Ratio, Ds & Dp			
				LB	BE	UB	HB	LB	BE	UB	HB				
25	7.0000	646.00	0.15	3219.80	4046.00	5084.10	5084.10	7318.80	9196.70	11556.00	11556.00	0.0259	0.0178	0.0122	0.0122
26	10.0000	639.00	0.15	3218.70	4045.00	5083.40	5083.40	7316.20	9194.40	11555.00	11555.00	0.0260	0.0179	0.0123	0.0123
27	7.0000	629.00	0.15	3218.70	4045.00	5083.40	5083.40	7316.20	9194.40	11555.00	11555.00	0.0260	0.0179	0.0123	0.0123
28	7.0000	622.00	0.13	2356.80	2950.00	3692.50	3692.50	6034.30	7553.10	9454.20	9454.20	0.0254	0.0174	0.0120	0.0120
29	7.5000	615.00	0.13	2356.80	2950.00	3692.50	3692.50	6034.30	7553.10	9454.20	9454.20	0.0254	0.0174	0.0120	0.0120
30	7.0000	607.50	0.13	2356.80	2950.00	3692.50	3692.50	6034.30	7553.10	9454.20	9454.20	0.0255	0.0175	0.0120	0.0120
31	7.5000	600.50	0.13	2356.80	2950.00	3692.50	3692.50	6034.30	7553.10	9454.20	9454.20	0.0255	0.0175	0.0120	0.0120
32	8.0000	593.00	0.135	2362.30	3153.00	4208.30	4208.30	5369.70	7166.90	9565.50	9565.50	0.0462	0.0313	0.0212	0.0212
33	8.0000	585.00	0.135	2362.30	3153.00	4208.30	4208.30	5369.70	7166.90	9565.50	9565.50	0.0462	0.0313	0.0212	0.0212
34	8.0000	577.00	0.135	2359.20	3150.00	4206.00	4206.00	5362.40	7160.10	9560.30	9560.30	0.0464	0.0315	0.0213	0.0213
35	8.0000	569.00	0.135	2359.10	3150.00	4206.00	4206.00	5362.40	7160.10	9560.30	9560.30	0.0464	0.0315	0.0213	0.0213
36	8.0000	561.00	0.135	2356.40	3147.00	4202.80	4202.80	5356.30	7153.20	9553.10	9553.10	0.0466	0.0316	0.0214	0.0214
37	8.0000	553.00	0.135	2356.40	3147.00	4202.80	4202.80	5356.30	7153.20	9553.10	9553.10	0.0466	0.0316	0.0214	0.0214

Table 3MM-11

SSI Analysis Cases for the East PSFSV

Analysis	Description	Backfill Soil	Rock Subgrade	Number of Frequencies Analyzed	Cut-off Frequency of Analysis	Mazimum Passing Frequency
1	Embedded Best Estimate	Best estimate	Best estimate	91	45	41.5
2	Embedded Lower Bound	Lower bound	Lower bound	71	35	30.5
3	Embedded Upper Bound	Upper bound	Upper bound	99	50	53.8
4	Embedded High Bound	High bound	Upper bound	99	50	69.8
5	Surface Best Estimate	N/A	Best estimate	99	50	76.1
6	Surface Lower Bound	N/A	Lower bound	99	50	58.9
7	Surface Upper Bound	N/A	Upper bound	99	50	93.2

Table 3MM-12

SSSI Analysis Cases for the PSFSVs

Analysis	Model/Description	Backfill Soil	Rock Subgrade	Number of frequencies analyzed	Cut-off frequency of Analysis	Maximum Passing frequency
1	T/B-E&W PSFSV Embedded Best Estimate	Best estimate	Best estimate	132	40	35.2
2	T/B-E&W PSFSV Embedded Lower Bound	Lower bound	Lower bound	109	30	25.2
3	T/B-E&W PSFSV Embedded Upper Bound	Upper bound	Upper bound	152	50	48.9
4	T/B-E&W PSFSV Embedded High Bound	High bound	Upper bound	152	50	67.8
5	R/B-T/B- W PSFSV Surface Best Estimate	Best estimate[(1)]	Best estimate	132	40	67.8
6	R/B-T/B- W PSFSV Surface Lower Bound	Lower bound [(1)]	Lower bound	109	30	54.8
7	R/B-T/B- W PSFSV Surface Upper Bound	Upper bound[(1)]	Upper bound	152	50	83.8
8	R/B-T/B- W PSFSV Surface High Bound	High bound[(1)]	Upper bound	152	50	83.8

Notes:

1) Massless solid elements are used in the surface models to represent the LB, BE, UB, and HB dynamic properties of the backfill around and between the buildings.

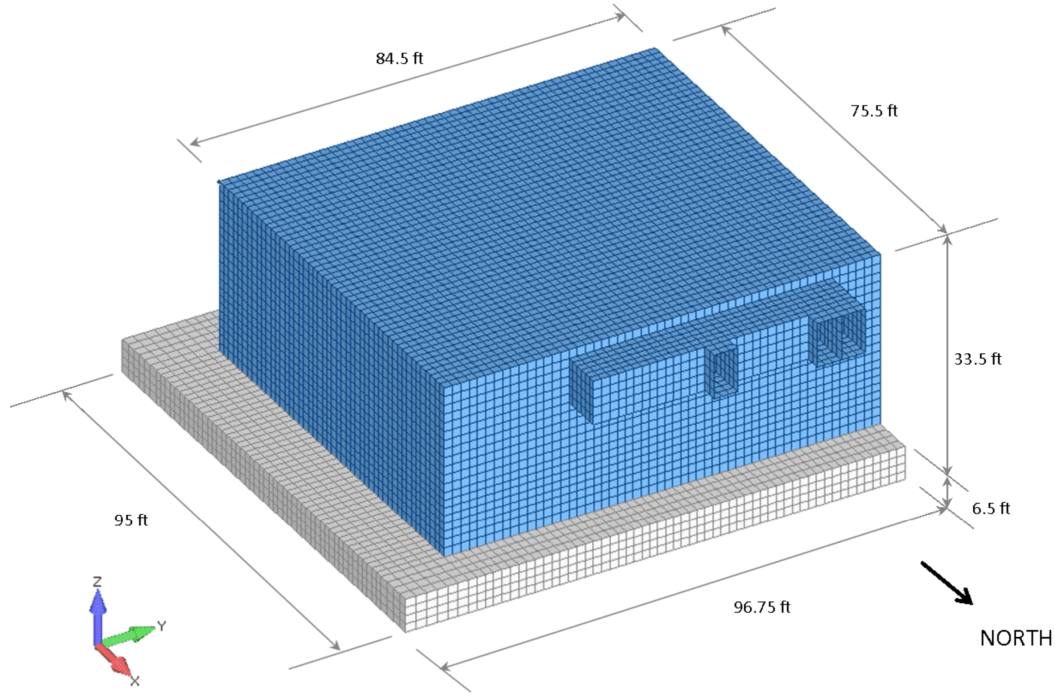

Note:

1) The vault pipe/access tunnel openings are on the north exterior wall as shown in the model above.

Figure 3MM-1 Structural Models of PSFSV Used for Seismic Analysis (Sheet 1 of 6) (SASSI Model of East PSFSV Used for SSI Analysis)

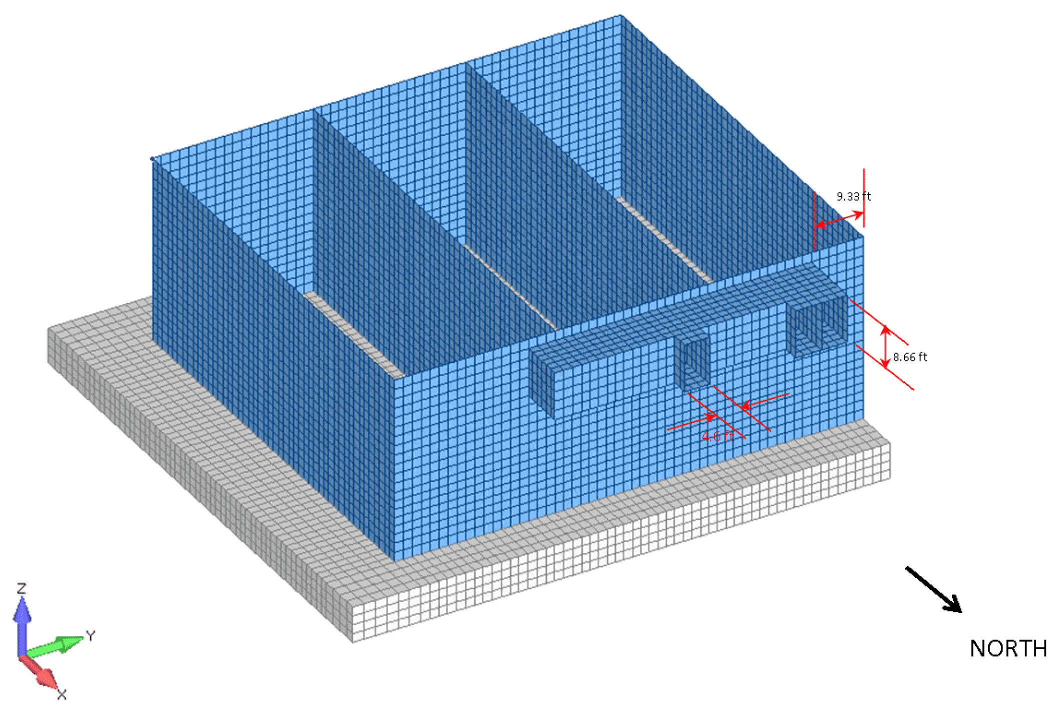

Figure 3MM-1 Structural Models of PSFSV Used for Seismic Analysis (Sheet 2 of 6) (SASSI Model of East PSFSV Used for SSI Analysis, with Roof Removed)

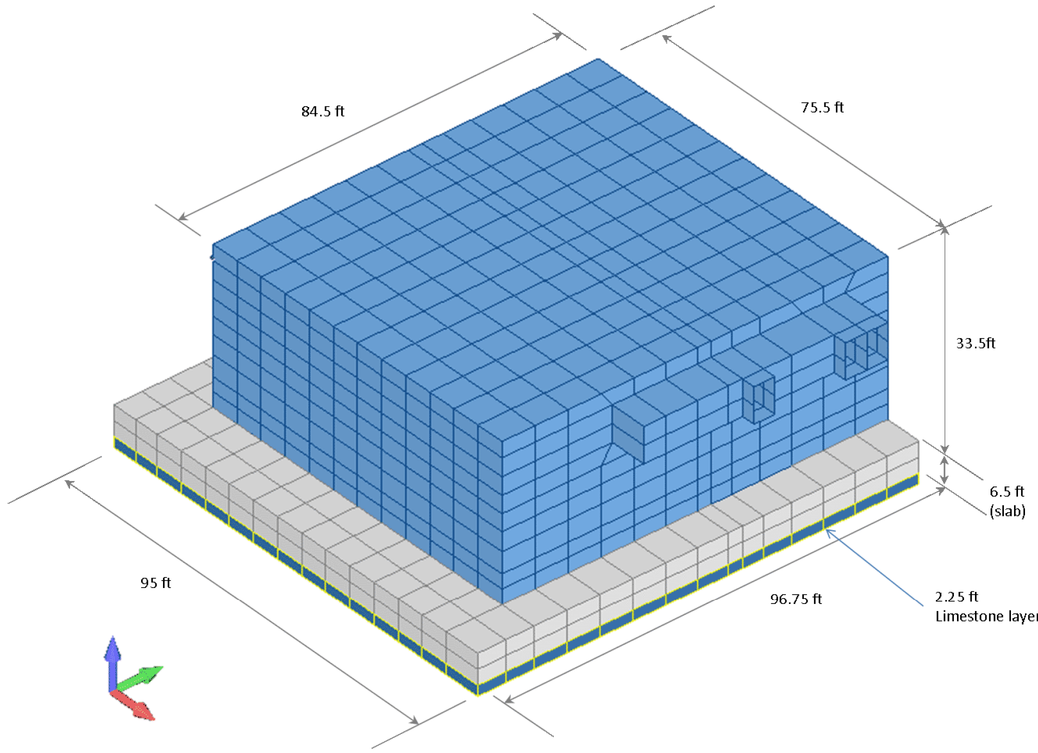

The layer of limestone elements shown in the figure is included below the PSFSV basemat so that the meshing aligns with the bottom elevation of the R/B complex basemat.

Figure 3MM-1 Structural Models of PSFSV Used for Seismic Analysis (Sheet 3 of 6) (SASSI Model of East PSFSV Used for SSSI Analysis)

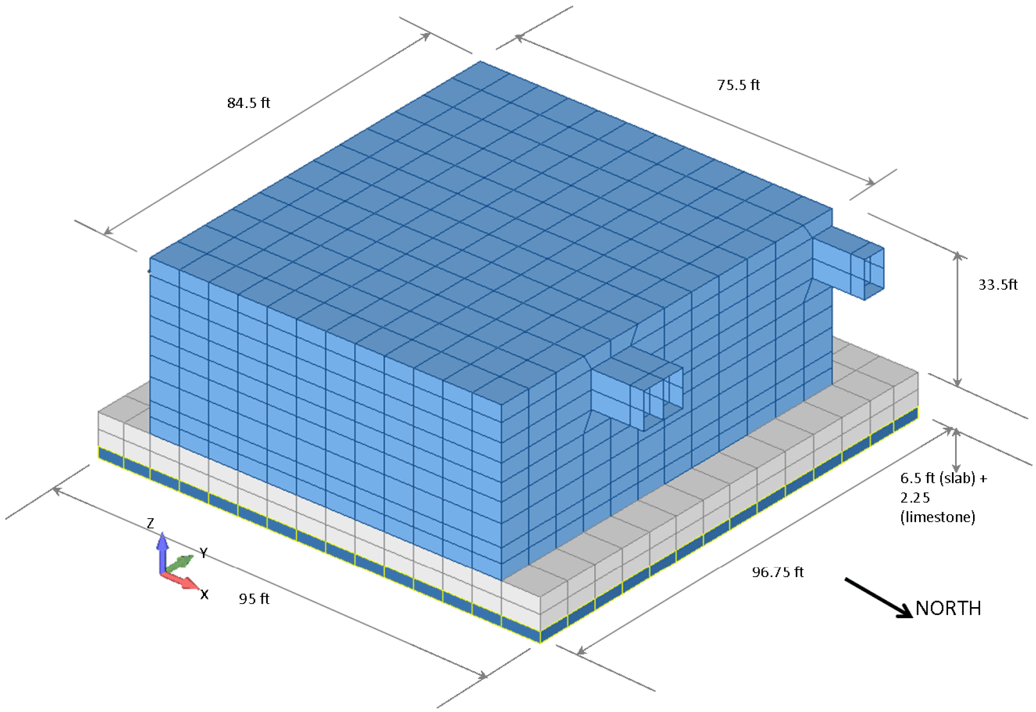

Figure 3MM-1 Structural Models of PSFSV Used for Seismic Analysis (Sheet 4 of 6) (SASSI Model of West PSFSV Used for SSSI Analysis)

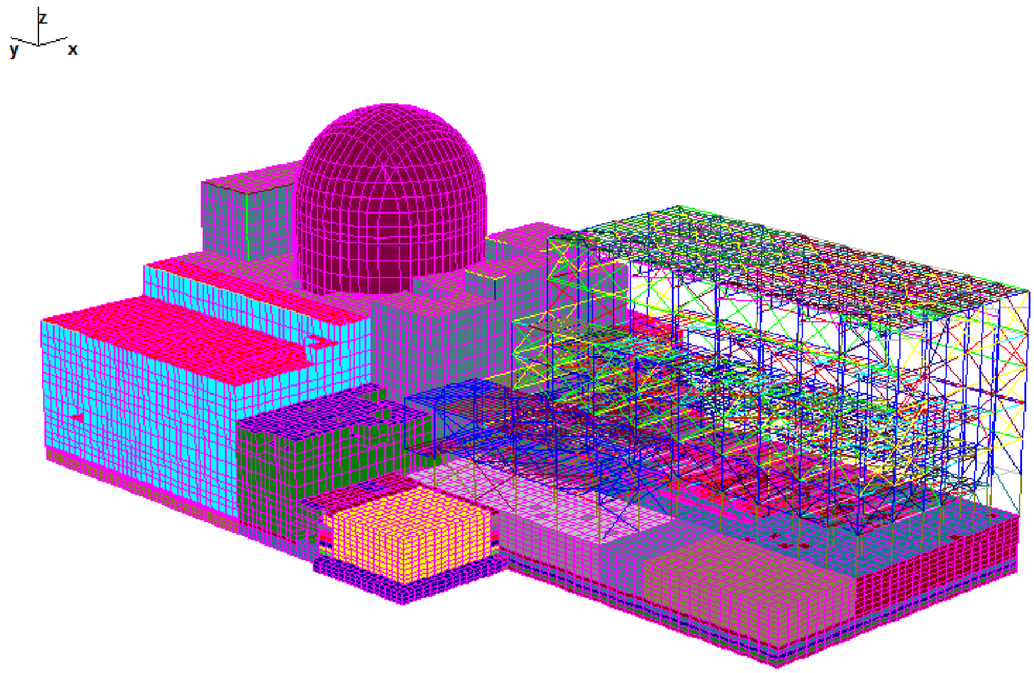

Figure 3MM-1 Structural Models of PSFSV Used for Seismic Analysis (Sheet 5 of 6) (SASSI Model of R/B Complex, T/B, and West PSFSV Used for SSSI Analysis)

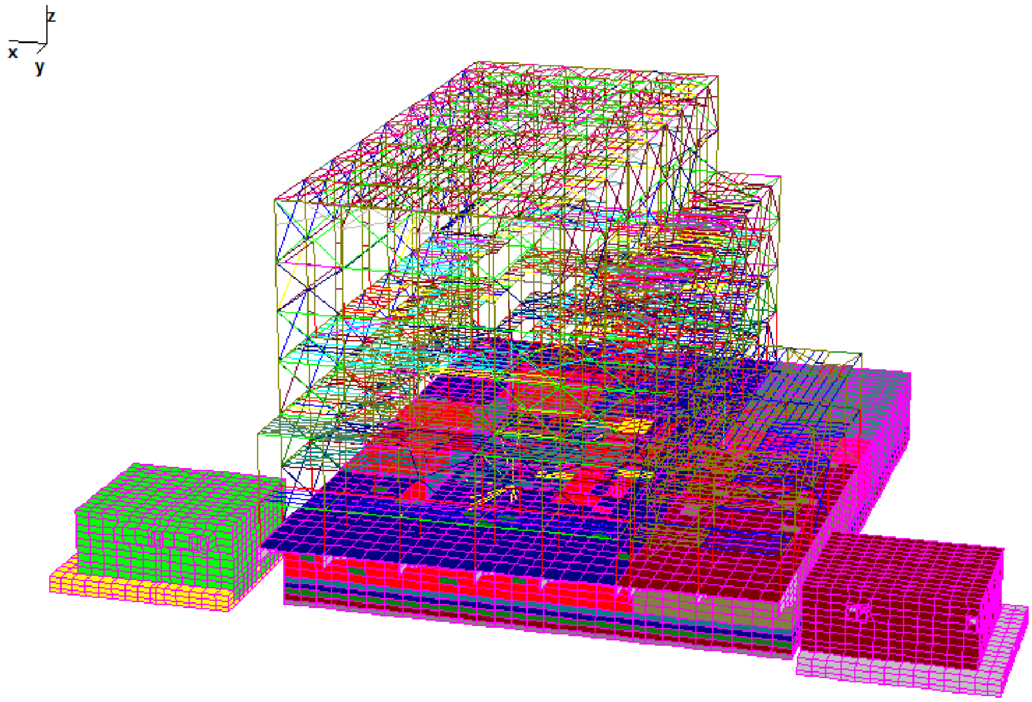

Figure 3MM-1 Structural Models of PSFSV Used for Seismic Analysis (Sheet 6 of 6) (SASSI Model of West PSFSV, T/B, and East PSFSV Used for SSSI Analysis)

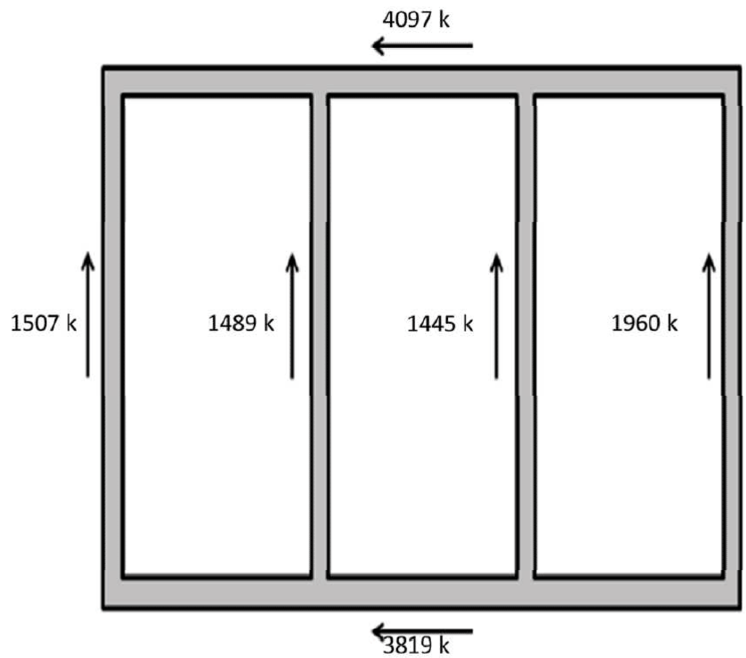

Notes:

1) The seismic shear forces shown above are computed for the east PSFSV at the bottom of each wall at the interface with the foundation mat, are the envelope of all load combinations and SSI and SSSI analysis cases, and account for accidental eccentricity and total seismic base shear to be resisted by in plane shear of walls.

Figure 3MM-2 Maximum Seismic Base Shear Forces in Walls

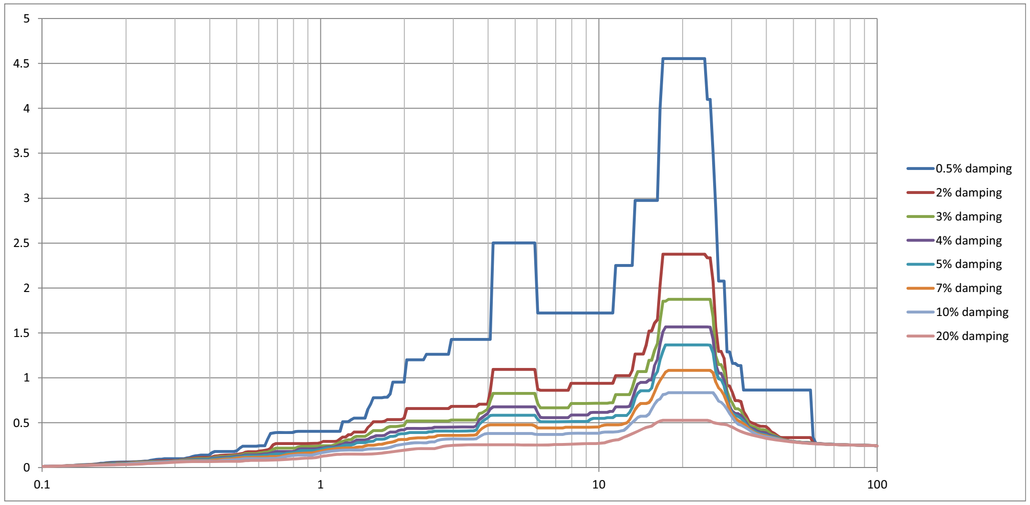

Figure 3MM-3 ISRS for PSFSV (Sheet 1 of 18)
Roof, X-direction (north-south)

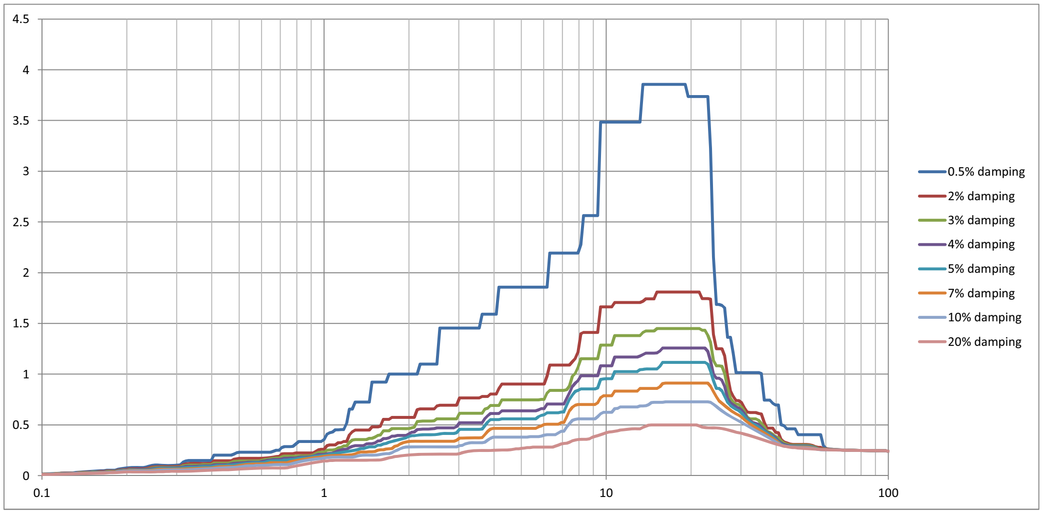

**Figure 3MM-3 ISRS for PSFSV (Sheet 2 of 18)
Roof, Y-direction (east-west)**

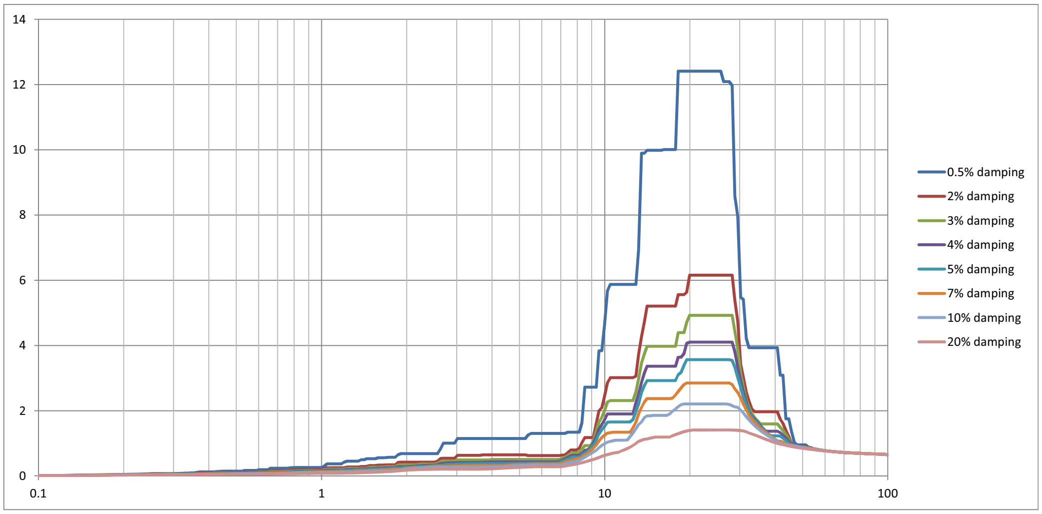

Figure 3MM-3 ISRS for PSFSV (Sheet 3 of 18)
Roof, Z-direction (vertical)

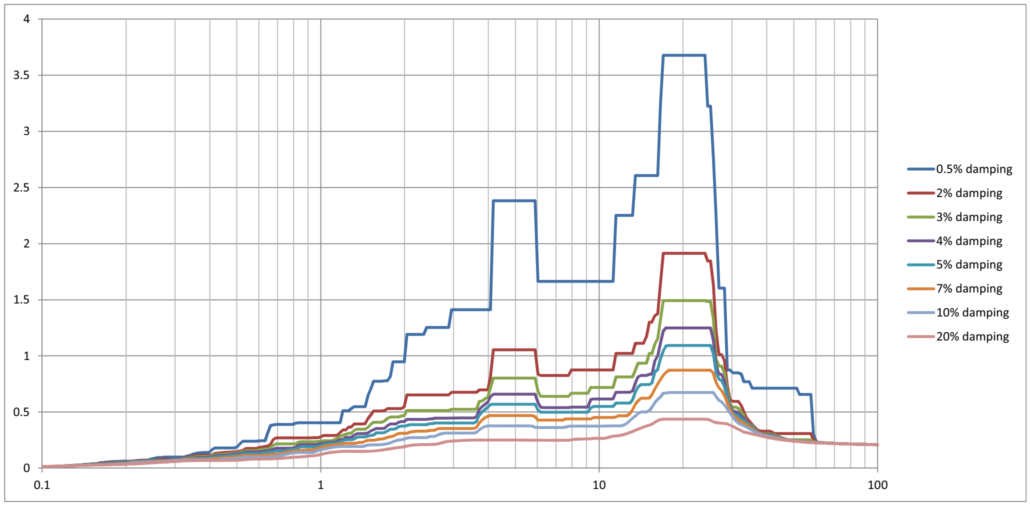

Figure 3MM-3 ISRS for PSFSV (Sheet 4 of 18)
East and West Exterior Walls X-direction (north-south)

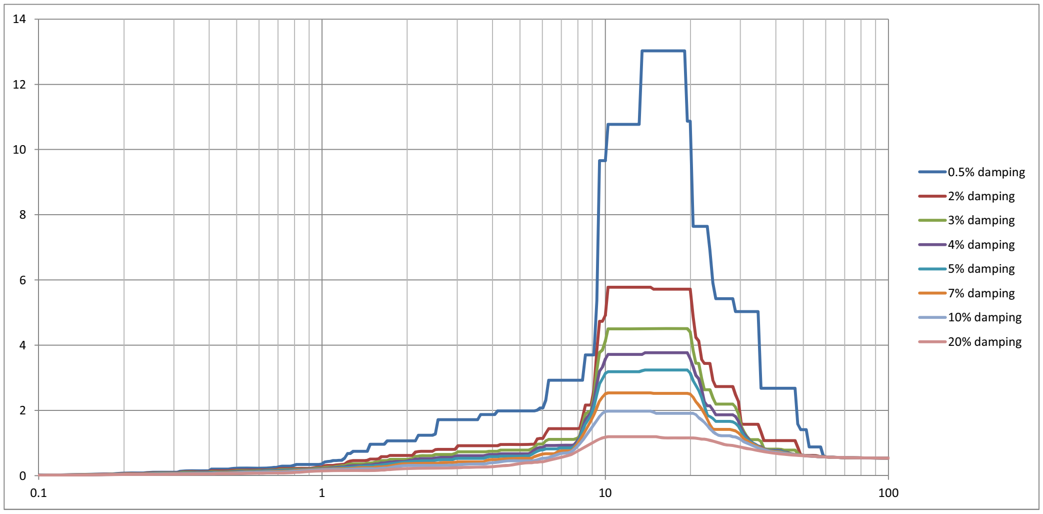

Figure 3MM-3 ISRS for PSFSV (Sheet 5 of 18)
East and West Exterior Walls Y-direction (east-west)

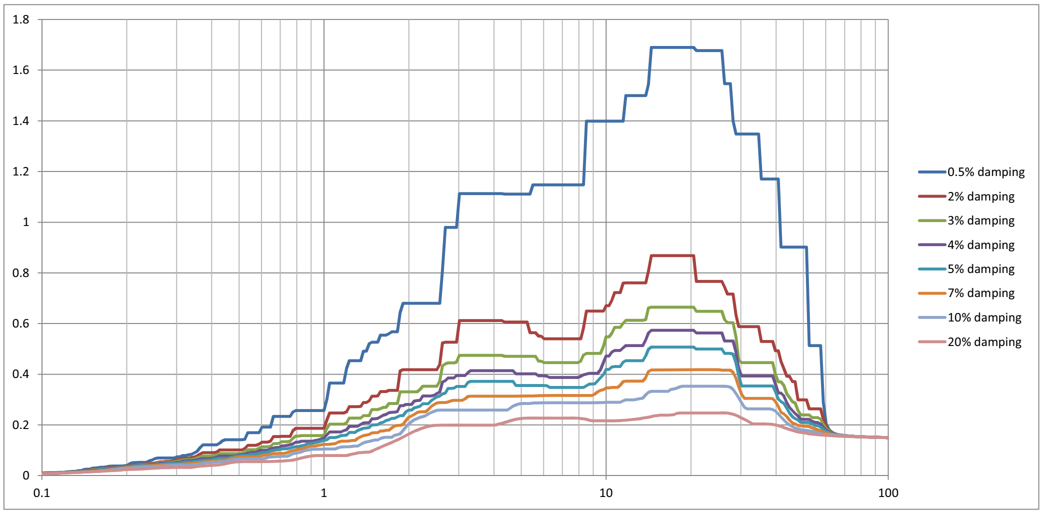

Figure 3MM-3 ISRS for PSFSV (Sheet 6 of 18)
East and West Exterior Walls Z-direction (vertical)

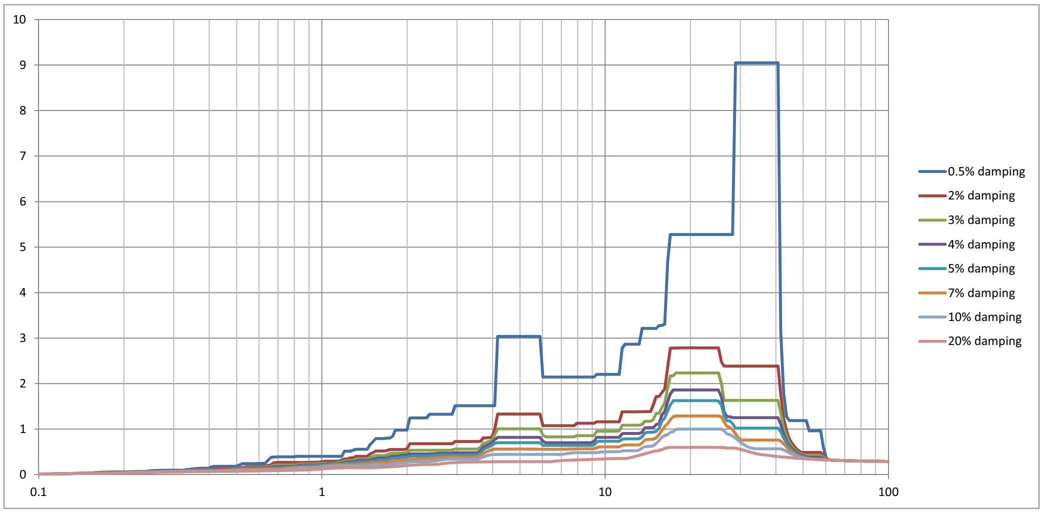

Figure 3MM-3 ISRS for PSFSV (Sheet 7 of 18)
North and South Exterior Walls X-direction (north-south)

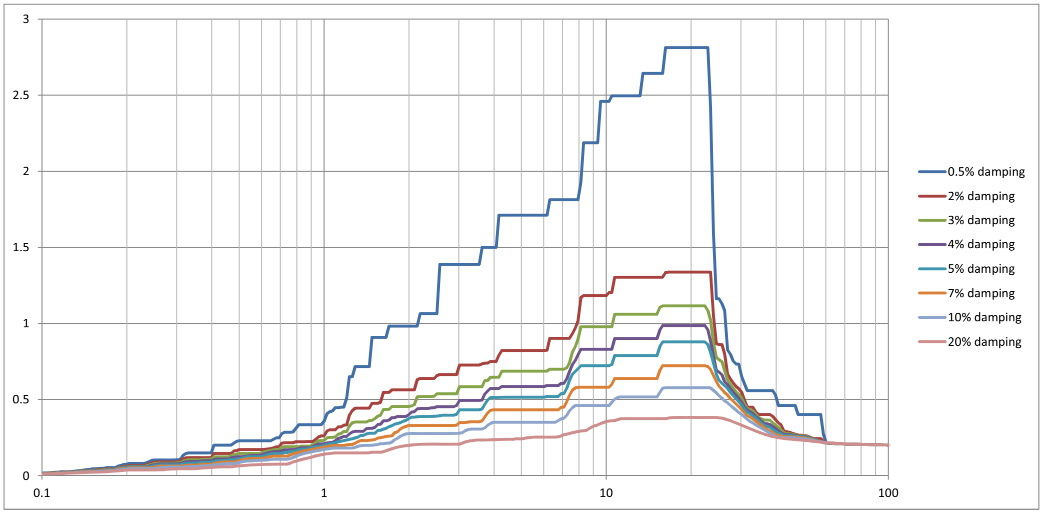

Figure 3MM-3 ISRS for PSFSV (Sheet 8 of 18)
North and South Exterior Walls Y-direction (east-west)

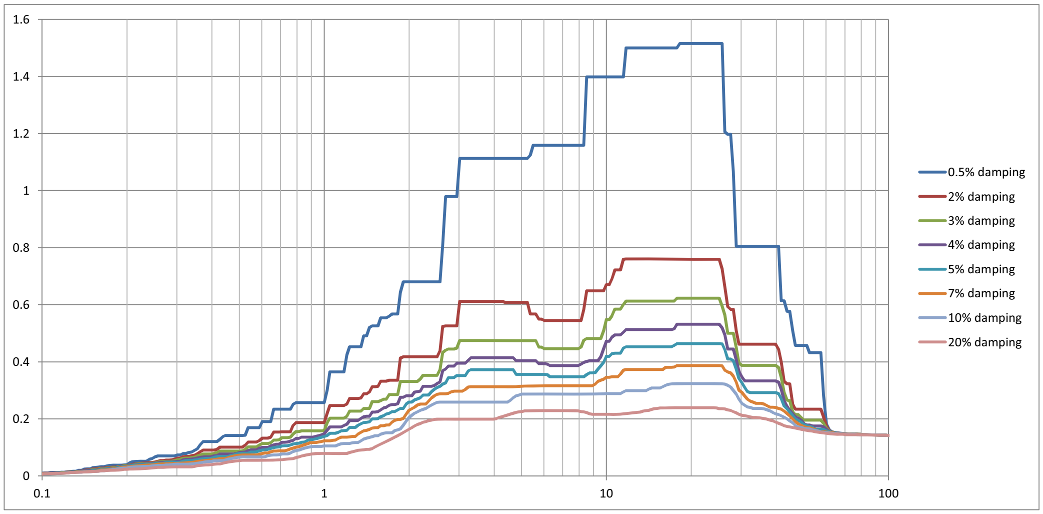

Figure 3MM-3 ISRS for PSFSV (Sheet 9 of 18)
North and South Exterior Walls Z-direction (vertical)

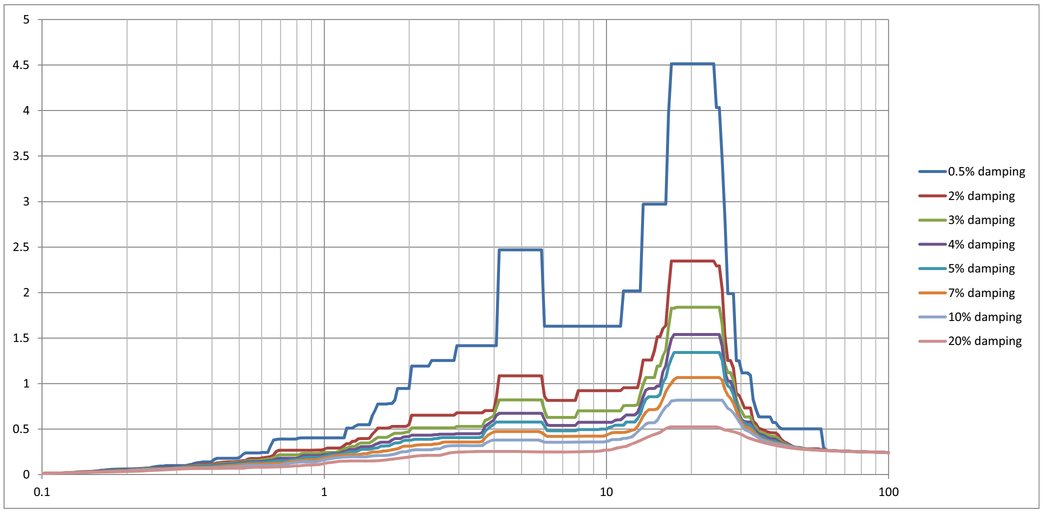

Figure 3MM-3 ISRS for PSFSV (Sheet 10 of 18)
Interior Walls X-direction (north-south)

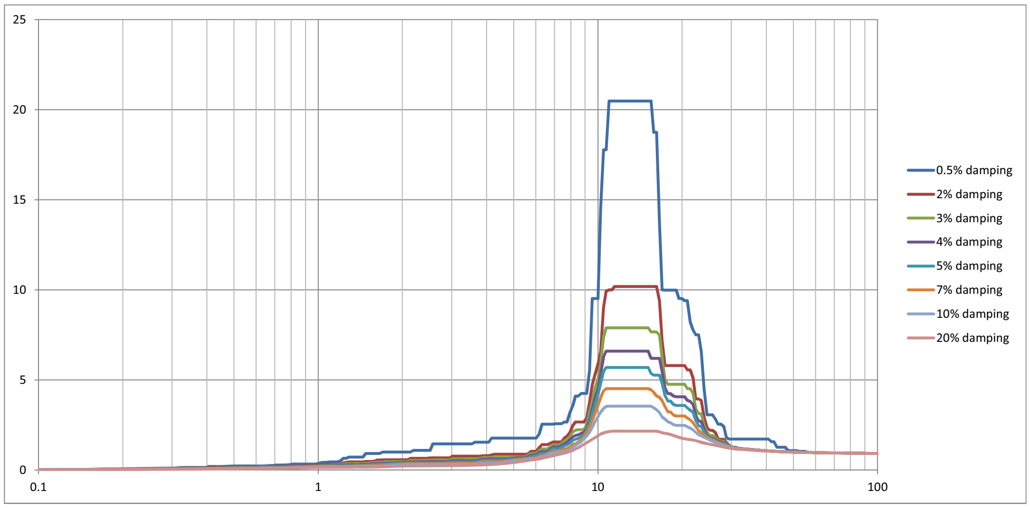

**Figure 3MM-3 ISRS for PSFSV (Sheet 11 of 18)
Interior Walls Y-direction (east-west)**

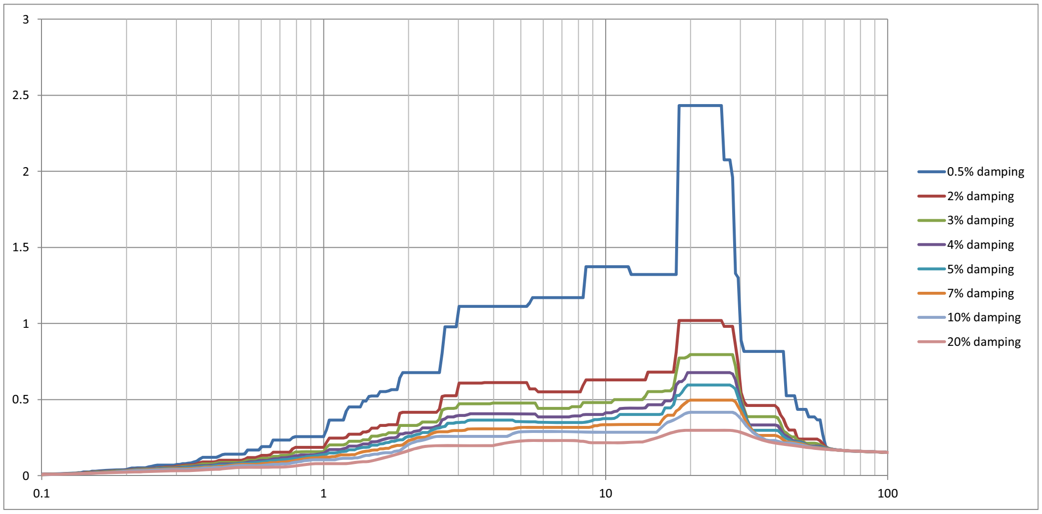

**Figure 3MM-3 ISRS for PSFSV (Sheet 12 of 18)
Interior Walls Z-direction (vertical)**

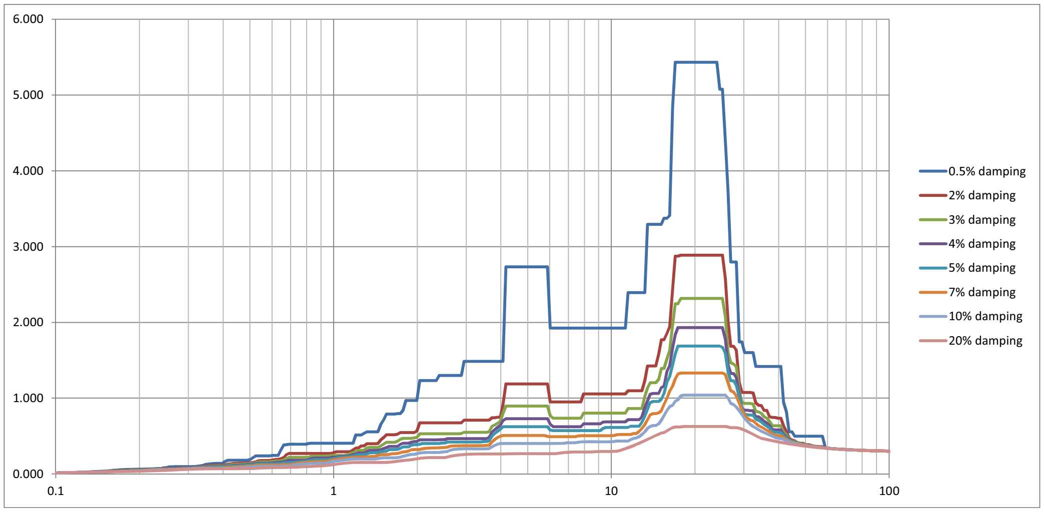

Figure 3MM-3 ISRS for PSFSV (Sheet 13 of 18)
Fuel Access Tunnel (all components) X-direction (north-south)

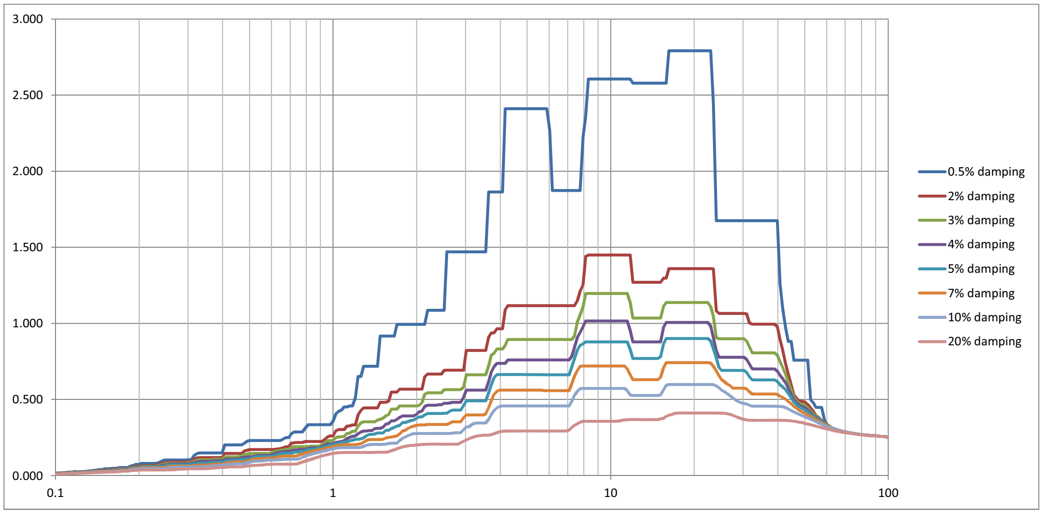

Figure 3MM-3 ISRS for PSFSV (Sheet 14 of 18)
Fuel Access Tunnel (all components) Y-direction (east-west)

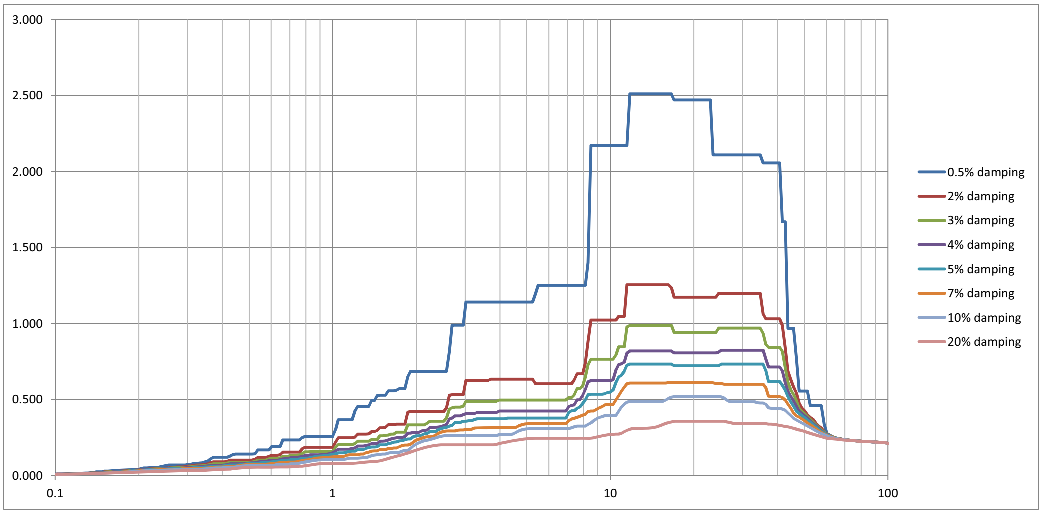

Figure 3MM-3 ISRS for PSFSV (Sheet 15 of 18)
Fuel Access Tunnel (all components) Z-direction (vertical)

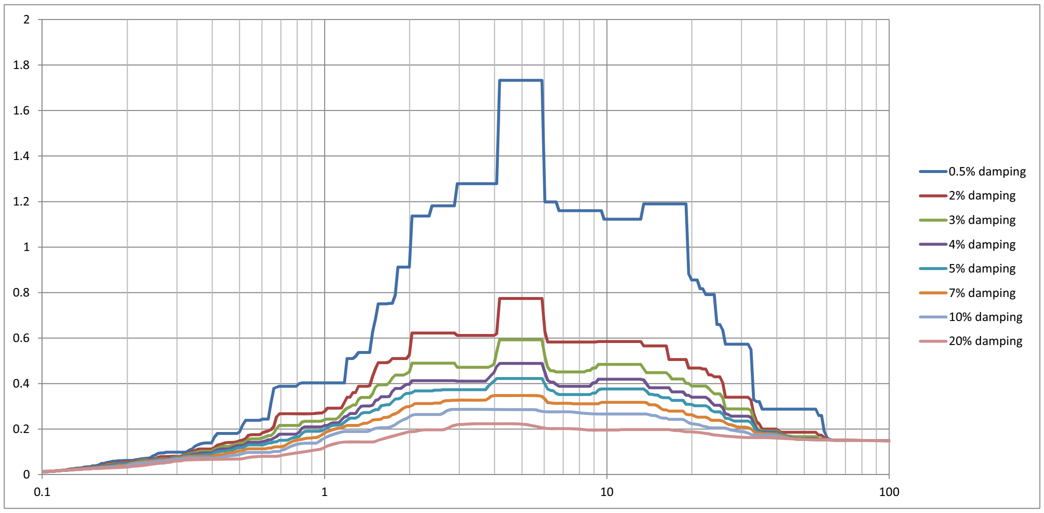

Figure 3MM-3 ISRS for PSFSV (Sheet 16 of 18)
Basemat X-direction (north-south)

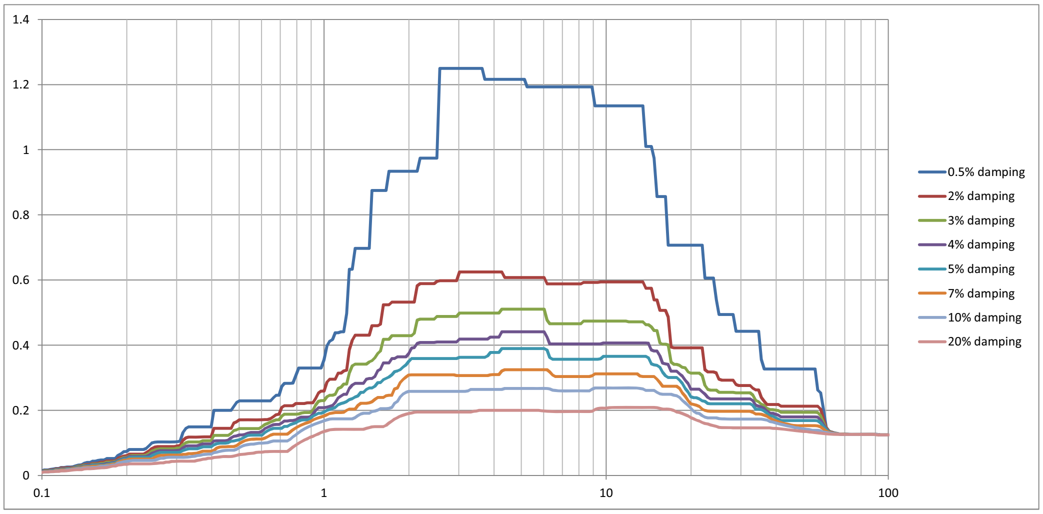

Figure 3MM-3 ISRS for PSFSV (Sheet 17 of 18)
Basemat Y-direction (east-west)

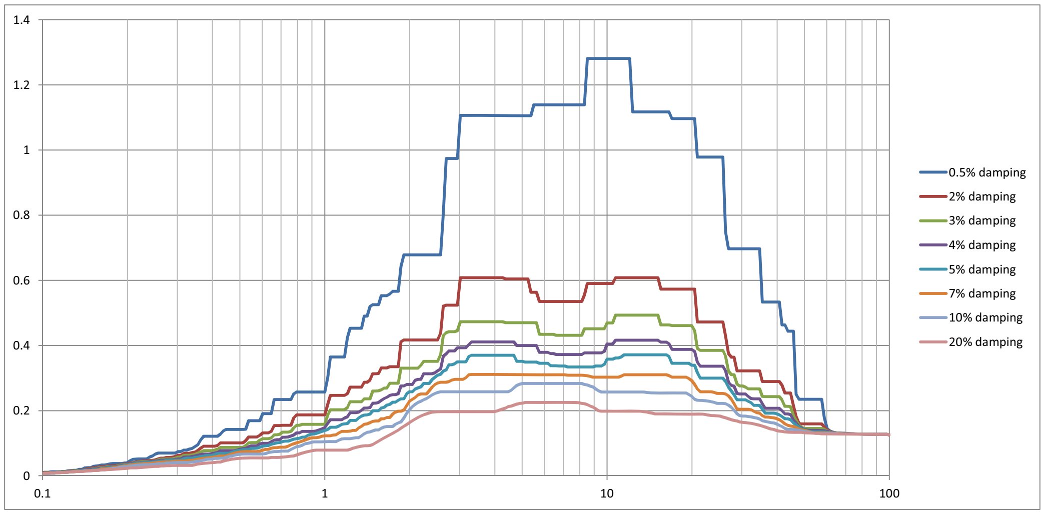

Figure 3MM-3 ISRS for PSFSV (Sheet 18 of 18)
Basemat Z-direction (vertical)

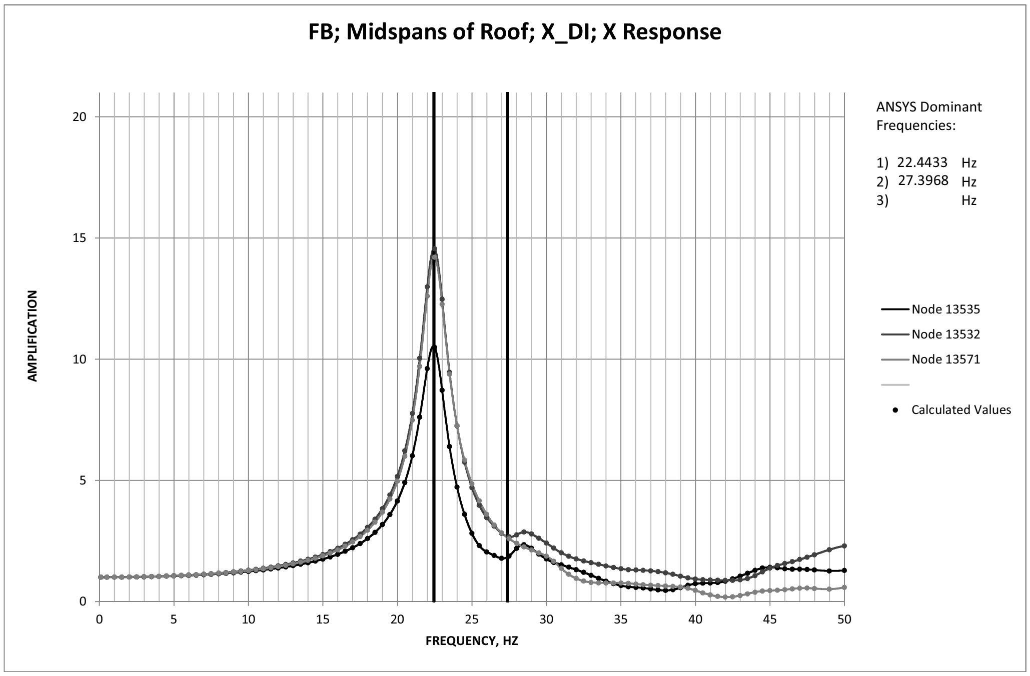

Figure 3MM-4 SASSI Fixed Base Transfer Functions for Midspans of PSFSV Roof Panels (Sheet 1 of 3)

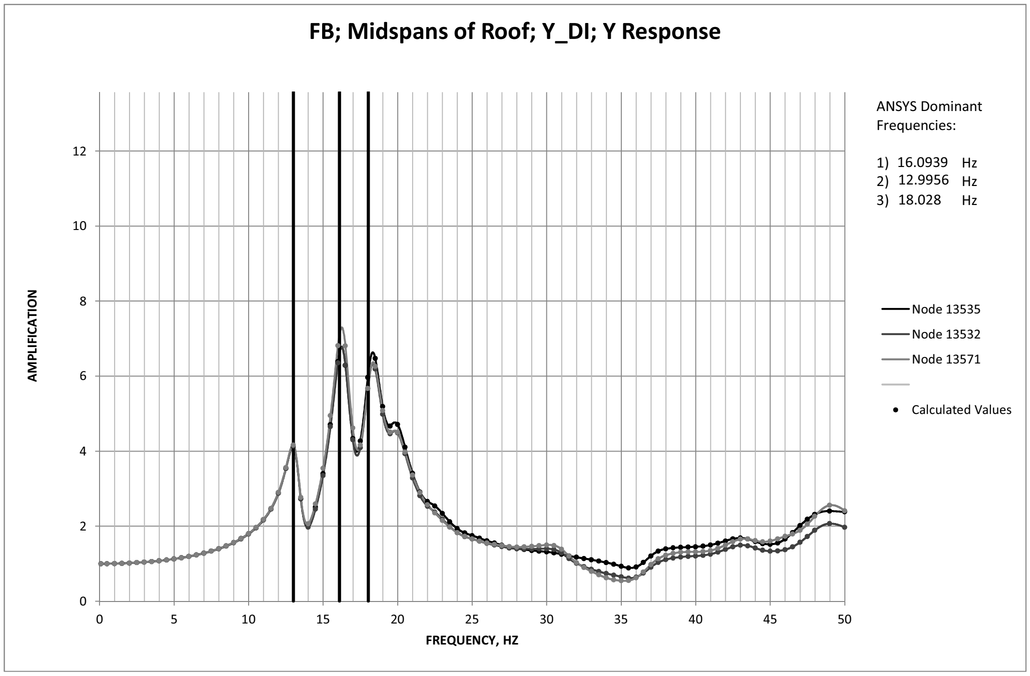

Figure 3MM-4 SASSI Fixed Base Transfer Functions for Midspans of PSFSV Roof Panels (Sheet 2 of 3)

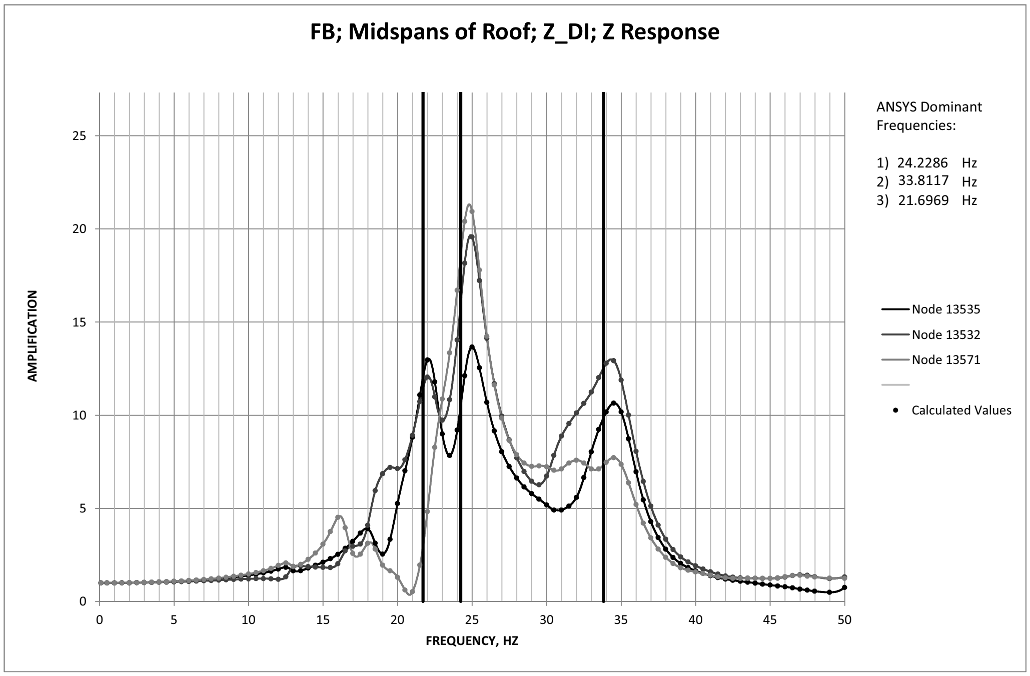

Figure 3MM-4 SASSI Fixed Base Transfer Functions for Midspans of PSFSV Roof Panels (Sheet 3 of 3)

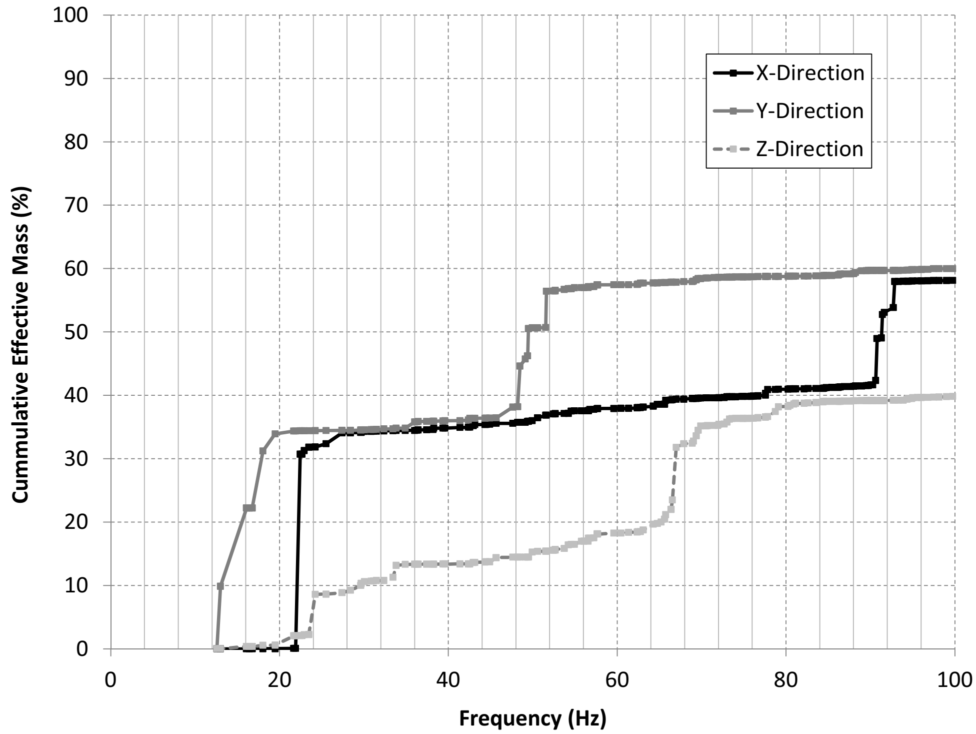

Figure 3MM-5 Cumulative Effective Mass from ANSYS Fixed Base Model

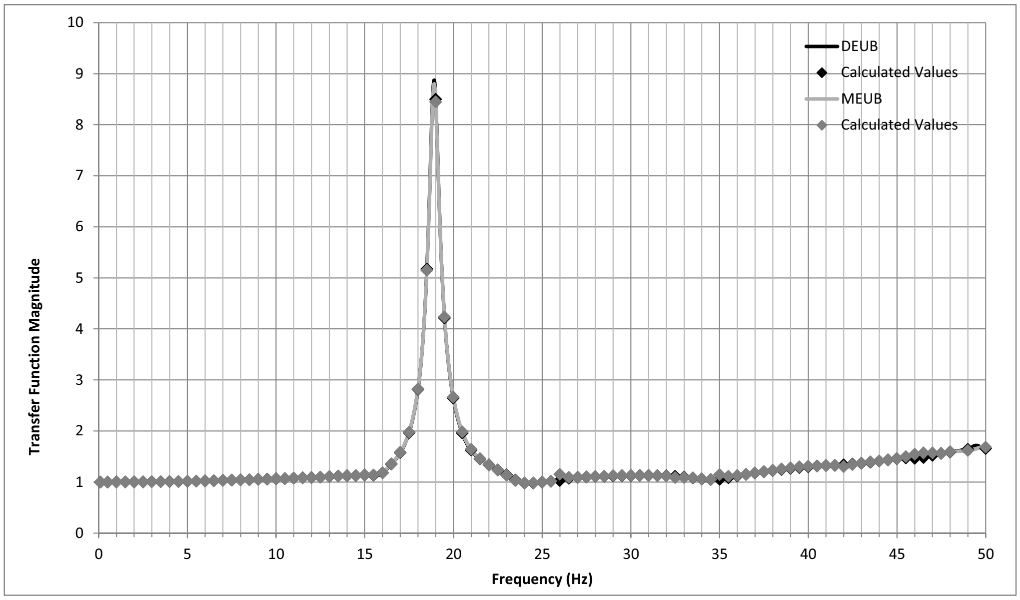

The above ATF plot is for the southeast corner of the PSFSV roof slab for the z-direction (vertical direction). The differences between results for the direct method versus the modified subtraction method are negligible.

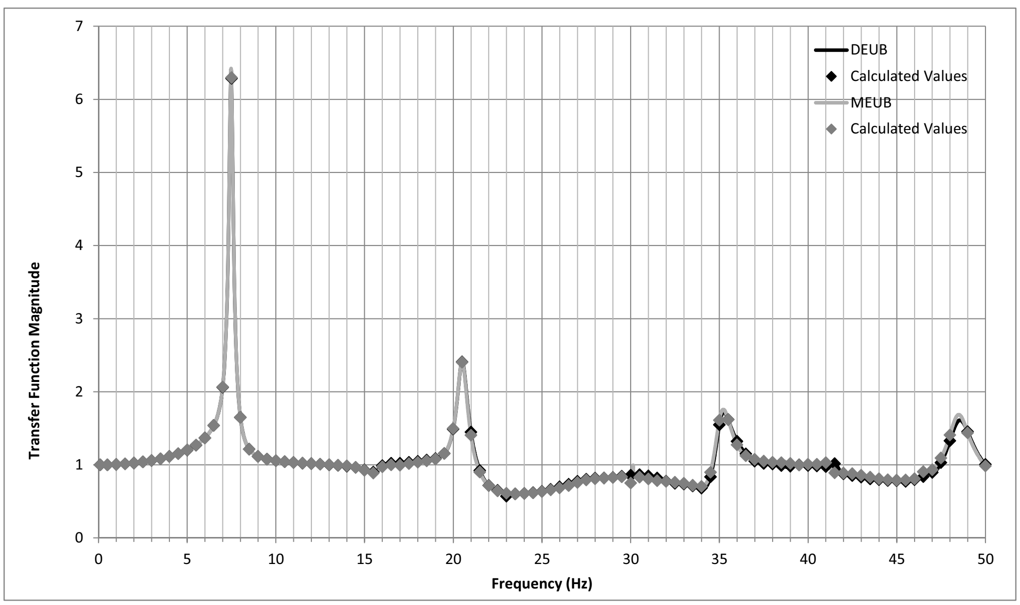

The above ATF plot is for the southeast corner of the PSFSV roof slab for the x-direction (north-south direction). The differences between results for the direct method versus the modified subtraction method are negligible.

Note: For Figure 3MM-6, DEUB = direct method embedded upper bound condition and MEUB = modified subtraction method embedded upper bound condition

Figure 3MM-6 Comparisons of Modified Subtraction Method versus Direct Method for PSFSV Embedded Analyses (Sheet 1 of 3)

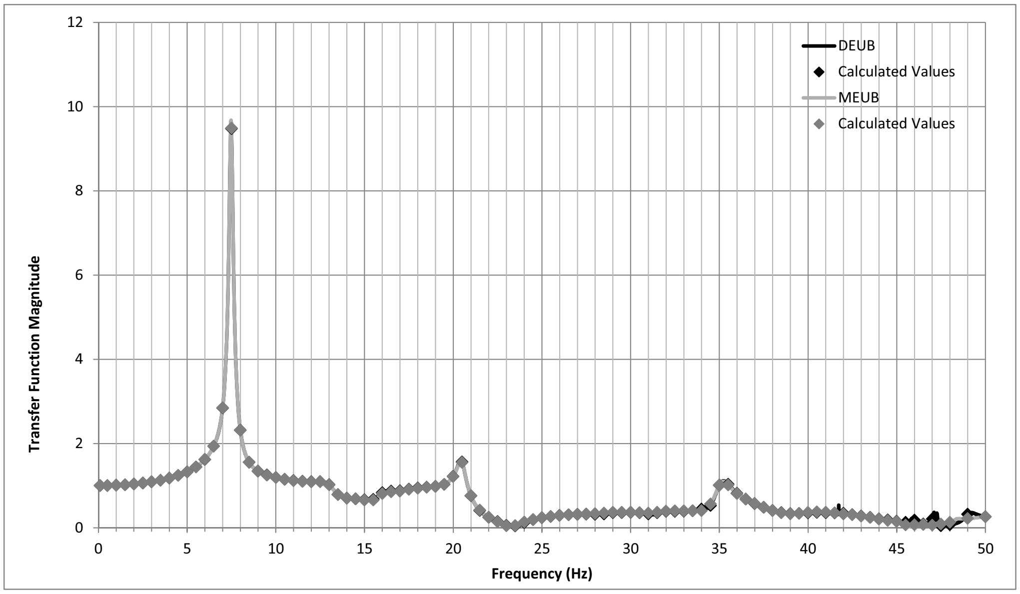

The above ATF plot is for the southeast corner of the PSFSV roof slab for the y-direction (east-west direction). The differences between results for the direct method versus the modified subtraction method are negligible.

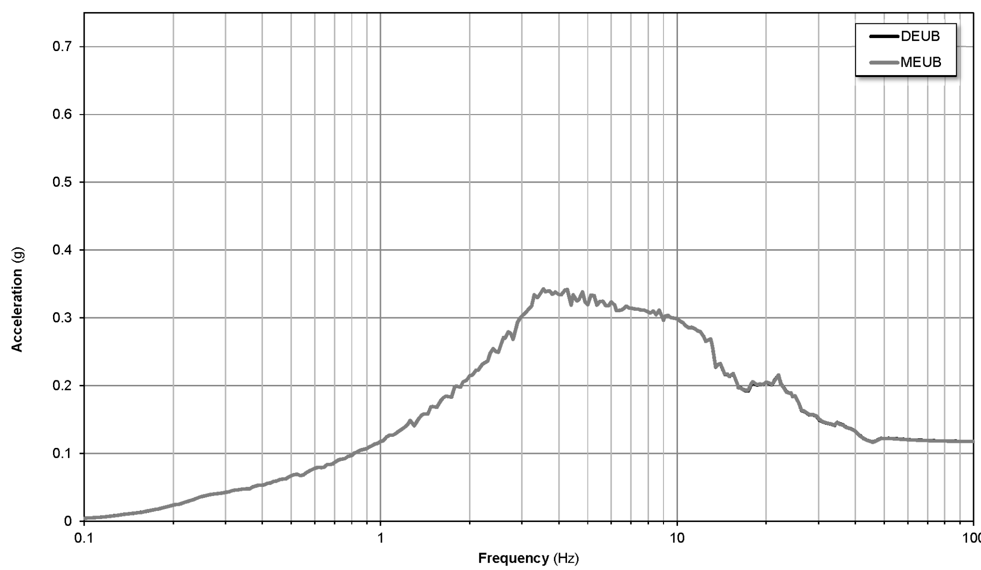

The ISRS at 5% damping in the above plot are for the center of the east PSFSV basemat for the z-direction (vertical). The differences between results for the direct method versus the modified subtraction method are negligible.

Figure 3MM-6 Comparisons of Modified Subtraction Method versus Direct Method for PSFSV Embedded Analyses (Sheet 2 of 3)

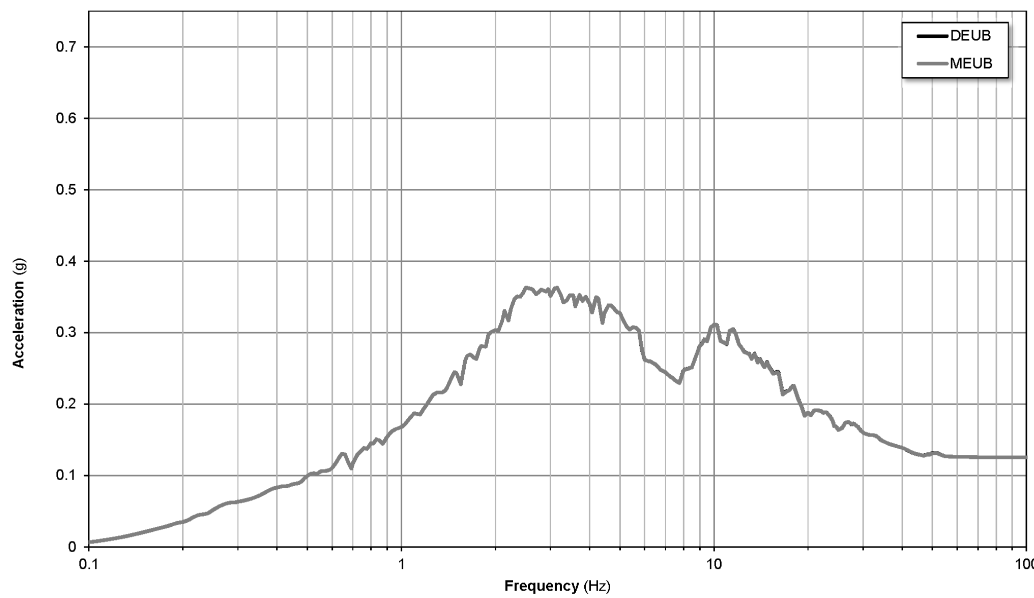

The ISRS at 5% damping in the above plot are for the center of the east PSFSV basemat for the x-direction (north-south). The differences between results for the direct method versus the modified subtraction method are negligible.

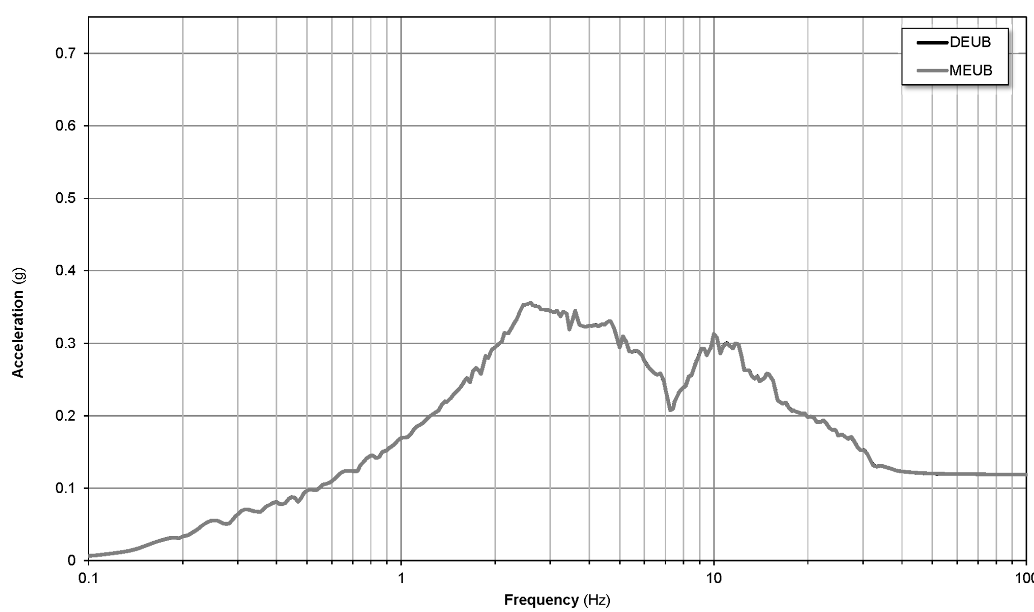

The ISRS at 5% damping in the above plot are for the center of the east PSFSV basemat for the y-direction (east-west). The differences between results for the direct method versus the modified subtraction method are negligible.

Figure 3MM-6 Comparisons of Modified Subtraction Method versus Direct Method for PSFSV Embedded Analyses (Sheet 3 of 3)

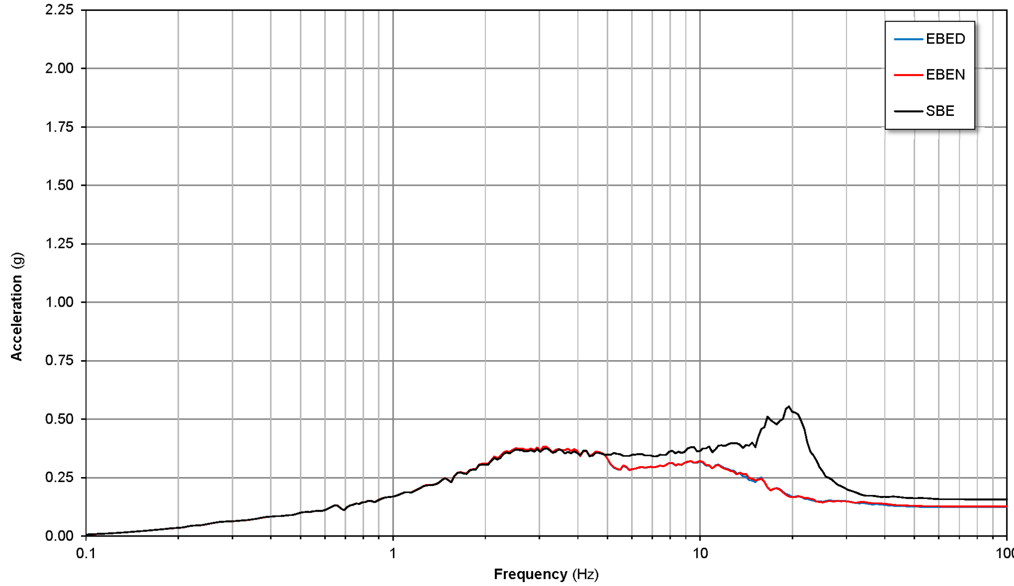

The above plot shows a comparison at the mid-height of the west wall of the PSFSV for the x-direction (north-south) response at 5% damping for saturated versus unsaturated conditions.

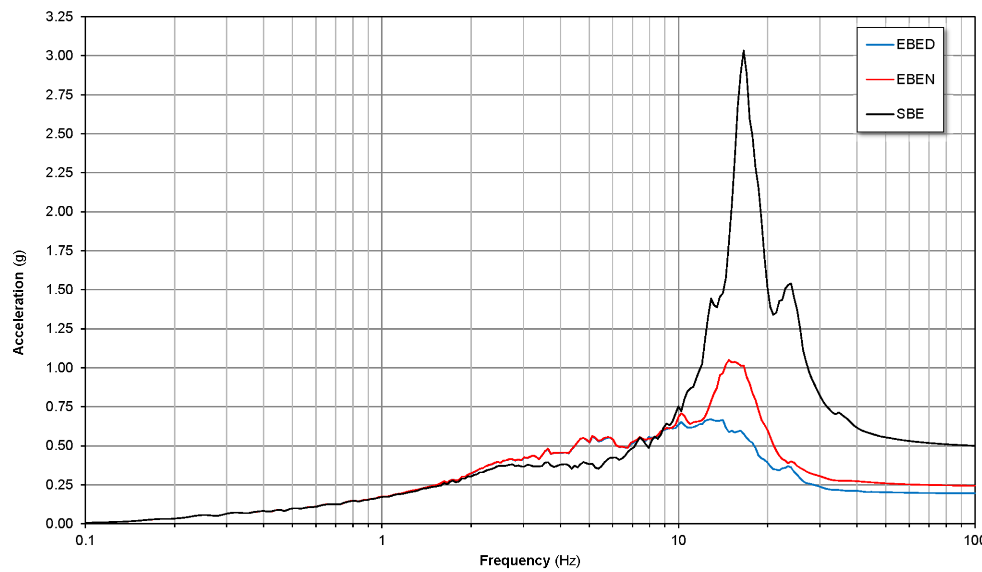

The above plot shows a comparison at the mid-height of the west wall of the PSFSV for the y-direction (east-west) response at 5% damping for saturated versus unsaturated conditions.

Note: For Figure 3MM-7, EBED = embedded best estimate dry (unsaturated); EBEN = embedded best estimate nominal (nominal GWL = 795'); and SBE = surface best estimate

Figure 3MM-7 Comparisons of In-structure Response Spectra for Saturated Versus Unsaturated Backfill Conditions (Sheet 1 of 3)

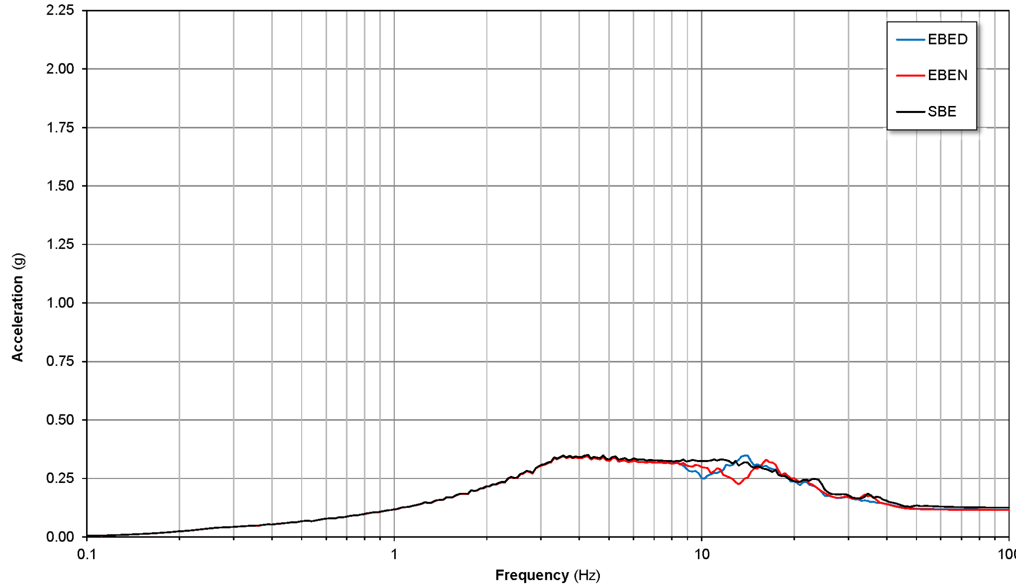

The above plot shows a comparison at the mid-height of the west wall of the PSFSV for the z-direction (vertical) response at 5% damping for saturated versus unsaturated conditions.

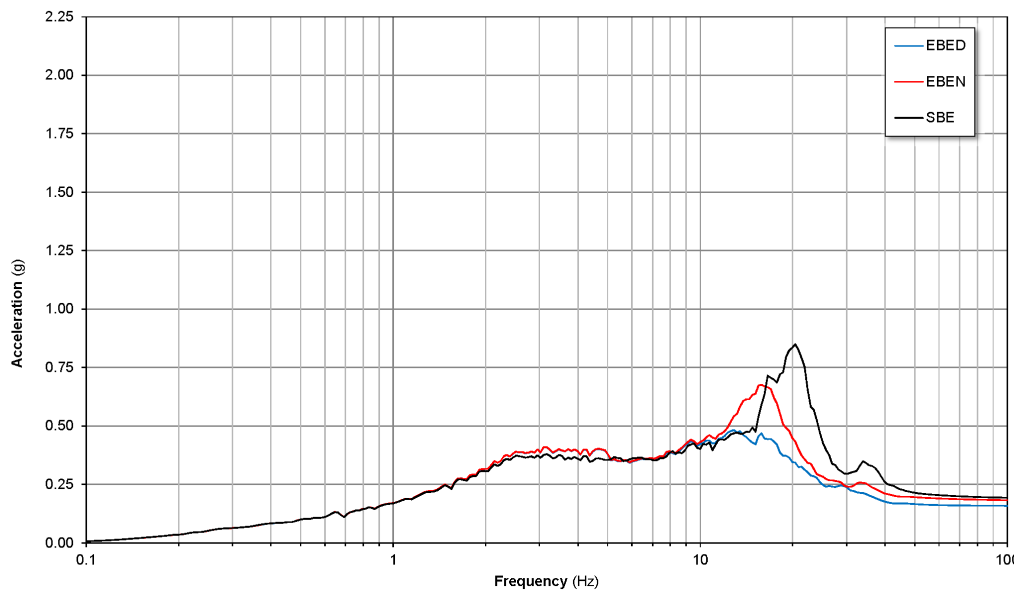

The above plot shows a comparison at the mid-height of the south wall of the PSFSV for the x-direction (north-south) response at 5% damping for saturated versus unsaturated conditions.

Figure 3MM-7 Comparisons of In-structure Response Spectra for Saturated Versus Unsaturated Backfill Conditions (Sheet 2 of 3)

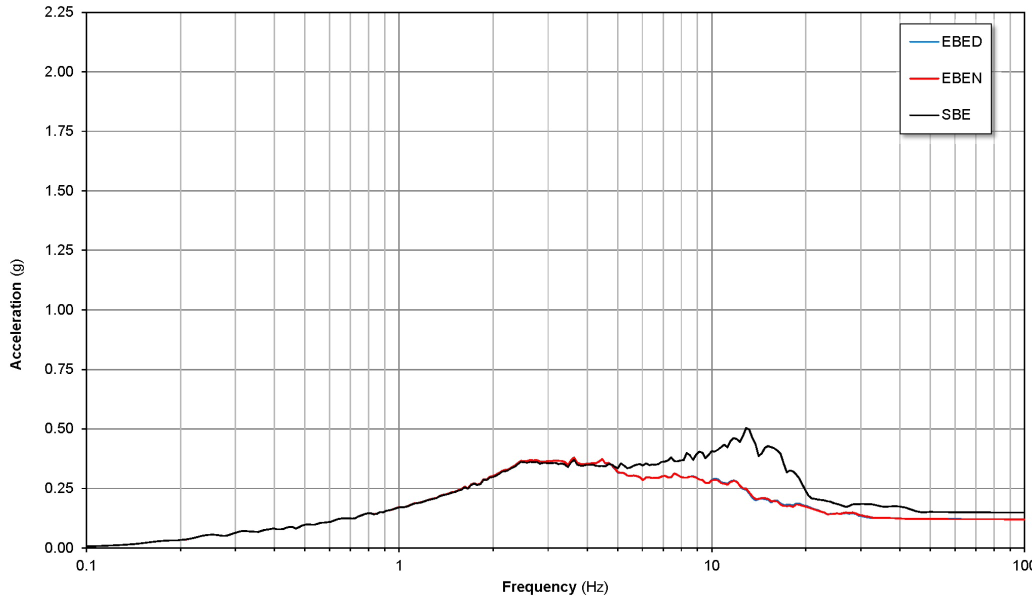

The above plot shows a comparison at the mid-height of the south wall of the PSFSV for the y-direction (east-west) response at 5% damping for saturated versus unsaturated conditions.

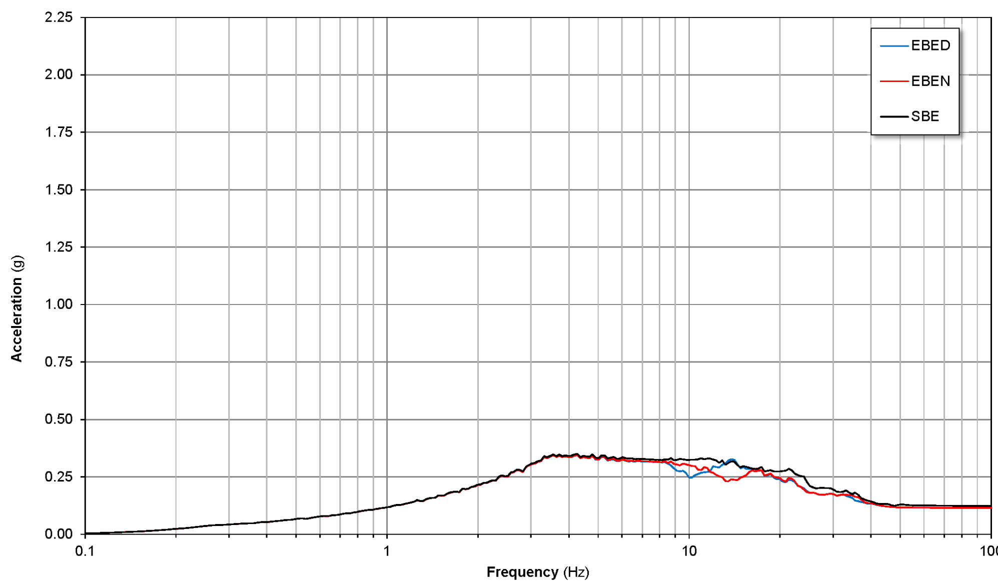

The above plot shows a comparison at the mid-height of the south wall of the PSFSV for the z-direction (vertical) response at 5% damping for saturated versus unsaturated conditions.

Figure 3MM-7 Comparisons of In-structure Response Spectra for Saturated Versus Unsaturated Backfill Conditions (Sheet 3 of 3)

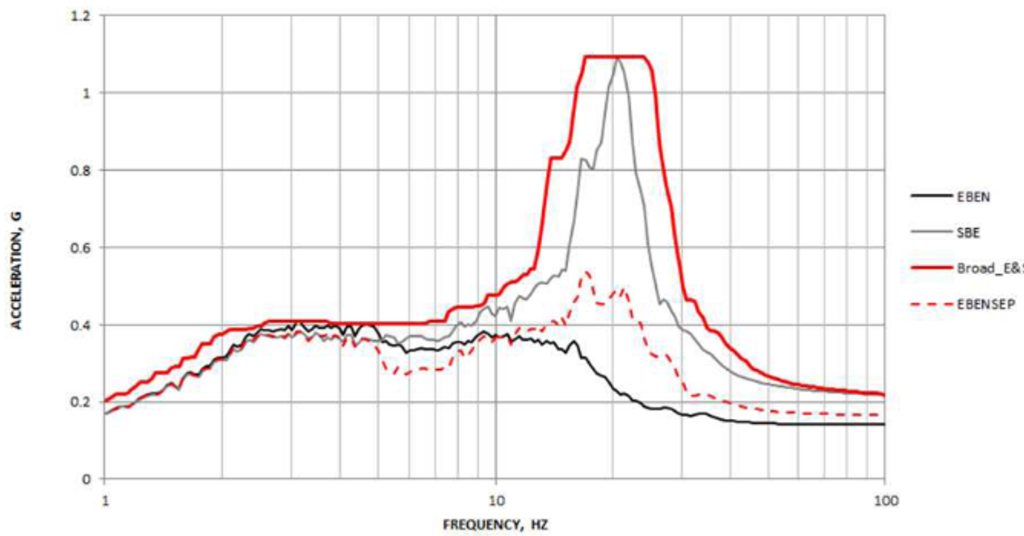

5% damping ISRS comparisons for PSFSV roof for x-direction (north-south)

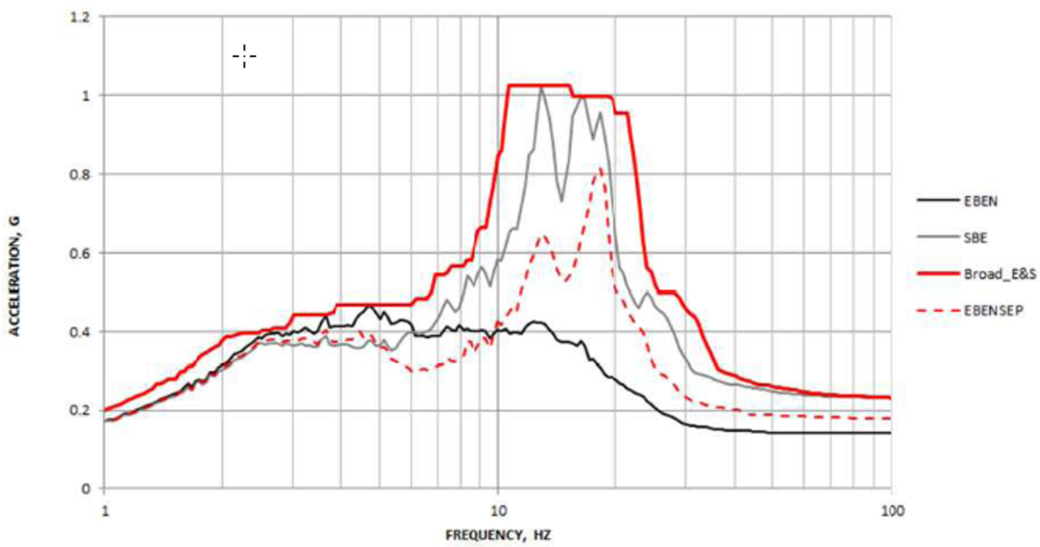

5% damping ISRS comparisons for PSFSV roof for y-direction (east-west)

Figure 3MM-8 Comparison of ISRS for Separated versus Non-separated Conditions (Sheet 1 of 3)

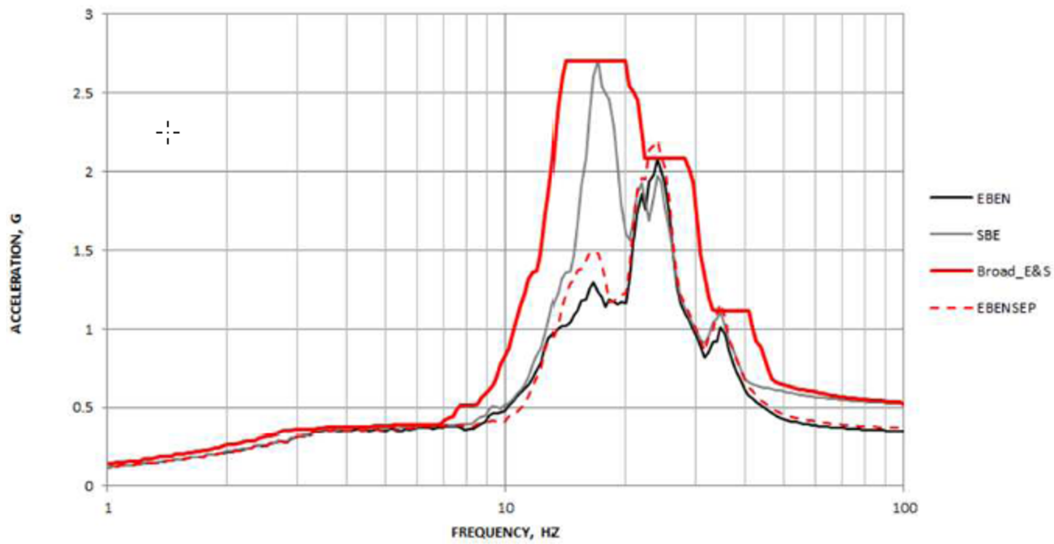

5% damping ISRS comparisons for PSFSV roof for z-direction (vertical)

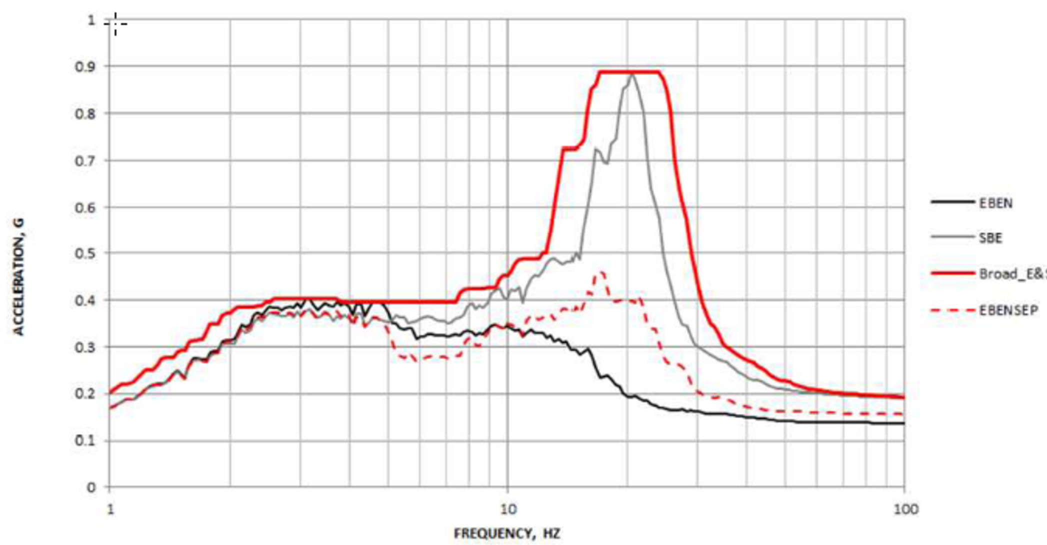

5% damping ISRS comparisons for PSFSV west wall for x-direction (north-south)

Figure 3MM-8 Comparison of ISRS for Separated versus Non-separated Conditions (Sheet 2 of 3)

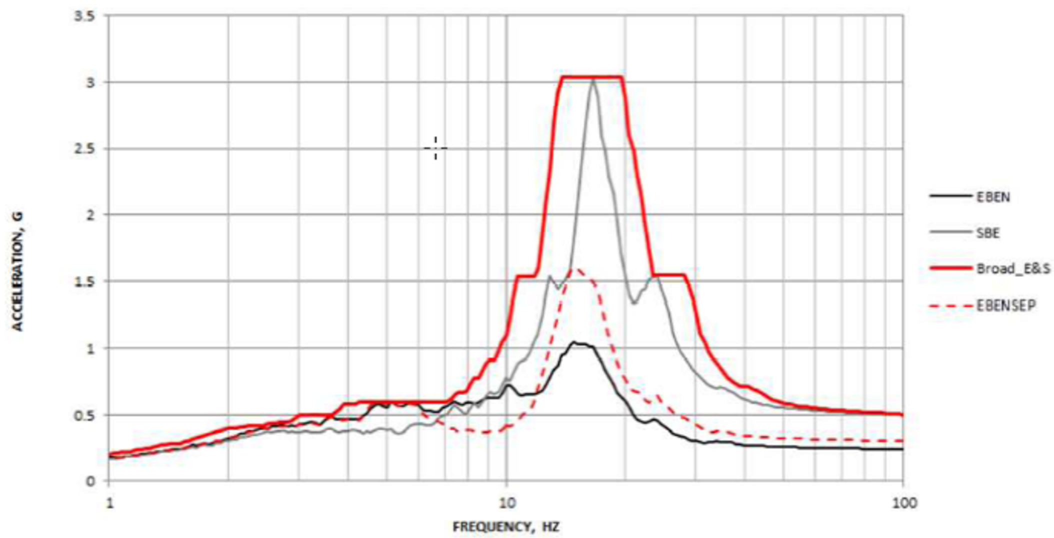

5% damping ISRS comparisons for PSFSV west wall for y-direction (east-west)

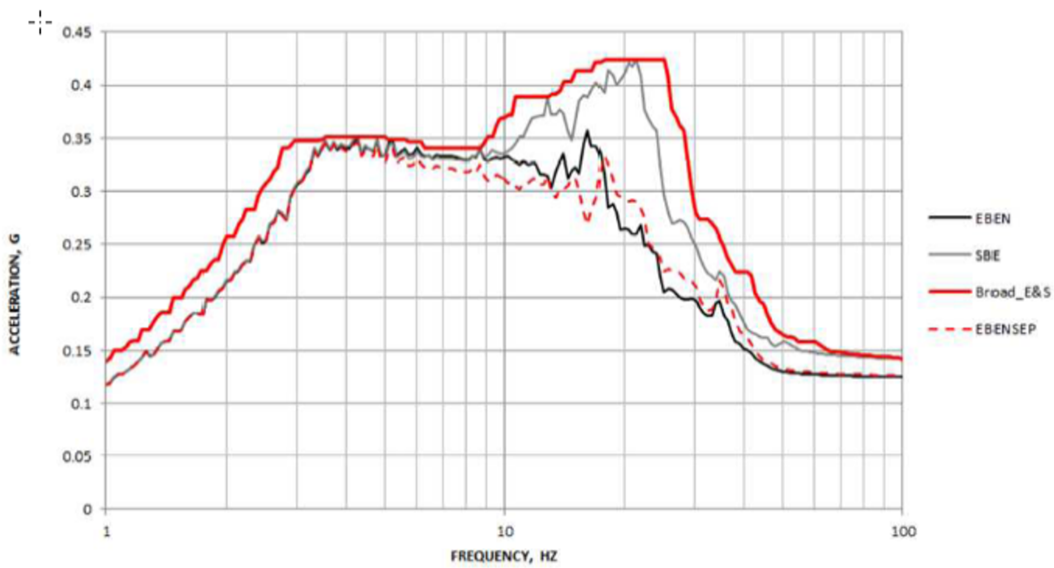

5% damping ISRS comparisons for PSFSV west wall for z-direction (vertical)

Figure 3MM-8 Comparison of ISRS for Separated versus Non-separated Conditions (Sheet 3 of 3)

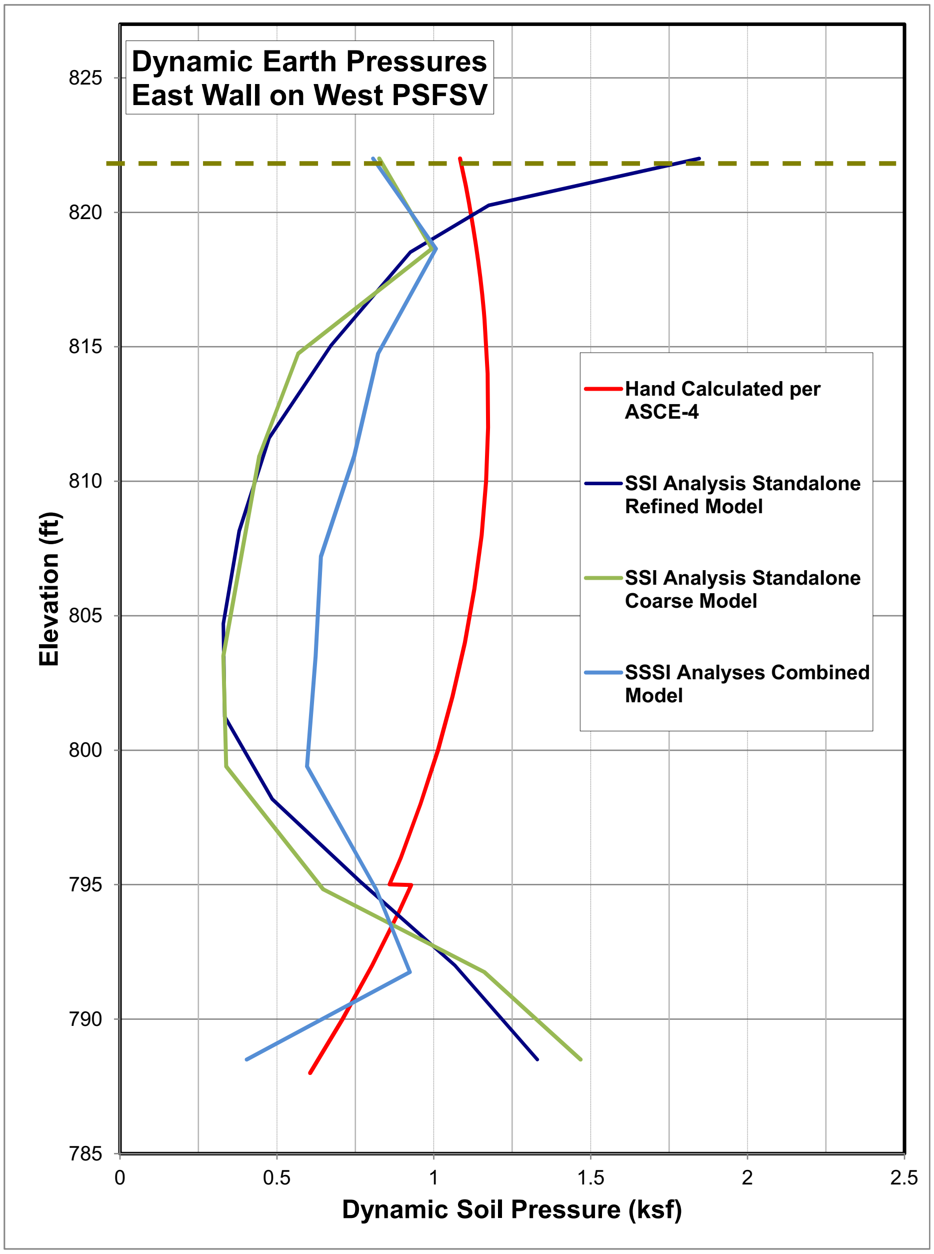

Figure 3MM-9 Example Comparison of Dynamic Soil Pressures Derived from ASCE 4 Versus SSI and SSSI Analysis Results for East Wall of West PSFSV

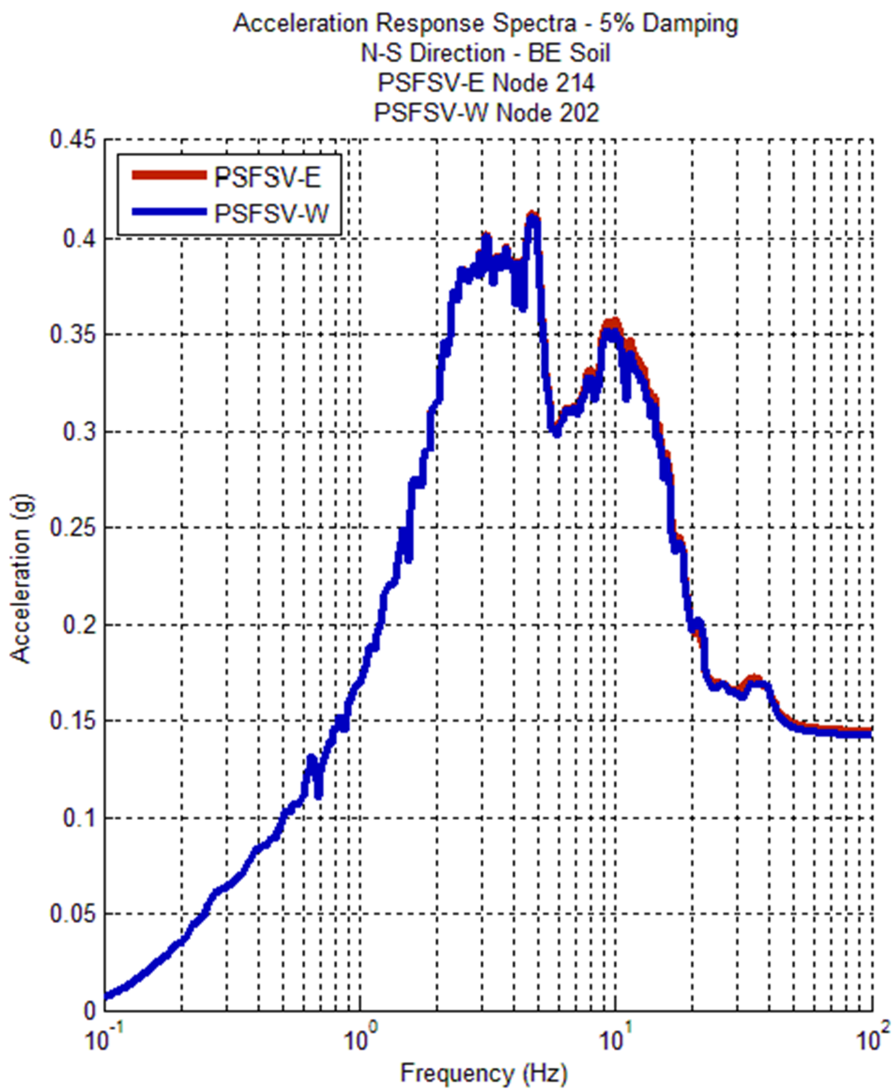

This plot shows the ARS obtained for a node at the southwest corner of the roof of the east PSFSV versus the ARS obtained at the "mirror image" node at the southeast corner of the roof of the west PSFSV, for the x-direction (north-south) at 5% damping.

Figure 3MM-10 Comparison of ISRS for East PSFSV versus West PSFSV (Sheet 1 of 3)

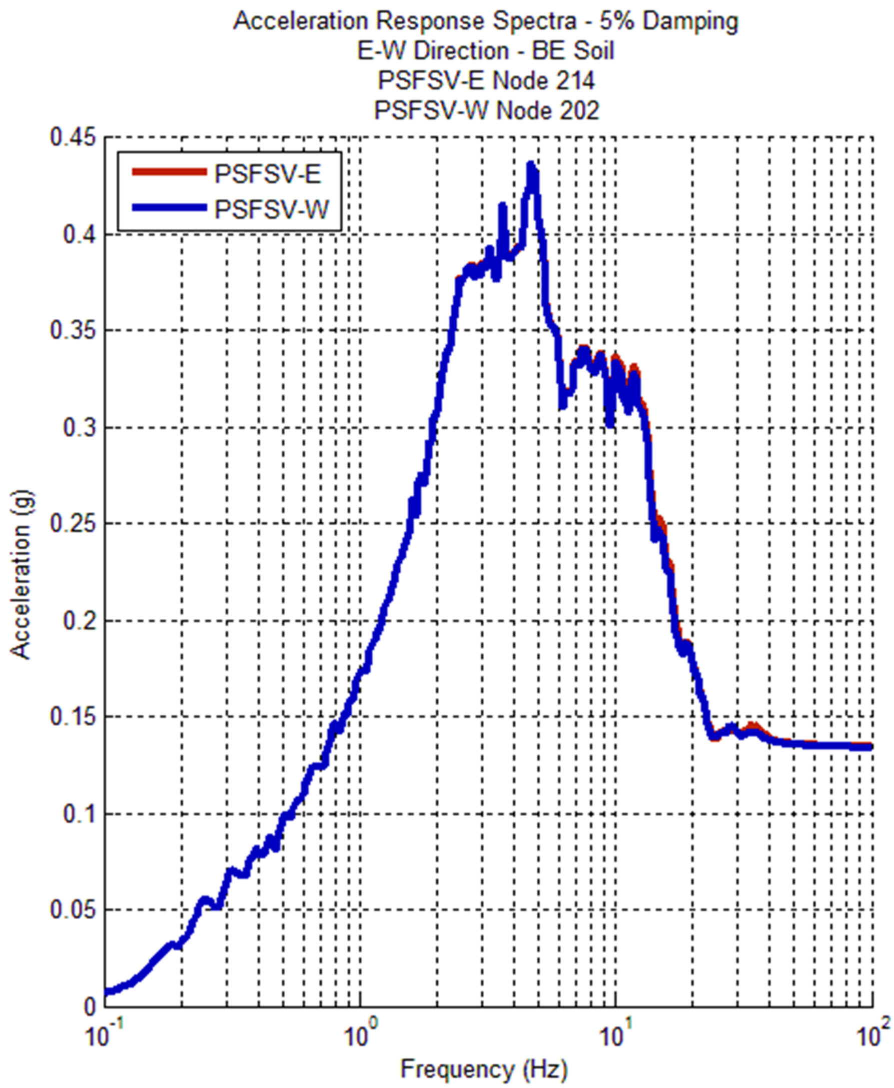

This plot shows the ARS obtained for a node at the southwest corner of the roof of the east PSFSV versus the ARS obtained at the "mirror image" node at the southeast corner of the roof of the west PSFSV, for the y-direction (east-west) at 5% damping.

Figure 3MM-10 Comparison of ISRS for East PSFSV versus West PSFSV (Sheet 2 of 3)

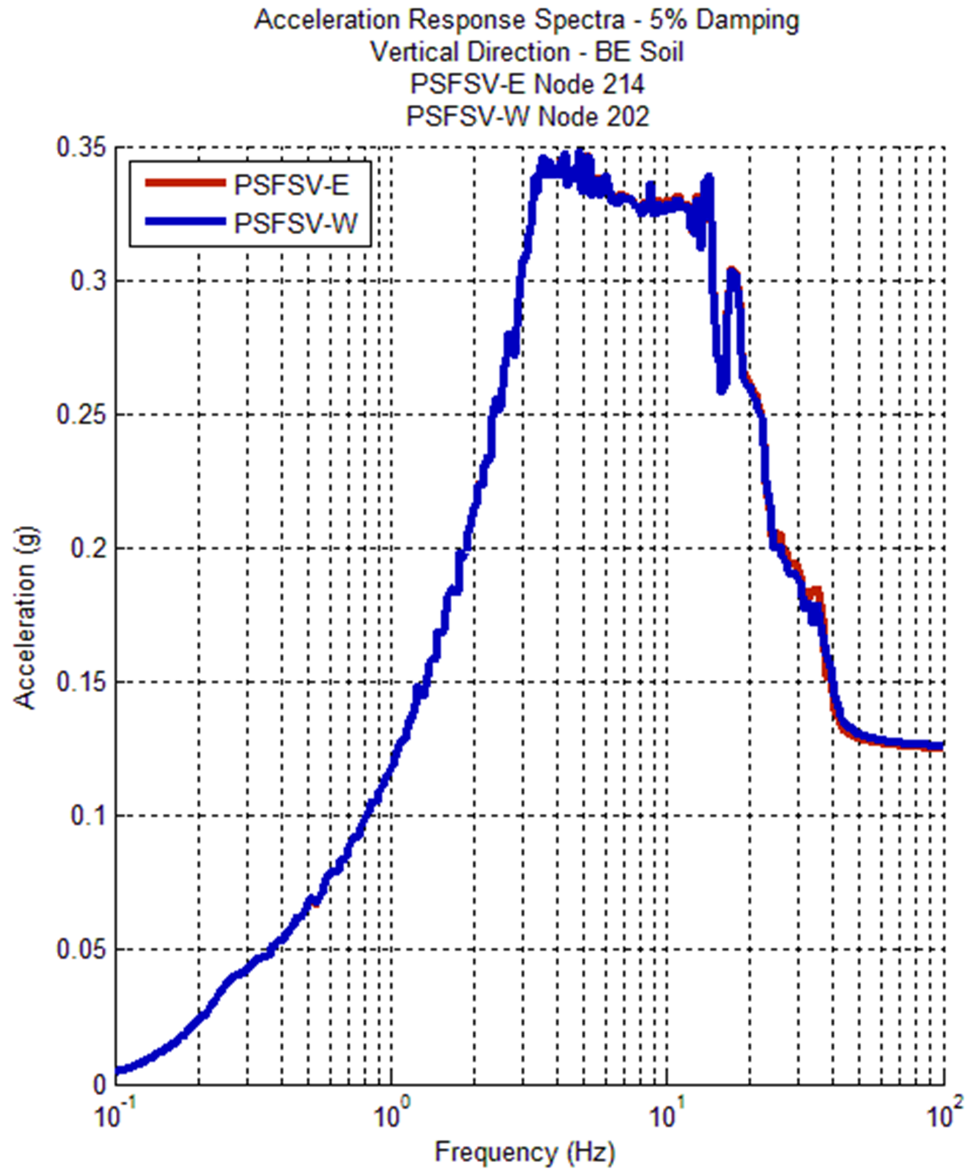

This plot shows the ARS obtained for a node at the southwest corner of the roof of the east PSFSV versus the ARS obtained at the "mirror image" node at the southeast corner of the roof of the west PSFSV, for the z-direction (vertical) at 5% damping.

Figure 3MM-10 Comparison of ISRS for East PSFSV versus West PSFSV(Sheet 3 of 3)

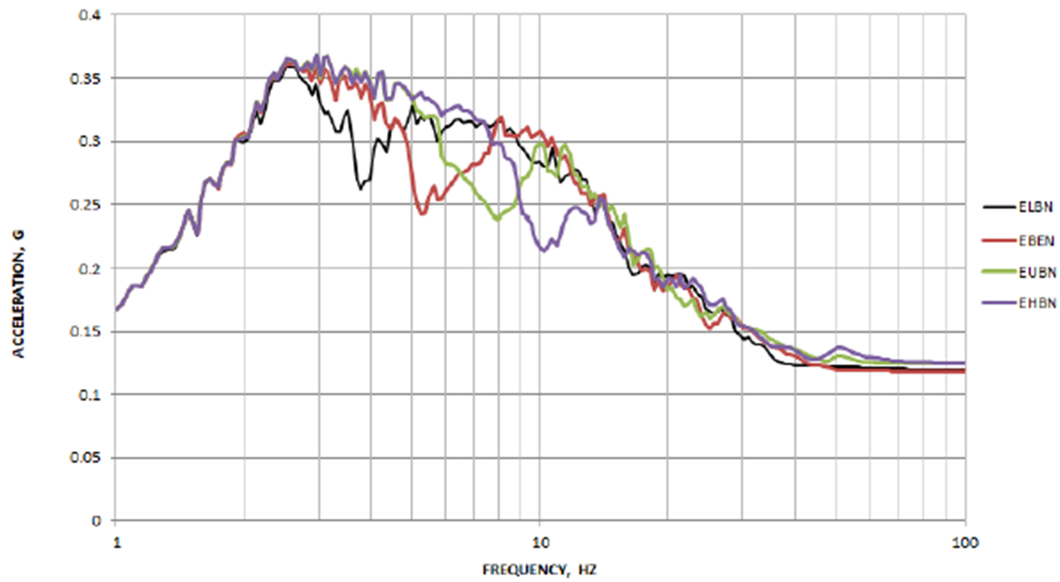

This plot is for a node located at the northwest corner of the PSFSV basemat, for the x-direction (north-south). The spectral values for this node beyond about 30 Hz are all controlled by the EUB and EHB soil case, compared to ELB or EBE.

Figure 3MM-11 Comparison of ISRS for Various Embedded Conditions (Sheet 1 of 3)

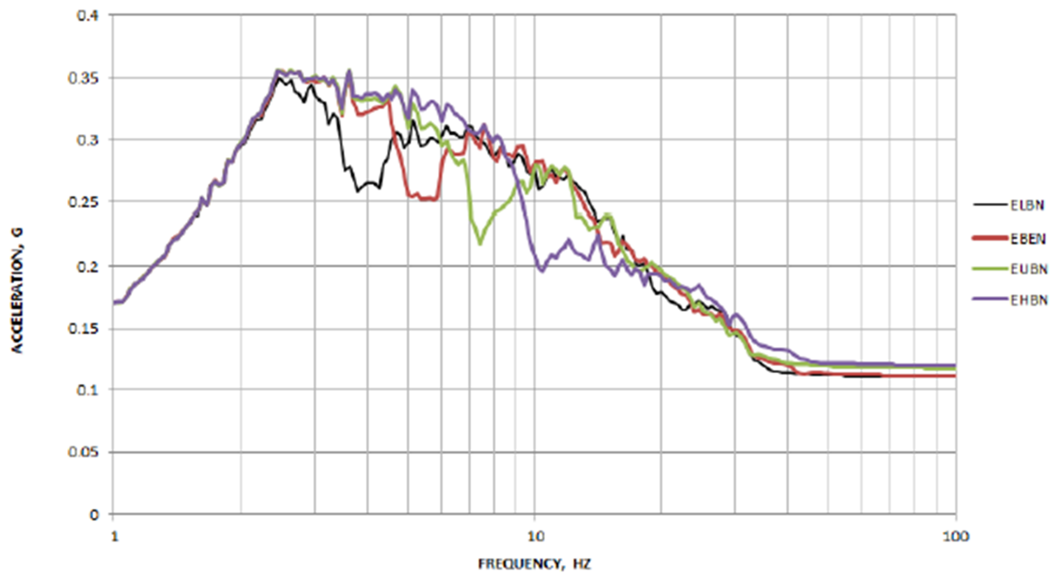

This plot is for a node located at the northwest corner of the PSFSV basemat, for the y-direction (east-west). The spectral values for this node beyond about 20 Hz are all controlled by the EHB and/or EUB soil cases, compared to ELB or EBE.

Figure 3MM-11 Comparison of ISRS for Various Embedded Conditions (Sheet 2 of 3)

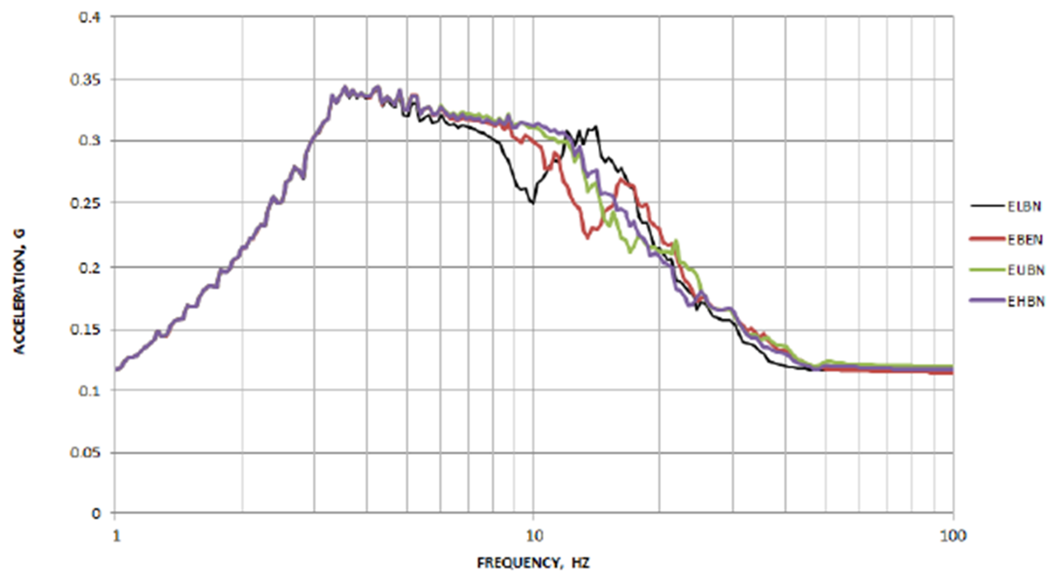

This plot is for a node located at the northwest corner of the PSFSV basemat, for the z-direction (vertical). The spectral values for this node beyond about 35 Hz are all controlled by the EHB and/or EUB soil cases, compared to ELB or EBE.

Figure 3MM-11 Comparison of ISRS for Various Embedded Conditions (Sheet 3 of 3)

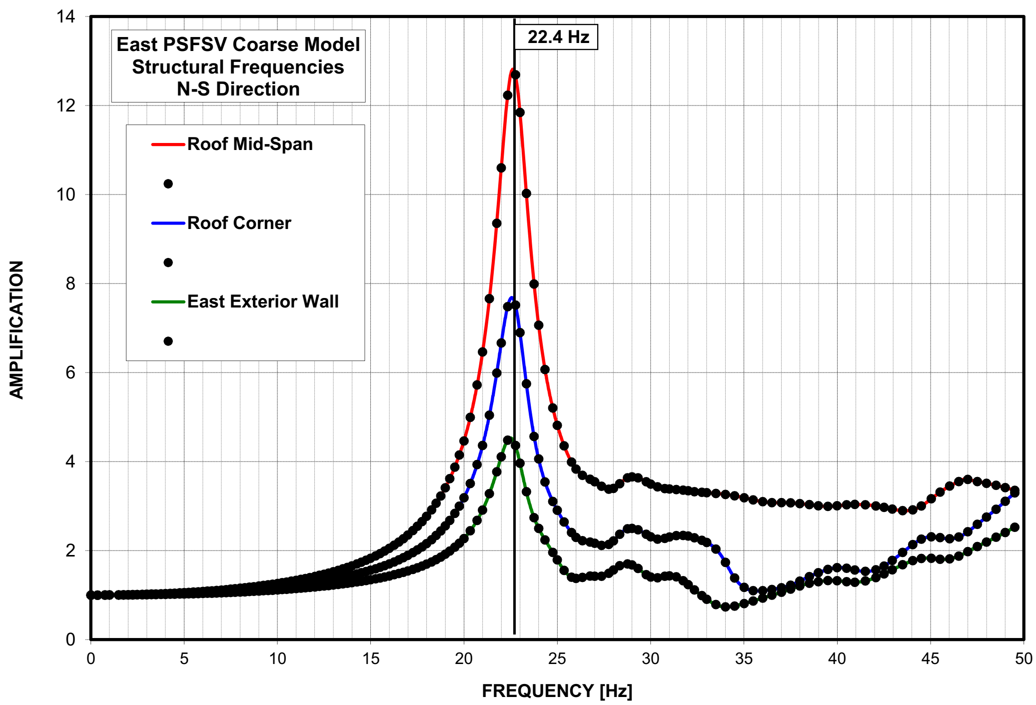

Figure 3MM-12 SASSI Fixed Base Transfer Function for Coarse Mesh Model of East PSFSV at Roof Locations, X-Direction (North-South) (Sheet 1 of 3)

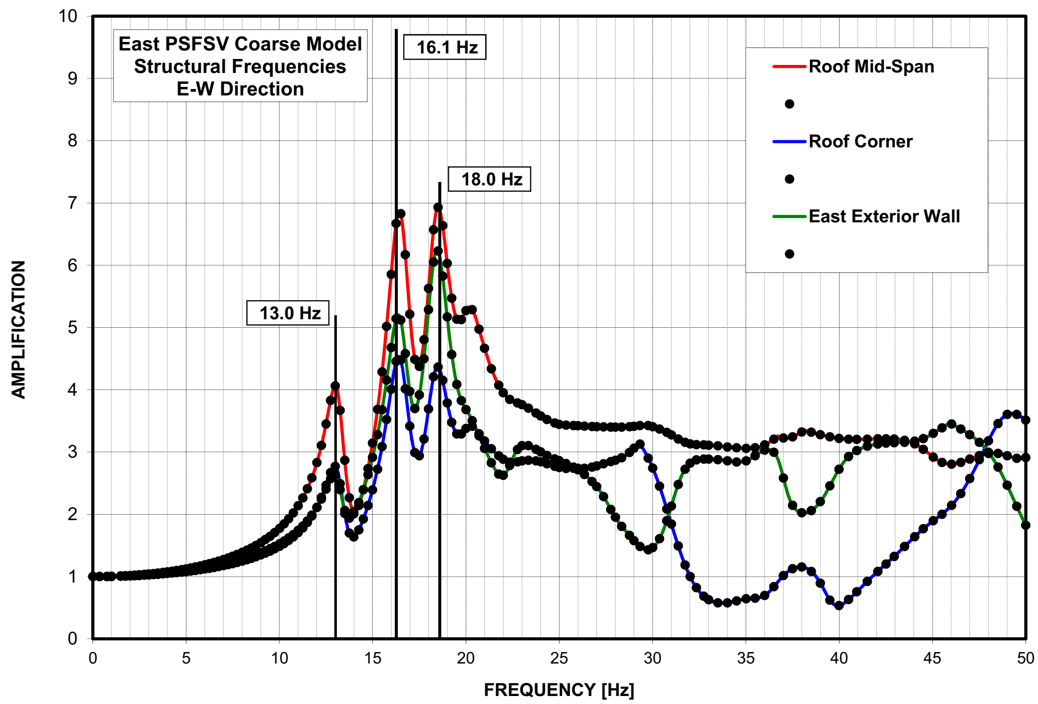

Figure 3MM-12 SASSI Fixed Base Transfer Function for Coarse Mesh Model of East PSFSV at Roof Locations, Y-Direction (East-West) (Sheet 2 of 3)

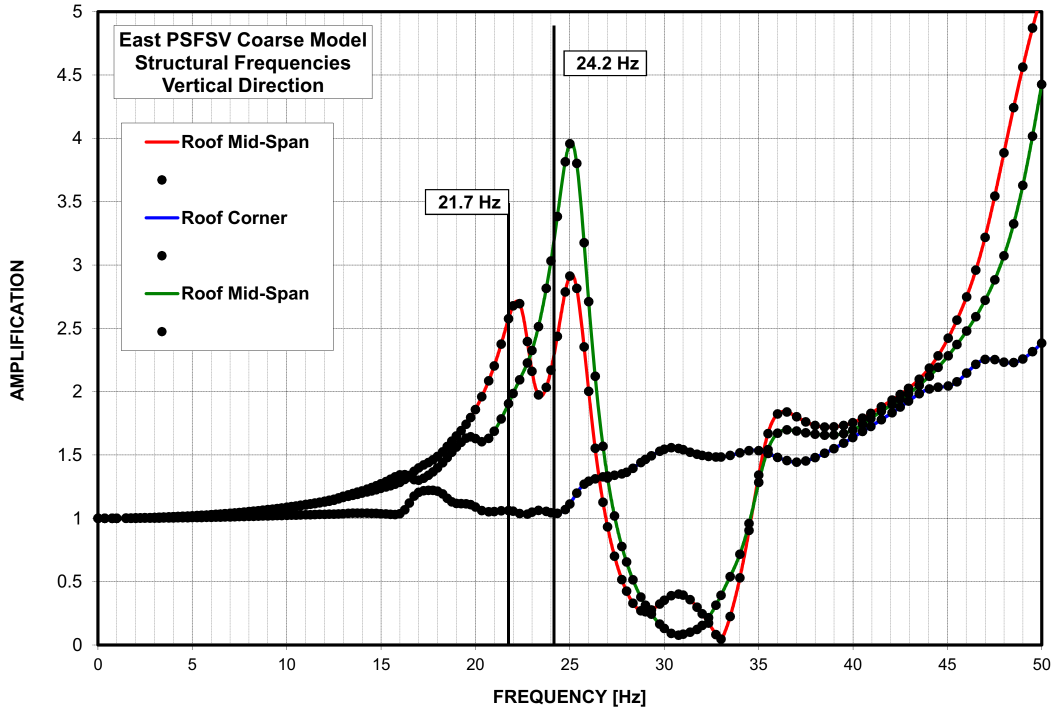

Figure 3MM-12 SASSI Fixed Base Transfer Function for Coarse Mesh Model of East PSFSV at Roof Locations, Z-Direction (Vertical) (Sheet 3 of 3)

CP COL 3.7(20)
CP COL 3.7(23)
CP COL 3.7(25)

APPENDIX 3NN

SITE-SPECIFIC SSI ANALYSIS OF R/B COMPLEX STRUCTURES

TABLE OF CONTENTS

LIST OF TABLES

LIST OF FIGURES

LIST OF FIGURES (Continued)

LIST OF FIGURES (Continued)

ACRONYMS AND ABBREVIATIONS

Acronyms	Definitions
3D	three-dimensional
A/B	auxiliary building
ARS	acceleration response spectra
ATF	acceleration transfer functions
BE	best estimate
CIS	containment internal structure
COV	coefficient of variation
CPNPP 3&4	Comanche Peak Nuclear Power Plant Units 3 and 4
CSDRS	certified seismic design response spectra
DCD	Design Control Document
FE	finite element
EBE	embedded best estimate
ELB	embedded lower bound
ESWPC	essential service water pipe chase
ESWPT	essential service water pipe tunnel
EHB	embedded high bound
EUB	embedded upper bound
FH/A	fuel handling area
GMRS	ground motion response spectra
GWL	ground water level
HB	high bound
ISRS	in-structure response spectra
LB	lower bound
MSM	modified subtraction method
NS	north-south
OBE	operating-basis earthquake

Acronyms	Definitions
P	compression
PCCV	prestressed concrete containment vessel
PS/B	power source building
PSFSV	power source fuel storage vault
R/B	reactor building
S	shear
SBE	surface best estimate
SDOF	single degree of freedom
SLB	surface lower bound
SUB	surface upper bound
SRSS	square root sum of the squares
SSE	safe-shutdown earthquake
SSI	soil-structure interaction
UB	upper bound
UHSRS	ultimate heat sink related structures
V_p	compression wave velocity
V_s	shear wave velocity

3NN SITE-SPECIFIC SSI ANALYSIS OF R/B COMPLEX STRUCTURES

3NN.1 Introduction

This Appendix documents the site-specific soil structure interaction (SSI) analysis of the US-APWR Reactor Building (R/B) complex of Comanche Peak Nuclear Power Plant Units 3 and 4 (CPNPP 3 & 4). The R/B complex is a US-APWR standard plant building which consists of the prestressed concrete containment vessel (PCCV), containment internal structure (CIS) and the reinforced concrete shear wall structure surrounding the reactor containment, all resting on a common reinforced basemat., This reinforced concrete shear wall structure integrates the reactor building (R/B), including the fuel handling area (FH/A), the power source buildings (East PS/B and West PS/B) and auxiliary building (A/B),Also included in the complex is the essential service water pipe chase (ESWPC) integrated at the south end of the basemat.

As stated in Subsection 3.7.2.4.5, site-specific SSI analyses of the R/B complex are performed to validate the US-APWR standard plant seismic design for the CPNPP 3 & 4 site, and to confirm that site-specific SSI effects are enveloped by the site-independent SSI analysis. The methodology and models used for these site-specific SSI analyses are consistent with those used for the standard design site-independent SSI analyses described in Subsection 3.7.2.4. The SASSI computer program (Reference 3NN-1) serves as a computational platform for the site-specific SSI analyses. Models of the R/B complex structures used in the site-specific SSI analyses are based on the design basis R/B complex dynamic finite element (FE) model used for standard plant design site-independent SSI analyses described in Subsection 3.7.2.3. The site-specific SSI analyses utilize input design ground motion as well as soil/rock properties and layering that are specific to the CPNPP 3 & 4 site. The approach utilized for the SSI analyses ensures that the following SSI site-specific effects are addressed:

- Dynamic properties of the R/B complex structures corresponding to site-specific stress levels under normal operating and accidental thermal conditions
- Variation of dynamic properties of soil and rock materials that are compatible with the strains generated by the site-specific ground motion
- Ground water level (GWL)
- Lateral soil separation

It is demonstrated that in-structure response spectra (ISRS) and lateral earth pressure loads developed from the site-specific SSI analyses are enveloped by the standard plant seismic design.

3NN.2 Seismological and Geotechnical Considerations

The R/B complex will be constructed on a rock subgrade by removing the native soil above the top of the limestone layer with shear wave velocity exceeding 5000 fps that is located at nominal elevation of 782 ft. The R/B complex basemat will be embedded in the limestone over a depth of approximately 2.75 ft. The foundation will be backfilled with a 40 ft. thick layer of engineered fill material to establish the nominal elevation of the plant ground surface at 822 ft.

The SSI analyses use dynamic properties of the rock and backfill materials that are compatible to the strains generated by the site-specific design ground motion. The strain-compatible properties are developed based on the results of the site response analyses of randomized site profiles described in Subsection 2.5.2.6.3. The best estimate (BE) properties of rock and backfill layers are obtained as log mean of the randomized strain-compatible full column profiles that include the 40-ft thick strata of engineered backfill soil and the in-situ rock layers below nominal elevation of 782 ft. Besides the BE values, the site-specific analyses address the variation of the rock subgrade properties by considering lower bound (LB) and upper bound (UB) properties. The LB and UB properties represent a coefficient of variation (COV) on the subgrade shear modulus of at least 50% as required by SRP 3.7.2 (Reference 3NN-5). The typical properties for a granular engineered backfill are adopted as the BE values for the dynamic properties of the backfill. Four profiles, LB, BE, UB, and high bound (HB) of input backfill properties are developed for the SASSI analyses considering also a coefficient of variation of soil shear modulus of at least 50% as required by SRP 3.7.2. The LB and BE backfill profiles are combined with corresponding LB and BE rock subgrade profiles, and the UB and HB backfill profiles are combined with the UB rock subgrade profile. The SSI analyses use identical values for the shear S-wave and compression P-wave velocity damping. Figure 3NN-1, Figure 3NN-2, and Figure 3NN-3 present, respectively, the strain-compatible rock subgrade LB, BE and UB profiles for shear (S) wave velocity (Vs), compression (P) wave velocity (Vp) and material damping. Figure 3NN-4, Figure 3NN-5, and Figure 3NN-6 present the strain-compatible backfill properties. The site-specific SSI analyses of the R/B complex consider the ground water level (GWL) to be located at the top of the essential service water pipe tunnel (ESWPT) located approximately at elevation of 804 ft, to account for the bounding case when the ground water gets trapped within the perimeter of the ESWPT. The sensitivity study presented in Technical Report MUAP-11007(R2) (Reference 3NN-6) show that the sensitivity of the R/B complex response to variations in GWL is small and that consideration of saturated generic profiles yields responses of the R/B complex structures that envelop at almost all frequencies responses obtained considering unsaturated soil properties. Conclusions from this GWL sensitivity study performed for the standard design concur with findings from the sensitivity studies performed for site-specific seismic category I structures described in Appendices 3LL, 3KK, and 3MM. These site-specific sensitivity studies also demonstrate that responses obtained using full column profiles with higher GWL envelop responses obtained considering lower GWL for almost all frequencies. Compared to the heavy R/B complex that has a shallow embedment, the site-specific seismic category I structures such as the PSFSVs, UHSRS, and ESWPT are light, deeply embedded structures. As a result, the observed GWL effects on the response of site-specific seismic category I structures are more pronounced than they are for the R/B complex.

The reconciliation of the standard design for the CPNPP 3 & 4 site is based on comparisons of the envelope of seismic responses obtained from site-specific SSI analyses of the R/B complex as an embedded structure in full contact with surrounding soil and as a surface-mounted structure with embedment soil removed. The consideration of these two bounding cases ensures that the reconciliation is based on site-specific responses that envelop effects of lateral soil separation and GWL variations. The results of the sensitivity studies performed for the PSFSV and described in Appendix 3MM demonstrate that the consideration of responses from embedded and surface-mounted models envelop effects of backfill separation and GWL effects. The results of these studies are applicable for the R/B complex because the PSFSV as a light deeply embedded structure is more sensitive to backfill separation and GWL effects than the heavy partially embedded R/B complex. Responses obtained from the analyses of surface-mounted models exceed the responses obtained from the embedded models at almost all frequencies. The consideration of surface models in addition to the standard design basis embedded model helps address effects of variations of the site-specific parameters in an efficient and conservative manner.

The SSI analyses of the embedded model are performed using the following four full column soil profiles described in Subsection 3.7.2.4.5 that include the backfill soil and the underlying rock strata below nominal elevation of 782 ft:

- EBE representing best estimate rock subgrade and backfill properties;
- ELB representing lower bound rock subgrade and backfill properties
- EUB representing upper bound rock subgrade and backfill properties; and
- EHB representing upper bound rock subgrade and high bound backfill properties

Analyses of the surface-mounted models are performed for the following three truncated column soil profiles:

- SBE representing best estimate rock subgrade properties;
- SLB representing lower bound rock subgrade properties; and
- SUB representing upper bound rock subgrade properties

As shown in Subsection 3.7.1, the minimum design spectra, tied to the shapes of the certified seismic design response spectra (CSDRS) and anchored at 0.1g, envelops the foundation input response spectra (FIRS) that define the safe-shutdown earthquake (SSE) design motion for the R/B complex structures defined as outcrop motion at the basemat bottom elevation 779.75 ft. Therefore, to simplify the reconciliation process, US-APWR standard plant design basis acceleration time histories are scaled by 1/3 and used directly as input control motion for site-specific SSI analyses of surface-mounted models. As described in Subsection 3.7.2.4.5, site response analyses are performed on the full column profiles of BE, LB, UB, and HB strain-compatible shear wave and compression wave velocities to convert these outcrop motion time histories into acceleration time histories of within-column motion at El. 779.75 ft. These within motion time histories serve as input control motion for the SSI analyses of the embedded R/B complex model. The three components of the input motions are applied to the SSI models separately by using vertically propagating shear and compression waves for the horizontal and vertical components, respectively. These input motions are discussed further in Subsection 3.7.1.

Due to the low frequency content of the seismic design motion at the CPNPP 3 & 4 site, the effects of spatial variation of the input ground motion on the response of the R/B complex are not significant. As a result, site-specific SSI analyses do not consider incoherence of the input control motion that may results in reduction of the seismic response at higher frequencies.

3NN.3 SASSI Model Description and Analysis Approach

Model Description

Figure 3NN-7 and Figure 3NN-8 shows the three-dimensional SSI surface and embedded FE models, respectively, used for site-specific seismic analysis of the R/B complex consisting of the R/B-FH/A, PCCV, CIS, East PS/B & West PS/B, A/B and the ESWPC, all supported on a common reinforced concrete basemat. The R/B, East PS/B, West PS/B, A/B and ESWPC are combined in an integral structure consisting of vertical shear and bearing walls and horizontal slabs/roofs. The containment structures (PCCV and CIS) are independent structures above plant grade elevation that share a common basemat with the other structures.

In order to address the effects of concrete cracking on the stiffness of the R/B complex structures under different operating conditions, the reconciliation of the standard design is based on an envelope of responses obtained from the site-specific SSI analyses of three SSI FE models:

a. Surface-mounted model with full (uncracked concrete) stiffness properties corresponding to the low structural stress levels during normal operating conditions

b. Embedded foundation model with full (uncracked concrete) stiffness properties

c. Surface-mounted model with reduced (cracked concrete) stiffness properties of containment structures corresponding to high thermal stresses during accident conditions

The geometry, the FE configuration, and the mass inertia properties of these models are identical to those of the design basis Dynamic FE model used for the standard design SSI analyses. Only minor modifications of the FE mesh, the stiffness and the damping properties of the design basis Dynamic FE model were made to address site-specific conditions.

All three models are established with reference to the Cartesian coordinate system with origin established 2 ft.-7 in. below the ground surface elevation at the center of the PCCV foundation. The origin location corresponds to the location of the coordinate system used as reference for the seismic analysis of the standard plant presented in Subsection 3.7.4. The orientation of the Z-axis is upward. The positive X-axis is oriented southward and the Y-axis is oriented eastward.

Models (a) and (b) are assigned stiffness properties identical to those of the design basis dynamic FE model with full stiffness properties. These two models with full stiffness properties are fitted with single degree of freedom (SDOF) oscillators that serve to capture the shift in the out-of-plane vibration frequencies of slabs in the seismic category I buildings (R/B and PS/Bs) that may crack under applicable loads. To address the effects of concrete cracking under accident thermal loads, the containment structures (CIS and PCCV) in the surface-mounted foundation model (c) are assigned reduced stiffness properties identical to those assigned to the PCCV and CIS in the design basis FE dynamic model with reduced stiffness properties as shown in DCD Table 3.7.2-3. Due to the low seismicity of the CPNPP site, stress levels are expected to be low and insufficient to cause considerable cracking of the shear walls of the concrete structure surrounding the containment and hosting the R/B, PS/B, and A/B. As a result, for the reduced stiffness model (c), full (uncracked concrete) stiffness properties are assigned to shear walls. Only the properties of the R/B, PS/Bs and A/B reinforced concrete slabs are adjusted to reflect full stiffness in slab in-plane direction and 50% reduction of slab stiffness in the out-of plane direction due to concrete cracking under vertical gravity loads. The lower level Operating Basis Earthquake (OBE) damping properties are assigned to all models used for site-specific SSI analyses of the R/B complex to account for energy dissipation in the different structural members.

The site-specific models utilize the same element types to model the members of the R/B complex structures as the design basis dynamic FE model. Shell elements are used to model the reinforced concrete shear walls and slabs, and 3-D beam elements model the reinforced concrete and steel columns and beams. Solid brick elements are used to model the basemat foundation and the massive concrete sections of the CIS. Spring elements are used to model the supports and connection of the CIS FE mesh with lumped-mass-stick model representing the dynamic properties of the RCL components. In the embedded foundation model (b), a row of solid brick elements assigned properties of the backfill soil are attached to the shell elements of the basement walls to enable calculation of dynamic earth pressures acting on the walls. Solid brick elements are also used to model the dynamic properties of the excavated soil as needed for the models used for SASSI analyses of embedded structures. Figure 3NN-9 and Figure 3NN-10 show the excavated soil volume and backfill soil brick elements, respectively.

The FE mesh of the basement exterior walls in the embedded foundation model (b) along the vertical direction is adjusted to allow passage of waves up to 50 Hz frequency in the upper bound backfill site model (EUB). The vertical element mesh size is determined from the requirement that the vertical size of the FE mesh be equal to or smaller than one fifth of the wave length, i.e. the mesh size is determined using the following equation

$$d = \frac{Vs}{5 \cdot f_{pass}}$$

where Vs is the shear wave velocity of the backfill soil in the EUB profile, *d* is either the thickness of the soil layer or FE mesh size and f_{pass} is the passing frequency of the model set to 50 Hz.

Table 3NN-1 presents the adjusted dynamic properties and corresponding passing frequencies for the backfill soil elements.

Field interaction nodes are added to the embedded model (b) to enable calculation of field motion at locations of the nearby standalone segments of the ESWPT. The comparison of responses at these field interactions nodes with the free field motion serves to assess the effects of the R/B complex on the free field motion and to address effects of SSSI on the ESWPT as described in Appendix 3LL.

The location of the lower boundary used in the SSI analyses is greater than 1078 feet below grade. The depth is greater than the embedment plus twice the depth of the largest base dimensions (i.e. 406.67’ x 2 + 42.25’ = 856’) as recommended by SRP 3.7.2. A ten layer half-space is used below the lower boundary in the SASSI analysis. The SASSI half-space simulation consists of additional layers with viscous dashpots added at the base of the half-space. The half-space layer has a thickness of 1.5 Vs/f, where Vs is the shear wave velocity of the half-space and f is the frequency of analysis. The half-space is sub-divided by the selected number of layers in the half-space.

Modeling of Cracked Out-of-Plane Slab Properties

The properties of the shell elements modeling the slabs in the reduced stiffness model (c) are adjusted to reflect a 50% reduction in the out-of-plane stiffness with full stiffness in the in-plane direction using the following equations. These equations demonstrate the relationships between the modified Young’s modulus, thickness, and unit weight properties of shell elements with reduced stiffness (Em, tm and γm) and the initial properties (E0, t0 and γ0) of the shell elements in the standard plant design basis model with full stiffness:

$$E_m = E_0 \cdot \sqrt{\frac{n_b}{n_a^3}}\,;\quad t_m = t_0 \cdot \sqrt{\frac{n_a}{n_b}}\,;\quad \gamma_m = \gamma_0 \cdot \sqrt{\frac{n_b}{n_a}}$$

where values of $n_b = 2$ and $n_a = 1$ are used to represent the condition when the slab out-of-plane stiffness is reduced by 50% to account for concrete cracking while the in-plane stiffness remains unchanged.

Single degree of freedom (SDOF) oscillators are added to the models with full stiffness properties (a) and (b) to capture the shift in out-of-plane vibration frequencies of slabs in the seismic category I buildings (R/B and PS/Bs) that may crack under applicable loads. The dynamic properties of the SDOF oscillators are based on results of modal analyses of floor models extracted from the R/B complex dynamic FE model (c) with the reduced stiffness properties. Each of the R/B complex major floor elevations is isolated as shown in Figure 3NN-11. Boundary conditions are established as shown in Figure 3NN-12 at the upper and lower border of the floor models to restrain horizontal displacements of the walls and accurately mimic the bending stiffness at the wall/slab interfaces. The horizontal and vertical displacements of the slab at the junctions of the slab with the supporting walls are also restrained in order to eliminate the effects of the axial stiffness of the walls on the modal analyses results and to disregard the slab horizontal modes as well. Where the slab is supported by columns, the vertical displacement is constrained. Modal analysis using ANSYS is then performed on the isolated floor models for different floor elevations of the R/B complex to obtain the natural frequencies of the vertical vibrations of the slabs. Slabs with a first dominant mode frequency less than 50 Hz in the reduced (cracked concrete) stiffness condition are considered flexible and assigned an SDOF oscillator.

The SDOF are included in models (a) and (b) in a manner that ensures their addition does not affect the dynamic properties of the models or the elements they are attached to. SDOF oscillators are independent of slabs and consist of a lumped mass with a unit weight of 1 kip supported by a number of springs with stiffness in the global vertical direction as shown in Figure 3NN-13. The small mass is assigned to the model to ensure that the mass properties of the model remain unaffected. Springs with stiffness in the global vertical direction are used to connect the lumped mass to the slab periphery nodes located at the intersection of slabs with walls and columns as shown in Figure 3NN-14. SDOF oscillators are assigned an OBE damping value of 4% and a vertical spring constant stiffness ($k_{cracked}$) computed as follows:

$$k_{cracked} = \frac{4}{n_s} \cdot f_{cracked}{}^2 \cdot \pi^2$$

where n_s is the number of vertical springs used to connect the SDOF lumped mass to the FE model.

Table 3NN-2 presents a sample of the 224 flexible slabs assigned SDOFs in the R/B and two PS/Bs.

Model Validation

The models used for site-specific SSI analyses are based on the design basis dynamic FE model of the R/B complex. The ability of this design basis model to adequately represent the dynamic properties of the R/B complex structures is demonstrated in Section 02.5 of MUAP-10006 (Reference 3NN-2). Since the modifications made to the design basis model are minor and do not change the configuration of the model, validations were performed on the site-specific models to ensure that these modifications do not result in errors that may impair the ability of the models to adequately represent the dynamic properties of the R/B complex structures.

The ability of the SDOF oscillators for capturing out-of-plane response of cracked slabs is evaluated by comparing results obtained from the SSI analyses of the full stiffness model (a) with SDOF oscillators against results obtained from the reduced (cracked concrete) stiffness model (c). 5% damped ISRS obtained from the SSI analyses of the full stiffness model (a) are calculated as an envelope of vertical responses of the full stiffness slab FE nodes and the response of the SDOF mass node. These ISRS are compared with the corresponding ISRS obtained from the SSI analyses of the reduced stiffness model in which the out-of-plane stiffness of slabs is reduced by 50%. Before being compared, the ISRS obtained from the SSI analyses of the two models are enveloped for the three soil cases and broadened by ± 15% in spectral frequency. The ISRS comparisons in Figure 3NN-17 indicate that SDOFs can effectively capture the peak frequency shifts in the design ISRS that are due to slab cracking. The results also indicate that the SDOF can underestimate the amplitude of the resonant responses of the mid-span FE nodes where the cracked slab experiences the largest vibrations. This shortcoming of the SDOF approach is not significant and does not affect the conclusions of the standard plant design reconciliation analyses that show that the standard design envelops the site-specific demands with very large margins.

SSI Analysis Approach

The methodology used for the site-specific SSI analyses are consistent with those used for the standard design site-independent SSI analyses described in Subsection 3.7.2.4. The site-specific SSI analyses are performed using the ACS SASSI computer program that employs the complex response method and finite element technique to solve the seismic response of the SSI system in the frequency domain. Responses are calculated at selected frequencies of analysis and then interpolated for the range of frequencies of interest. The initial set of frequencies of analysis is selected as follows:

- for frequency range 0 to 20 Hz, the spacing of analyzing frequency points is about 0.25 Hz, i.e. four frequency points per 1.0 Hz frequency interval,
- for frequency range 20 Hz to 33 Hz, the spacing of analyzing frequency points is about 0.33 Hz, i.e. three frequency points per 1.0 Hz interval
- for frequency range 33 Hz to 50 Hz, the spacing of analyzing frequency points is about 0.5 Hz, i.e. two frequency points per 1.0 Hz interval.

For each set of SSI analysis, a cut-off frequency is selected based on the wave passage frequency accurately transmitted through the soil layers of the model. The cut-off frequency for the LB profile is 33 Hz. The cut-off frequency for the BE profile is 44 Hz and the cut-off frequency for the UB and HB profiles is 50Hz. Acceleration transfer functions (ATF) results are reviewed to ensure that the selected frequencies of analysis yield reasonable results and capture critical seismic responses. The accuracy of the interpolated ATFs is improved when needed by adding additional frequencies.

In each set of SASSI runs, the input motion is applied to the models at the foundation bottom elevation in the north-south (NS)(H1), east-west (EW)(H2), and vertical directions. Responses obtained for the earthquake components in the three global orthogonal directions are combined in accordance with RG 1.92 (Reference 3NN-3) using the square root sum of the squares (SRSS) method.

The SSI analyses of the embedded model employ the modified subtraction method (MSM) to represent the continuity between the excavated soil model, the structural model, and the site model. MSM provides a solution to the seismic response of embedded foundations by specifying only the nodes at the outer face of the excavated soil volume as interaction nodes for which impedances are calculated. Results of the validation studies performed for the standard plant as well as for the site-specific seismic category I structures presented in Appendices 3KK, 3LL, and 3MM demonstrate that the use of MSM provides accurate solutions for the embedded R/B complex model SSI response.

3NN.4 Seismic Analysis Results

The reconciliation of the standard design for the site is based on an envelope of responses obtained from the following three types of site-specific SSI analyses:

(a) Surface-mounted SSI analyses of the R/B complex structures with full (uncracked concrete) stiffness properties corresponding to the low seismic response of the building at the site during normal operating conditions

(b) Embedded foundation SSI analyses of the R/B complex structures also with full (uncracked concrete) stiffness properties

(c) Surface-mounted SSI analyses of the R/B complex structures with reduced (cracked concrete) stiffness properties of containment structures corresponding to high thermal stresses during accident conditions

The applicability of the standard design is demonstrated by showing that ISRS and lateral earth pressures obtained from the site-specific SSI analyses are enveloped by the standard design basis ISRS documented in Section 03.4.2 of MUAP-10006 (Reference 3NN-2) and lateral earth pressure loads presented in Table 3.8.4-23 that are used for the standard design of R/B complex structures. Results are also used to compute base reactions for stability evaluation and dynamic bearing pressures for the CPNPP 3 & 4 R/B complex.

3NN.5 Site-Specific In-Structure Response Spectra (ISRS)

The methodology used for the development of site-specific ISRS for the R/B complex is consistent with the methodology used for the development of the standard design ISRS described in Subsection 3.7.2.4.5. The site-specific ISRS are developed using the site-specific SSI analyses results for 3, 4, and 5 percent damping acceleration response spectra (ARS) for the three orthogonal directions. The ARS results for the three components of the input earthquake are combined using the SRSS method. Site-specific ISRS are developed as an envelope of ARS results obtained from the three types of site-specific SSI analyses (a), (b), and (c) described in Section 3NN.4 using seven different soil profiles. ISRS are broadened by ± 15% in spectral frequency.

As part of the reconciliation process of the standard plant design to the site, 5% damped ISRS are developed at node locations specified in Table 3NN-3 and compared with the corresponding standard design ISRS. These node locations include the corners of the R/B complex, the top of the basemat elevation, ground elevation, and roof elevations to detect rocking and torsion of the building as well as possible amplifications at plant grade due to site-specific embedment effects. Comparisons are also carried at the top of the PCCV at node locations within the CIS where these structures experience the largest amplifications of their seismic responses. Figure 3NN-20 through Figure 3NN-68 compare the site-specific ISRS at the specified nodal location in all three directions with the corresponding standard plant ISRS.

Site-specific ISRS are also developed for key systems and equipment at damping values identified in Table 3NN-4. These site-specific ISRS are developed by grouping the responses at multiple node locations following the same methodology described in Subsection 3.7.2.4.5 for development of ISRS for the standard design of equipment and components. The only difference is that the site-specific vertical ISRS for the key systems and equipment supported by flexible slabs also include the responses at the corresponding SDOF mass nodes in order to account for possible shifts of ISRS peak frequencies due to concrete cracking. Figure 3NN-71 through Figure 3NN-78 compare the site-specific ISRS for key systems and equipment with the corresponding standard plant ISRS.

As shown in Figure 3NN-20 through Figure 3NN-78, the standard plant ISRS envelop by a high margin all of the site-specific ISRS at all locations and for all frequencies ranging from 0.1 Hz to 100 Hz. Therefore, the comparisons of the ISRS confirm the validity of the US-APWR R/B complex standard plant seismic design for the CPNPP 3 & 4 site.

3NN.6 Site-Specific Lateral Earth Pressure

Following the requirements of SRP 3.8.4 Section II.4.H (Reference 3NN-7), the reconciliation of the standard design is based on comparison of the lateral earth pressure loads used for standard design of US-APWR structures to the site-specific lateral pressure loads calculated as:

i. The sum of static earth pressure, hydrostatic pressure, and total dynamic earth pressure calculated in accordance with ASCE 4-98, Section 3.5.3.2 (Reference 3NN-8) due to horizontal and vertical component of the site-specific design earthquake.

ii. The sum of static pressure, hydrostatic pressure and passive lateral earth pressure generated by the wall motion as calculated by the site-specific SSI analyses.

Pressures based on the passive resistance of the backfill are not considered since the seismicity of the CPNPP 3 & 4 site is low and the resulting lateral displacements of the below-grade walls are too small to initiate plastic yield in the backfill soil mass. High site-specific GWL is considered to be at the top of the ESWPT to address the bounding case when the ground water is trapped within the perimeter of the ESWPT. To include the hydrodynamic pressure from the ground water, the calculated dynamic earth pressures due to the horizontal component of the earthquake using ASCE 4-98 methodology and the dynamic pressures obtained from the SSI analyses of the embedded R/B complex model are computed using saturated soil weight of 135 pcf for the backfill soil located below GWL.

The methodology used in the calculations of the site-specific lateral pressures using ASCE 4-98 methodology is consistent with the one used for standard design described in Subsection 3.8.4.4.1.4. This methodology is based on small strain "at-rest" or elastic solutions of a uniform soil body trapped between two rigid walls connected by a rigid base and excited in the horizontal direction. The effects of groundwater on the dynamic pressures are addressed by considering the soil as a one-phase-system where the pore water within the saturated backfill soil moves together with the soil skeleton. The used horizontal seismic coefficient is obtained from the site-specific SSI analyses results for maximum accelerations of the near field backfill elements following the approach used for calculation of dynamic lateral pressures for the standard design. The methodology used to calculate the dynamic pressure due to the vertical component of the earthquake also considers the building walls to be rigid and non-yielding. The lateral dynamic earth pressure due to the vertical component of the earthquake is calculated by multiplying the static lateral pressures (earth pressure at-rest plus hydrostatic pressure) by a vertical seismic coefficient. The value of the vertical seismic coefficient is obtained from the results of SSI analyses for maximum accelerations of the near field backfill elements. The total value of the calculated dynamic lateral pressure using ASCE 4-98 methodology is calculated as the sum of the dynamic earth pressures due to horizontal and vertical component of the earthquake.

The dynamic lateral pressures are calculated from the numerical results of the site-specific SSI analyses of the embedded model. They are obtained as the SRSS of stress results calculated at the centroid of the 3-D solid backfill elements along the perimeter basement walls of the R/B complex, due to each of the three directions of earthquake and for each of the four full column soil profiles, ELB, EBE, EUB and EHB. Figure 3NN-79 through Figure 3NN-83 compare the maximum SSI dynamic earth pressures calculated along each perimeter wall of the R/B complex basement to the corresponding calculated dynamic pressure using ASCE 4-98 methodology. These figures also show that both sets of site-specific lateral pressure loads are enveloped by the corresponding standard plant dynamic pressure load. Figure 3NN-84 through Figure 3NN-88 further demonstrate the applicability of the standard plant for the CPNPP 3 & 4 site by showing that the total site-specific lateral earth pressure loads are enveloped by the lateral earth pressure loads presented in Table 3.8.4-23 that are used for the standard plant design.

3NN.7 Site-Specific Seismic Stability and Bearing Pressures Evaluation

The reconciliation of the standard design for site-specific conditions requires a seismic stability evaluation to be performed to demonstrate the sliding and overturning stability of the R/B complex during a site-specific design earthquake event. The site-specific stability of the R/B complex is evaluated by means of pseudo-static analysis showing that no sliding of the R/B complex occurs and that a safety factor against sliding larger than 1.1 is maintained as required by the acceptance criteria specified in Subsection 3.8.5.5.2. The R/B complex overturning stability is demonstrated following the criteria and methodology used for standard plant stability evaluations described in Subsection 3.8.5.5. To evaluate the stability of the CPNPP site subgrade under site-specific seismic loads, dynamic bearing pressure is calculated from the results of quasi-static analysis using a methodology that is consistent with the methodology used for standard plant design.

Site-specific base reactions that serve as input for the seismic stability evaluations and calculations of maximum dynamic bearing pressures for the R/B complex are calculated using results obtained from the site-specific SSI analyses of the surface foundation models of the R/B complex with full stiffness properties (a) and reduced stiffness properties (c) performed for the three truncated soil profiles SLB, SBE and SUB. Acceleration responses obtained from these analyses in all three directions for each direction of seismic motions are used to derive the dynamic inertia forces acting on the R/B complex structures and foundations due to the earthquake. Inertia forces are computed by multiplying the nodal masses of the R/B complex with the corresponding accelerations for each nodal direction at each time step. Base reactions and overturning moments are calculated by summing the inertia forces with respect to the centroid of the R/B complex basemat bottom. In addition to the inertia forces obtained from the site-specific SSI analyses, the dynamic lateral earth pressures using ASCE 4-98 methodology described in Section 3NN.6 are also considered to act on the exterior basement walls of the R/B complex. The dynamic lateral pressure is considered to act in the same direction as the driving inertia forces. Since the R/B complex is an asymmetric structure, all eight permutations of the seismic load directional combinations (±X, ±Y, ±Z) are considered in the calculations.

Table 3.8-202 presents the site-specific sliding and overturning safety factors for the R/B complex as well as the maximum seismic toe bearing pressures. The calculated site-specific safety factors show large margins of safety for sliding and overturning stability of the R/B complex. The calculated value for the maximum bearing pressure at the toe of the R/B complex foundation is significantly lower than the maximum allowable dynamic pressure specified in Subsection 3.8.5.4.1.

3NN.8 References

3NN-1 ACS SASSI NQA Version 2.3.0 Including Options A and FS Rev 1, “An Advanced Computational Software for 3D Dynamic Analysis Including Soil-Structure Interaction”, User Manual Rev 7, Installation Kit IKTR5, Ghiocel Predictive Technologies Inc., September 26, 2012.

3NN-2 Soil-Structure Interaction Analyses and Results for the US-APWR Standard Plant, Mitsubishi Heavy Industries, Ltd., Technical Report MUAP 10006, Revision 3, November 2012.

3NN-3 *Combining Responses and Spatial Components in Seismic Response Analysis*, Regulatory Guide 1.92, Rev. 2, U.S. Nuclear Regulatory Commission, Washington, DC, July 2006.

3NN-4 *Damping Values for Seismic Design of Nuclear Power Plants*, Regulatory Guide 1.61, Rev. 1, U.S. Nuclear Regulatory Commission, Washington, DC, March 2007.

3NN-5 Seismic System Analysis NUREG-0800 US NRC Standard Review Plan (SRP) Section 3.7.2, Revision 3, March 2007.

3NN-6 Ground Water Effects on SSI, Mitsubishi Heavy Industries, Ltd., Technical Report MUAP 11007, Revision 2, November 2012.

3NN-7 Other Seismic Category I Structures, NUREG-0800 US NRC Standard Review Plan (SRP) Section 3.8.4, Draft Revision 4, December 2012.

3NN-8 Seismic Analyses of Safety Related Nuclear Structures and Commentary, ASCE 4-98, American Society of Civil Engineers, Reston, VA, 2000.

Table 3NN-1

Properties and Passing Frequencies for Backfill Elements

Layer	Thick. (ft)	Unit weight (lb/ft^3)	Vs (ft/s)				Vp (ft/s)				Damping (%)				Passing Frequency			
			LB	BE	UB	HB	LB	BE	UB	HB	LB	BE	UB	HB	LB	BE	UB	HB
1	3.100	125	505	656	851	1,105	1,051	1,365	1,772	2,300	2.8	1.7	1.0	0.6	32.6	42.3	54.9	71.3
2	4.033	125	571	763	1,020	1,363	1,189	1,589	2,123	2,836	3.5	2.1	1.2	0.7	28.3	37.8	50.6	**67.6**
3	4.033	125	552	748	1,012	1,371	1,149	1,556	2,108	2,854	4.3	2.5	1.5	0.9	**27.4**	**37.1**	**50.2**	68.0
4	3.500	125	535	733	1,005	1,378	1,114	1,527	2,093	2,868	5.0	2.9	1.7	1.0	30.6	41.9	57.4	78.7
5	3.500	125	523	723	999	1,381	1,089	1,505	2,080	2,875	5.6	3.2	1.8	1.1	29.9	41.3	57.1	78.9
6	3.583	125	579	797	1,099	1,513	2,908	4,006	5,519	7,603	5.0	2.9	1.7	1.0	32.3	44.5	61.3	84.4
7	3.583	125	684	931	1,268	1,727	3,486	4,748	6,467	8,808	4.0	2.3	1.3	0.8	38.2	52.0	70.8	96.4
8	3.583	125	676	924	1,264	1,728	3,448	4,714	6,445	8,811	4.3	2.5	1.4	0.8	37.7	51.6	70.5	96.4
9	3.694	125	671	920	1,261	1,729	3,423	4,692	6,430	8,814	4.5	2.6	1.5	0.8	36.3	49.8	68.3	93.6
10	3.694	125	667	916	1,259	1,729	3,401	4,671	6,417	8,816	4.6	2.7	1.5	0.9	36.1	49.6	68.1	93.6
11	3.694	125	663	912	1,256	1,729	3,379	4,652	6,404	8,816	4.8	2.7	1.6	0.9	35.9	49.4	68.0	93.6
12	2.250	155	4,603	5,720	7,108	7,108	9,138	11,356	14,112	14,112	2.8	1.9	1.3	1.3	409	508	632	632

Table 3NN-2

Sample of Flexible Slabs with SDOF Oscillators

Elevation	Slab Name	Slab Coordinates				Cracked Slab Frequency (Hz)	Springs	
		X1	X2	Y1	Y2		No.	Constant (K/ft)
EL.-14'-2"	PSEB1M12	HR	H1R	19R	20R	25.0	4	6169
EL.-8'-7"	Sb30AB1	CR	D2R	9R	11bR	44.7	4	19720
EL. 3'-7"	PSW1F15a	KR	LR	7R	8R	23.6	4	5497
EL. 13'-6"	S12A4	BR	CR	13R	13aR	49.6	4	24281
EL. 50'-2"	S28C1c	JR	KR	9aR	10R	37.7	4	14028
EL. 65'-0"	S40C7b	KR	LR	12aR	13R	40.3	4	16029
EL. 76'-5"	S28A25a	JR	KR	9aR	11R	34.0	4	11409
EL. 86'-4"	S20A3a	CR	DR	10R	11bR	42.1	4	17493
EL. 101'-0"	S28F2a	JR	KR	11R	12R	37.0	4	13511
EL. 131'-6"	S15E123b	HR	JR	15bR	16bR	15.4	4	2341

Table 3NN-3

Locations of Structural Nodes Used for Comparison of 5% Damped ISRS

	Location	Nodal Coordinates (ft)			Node Numbers		
		X (NS)	Y (EW)	Z (Vt.)	CPNPP 3 & 4		Standard Design
					Surface	Embed.	
1	Bottom of basemat foundation, center of PCCV at CL. FR & 13R	0.221	-0.078	-39.667	1690	1817	1937
2	Top of basemat foundation, center of PCCV at CL. FR & 13R	0.221	-0.078	-8.583	11754	48061	31873
3	Top of basemat foundation, building corner at CL. AR & 1R	-145.58	-238.67	-26.33	8424	30912	19831
4	Top of basemat foundation, building corner at CL. AR & 18R	-145.58	105.00	-26.33	8378	30866	19785
5	Top of basemat foundation, building corner at CL. LR & 1R	161.00	-238.67	-26.33	5901	25856	14573
6	Top of basemat foundation, building corner at CL. LR & 20R	161.00	171.00	-26.33	5845	25801	14517
7	Plant grade elevation, building corner at CL. AR & 1R	-145.58	-238.67	2.583	15563	59517	40761
8	Plant grade elevation, building corner at CL. AR & 18R	-145.58	105.00	2.583	15517	59471	40715
9	Plant grade elevation, building corner at CL. LR & 1R	161.00	-238.67	2.583	13106	57059	38202
10	Plant grade elevation, building corner at CL. LR & 20R	161.00	171.00	2.583	13050	57003	41111
11	West PS/B roof corner at CL. LR & 1R (Node 21566)	161.00	-238.67	48.50	22804	69835	50875
12	East PS/B roof corner at CL. LR & 20R	161.00	171.00	48.50	22755	69786	50826
13	Auxiliary building (A/B) roof corner at CL. AR & 1R	-145.58	-238.67	74.83	28728	74414	55464
14	FH/A roof corner at CL. AR & 18R	-151.58	105.00	156.00	33073	80400	61794
15	PCCV top	0.00	0.00	232.00	33564	81358	62749
16	Containment internal structure Steam Generator compartment top	-8.511	47.833	112	31259	78018	59432
		13.767	47.833	112	31243	78002	59416
		14.339	-47.833	112	31242	78001	59415
		-7.798	-47.833	112	31258	78017	59431
17	Containment internal structure Pressurizer compartment top	41.858	0.085	138.583	32463	79531	60943
		35.44	-2.599	138.583	32470	79538	60927
		35.136	2.853	138.583	32471	79539	60928

Table 3NN-4

ISRS for Design of Key Components and Equipment

No.	Equipment/Component	ISRS Damping	Location	
			Structure	Elev. (ft)
1	Reactor Vessel Support	3%	CIS Center	35.90
2	Sump Strainer Supports	3%	Containment Foundation	2.58
3	Steam Generators Bottom Supports	3%	CIS	45.64
4	Steam Generators Top Supports	3%	CIS	96.583
5	Spent Fuel Pool	4%	R/B-FH/A	25.25
6	New Fuel Storage Pit	4%	R/B-FH/A	63.33
7	Gas Turbine Generator Power Source Building (PS/B) - A-AAC	5%	East PS/B	2.583
8	Gas Turbine Generator Power Source Building (PS/B) - B-AAC	5%	West PS/B	2.583

Table 3NN-5

Site-Specific Seismic Stability Safety Factors and Foundation Bearing Pressures

CPNPP 3 & 4	
Factor of Safety for Sliding	2.8
Factor of Safety for Overturning	5.7
Maximum Dynamic Toe Bearing Pressure (ksf)	20.9

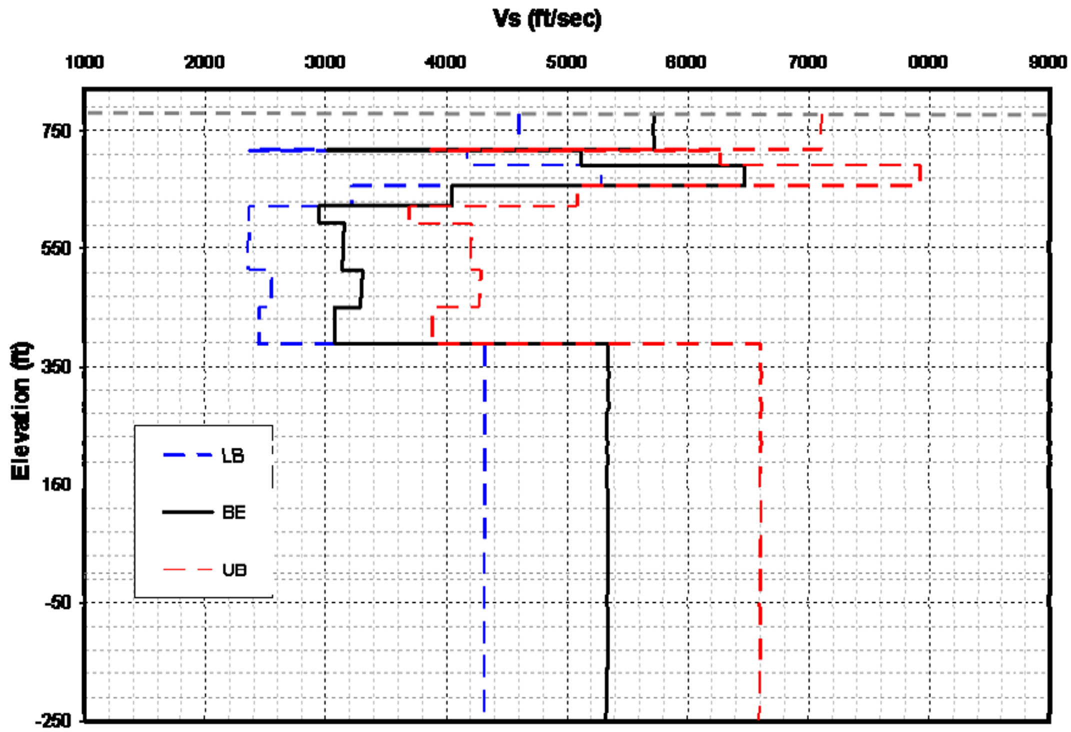

Figure 3NN-1 Rock Subgrade S-Wave Velocity Profiles

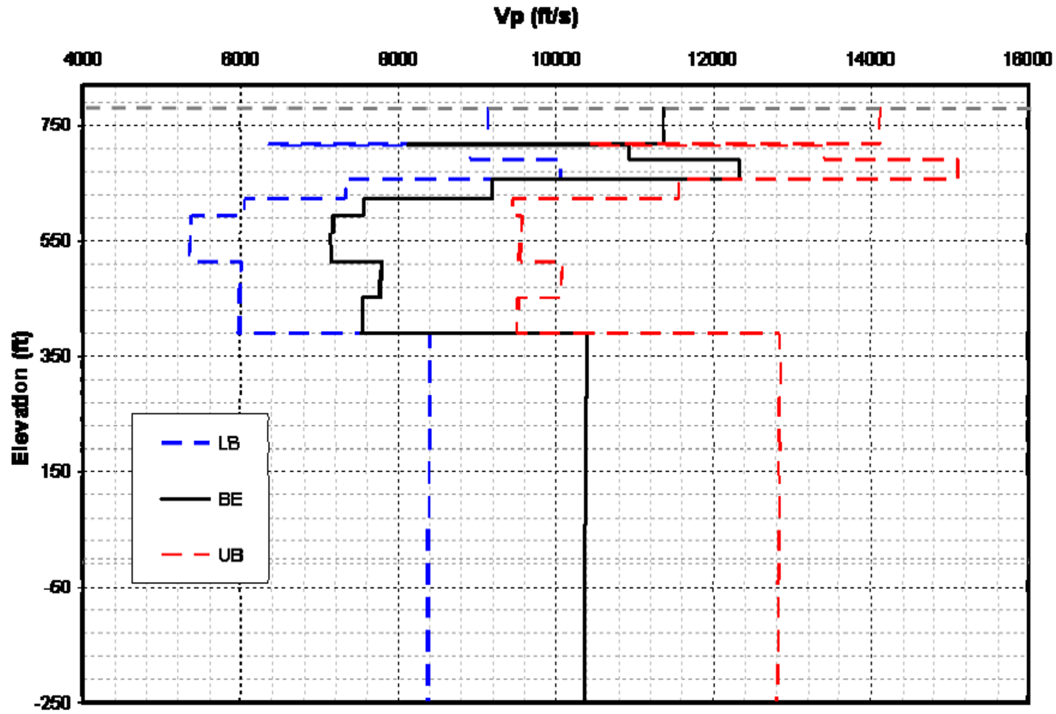

Figure 3NN-2 Rock Subgrade P-Wave Velocity Profiles

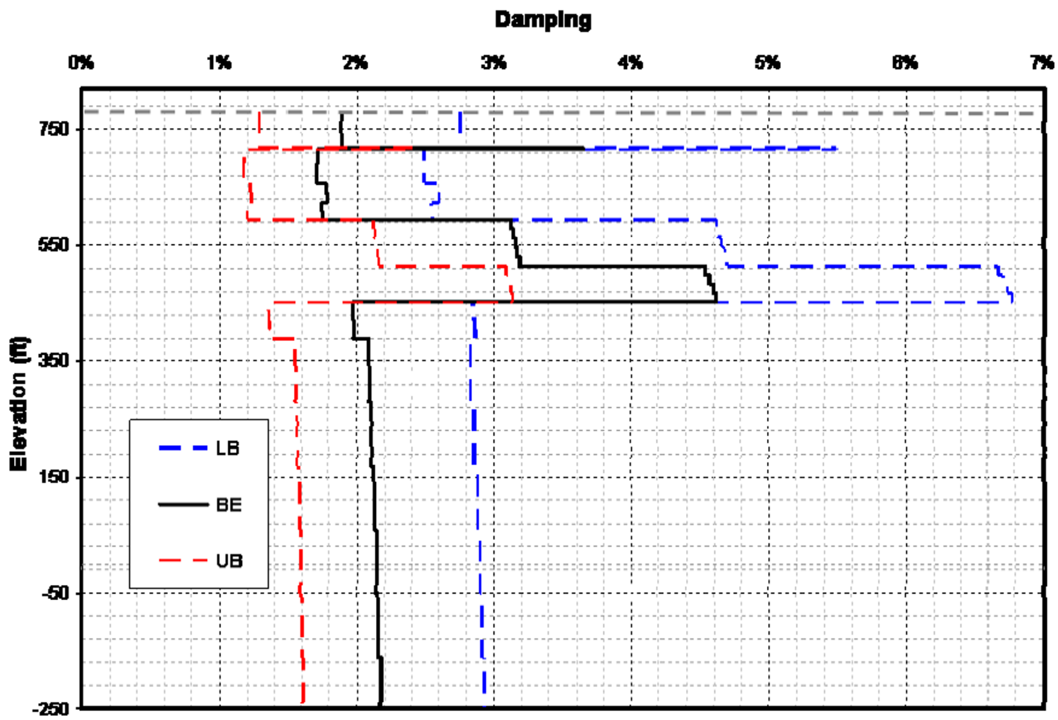

Figure 3NN-3 Rock Subgrade Damping Profiles

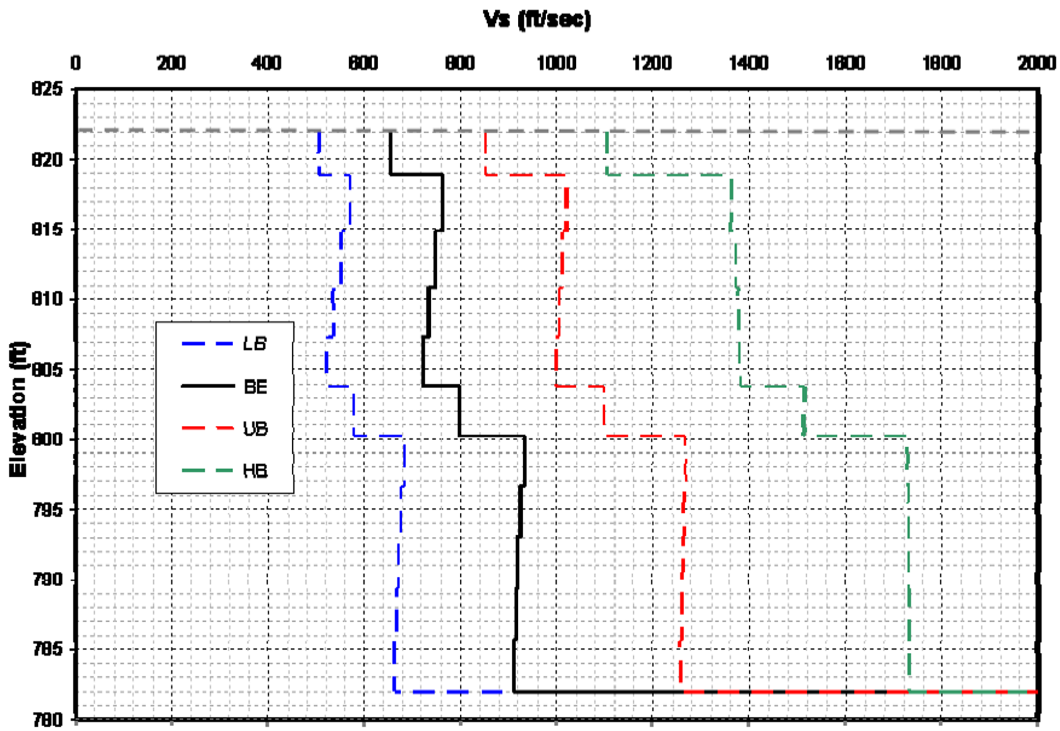

Figure 3NN-4 Backfill Strain-Compatible S-Wave Velocity Profiles

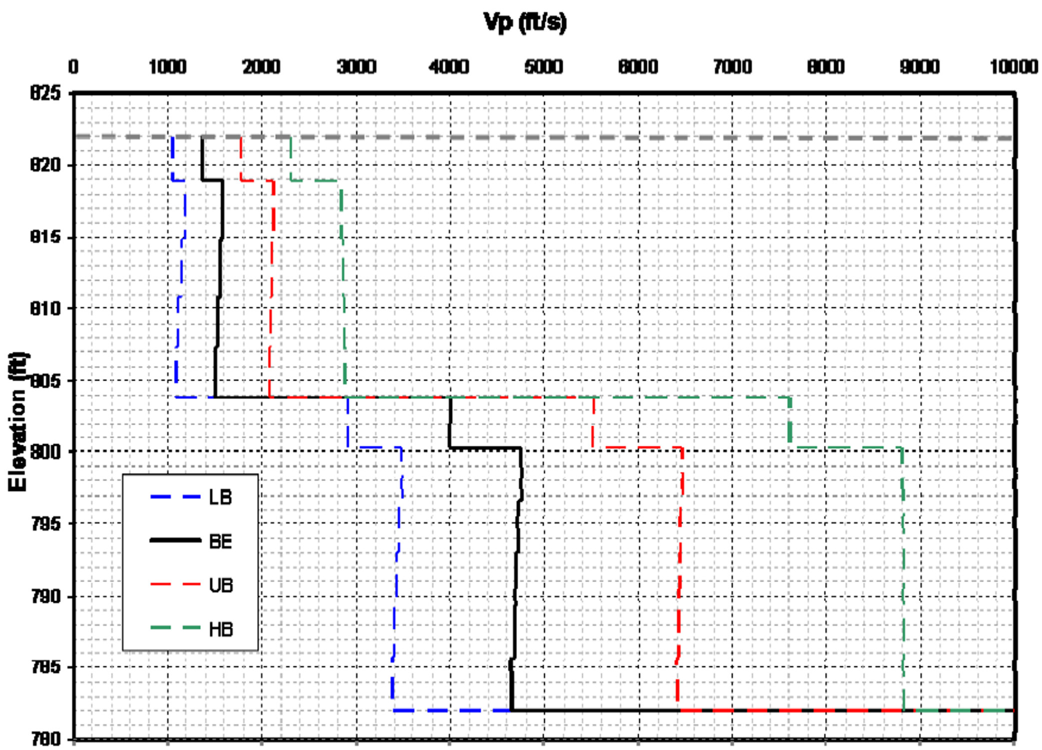

Figure 3NN-5 Backfill Strain-Compatible P-Wave Velocity Profiles

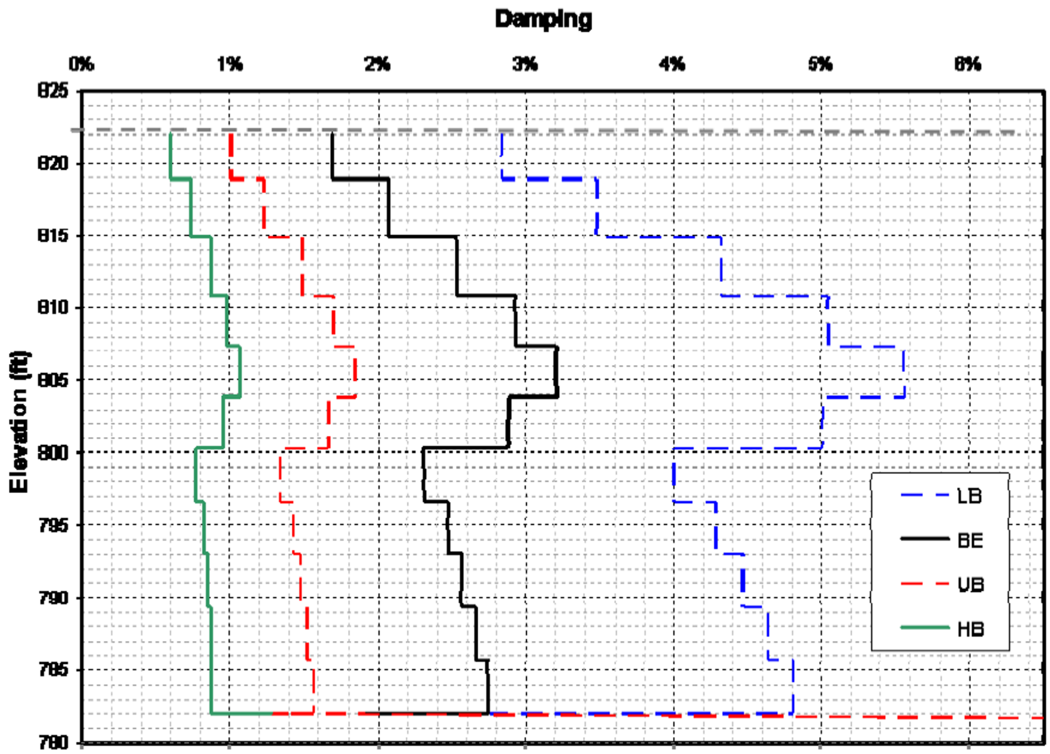

Figure 3NN-6 Backfill Strain-Compatible Damping Profiles

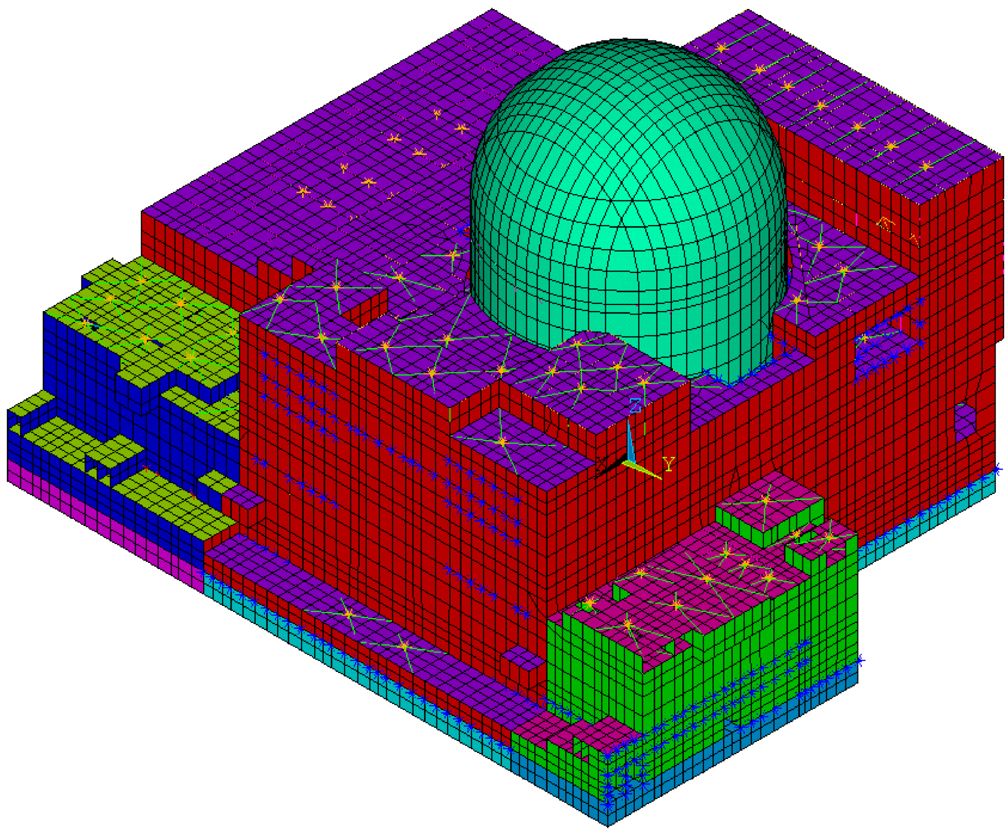

Figure 3NN-7 SASSI Surface Model of R/B Complex

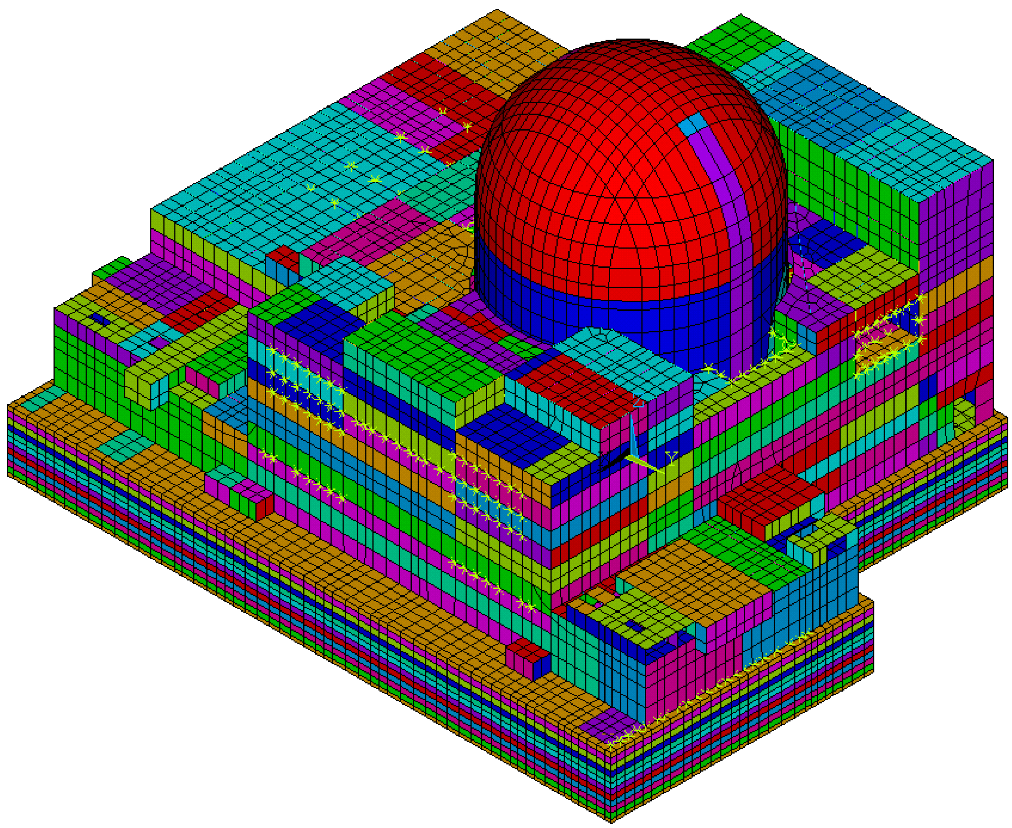

Figure 3NN-8 Structural Component of SASSI Embedded FE Model of R/B Complex

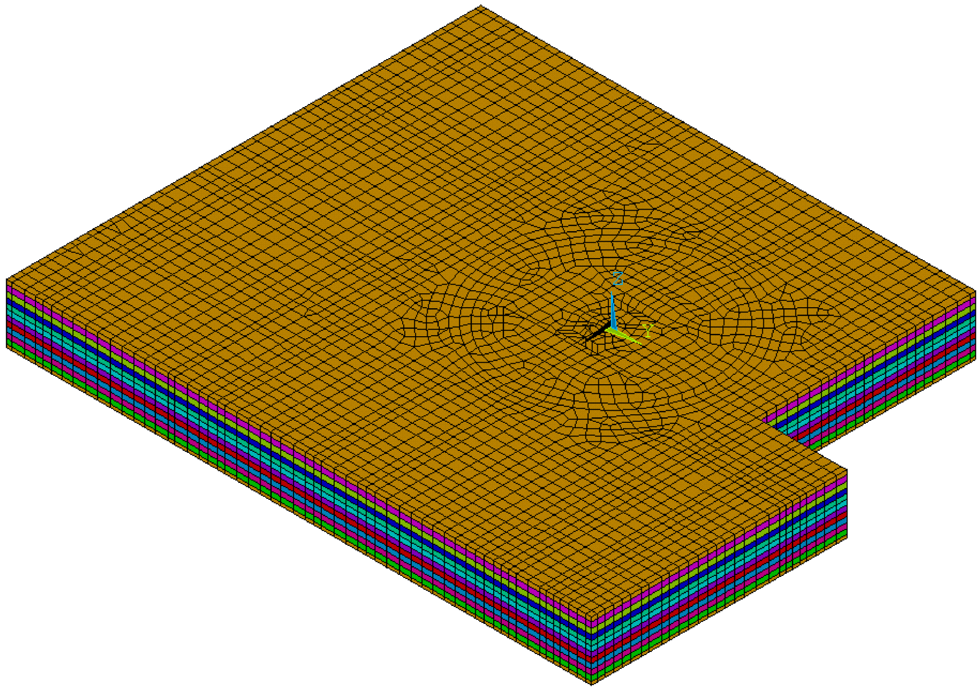

Figure 3NN-9 Excavated Soil Volume Elements

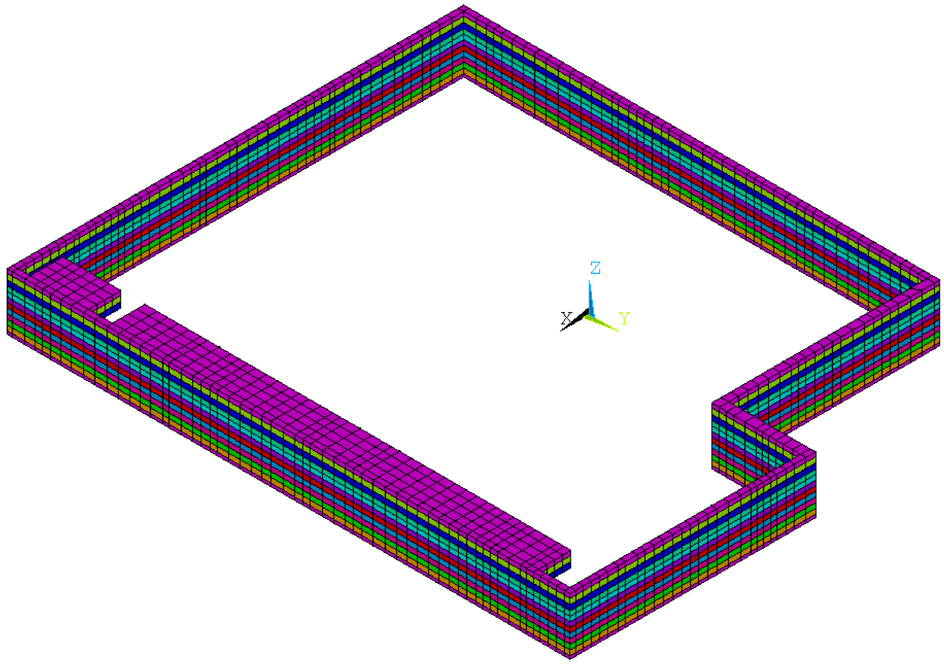

Figure 3NN-10 Backfill Elements

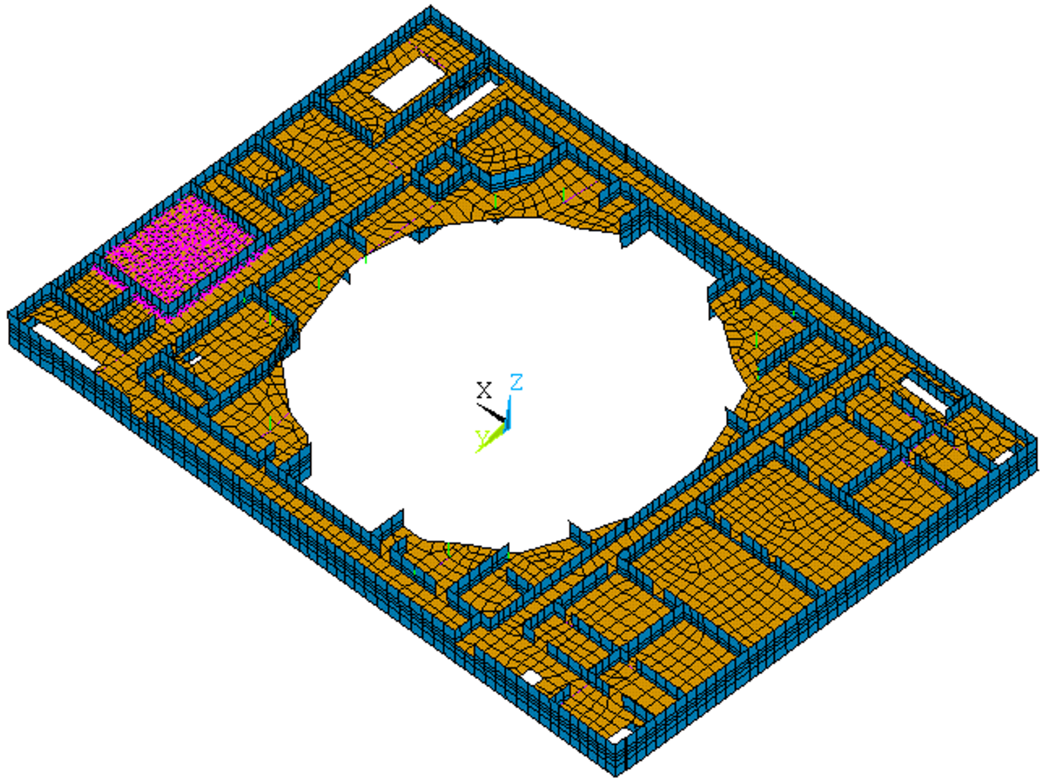

Figure 3NN-11 Extracted Dynamic FE Model of Floor Slabs

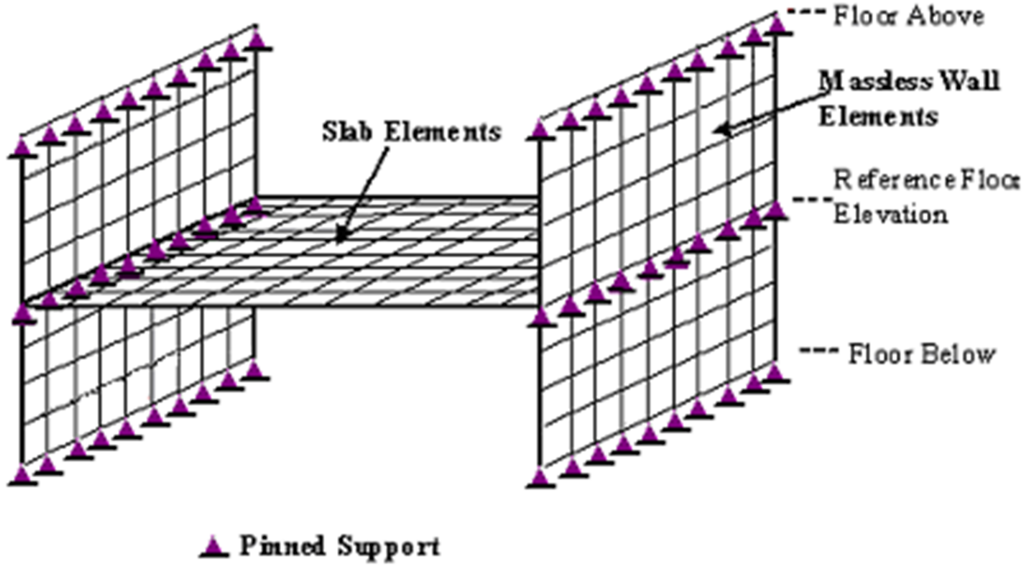

Figure 3NN-12 Floor Slab Model Boundary Conditions

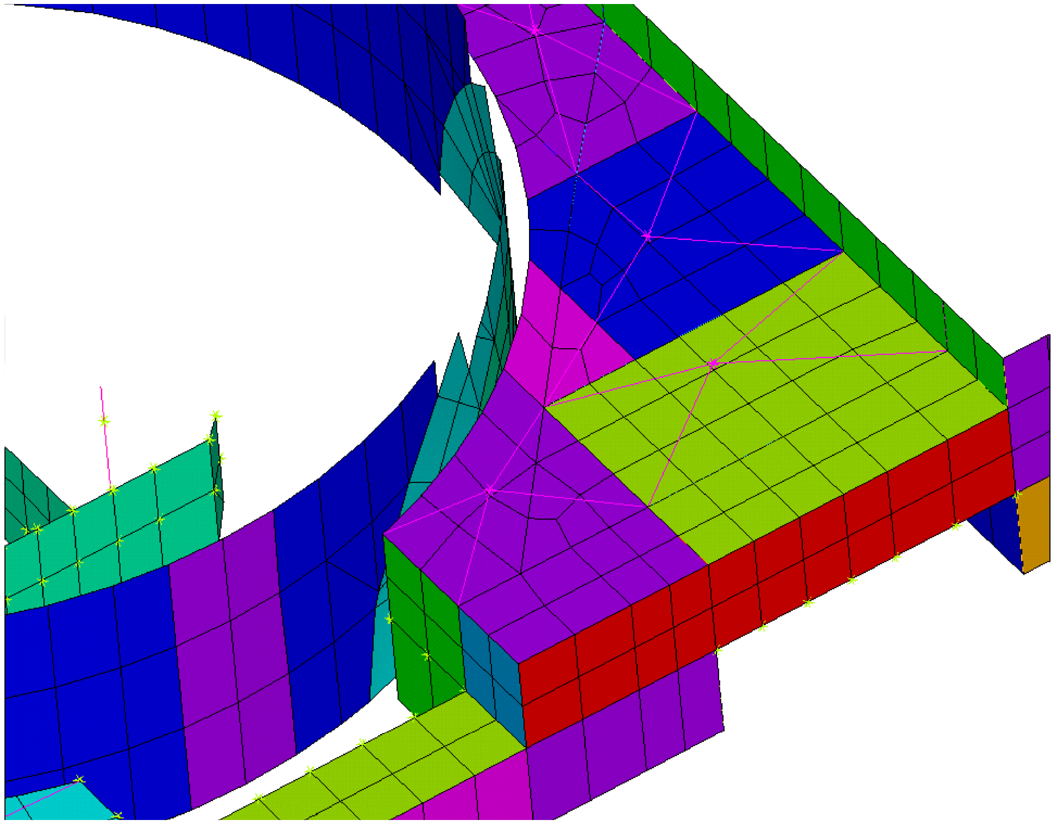

Figure 3NN-13 Flexible Slabs with SDOF

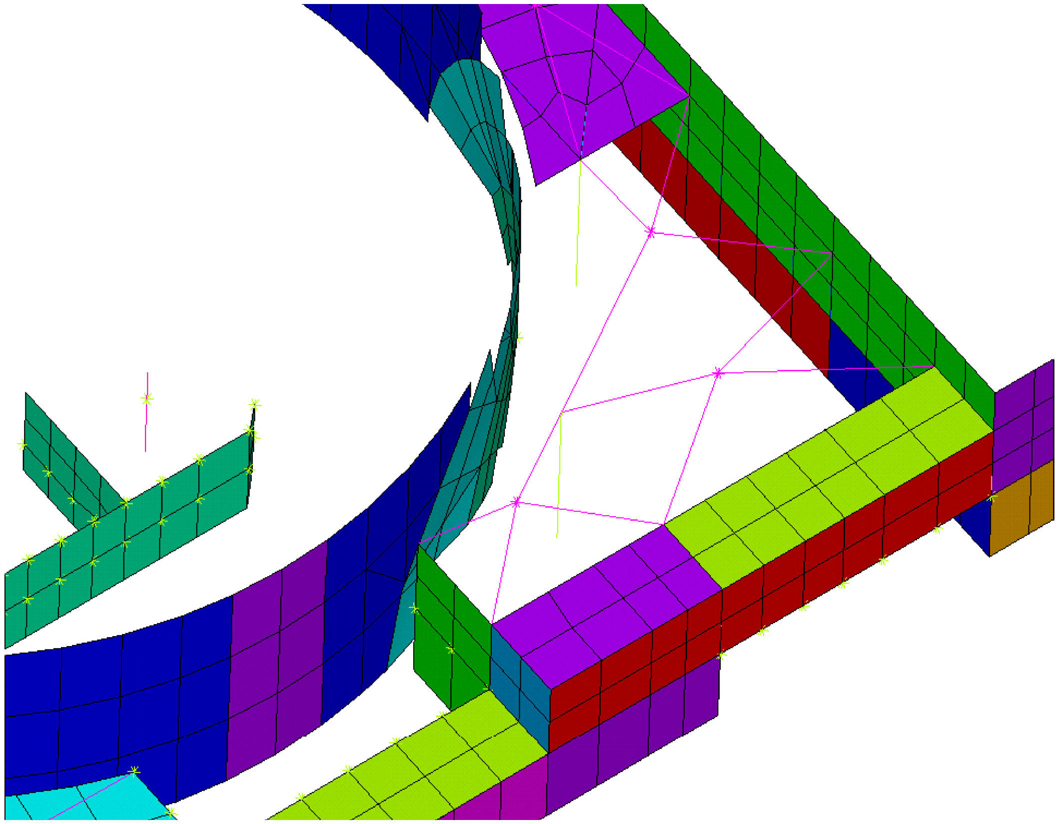

Figure 3NN-14 Typical Supports for SDOFs

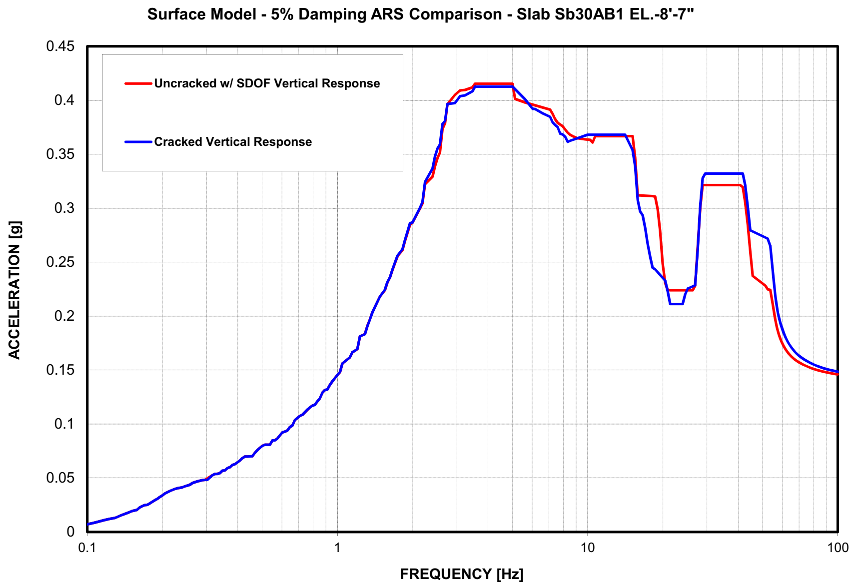

Figure 3NN-15 Evaluation of SDOF Oscillators (sheet 1 of 3)

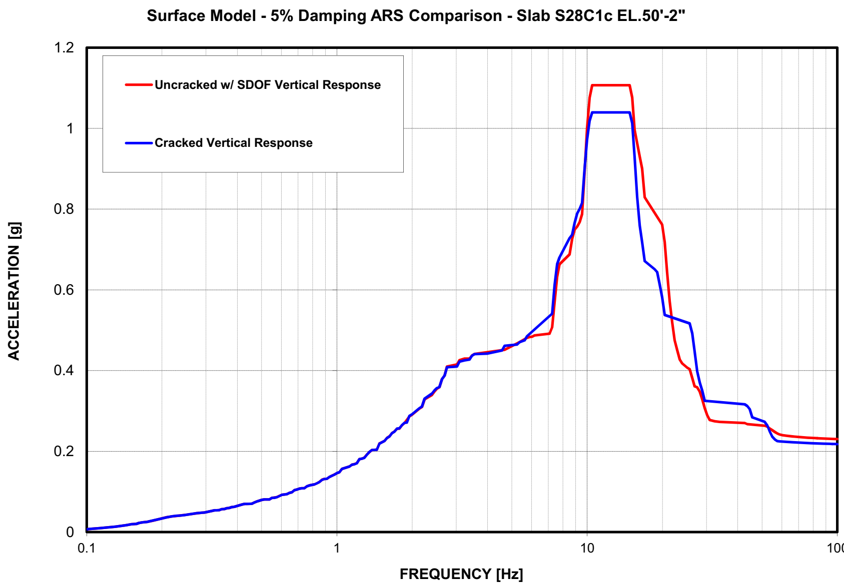

Figure 3NN-15 Evaluation of SDOF Oscillators (sheet 2 of 3)

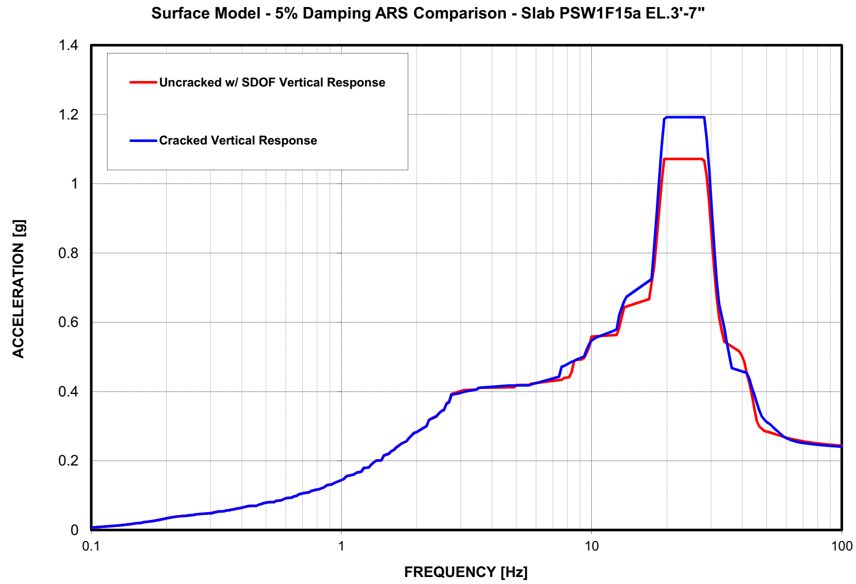

Figure 3NN-15 Evaluation of SDOF Oscillators (sheet 3 of 3)

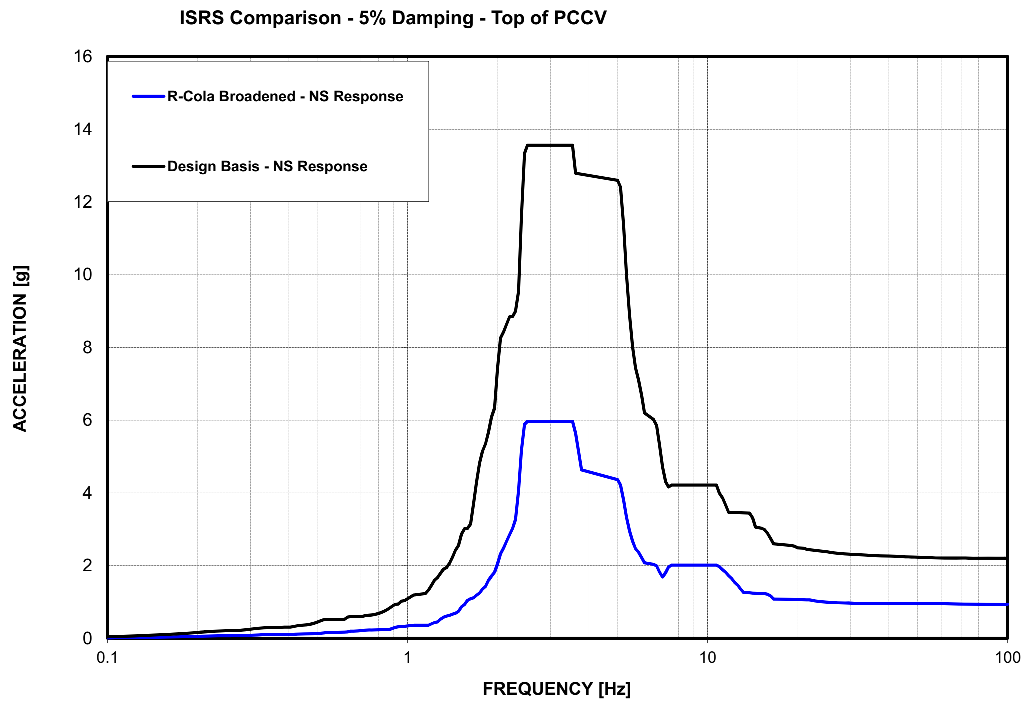

Figure 3NN-16 ISRS Comparison – 5% Damping – Top of PCCV EL. 232 ft (Sheet 1 of 3)

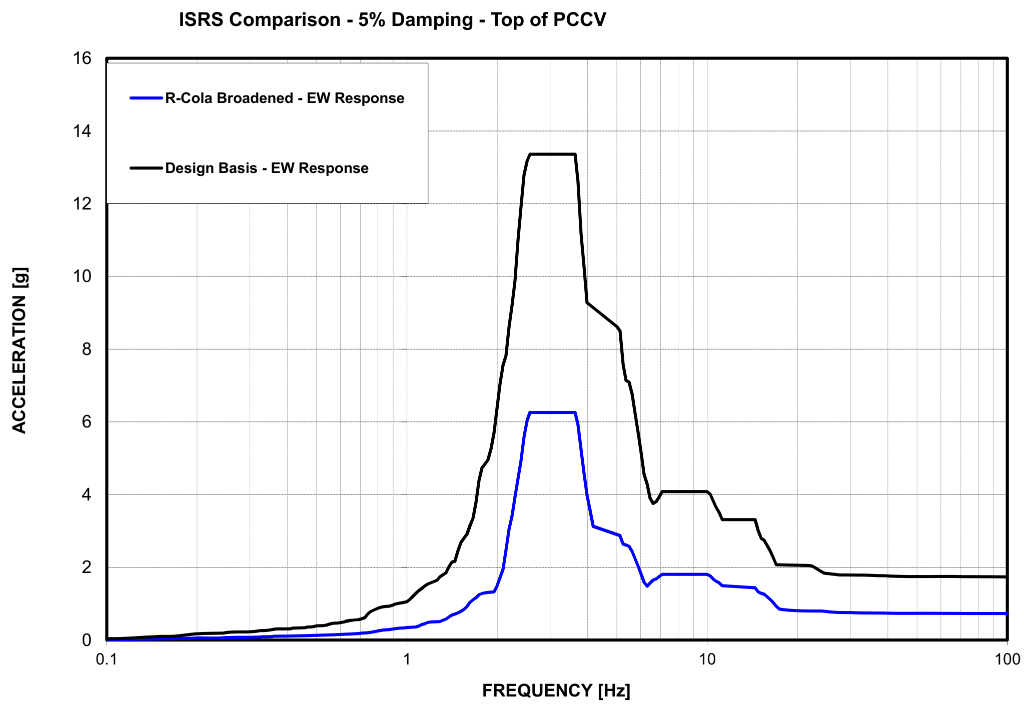

Figure 3NN-16 ISRS Comparison – 5% Damping – Top of PCCV EL. 232 ft (Sheet 2 of 3)

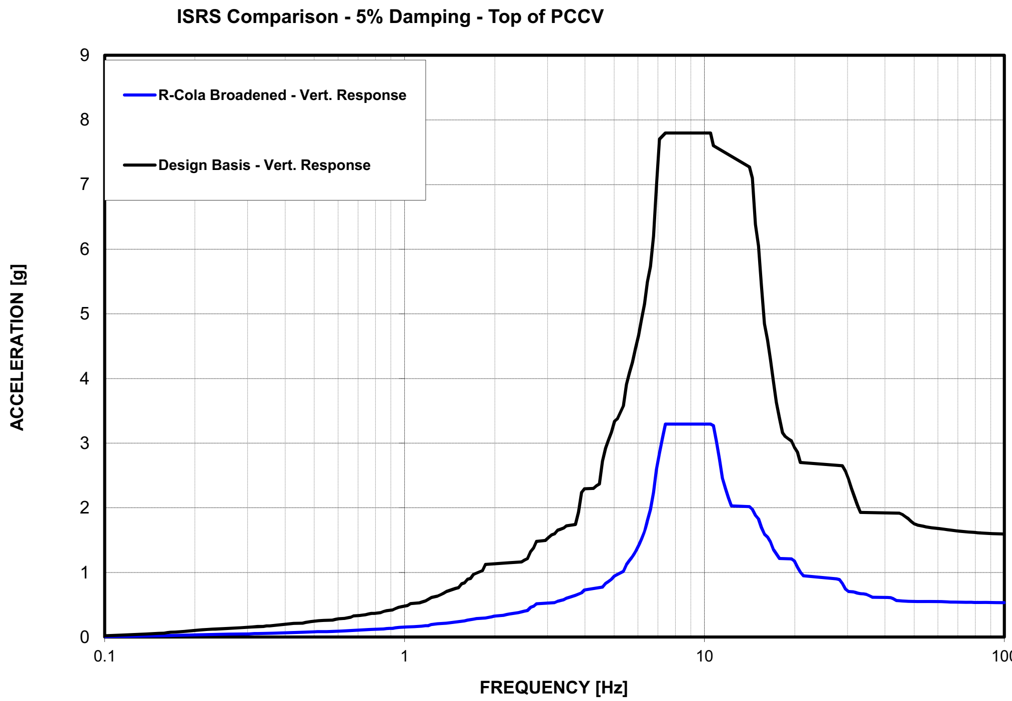

Figure 3NN-16 ISRS Comparison – 5% Damping – Top of PCCV EL. 232 ft (Sheet 3 of 3)

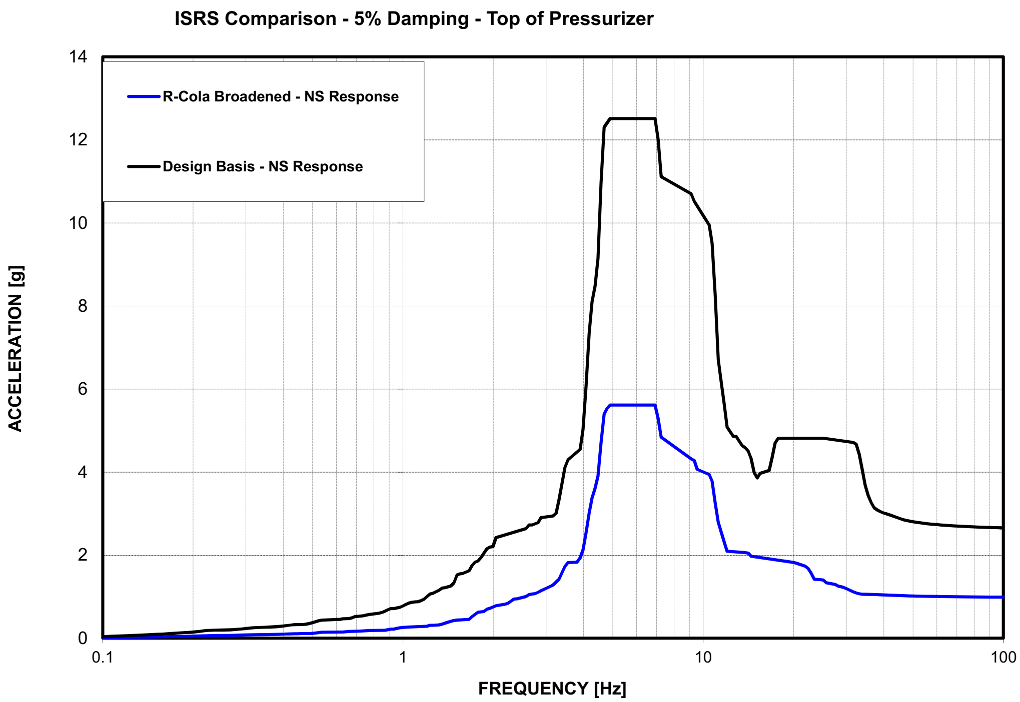

Figure 3NN-17 ISRS Comparison – 5% Damping – Top of Pressurizer House EL. 138.583 ft (Sheet 1 of 3)

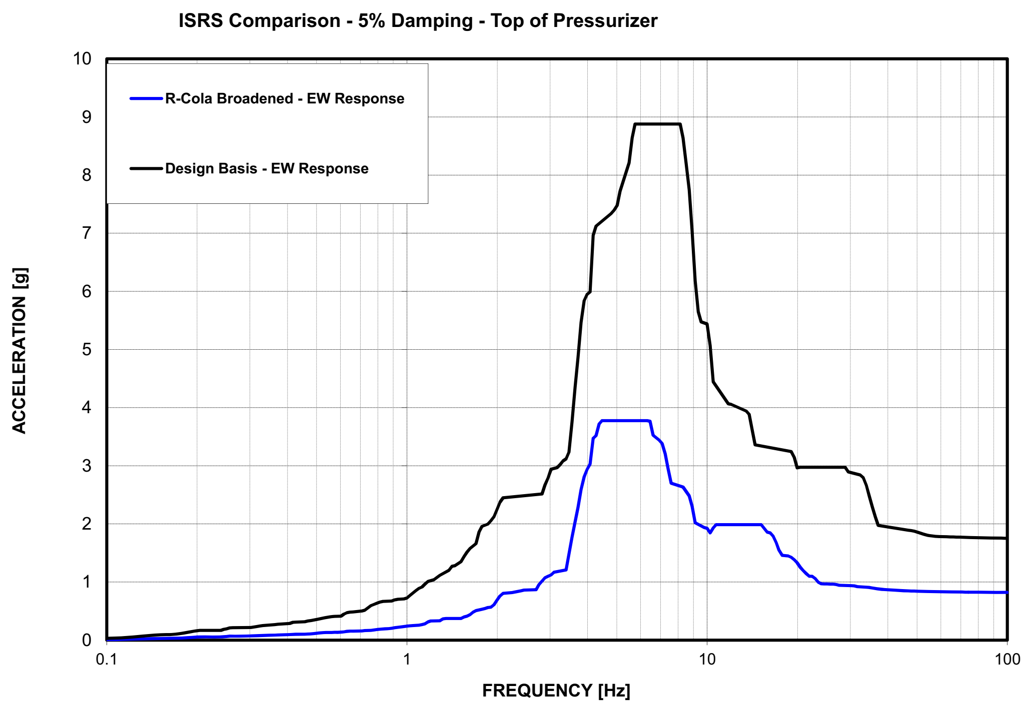

Figure 3NN-17 ISRS Comparison – 5% Damping – Top of Pressurizer House EL. 138.583 ft (Sheet 2 of 3)

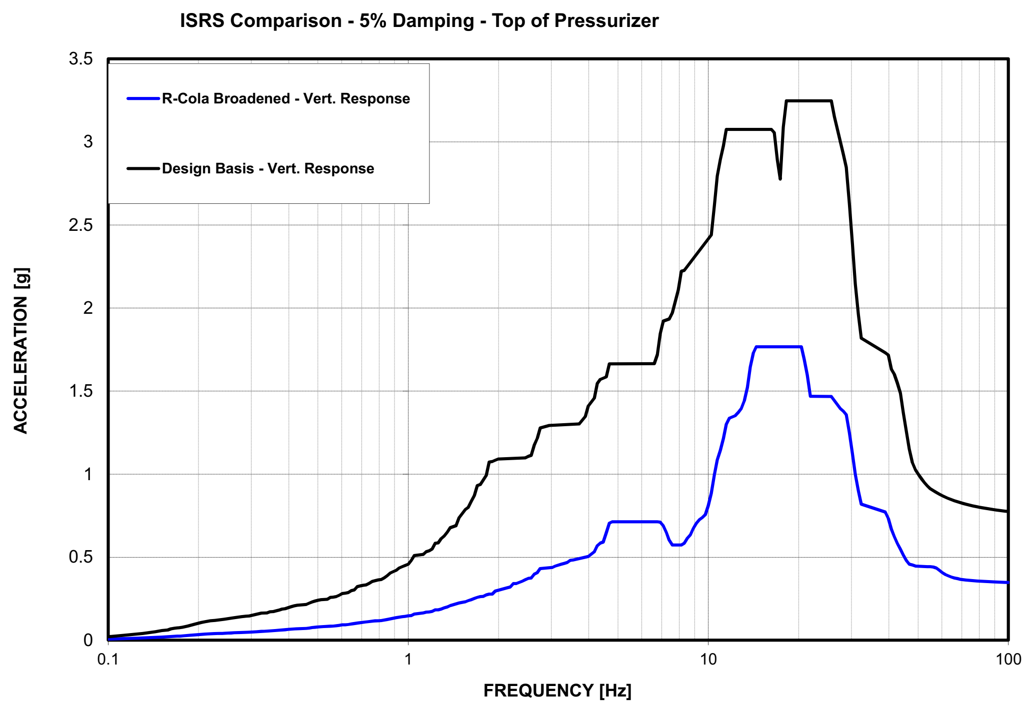

Figure 3NN-17 ISRS Comparison – 5% Damping – Top of Pressurizer House EL. 138.583 ft (Sheet 3 of 3)

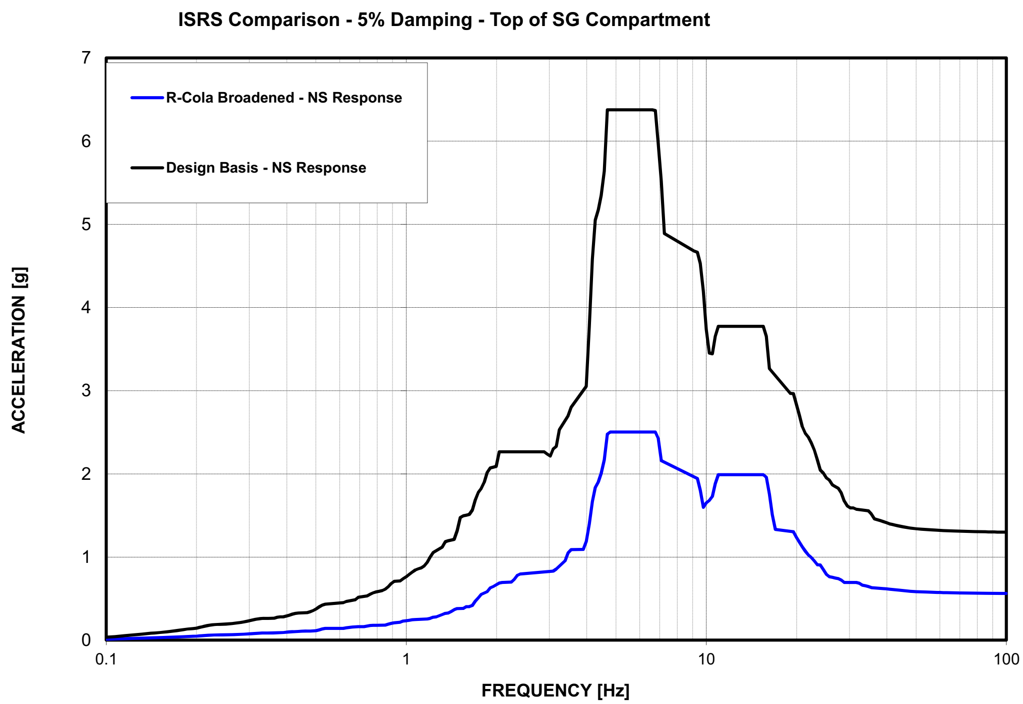

Figure 3NN-18 ISRS Comparison - 5% Damping – Top of Steam Generator Compartment EL. 112 ft (Sheet 1 of 3)

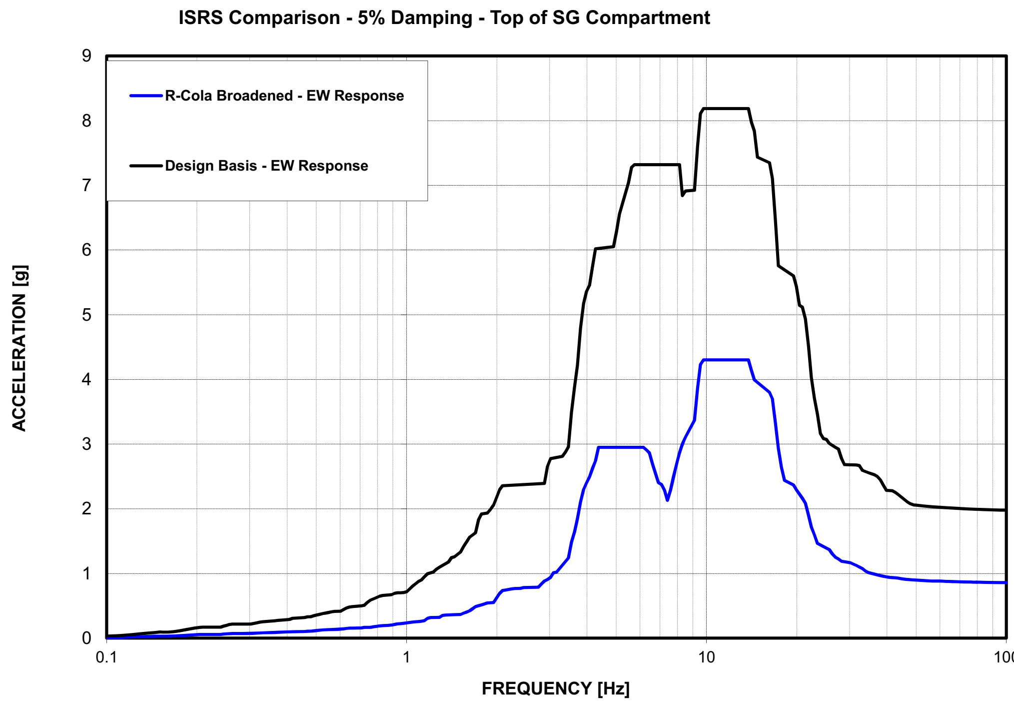

Figure 3NN-18 ISRS Comparison - 5% Damping – Top of Steam Generator Compartment EL. 112 ft (Sheet 2 of 3)

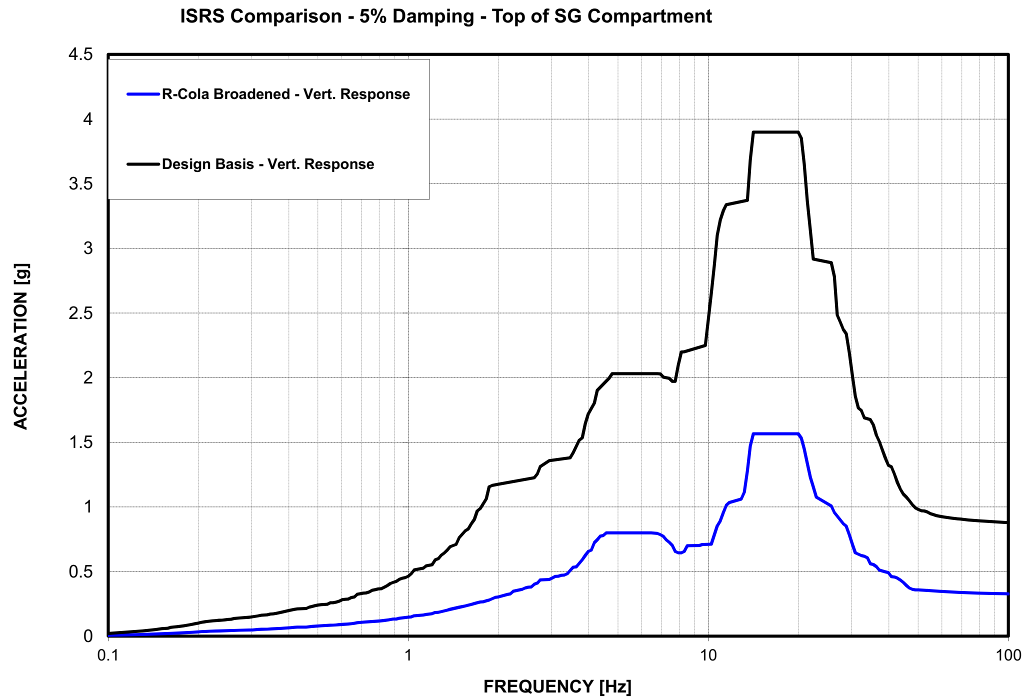

Figure 3NN-18 ISRS Comparison - 5% Damping – Top of Steam Generator Compartment EL. 112 ft (Sheet 3 of 3)

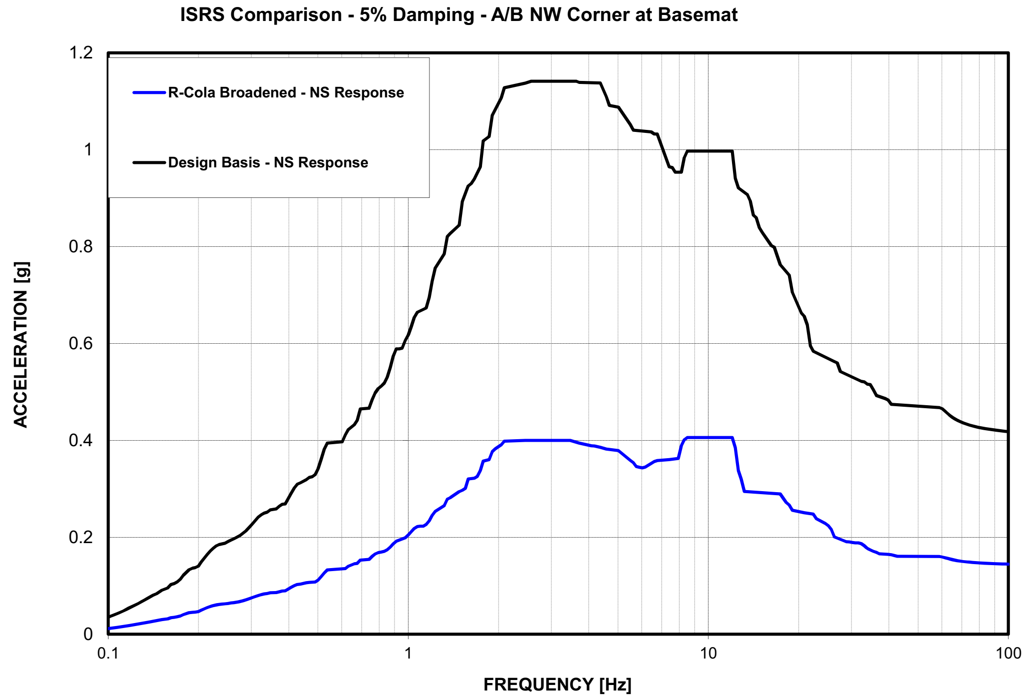

Figure 3NN-19 ISRS Comparison - 5% Damping – A/B Northwest Corner at Top of Basemat EL. -26.333 ft (Sheet 1 of 3)

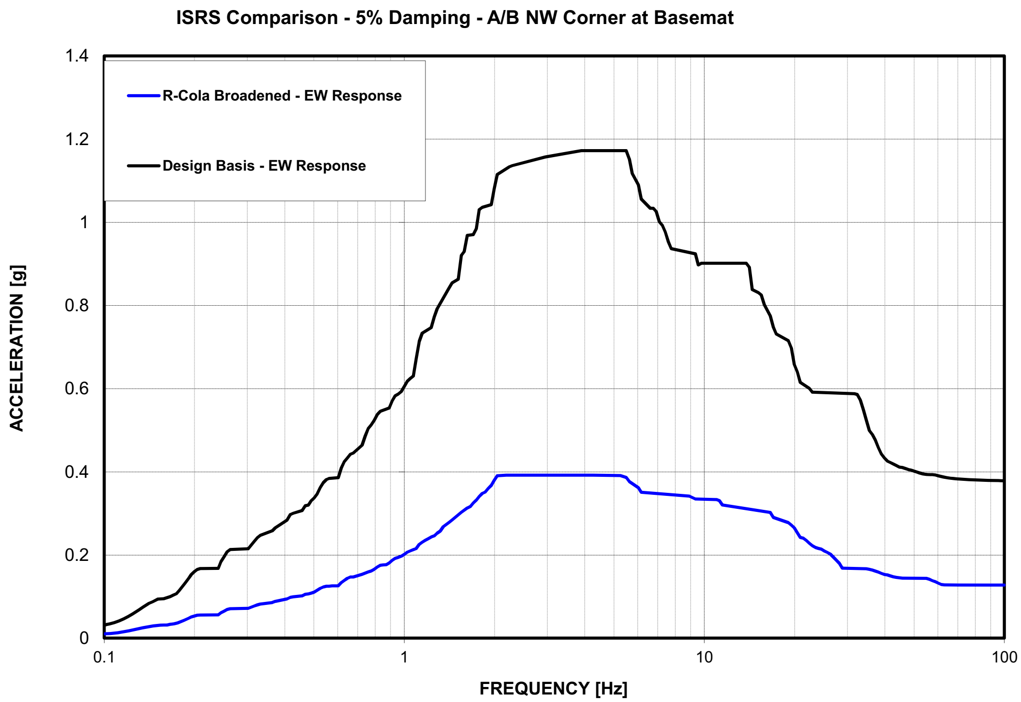

Figure 3NN-19 ISRS Comparison - 5% Damping – A/B Northwest Corner at Top of Basemat EL. -26.333 ft (Sheet 2 of 3)

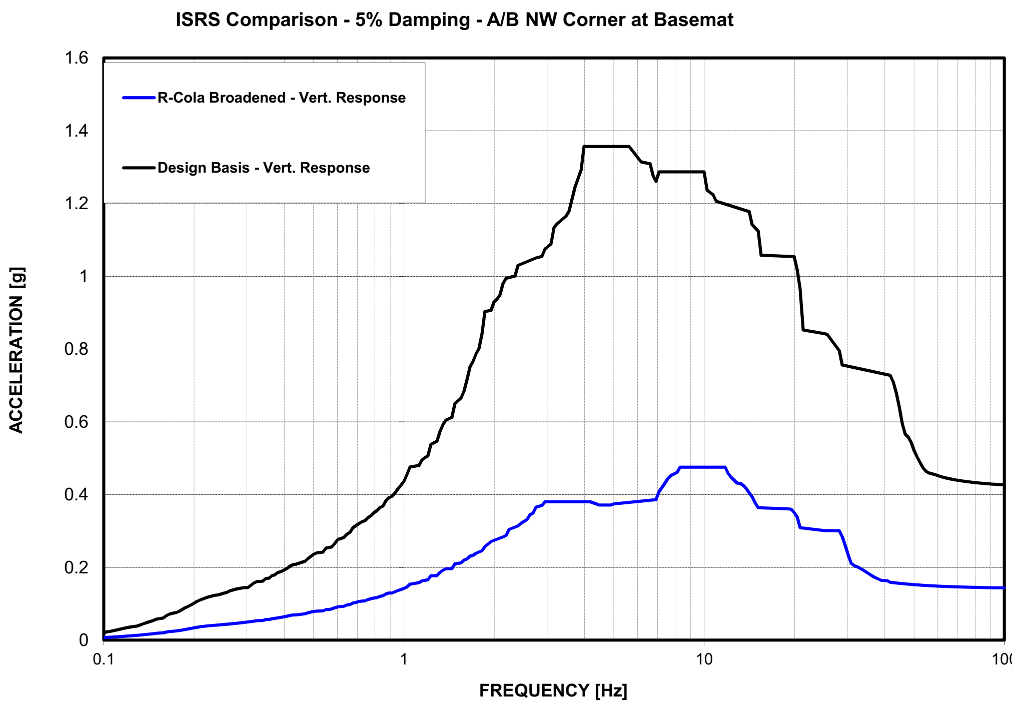

Figure 3NN-19 ISRS Comparison - 5% Damping – A/B Northwest Corner at Top of Basemat EL. -26.333 ft (Sheet 3 of 3)

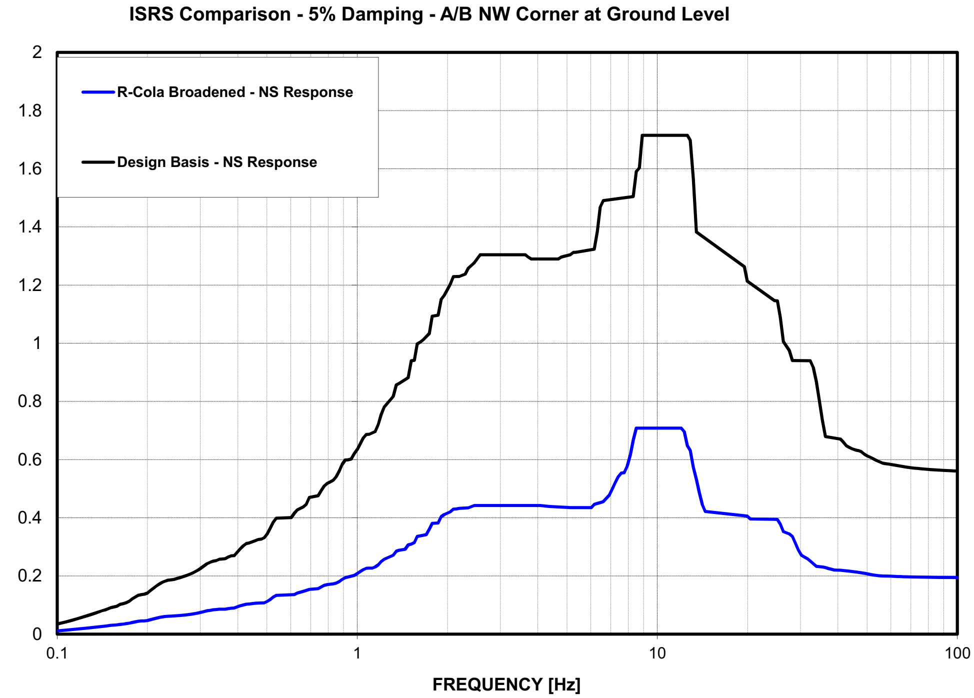

Figure 3NN-20 ISRS Comparison - 5% Damping – A/B Northwest Corner at Grade Level EL. 2.583 ft (Sheet 1 of 3)

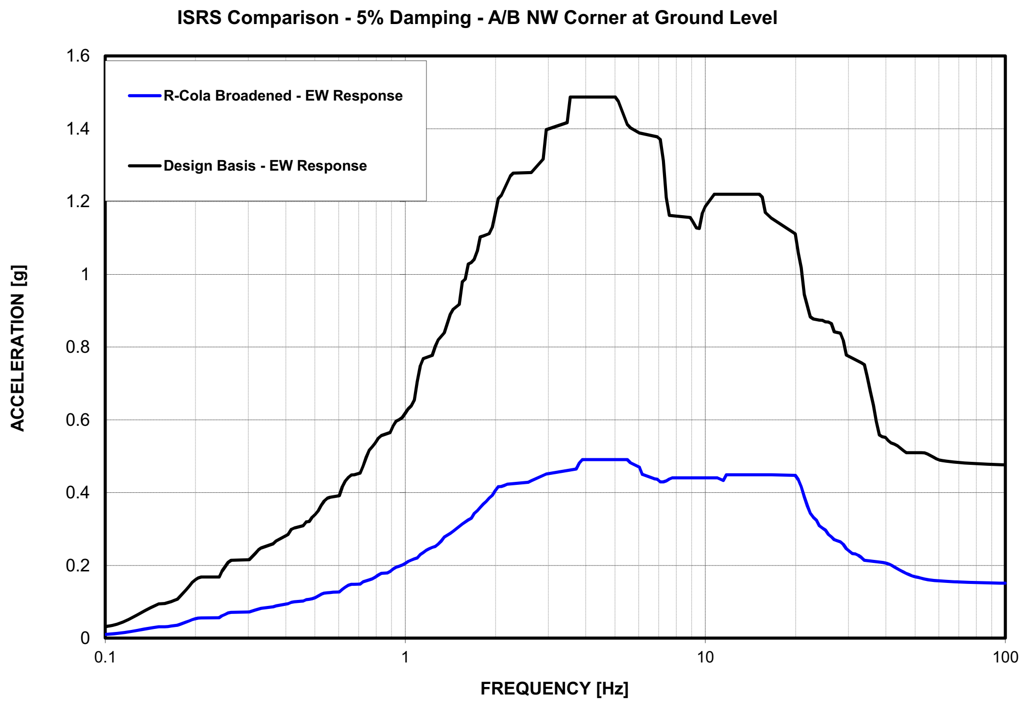

Figure 3NN-20 ISRS Comparison - 5% Damping – A/B Northwest Corner at Grade Level EL. 2.583 ft (Sheet 2 of 3)

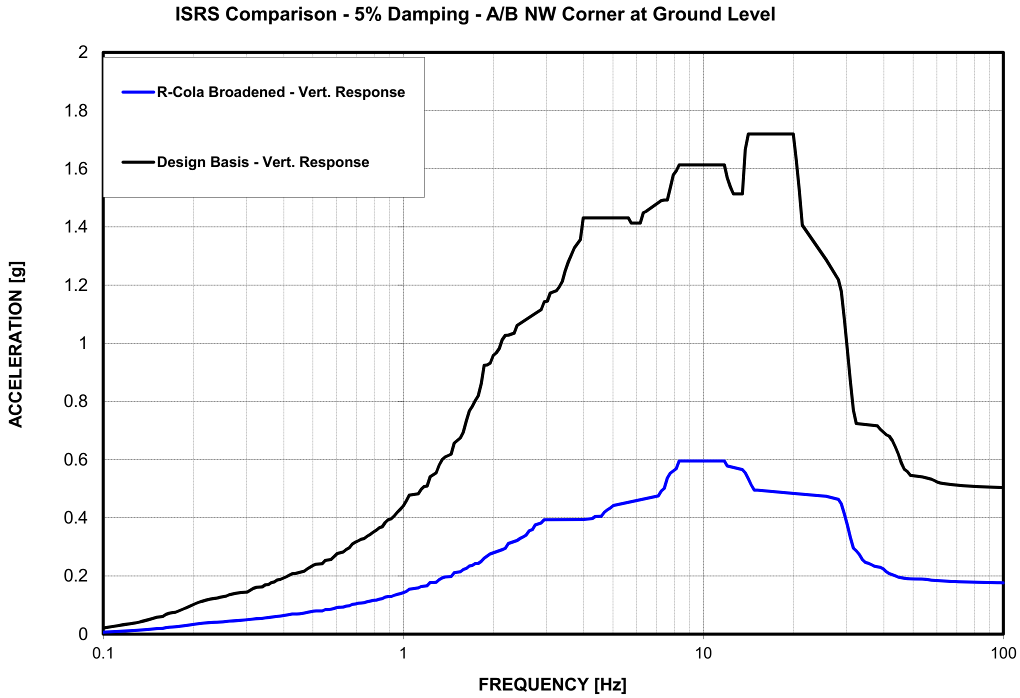

Figure 3NN-20 ISRS Comparison - 5% Damping – A/B Northwest Corner at Grade Level EL. 2.583 ft (Sheet 3 of 3)

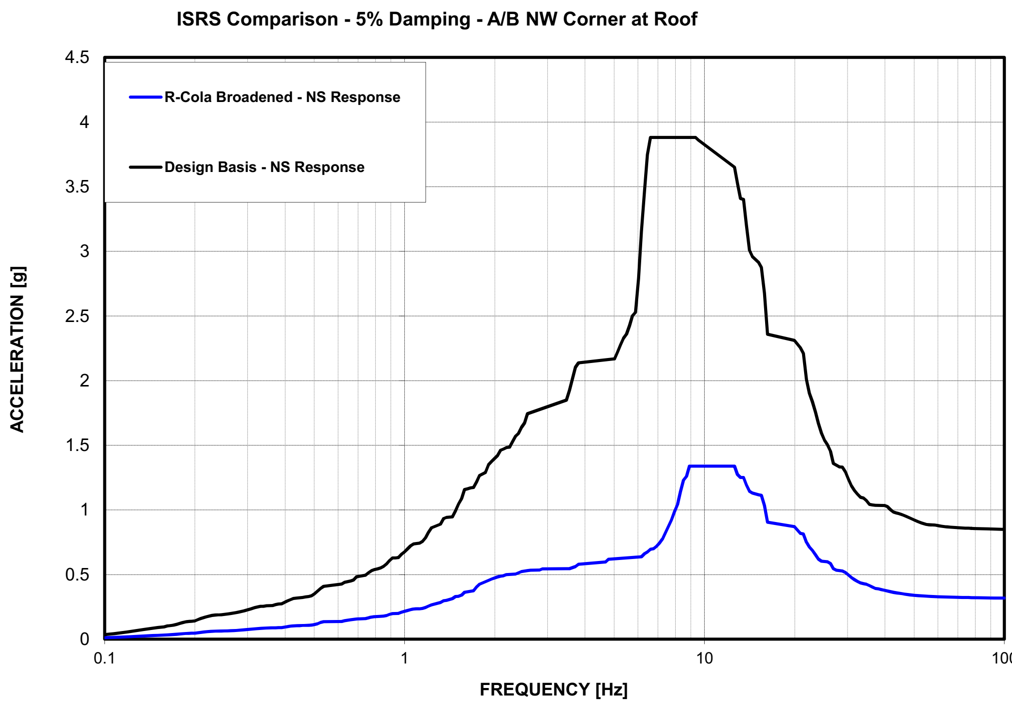

Figure 3NN-21 ISRS Comparison - 5% Damping – A/B Northwest Corner at Roof EL. 74.83 ft (Sheet 1 of 3)

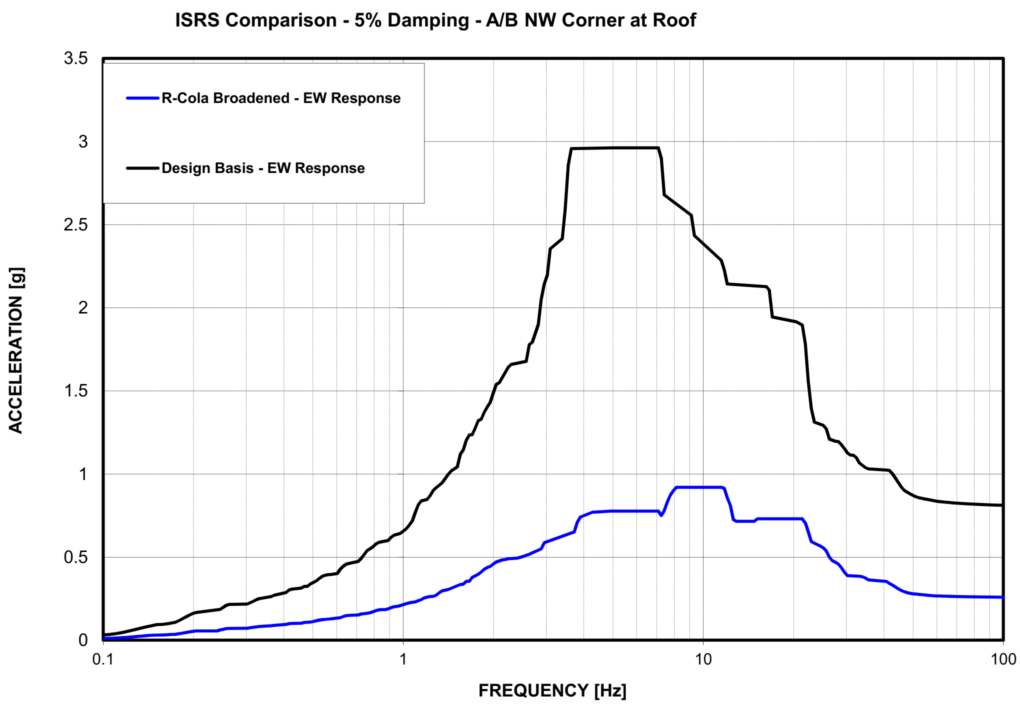

Figure 3NN-21 ISRS Comparison - 5% Damping – A/B Northwest Corner at Roof EL. 74.83 ft (Sheet 2 of 3)

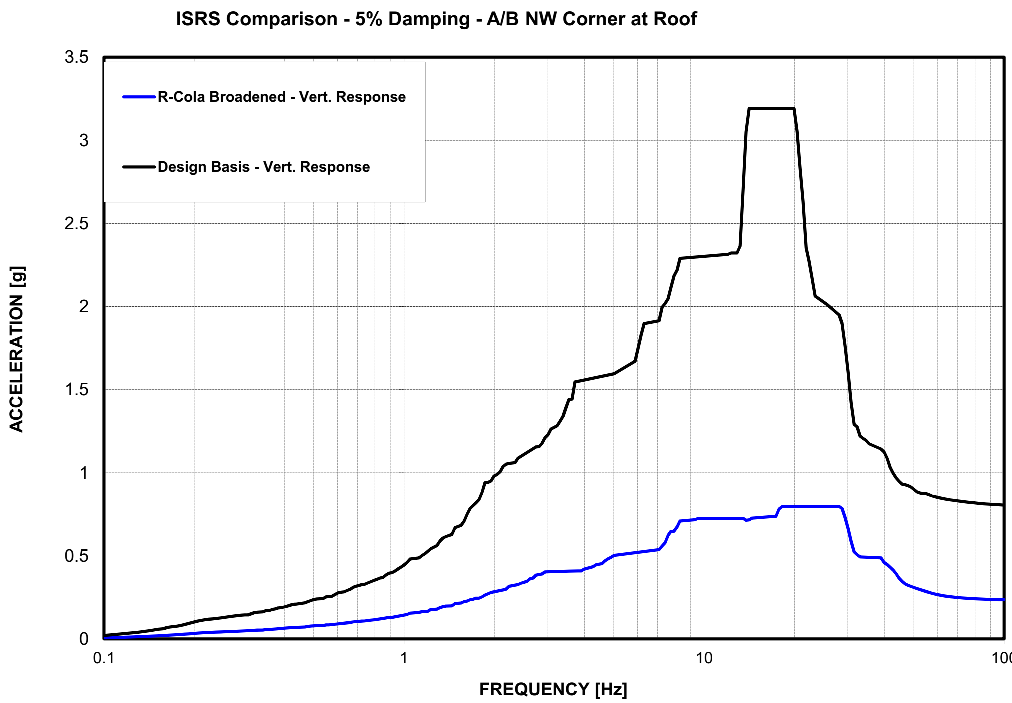

Figure 3NN-21 ISRS Comparison - 5% Damping – A/B Northwest Corner at Roof EL. 74.83 ft (Sheet 3 of 3)

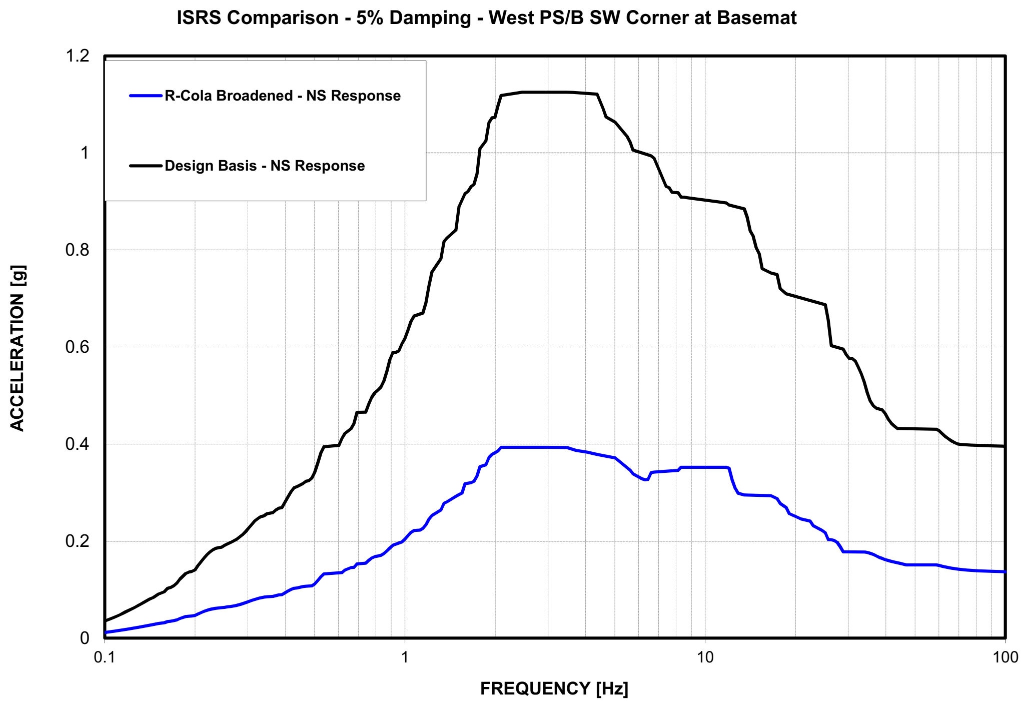

Figure 3NN-22 ISRS Comparison - 5% Damping – West PS/B Southwest Corner at Top of Basemat EL. -26.333 ft
(Sheet 1 of 3)

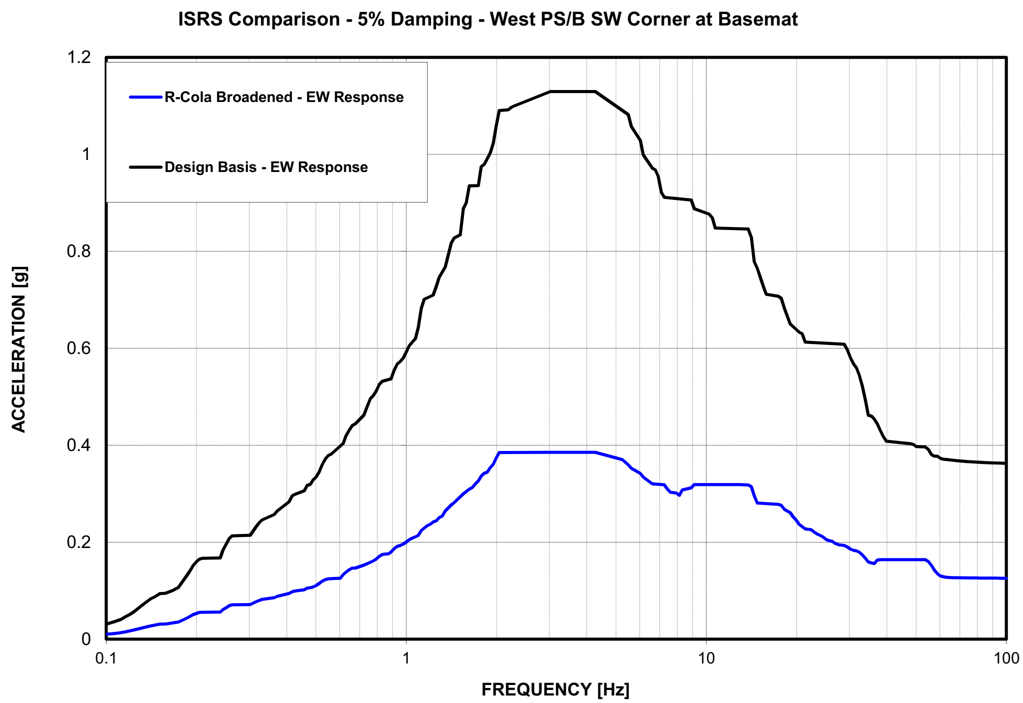

Figure 3NN-22 ISRS Comparison - 5% Damping – West PS/B Southwest Corner at Top of Basemat EL. -26.333 ft (Sheet 2 of 3)

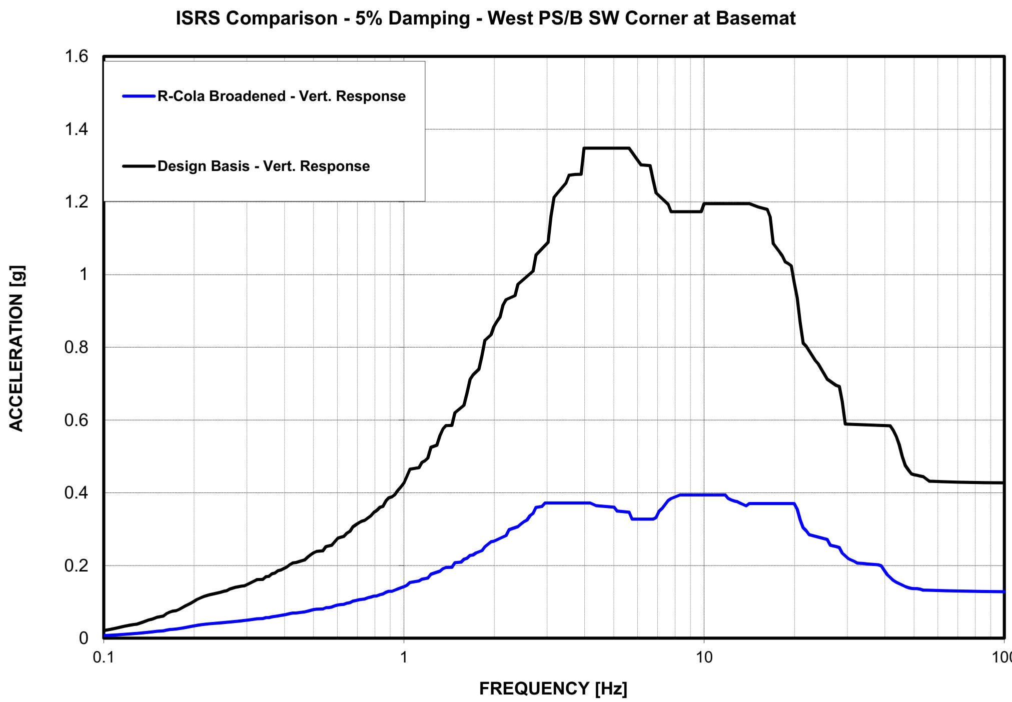

Figure 3NN-22 ISRS Comparison - 5% Damping – West PS/B Southwest Corner at Top of Basemat EL. -26.333 ft (Sheet 3 of 3)

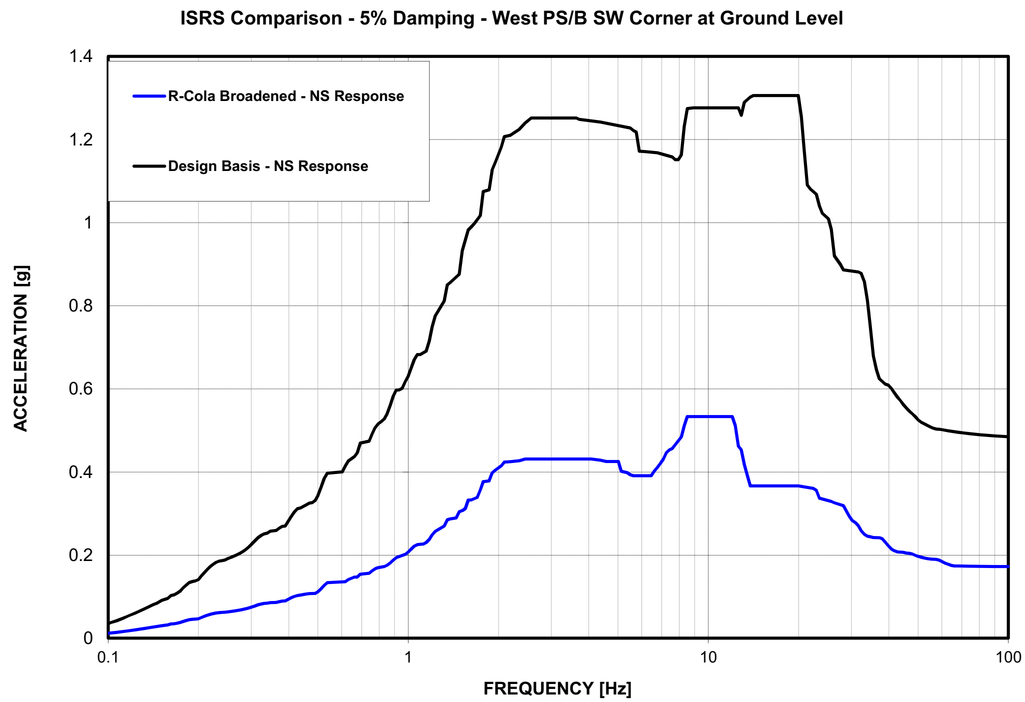

Figure 3NN-23 ISRS Comparison - 5% Damping – West PS/B Southwest Corner at Grade Level EL. 2.583 ft (Sheet 1 of 3)

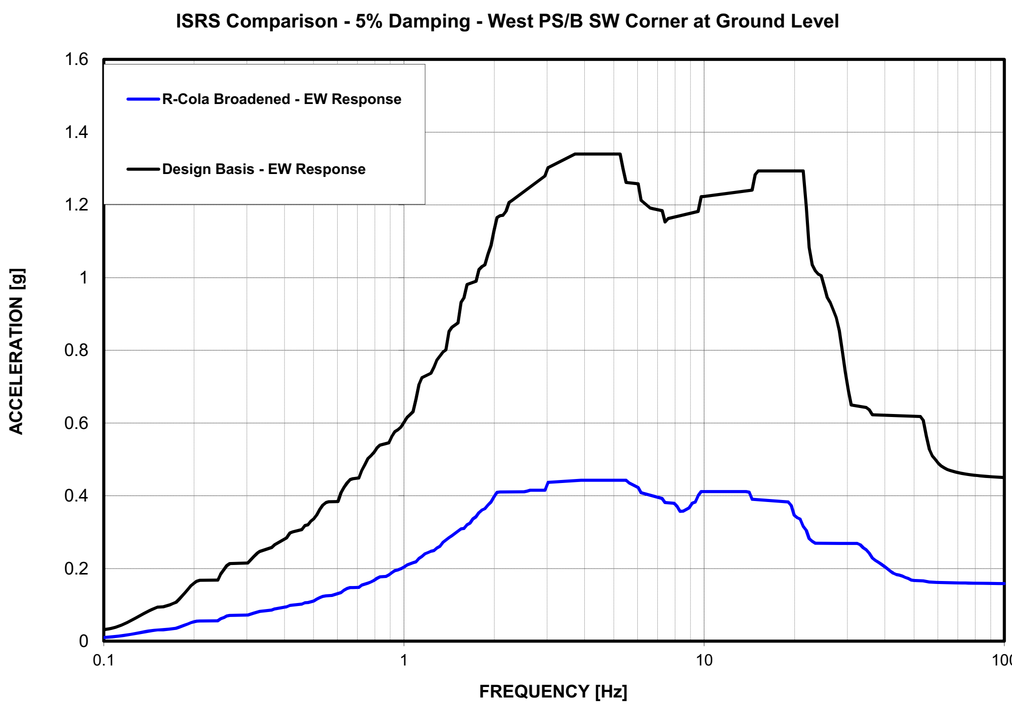

Figure 3NN-23 ISRS Comparison - 5% Damping – West PS/B Southwest Corner at Grade Level EL. 2.583 ft (Sheet 2 of 3)

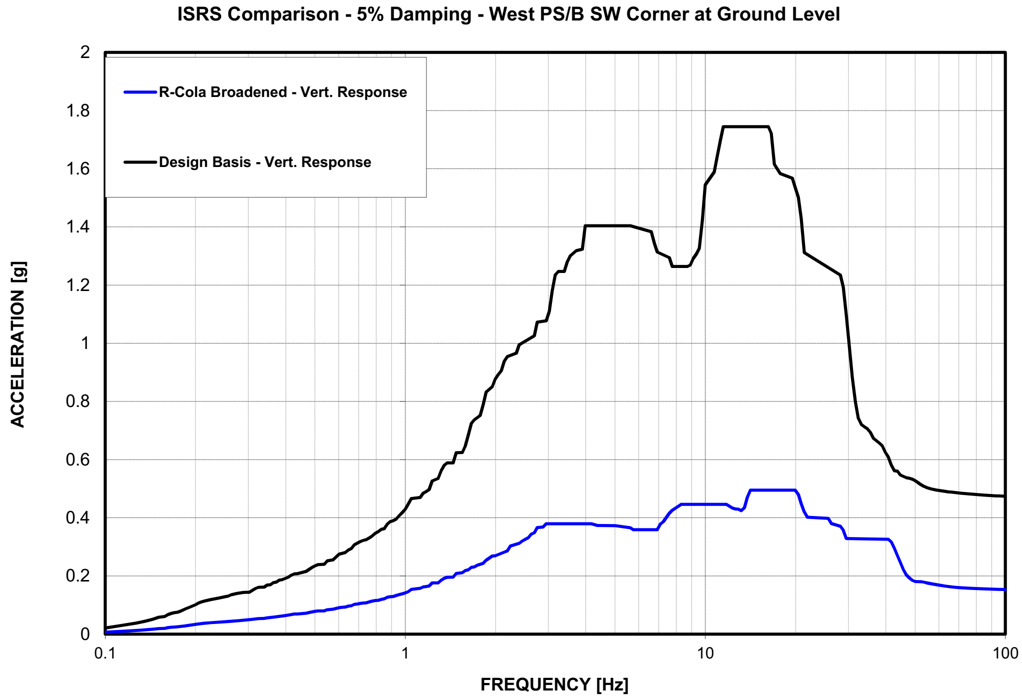

Figure 3NN-23 ISRS Comparison - 5% Damping – West PS/B Southwest Corner at Grade Level EL. 2.583 ft (Sheet 3 of 3)

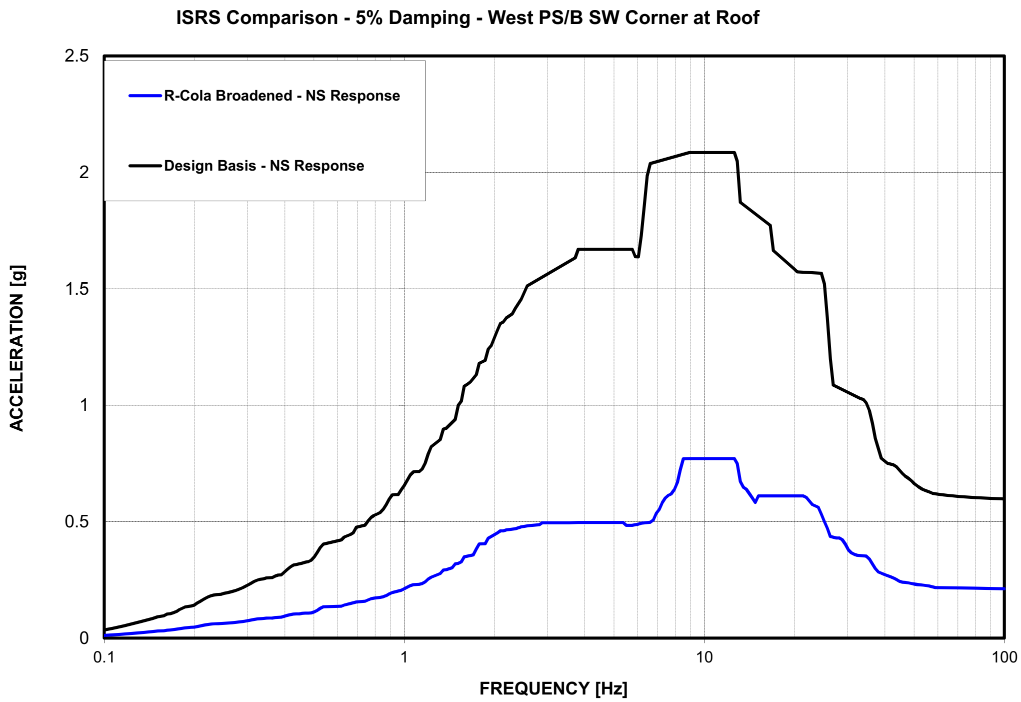

Figure 3NN-24 ISRS Comparison - 5% Damping – West PS/B Southwest Corner at Roof EL. 48.5 ft (Sheet 1 of 3)

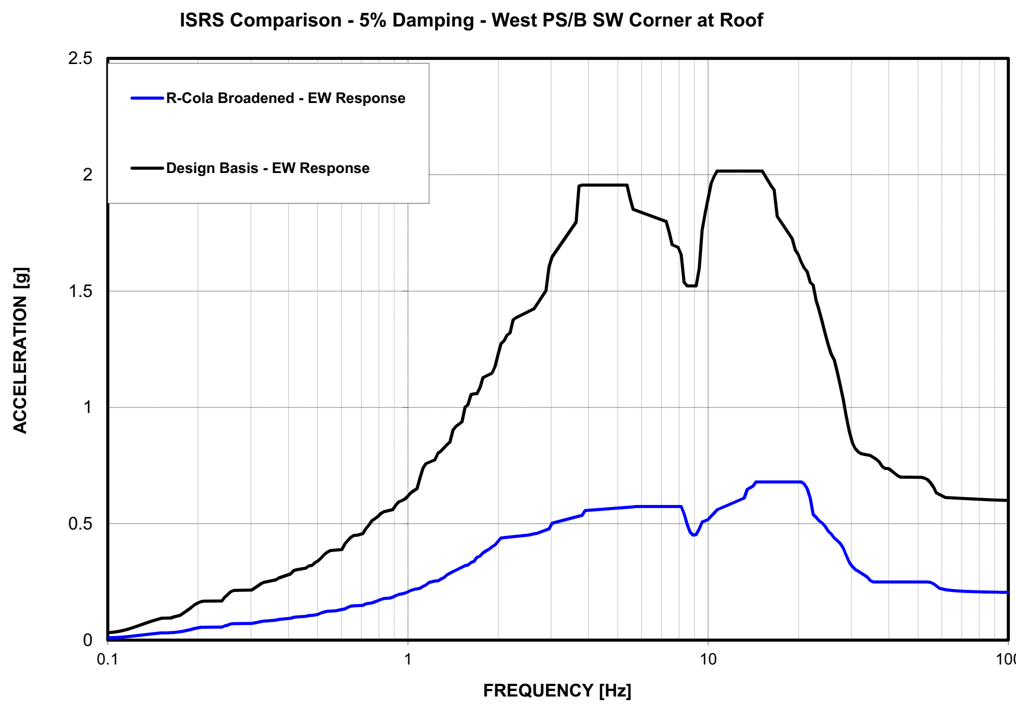

Figure 3NN-24 ISRS Comparison - 5% Damping – West PS/B Southwest Corner at Roof EL. 48.5 ft (Sheet 2 of 3)

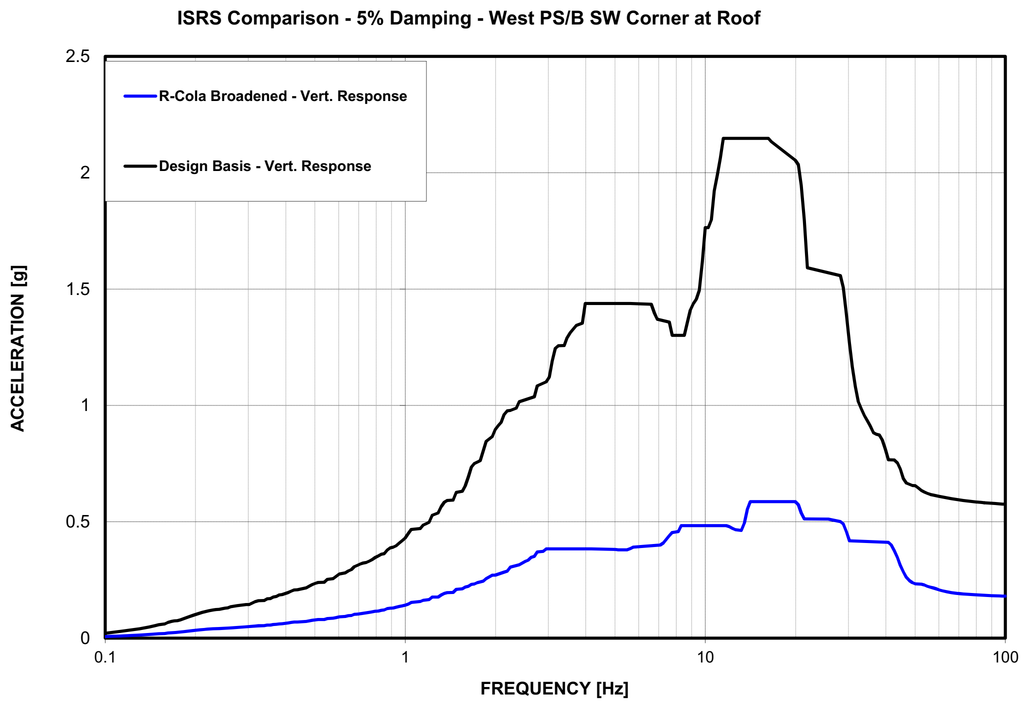

Figure 3NN-24 ISRS Comparison - 5% Damping – West PS/B Southwest Corner at Roof EL. 48.5 ft (Sheet 3 of 3)

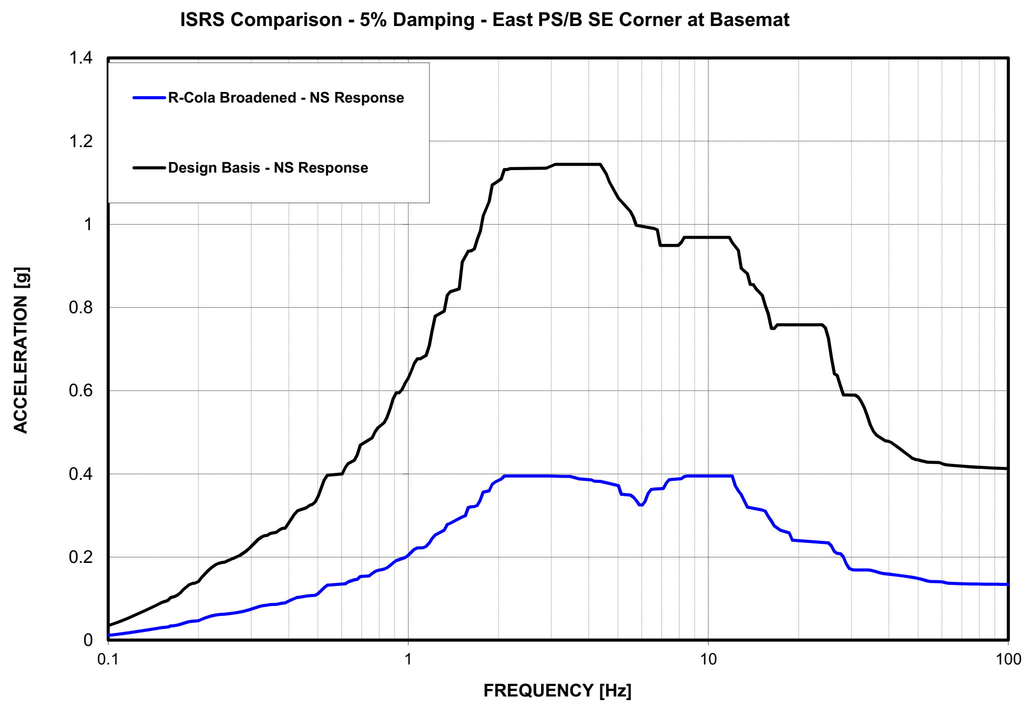

Figure 3NN-25 ISRS Comparison - 5% Damping – East PS/B Southeast Corner at Top of Basemat EL. -26.333 ft (Sheet 1 of 3)

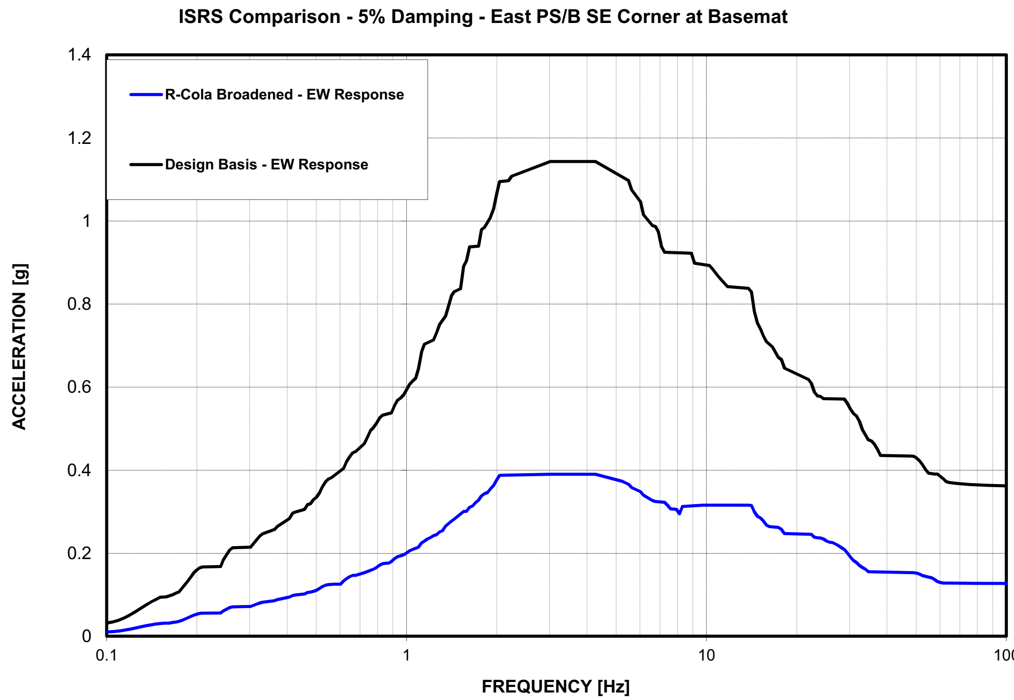

Figure 3NN-25 ISRS Comparison - 5% Damping – East PS/B Southeast Corner at Top of Basemat EL. -26.333 ft (Sheet 2 of 3)

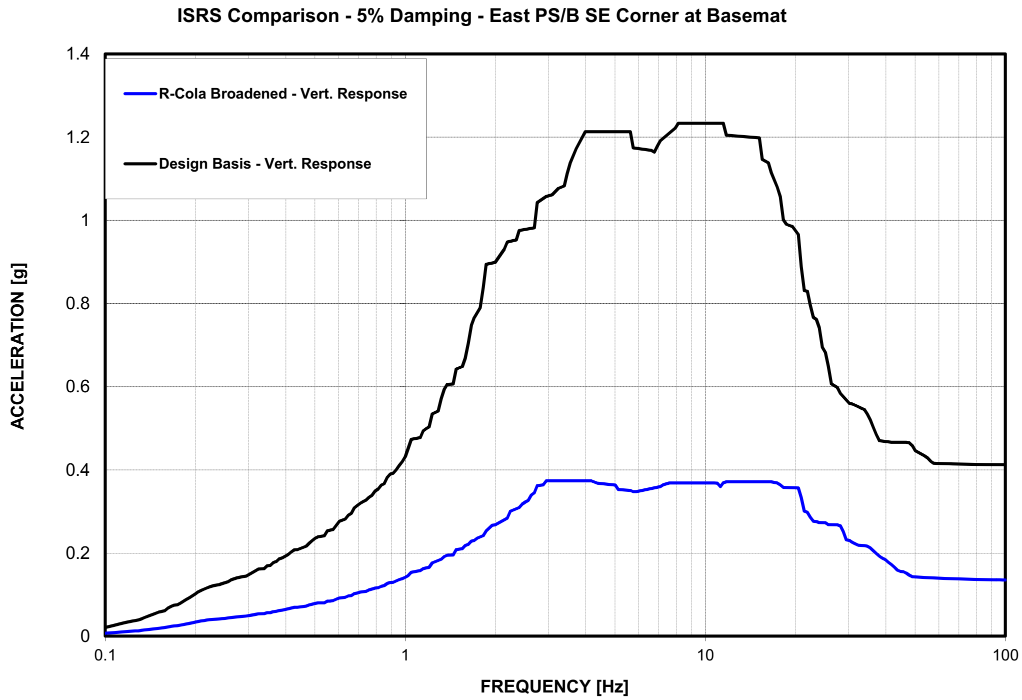

Figure 3NN-25 ISRS Comparison - 5% Damping – East PS/B Southeast Corner at Top of Basemat EL. -26.333 ft (Sheet 3 of 3)

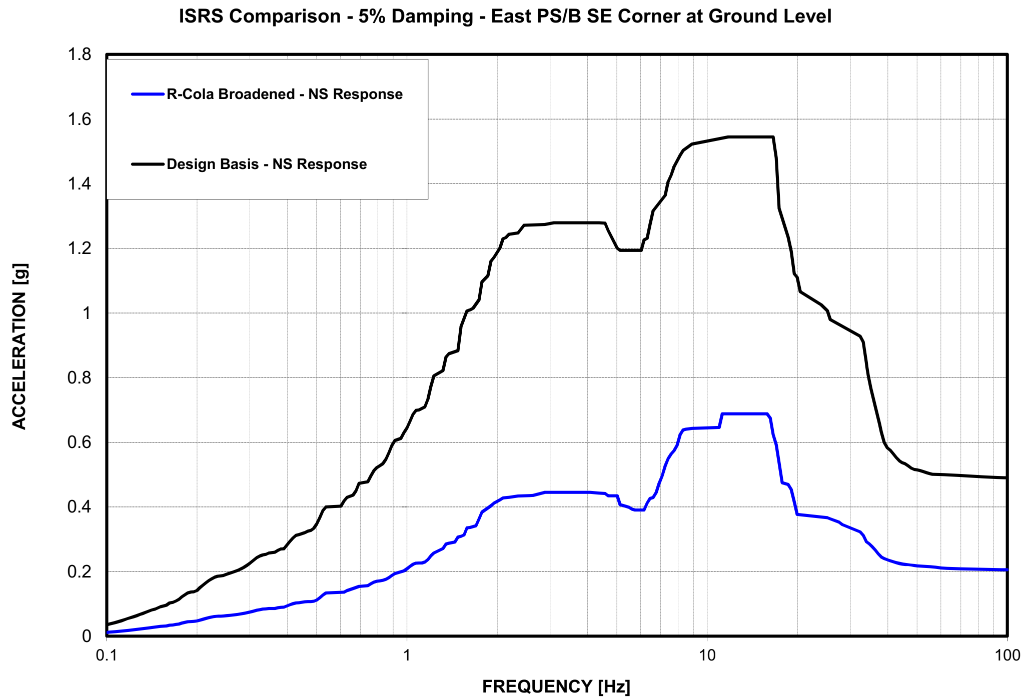

Figure 3NN-26 ISRS Comparison - 5% Damping – East PS/B Southeast Corner at Grade Level EL. 2.583 ft (Sheet 1 of 3)

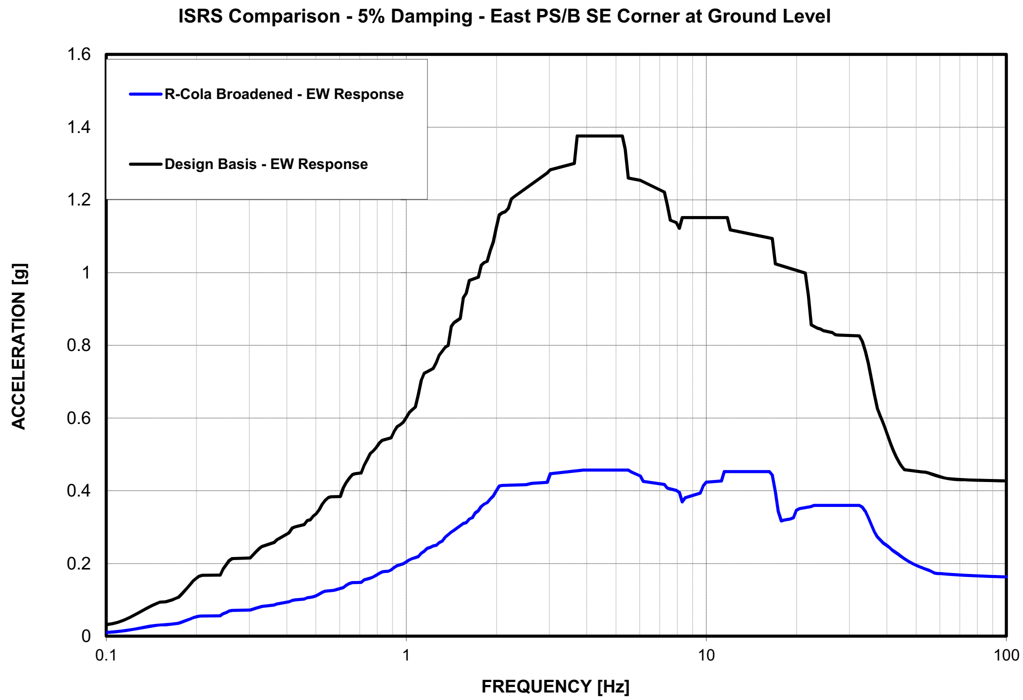

Figure 3NN-26 ISRS Comparison - 5% Damping – East PS/B Southeast Corner at Grade Level EL. 2.583 ft (Sheet 2 of 3)

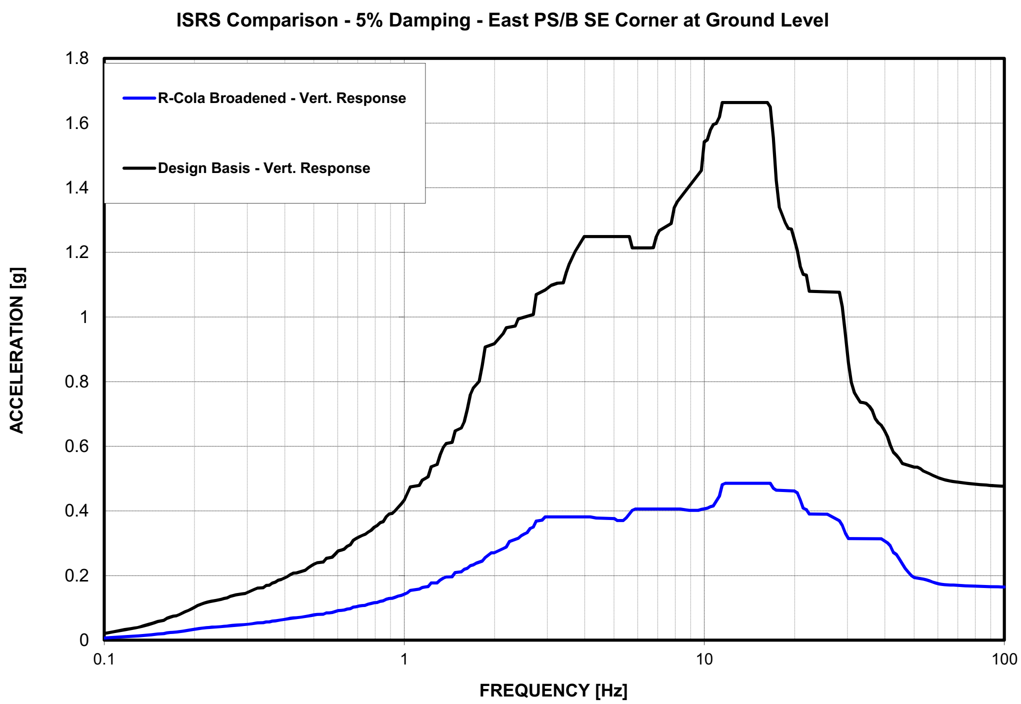

Figure 3NN-26 ISRS Comparison - 5% Damping – East PS/B Southeast Corner at Grade Level EL. 2.583 ft (Sheet 3 of 3)

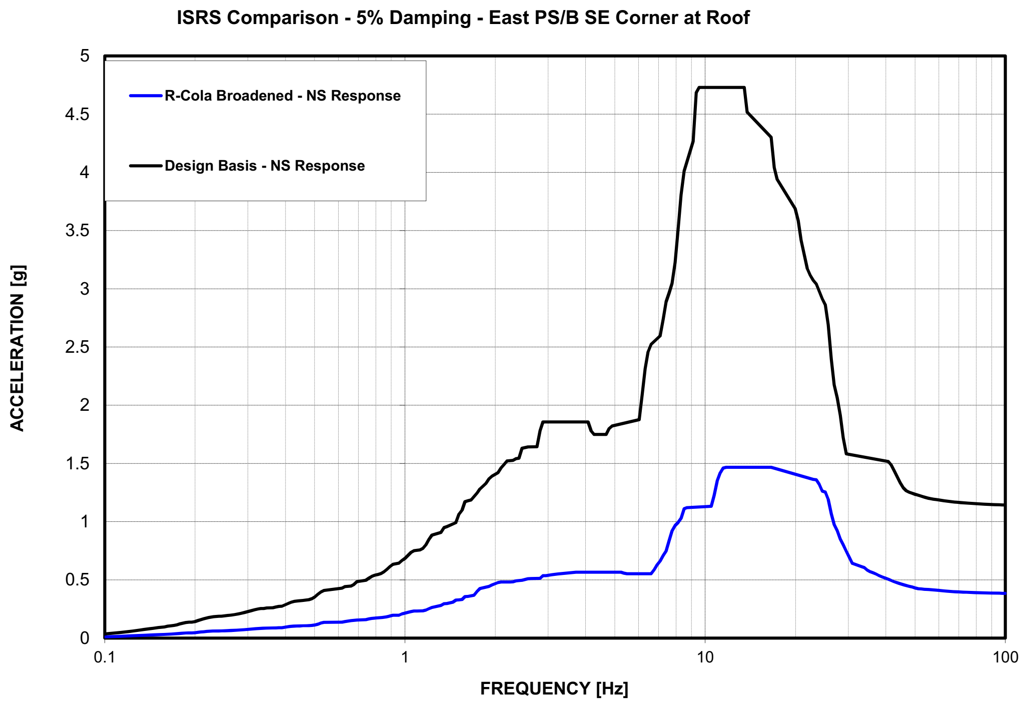

Figure 3NN-27 ISRS Comparison - 5% Damping – East PS/B Southeast Corner at Roof EL. 48.5 ft (Sheet 1 of 3)

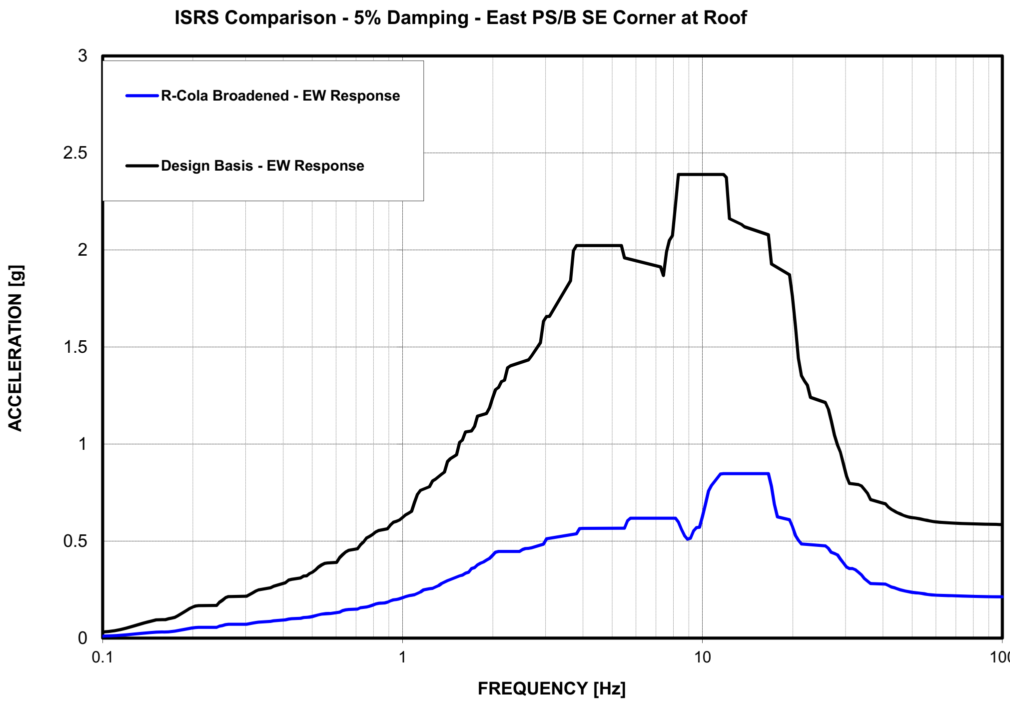

Figure 3NN-27 ISRS Comparison - 5% Damping – East PS/B Southeast Corner at Roof EL. 48.5 ft (Sheet 2 of 3)

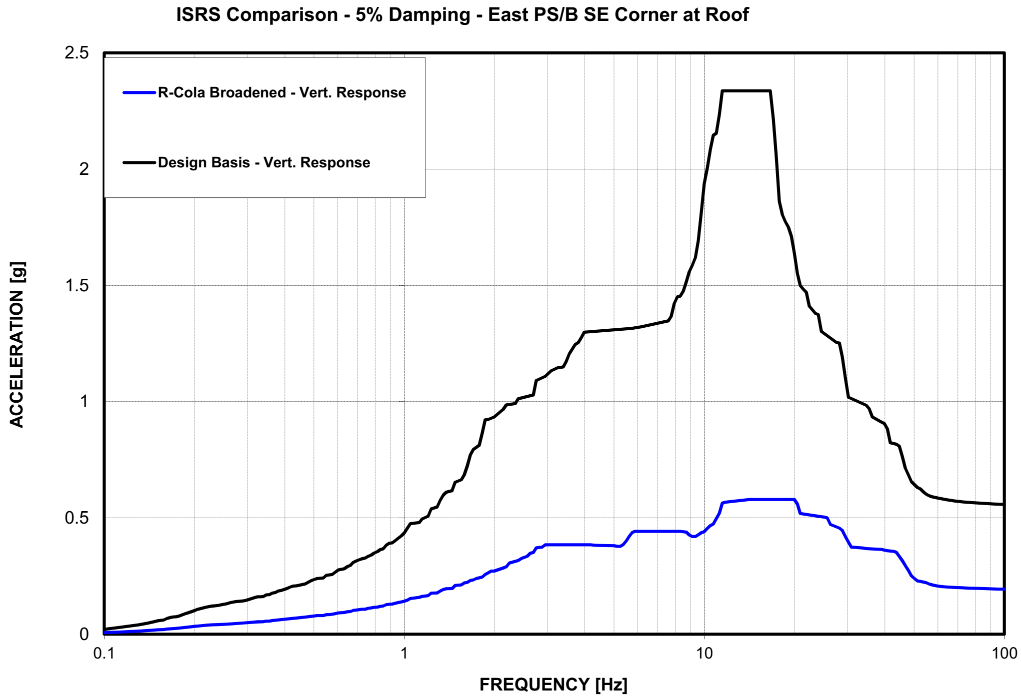

Figure 3NN-27 ISRS Comparison - 5% Damping – East PS/B Southeast Corner at Roof EL. 48.5 ft (Sheet 3 of 3)

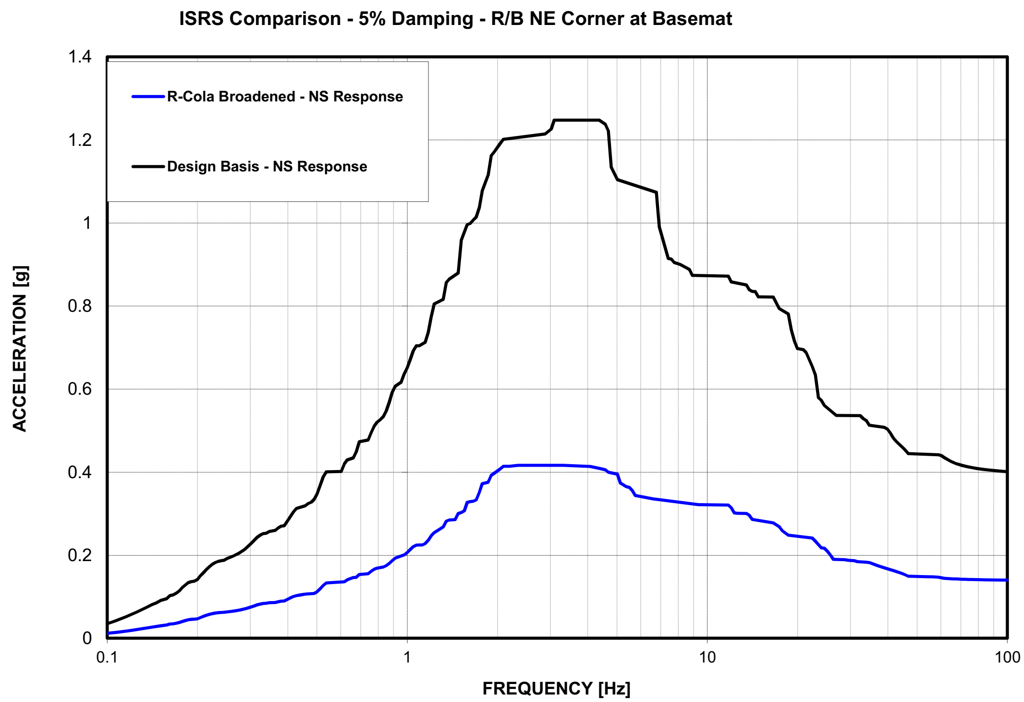

Figure 3NN-28 ISRS Comparison - 5% Damping – R/B Northeast Corner at Top of Basemat EL. -26.333 ft (Sheet 1 of 3)

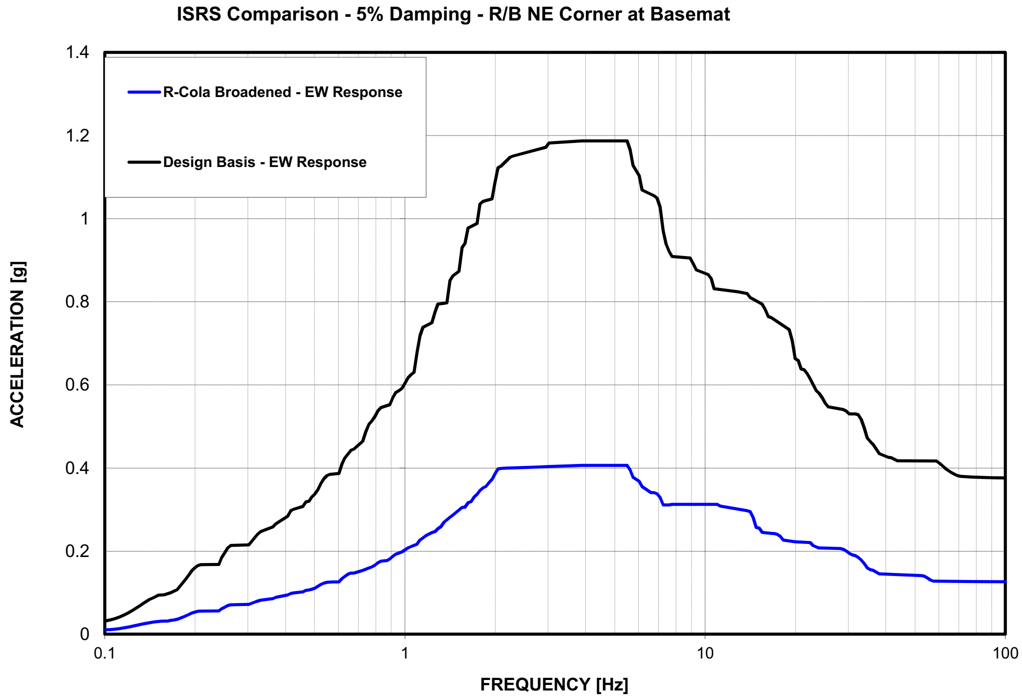

Figure 3NN-28 ISRS Comparison - 5% Damping – R/B Northeast Corner at Top of Basemat EL. -26.333 ft (Sheet 2 of 3)

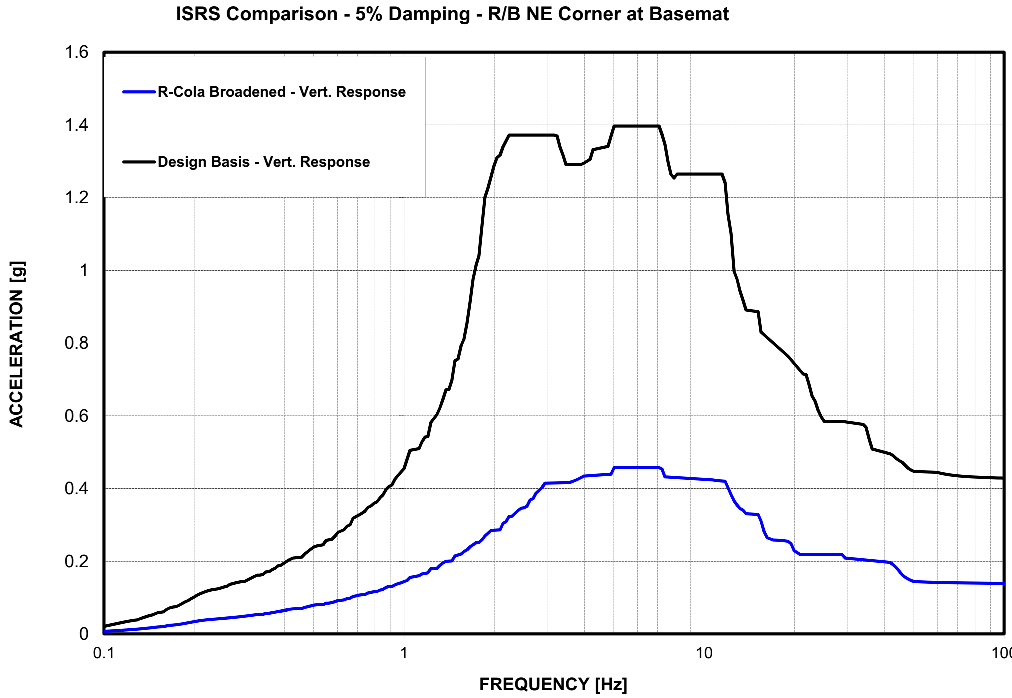

Figure 3NN-28 ISRS Comparison - 5% Damping – R/B Northeast Corner at Top of Basemat EL. -26.333 ft (Sheet 3 of 3)

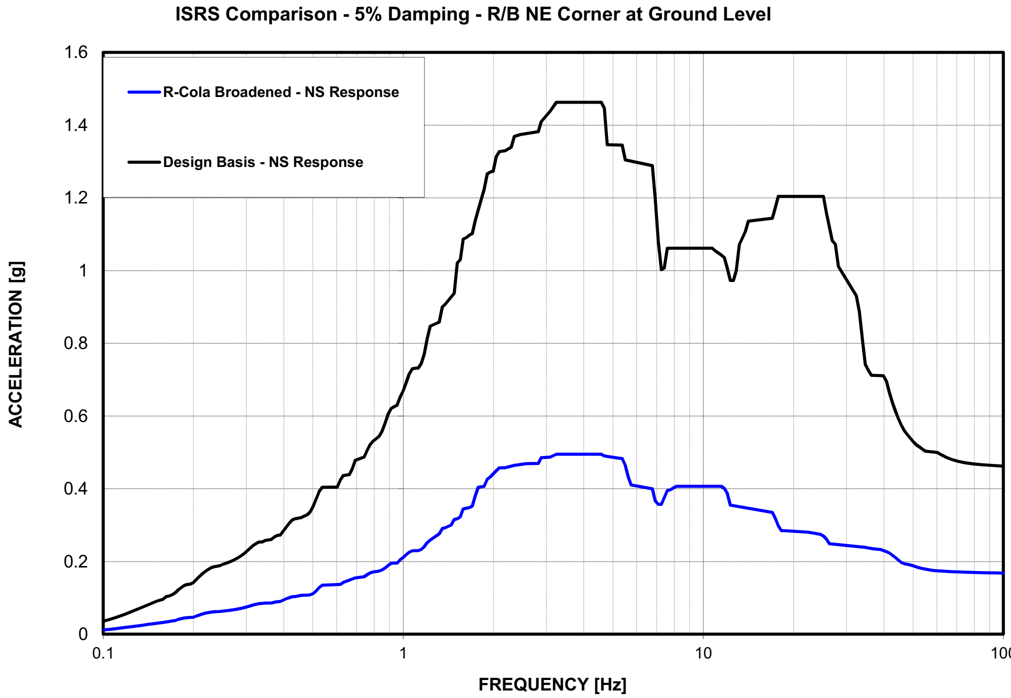

Figure 3NN-29 ISRS Comparison - 5% Damping – R/B Northeast Corner at Grade Level EL. 2.583 ft (Sheet 1 of 3)

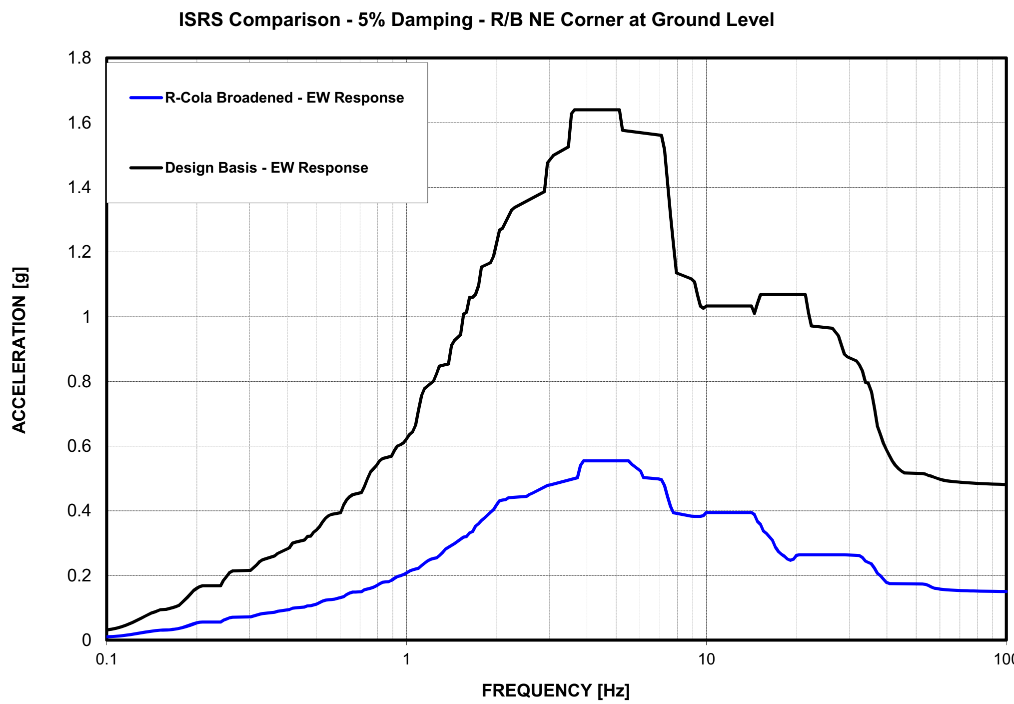

Figure 3NN-29 ISRS Comparison - 5% Damping – R/B Northeast Corner at Grade Level EL. 2.583 ft (Sheet 2 of 3)

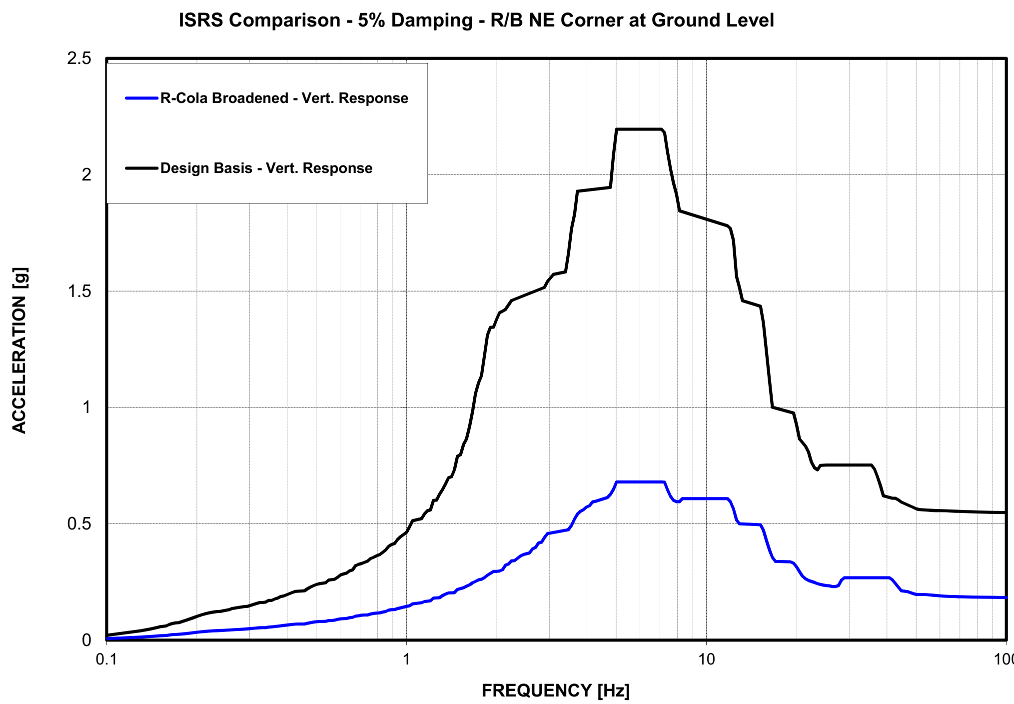

Figure 3NN-29 ISRS Comparison - 5% Damping – R/B Northeast Corner at Grade Level EL. 2.583 ft (Sheet 3 of 3)

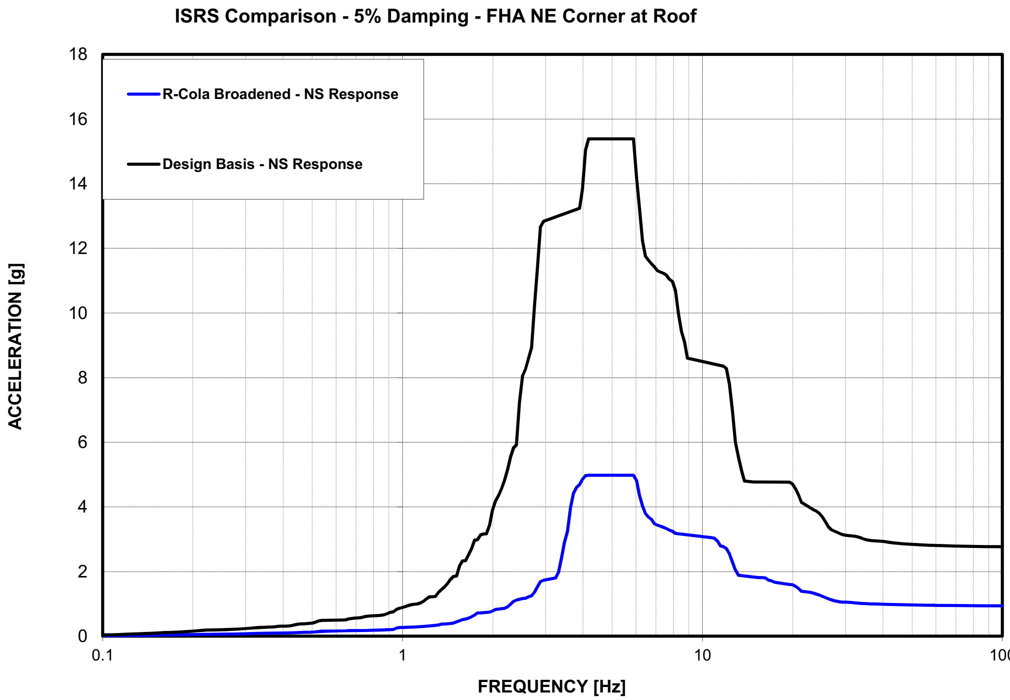

Figure 3NN-30 ISRS Comparison - 5% Damping – FH/A Northeast Corner at Roof EL. 156 ft (Sheet 1 of 3)

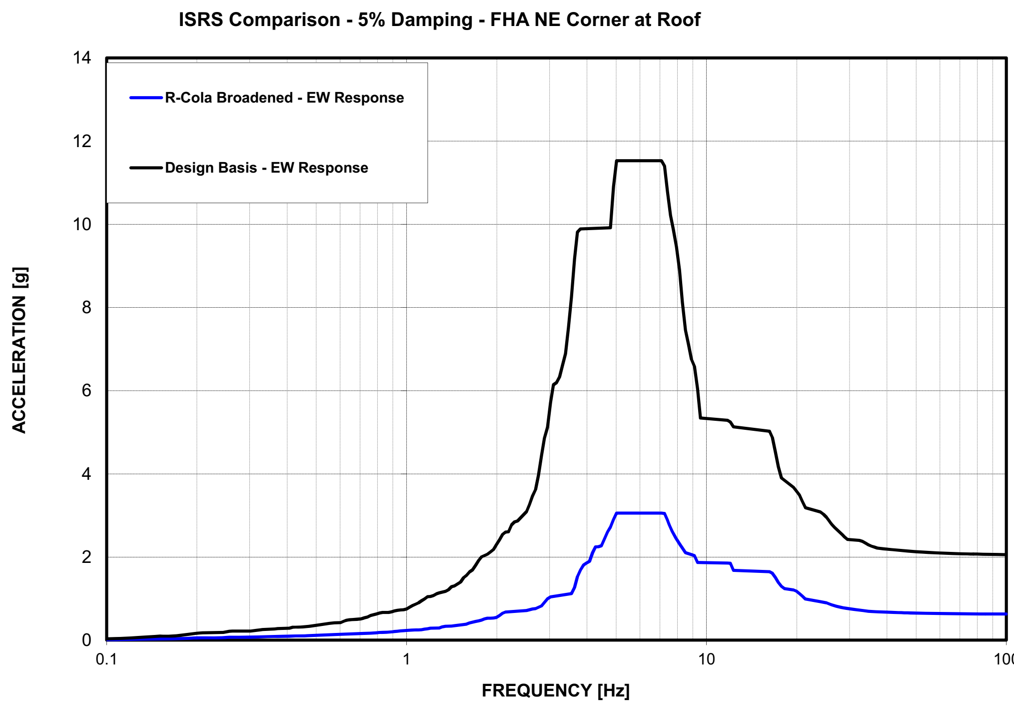

Figure 3NN-30 ISRS Comparison - 5% Damping – FH/A Northeast Corner at Roof EL. 156 ft (Sheet 2 of 3)

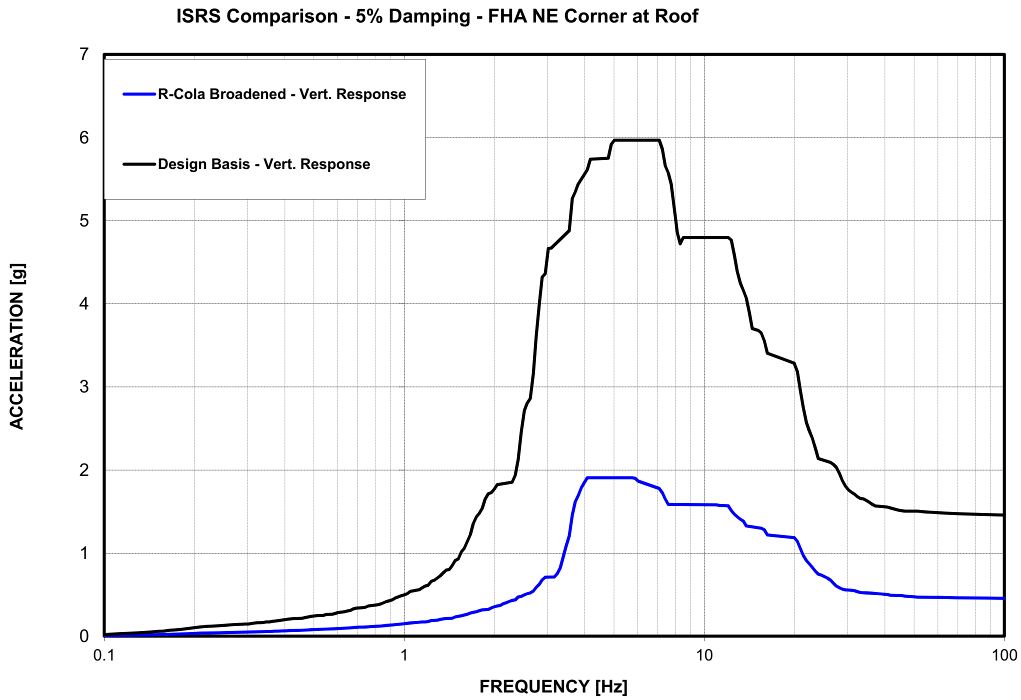

Figure 3NN-30 ISRS Comparison - 5% Damping – FH/A Northeast Corner at Roof EL. 156 ft (Sheet 3 of 3)

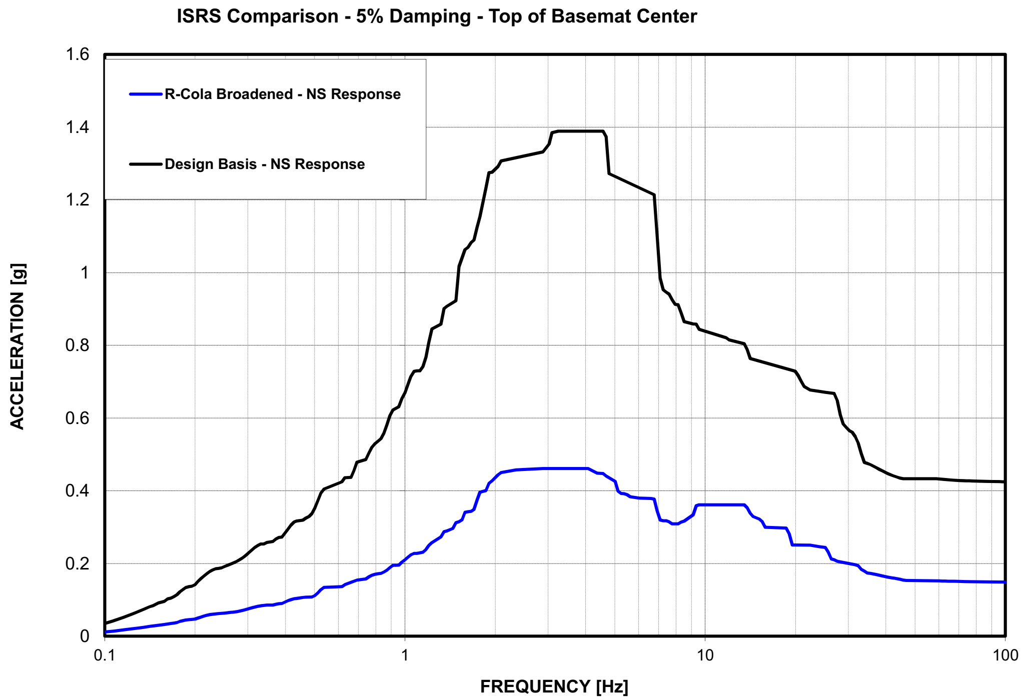

Figure 3NN-31 ISRS Comparison - 5% Damping – Top of Center of Basemat EL. -8.583 ft (Sheet 1 of 3)

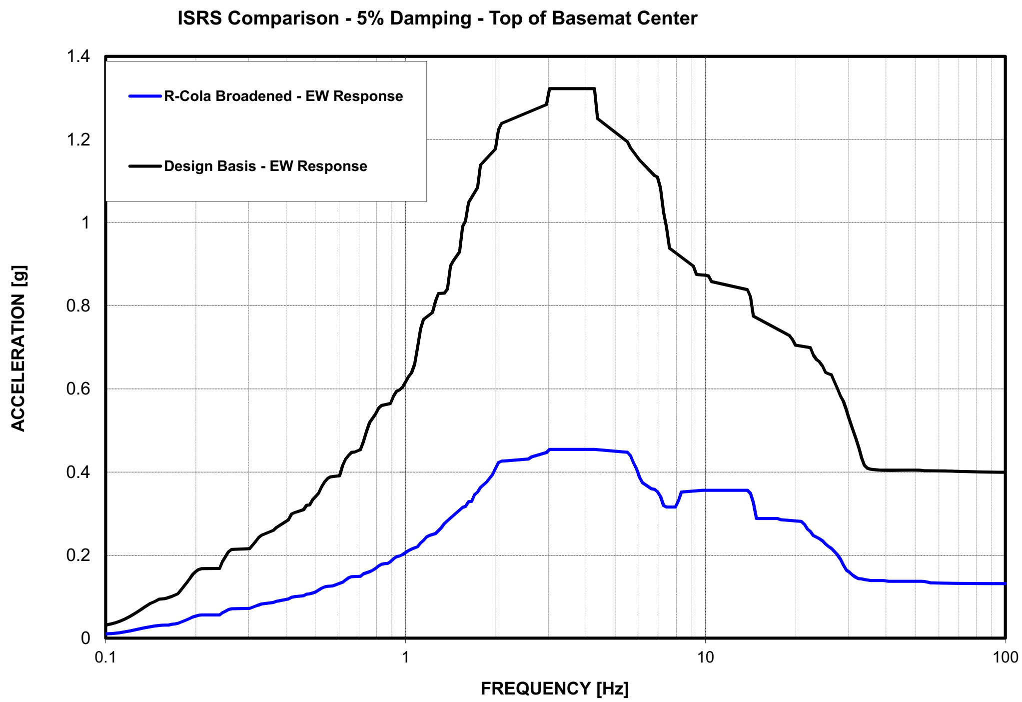

Figure 3NN-31 ISRS Comparison - 5% Damping – Top of Center of Basemat EL. -8.583 ft (Sheet 2 of 3)

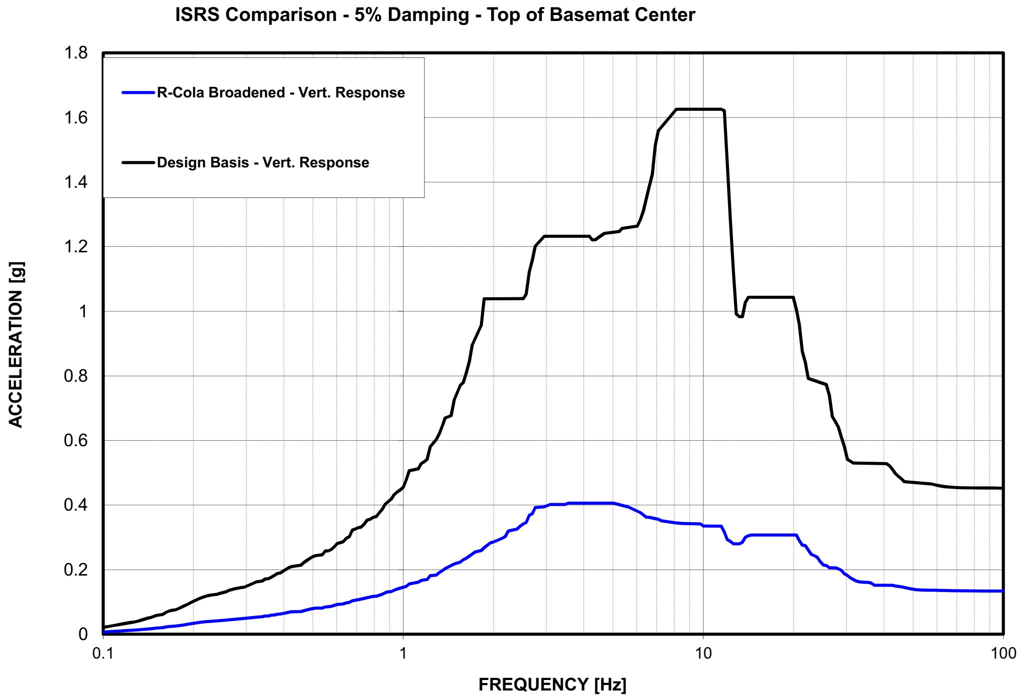

Figure 3NN-31 ISRS Comparison - 5% Damping – Top of Center of Basemat EL. -8.583 ft (Sheet 3 of 3)

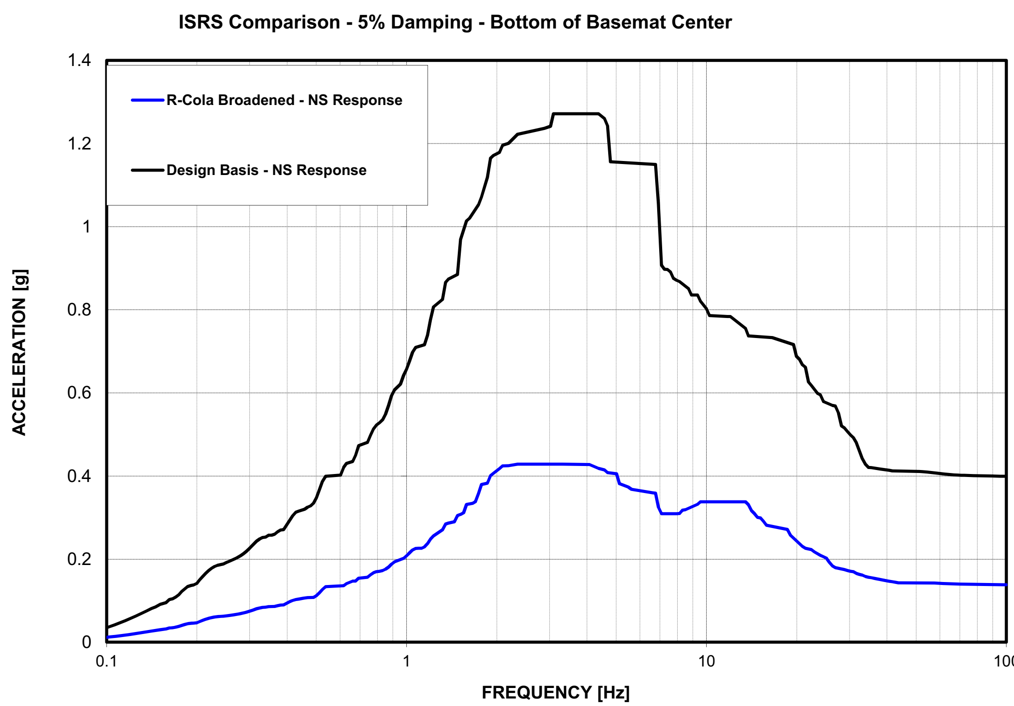

Figure 3NN-32 ISRS Comparison - 5% Damping – Bottom of Center of Basemat EL. -39.667 ft (Sheet 1 of 3)

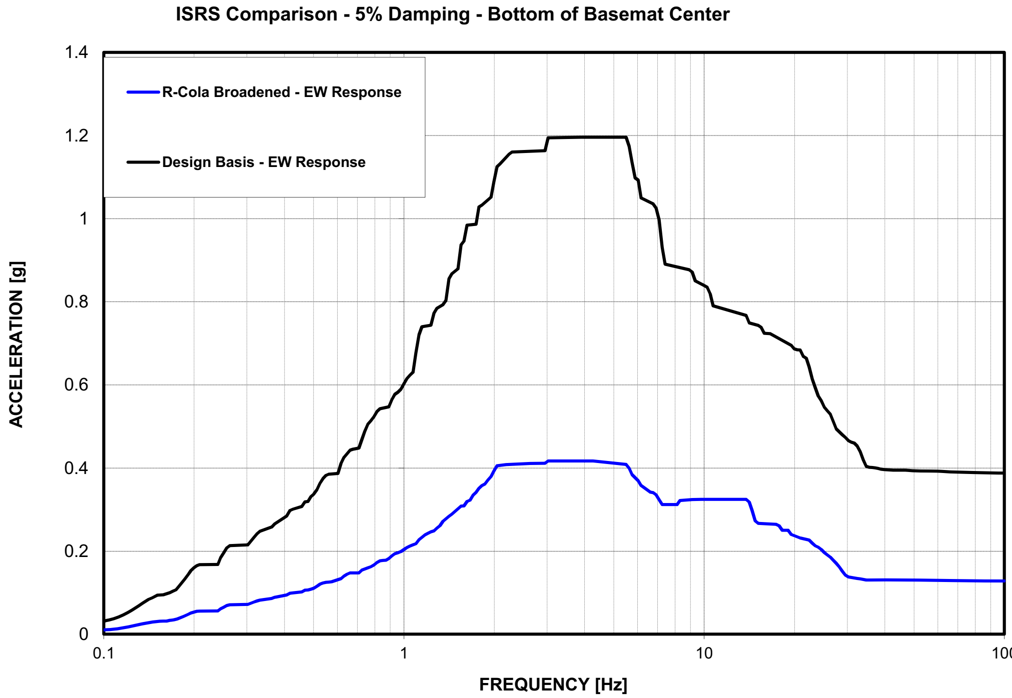

Figure 3NN-32 ISRS Comparison - 5% Damping – Bottom of Center of Basemat EL. -39.667 ft (Sheet 2 of 3)

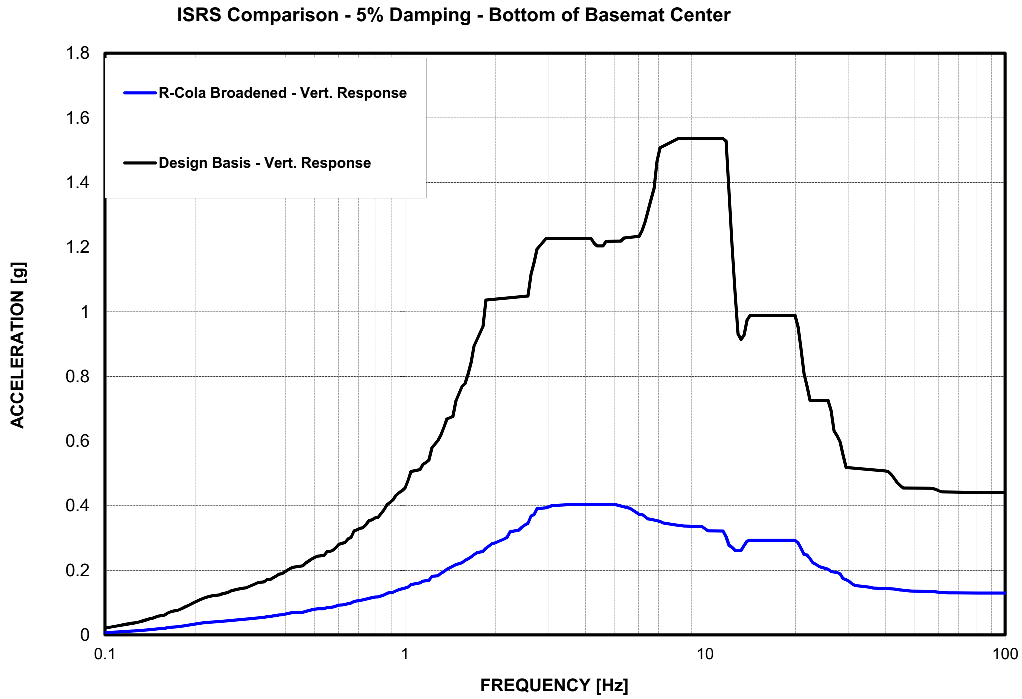

Figure 3NN-32 ISRS Comparison - 5% Damping – Bottom of Center of Basemat EL. -39.667 ft (Sheet 3 of 3)

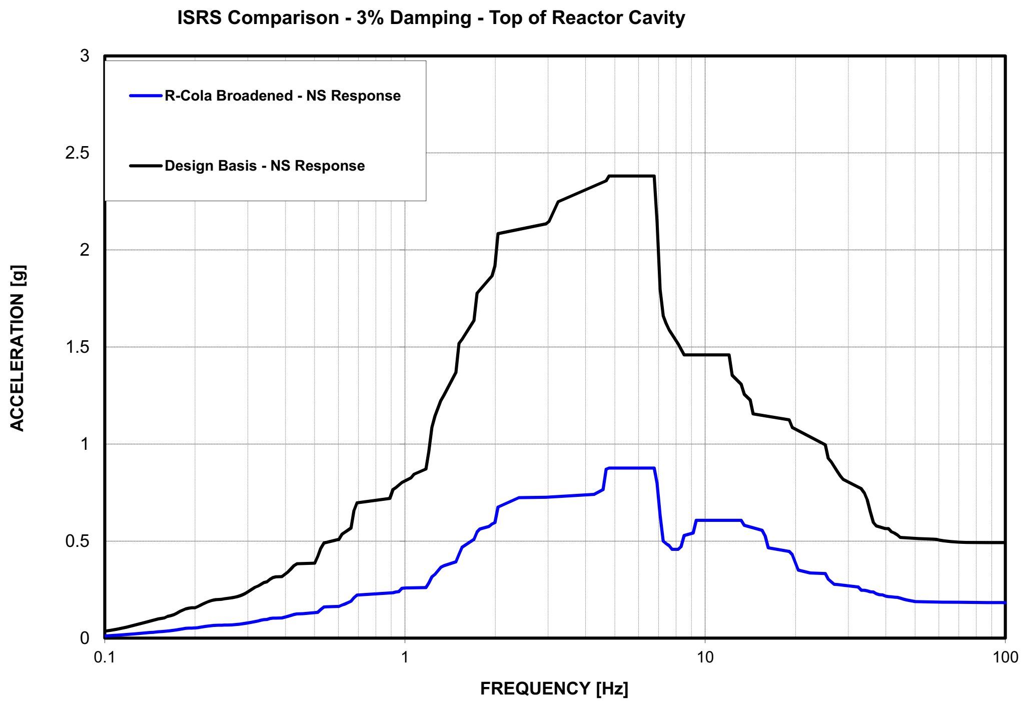

Figure 3NN-33 ISRS Comparison - 3% Damping - Top of Reactor Cavity EL. 35.906 ft (Sheet 1 of 3)

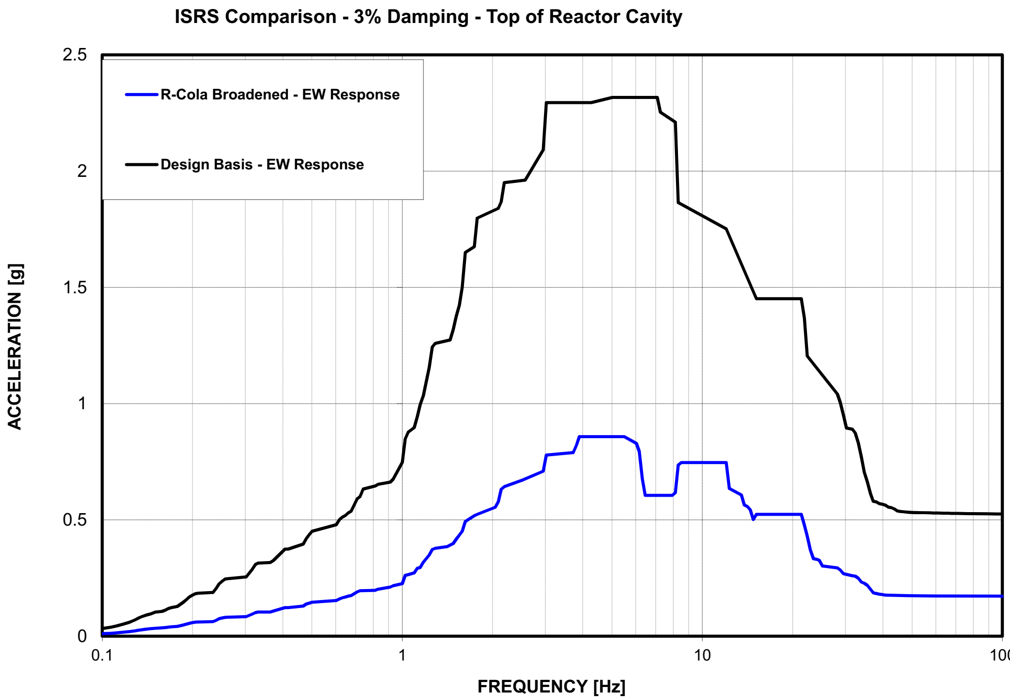

Figure 3NN-33 ISRS Comparison - 3% Damping - Top of Reactor Cavity EL. 35.906 ft (Sheet 2 of 3)

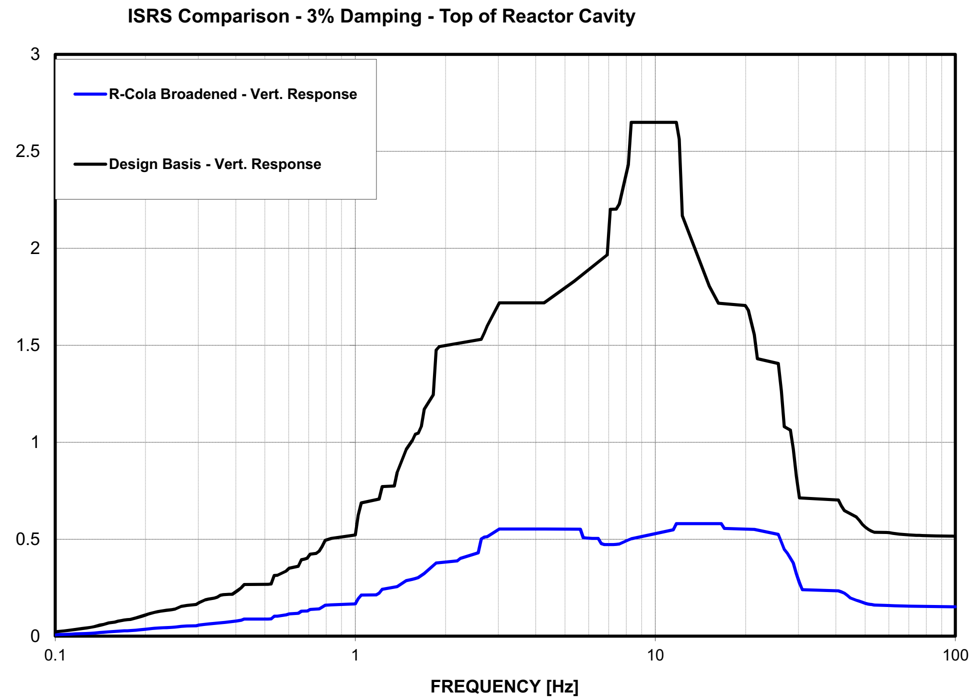

Figure 3NN-33 ISRS Comparison - 3% Damping - Top of Reactor Cavity EL. 35.906 ft (Sheet 3 of 3)

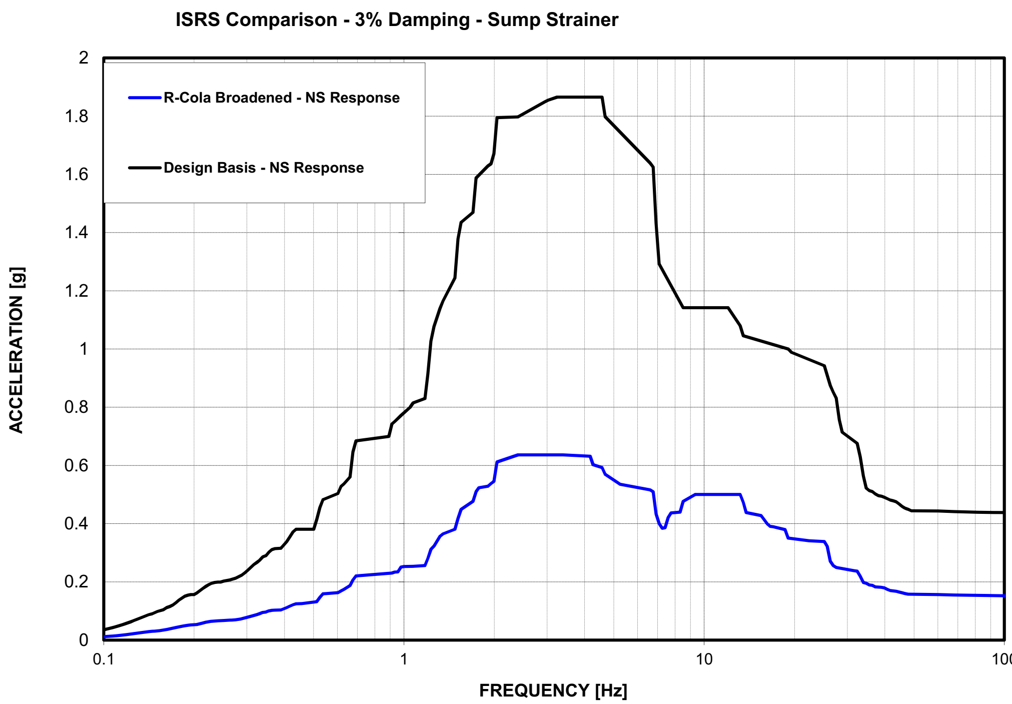

Figure 3NN-34 ISRS Comparison - 3% Damping – Sump Strainer EL. 2.583 ft (Sheet 1 of 3)

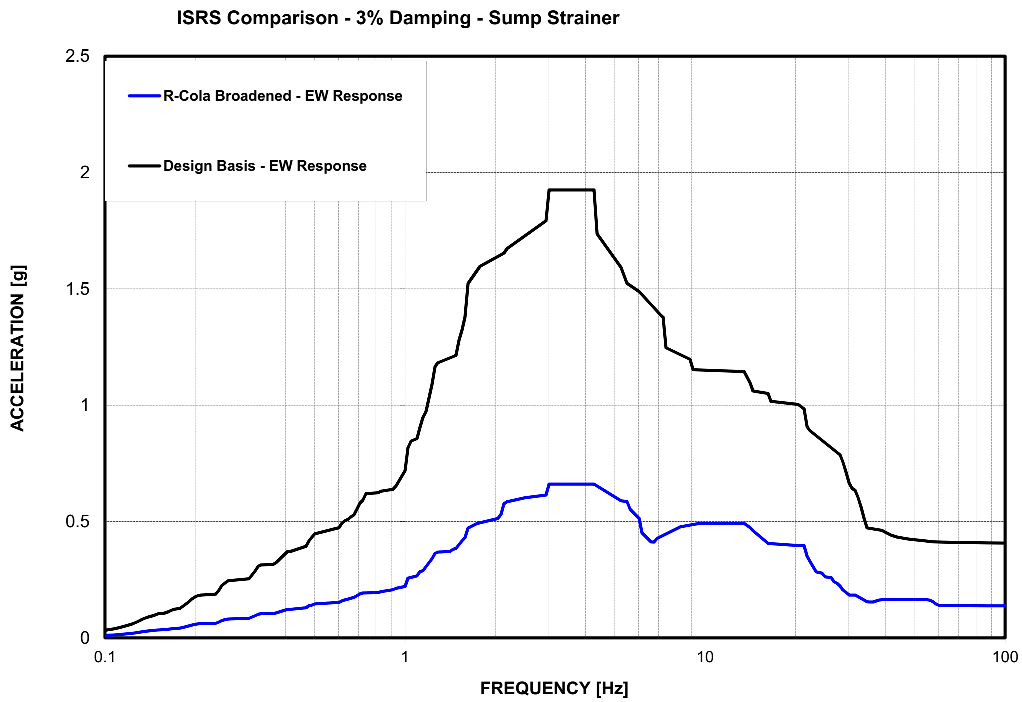

Figure 3NN-34 ISRS Comparison - 3% Damping – Sump Strainer EL. 2.583 ft (Sheet 2 of 3)

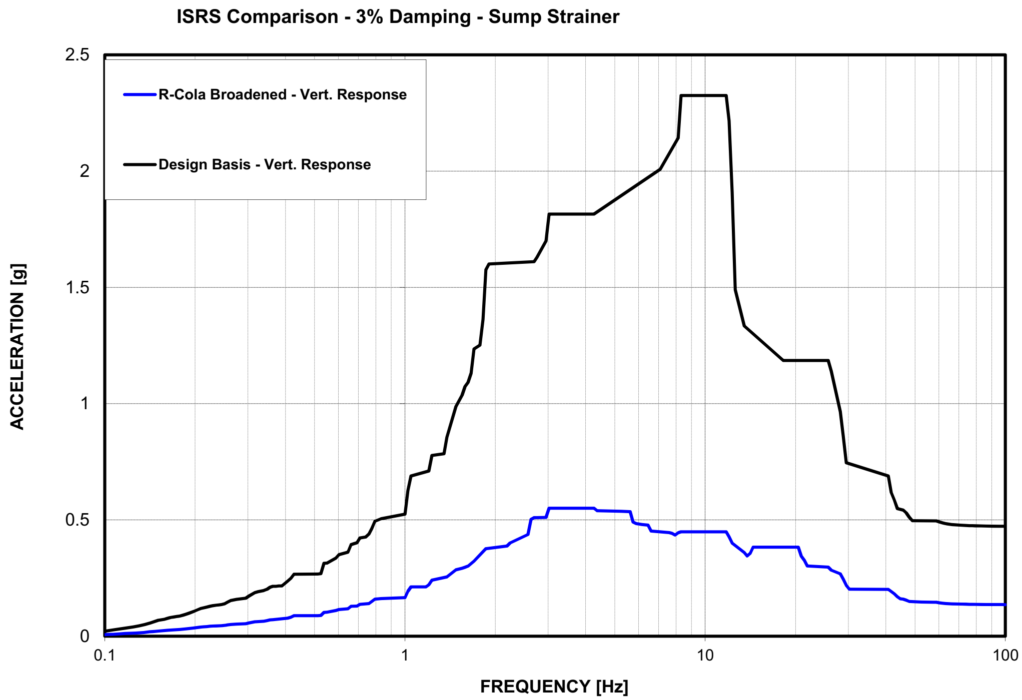

Figure 3NN-34 ISRS Comparison - 3% Damping – Sump Strainer EL. 2.583 ft (Sheet 3 of 3)

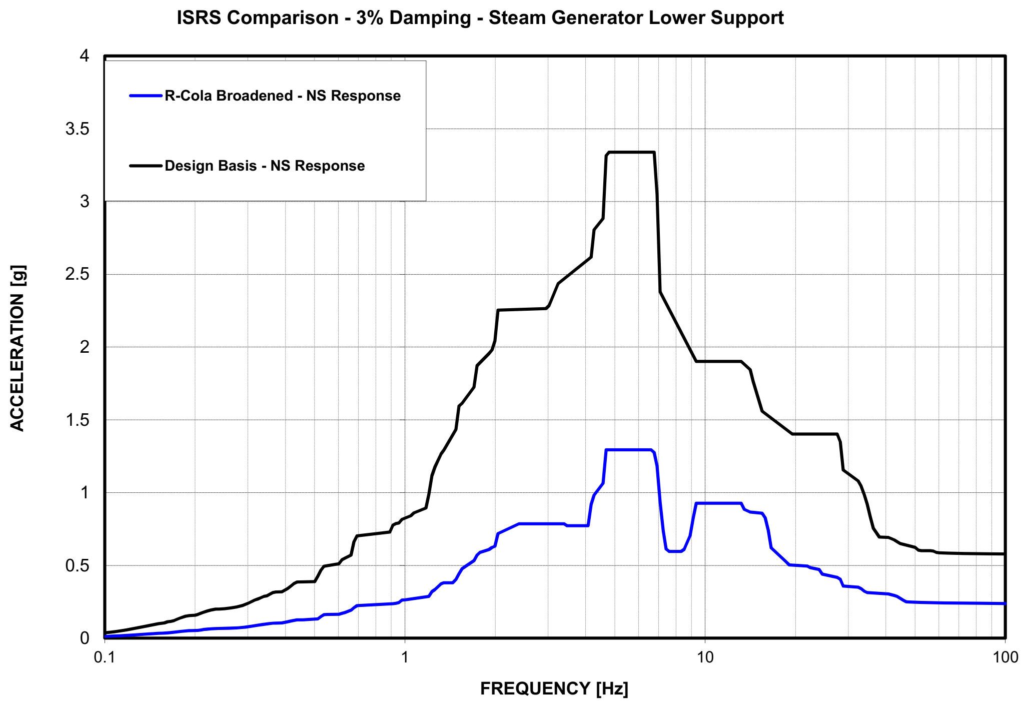

Figure 3NN-35 ISRS Comparison - 3% Damping – Steam Generators Lower Supports EL. 45.637 ft (Sheet 1 of 3)

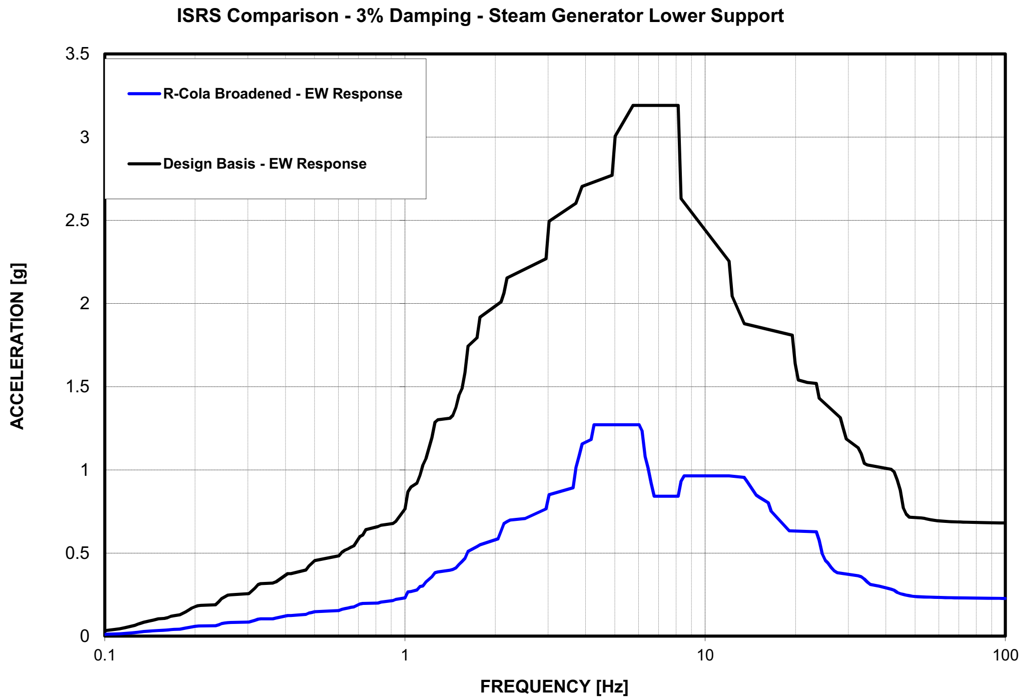

Figure 3NN-35 ISRS Comparison - 3% Damping – Steam Generators Lower Supports EL. 45.637 ft (Sheet 2 of 3)

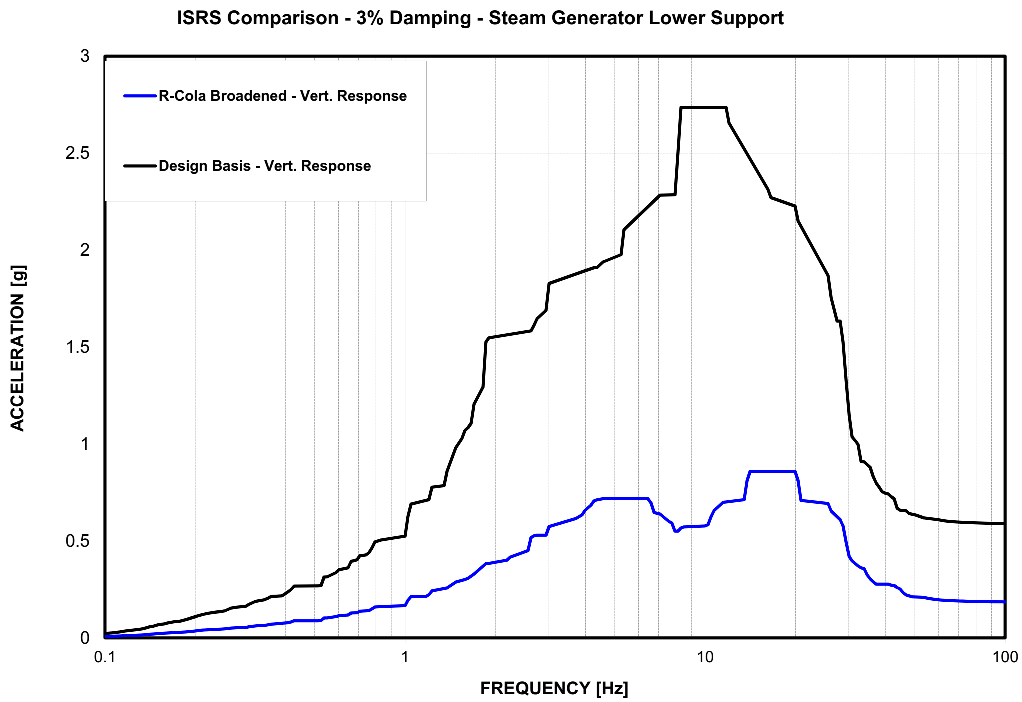

Figure 3NN-35 ISRS Comparison - 3% Damping – Steam Generators Lower Supports EL. 45.637 ft (Sheet 3 of 3)

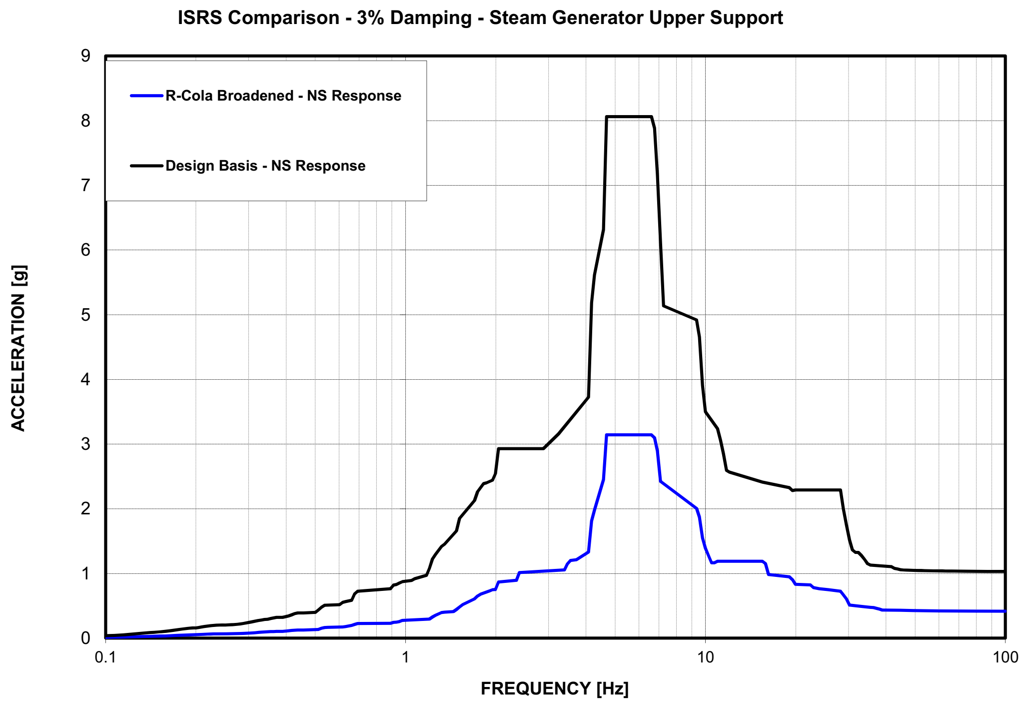

Figure 3NN-36 ISRS Comparison - 3% Damping – Steam Generators Upper Supports EL. 96.583 ft (Sheet 1 of 3)

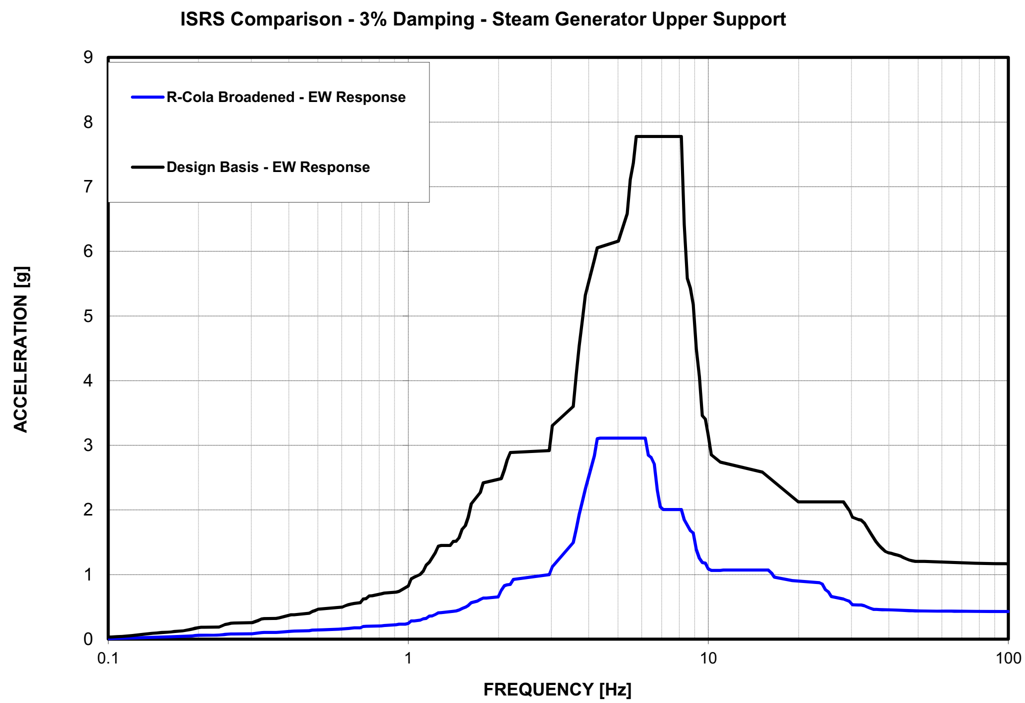

Figure 3NN-36 ISRS Comparison - 3% Damping – Steam Generators Upper Supports EL. 96.583 ft (Sheet 2 of 3)

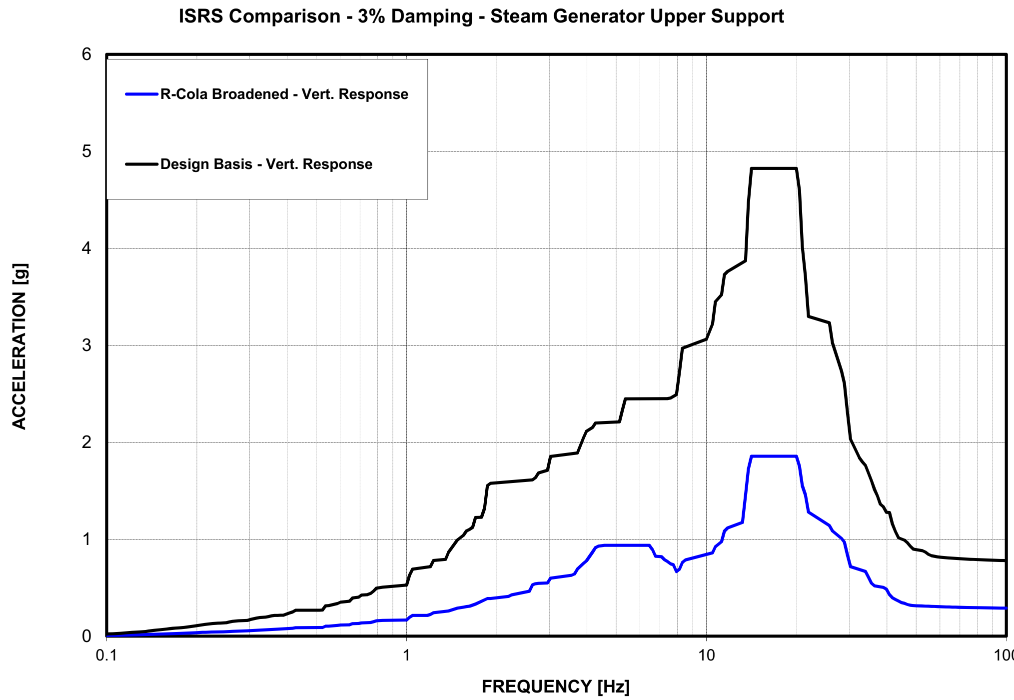

Figure 3NN-36 ISRS Comparison - 3% Damping – Steam Generators Upper Supports EL. 96.583 ft (Sheet 3 of 3)

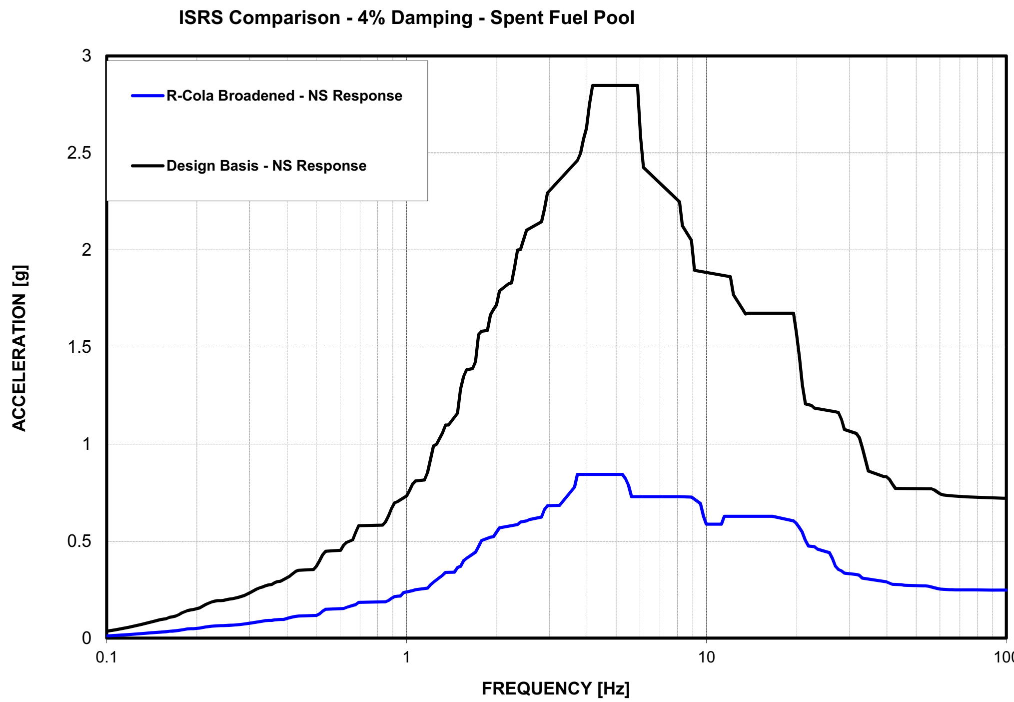

Figure 3NN-37 ISRS Comparison - 4% Damping – Spent Fuel Pool EL. 25.25 ft (Sheet 1 of 3)

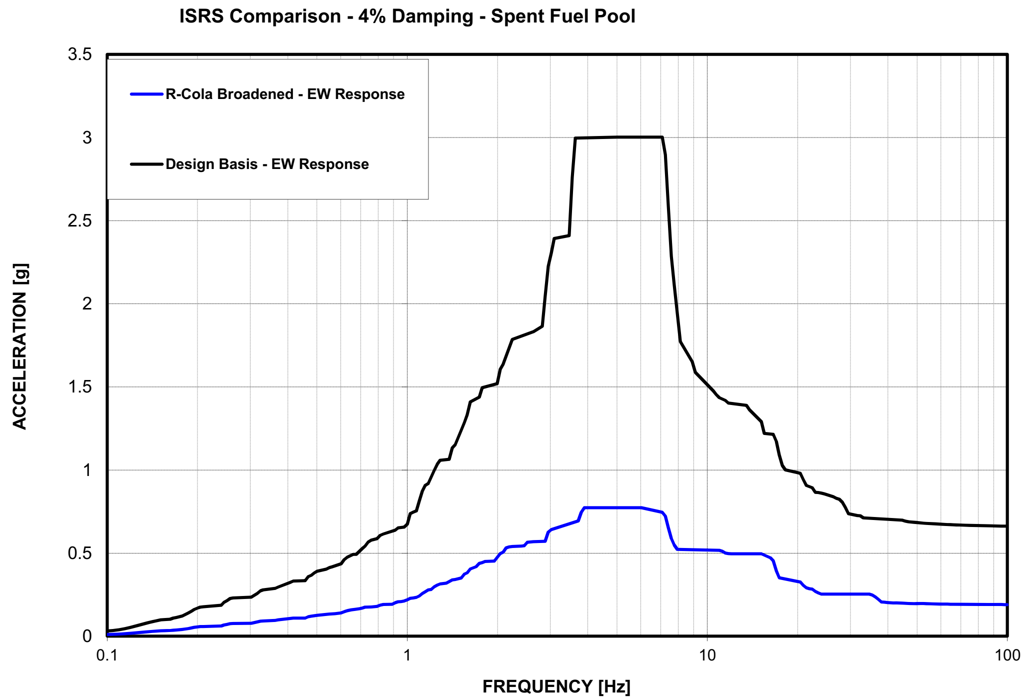

Figure 3NN-37 ISRS Comparison - 4% Damping – Spent Fuel Pool EL. 25.25 ft (Sheet 2 of 3)

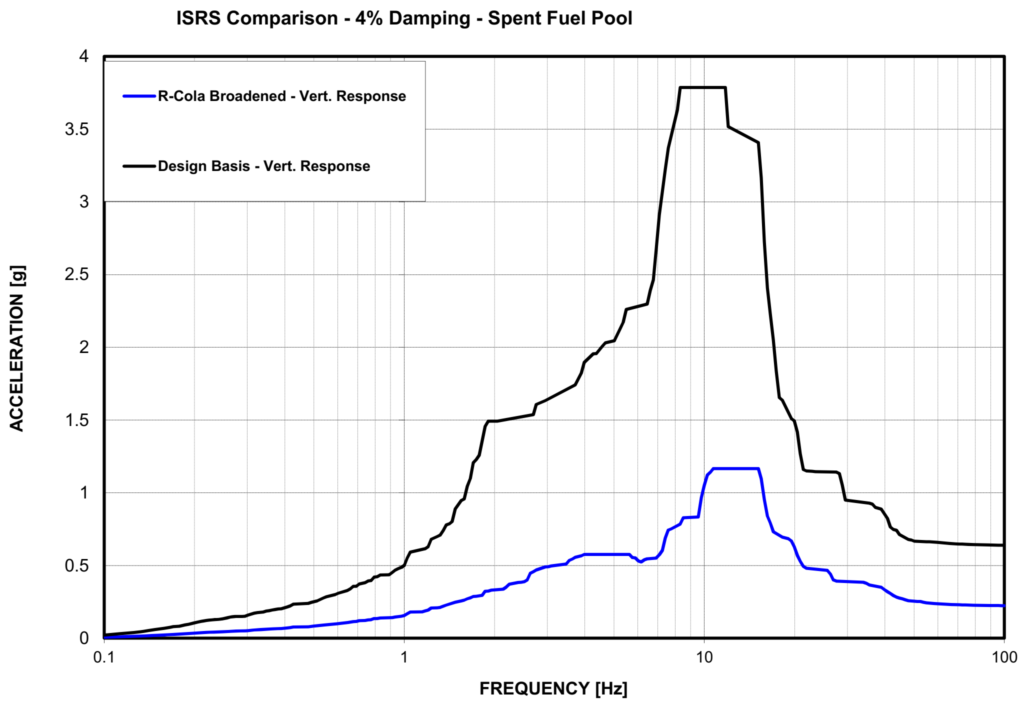

Figure 3NN-37 ISRS Comparison - 4% Damping – Spent Fuel Pool EL. 25.25 ft (Sheet 3 of 3)

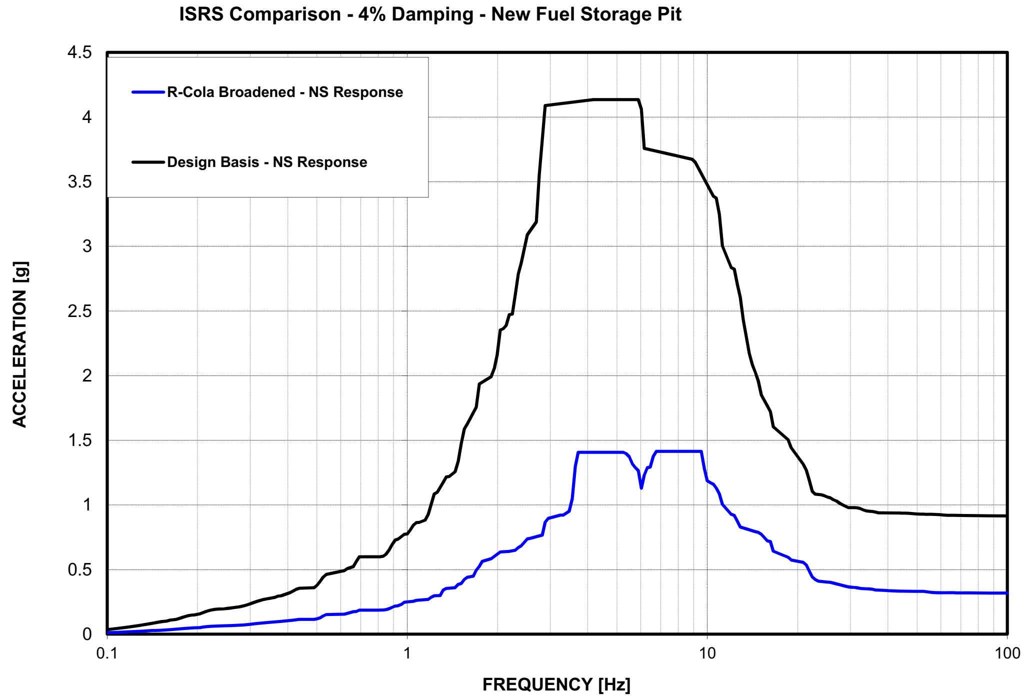

Figure 3NN-38 ISRS Comparison - 4% Damping – New Fuel Storage Pit EL. 63.33 ft (Sheet 1 of 3)

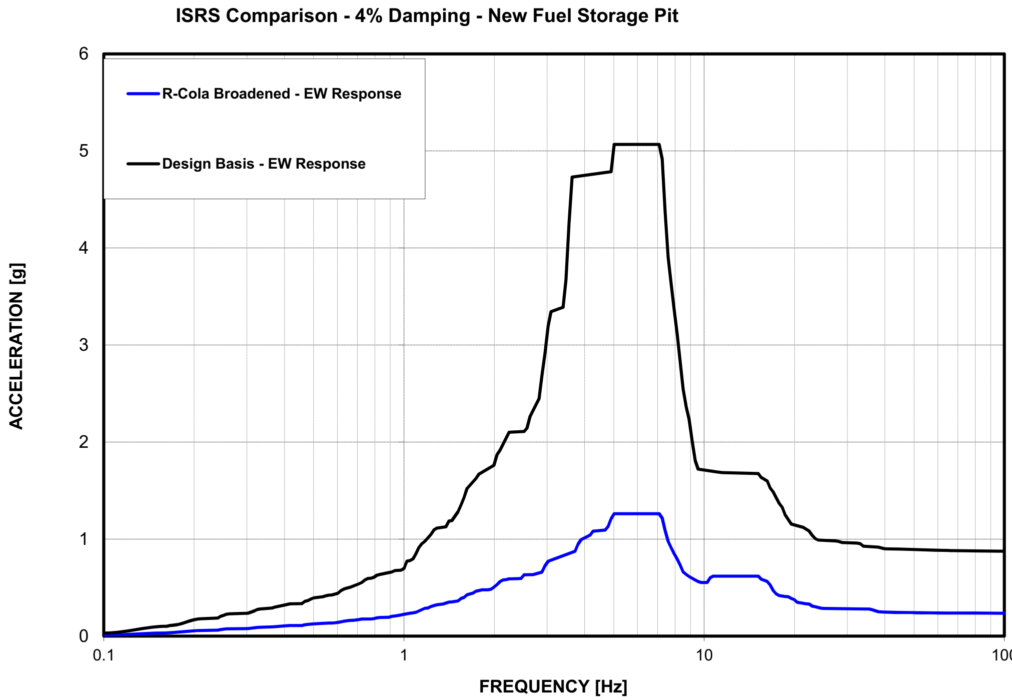

Figure 3NN-38 ISRS Comparison - 4% Damping – New Fuel Storage Pit EL. 63.33 ft (Sheet 2 of 3)

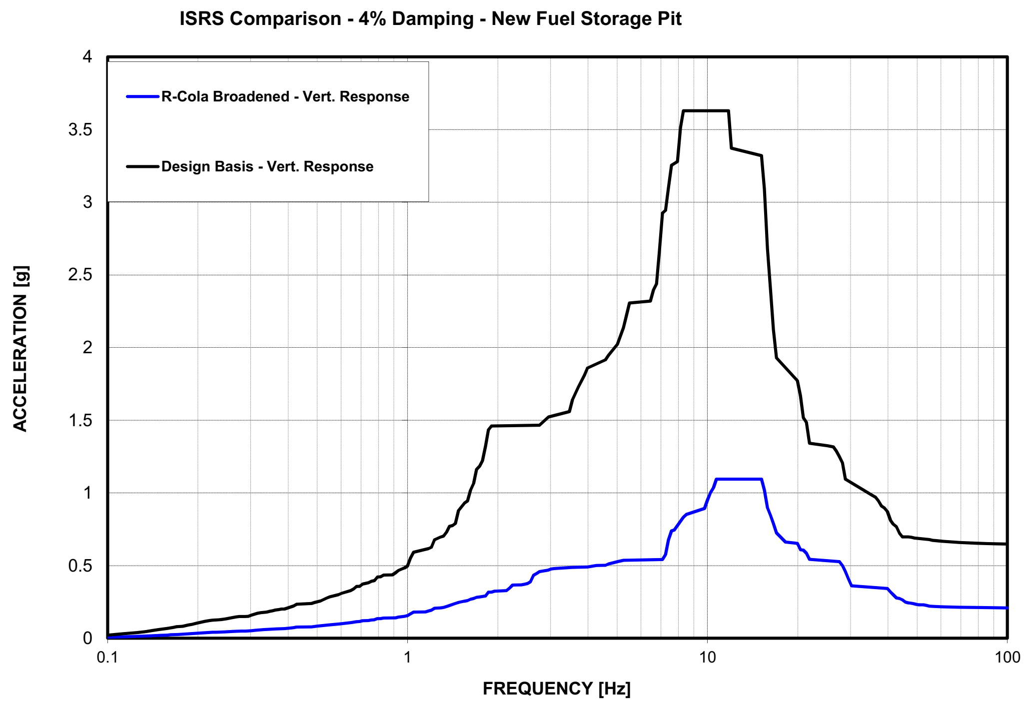

Figure 3NN-38 ISRS Comparison - 4% Damping – New Fuel Storage Pit EL. 63.33 ft (Sheet 3 of 3)

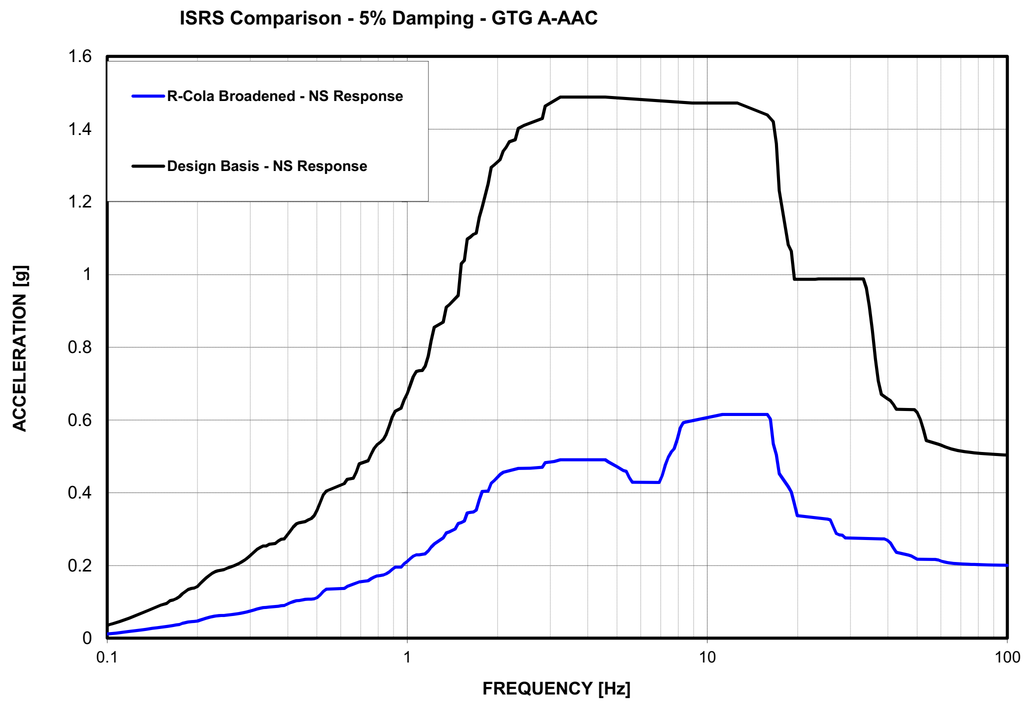

Figure 3NN-39 ISRS Comparison - 5% Damping – Gas Turbine Generator A-AAC EL. 2.583 ft (Sheet 1 of 3)

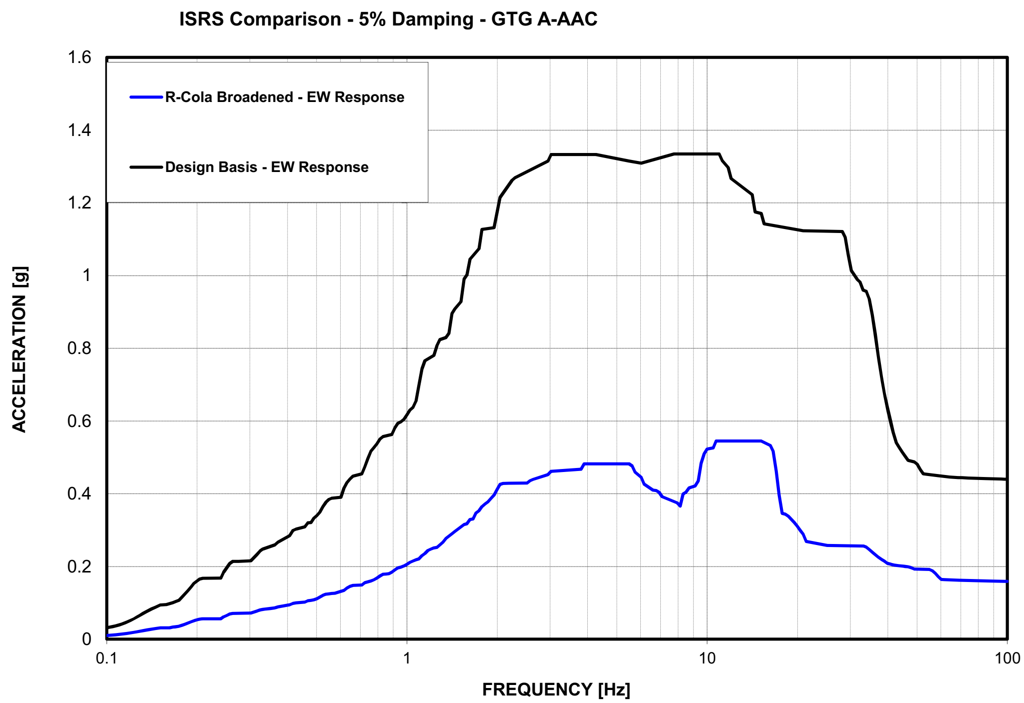

Figure 3NN-39 ISRS Comparison - 5% Damping – Gas Turbine Generator A-AAC EL. 2.583 ft (Sheet 2 of 3)

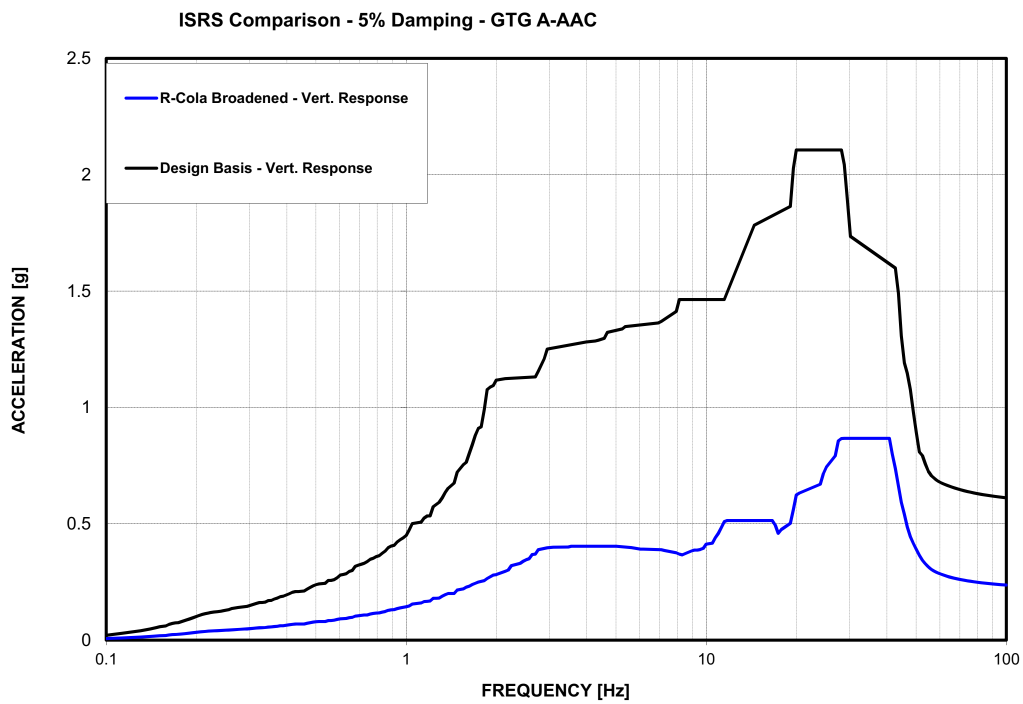

Figure 3NN-39 ISRS Comparison - 5% Damping – Gas Turbine Generator A-AAC EL. 2.583 ft (Sheet 3 of 3)

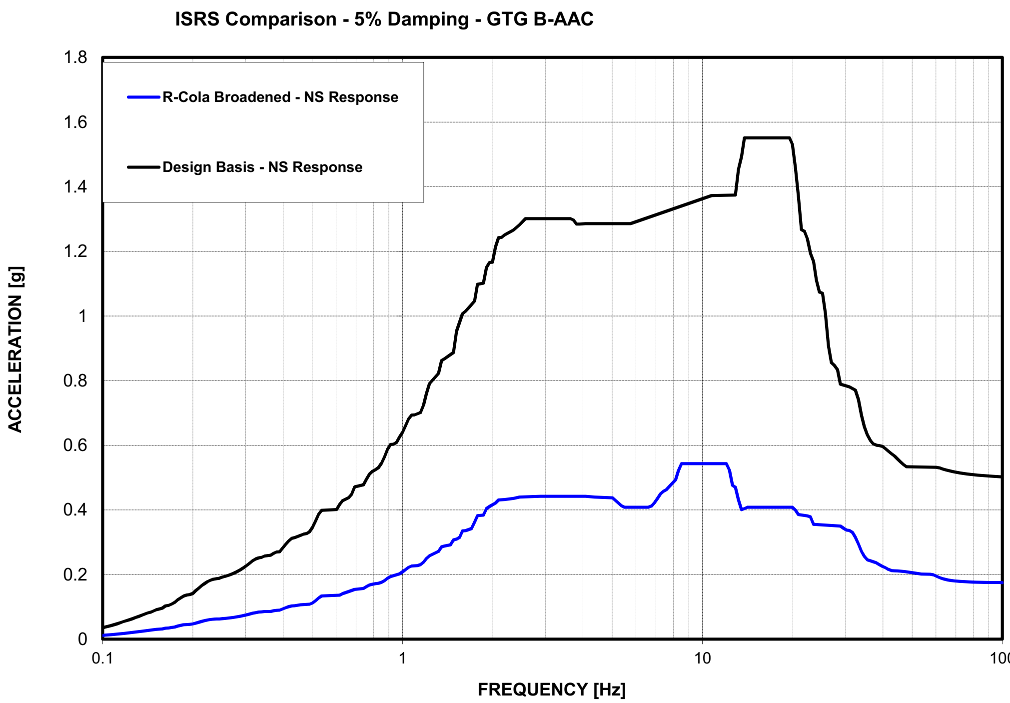

Figure 3NN-40 ISRS of Comparison - 5% Damping –Gas Turbine Generator B-AAC EL. 2.583 ft (Sheet 1 of 3)

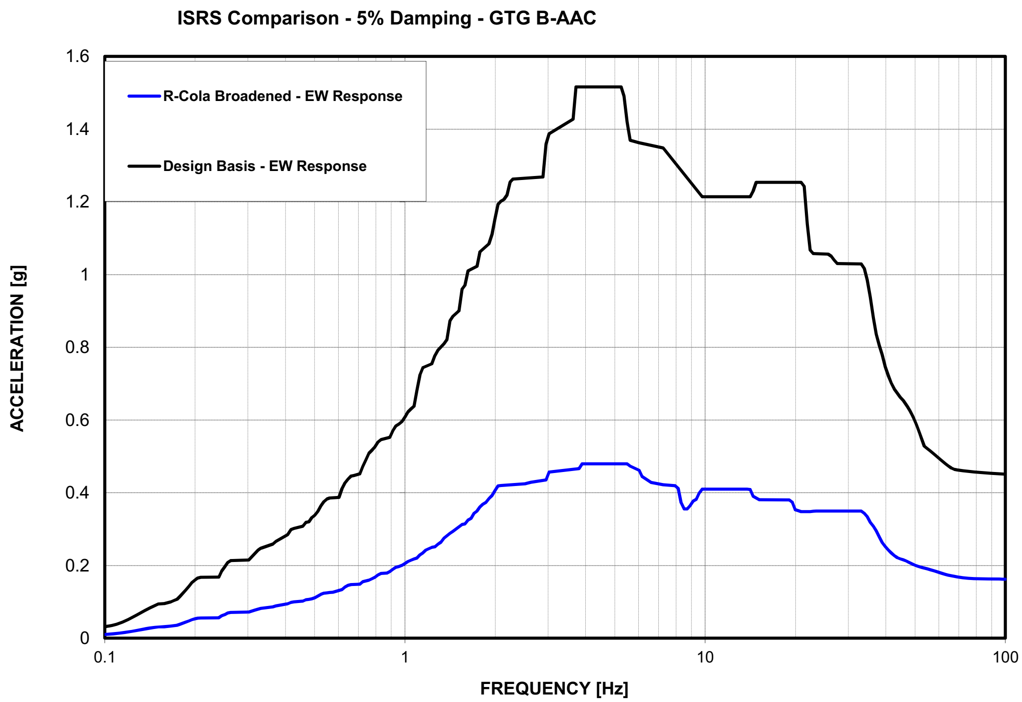

Figure 3NN-40 ISRS of Comparison - 5% Damping –Gas Turbine Generator B-AAC EL. 2.583 ft (Sheet 2 of 3)

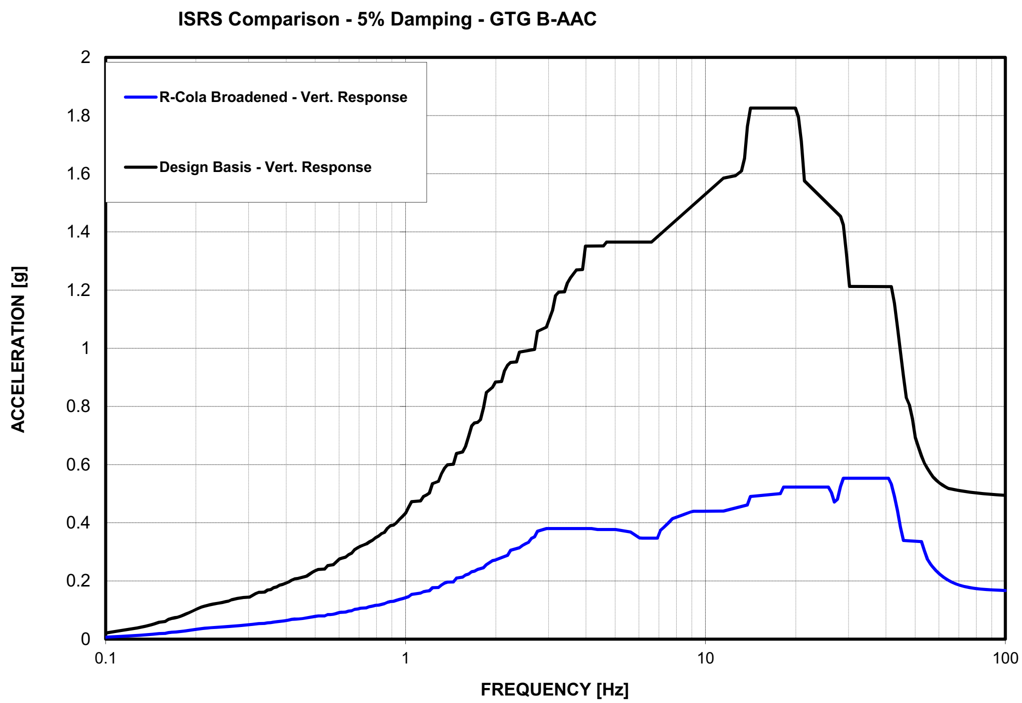

Figure 3NN-40 ISRS of Comparison - 5% Damping –Gas Turbine Generator B-AAC EL. 2.583 ft (Sheet 3 of 3)

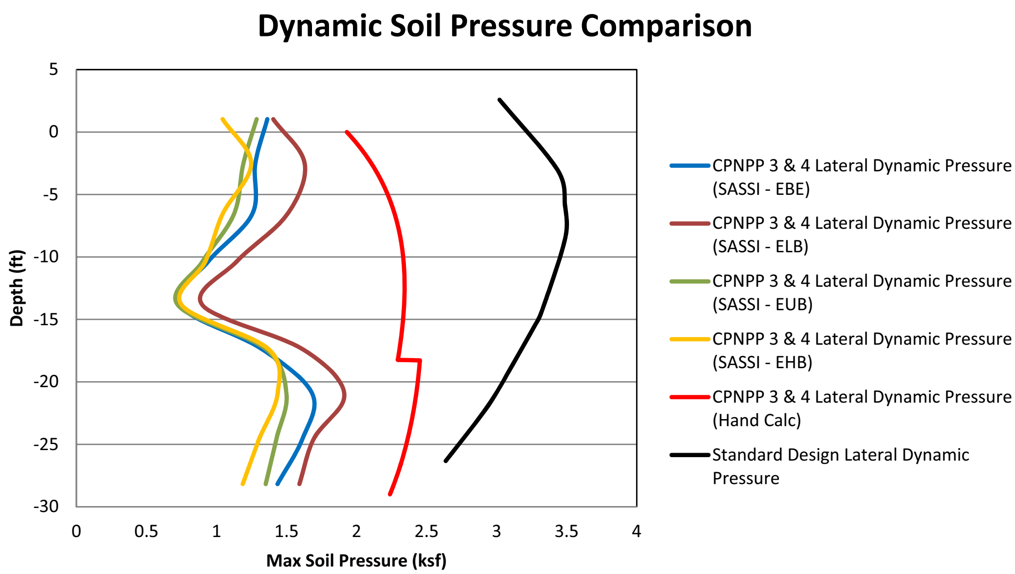

Figure 3NN-41 Lateral Dynamic Pressure Comparison – East Wall of East PS/B

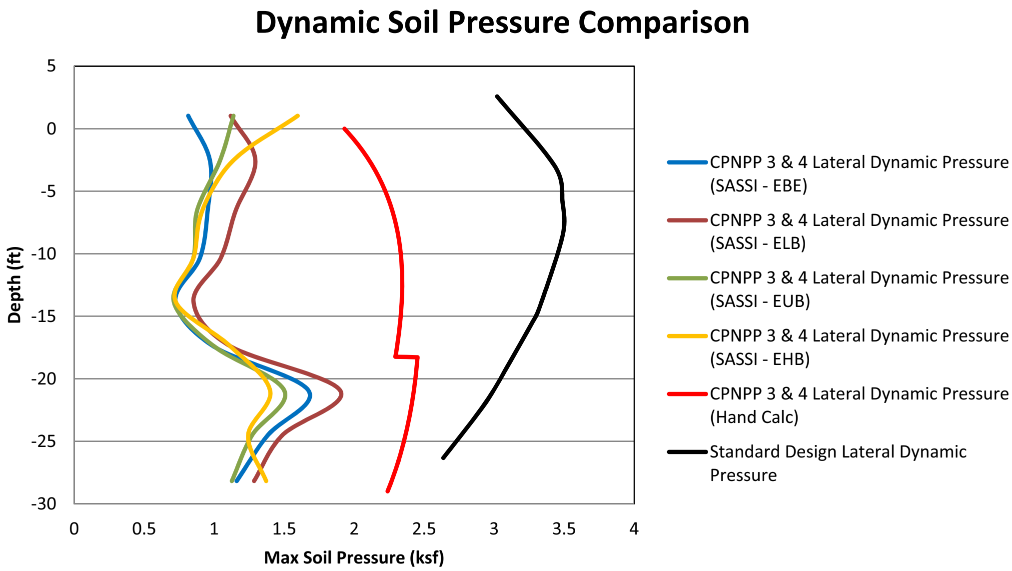

Figure 3NN-42 Lateral Dynamic Pressure Comparison – East Wall of Reactor Building

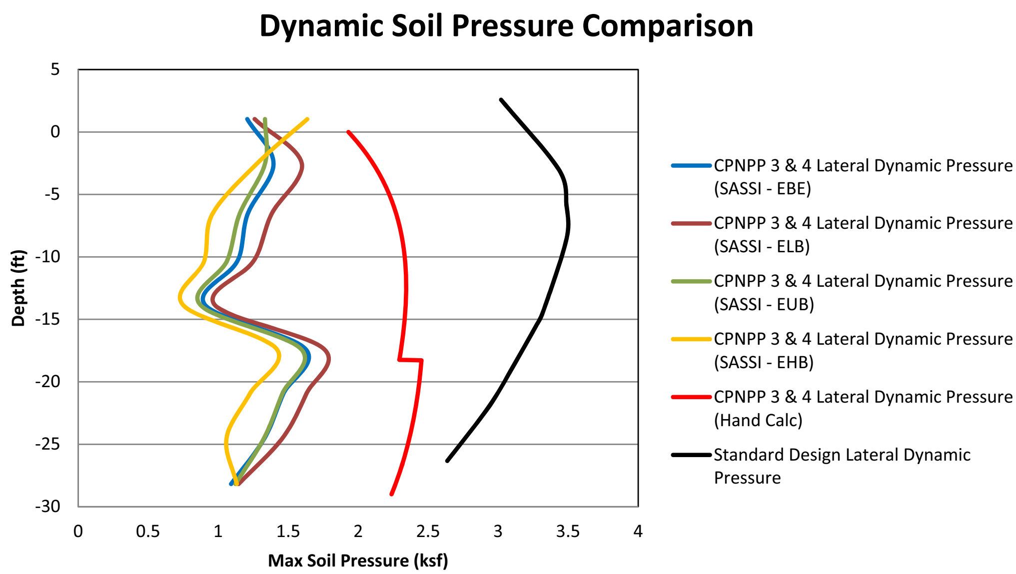

Figure 3NN-43 Lateral Dynamic Pressure Comparison – North Wall of Reactor Building

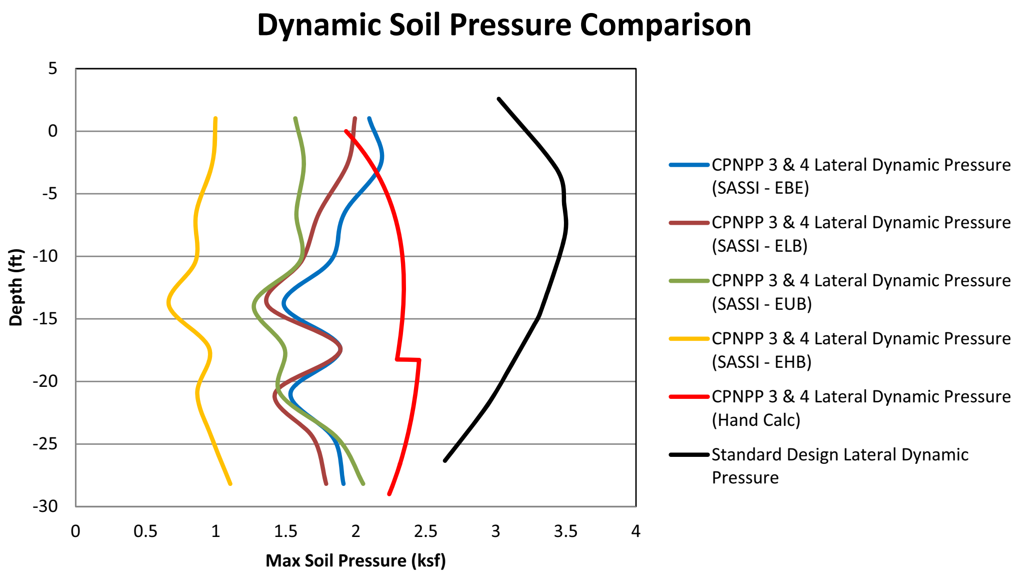

Figure 3NN-44 Lateral Dynamic Pressure Comparison – West Wall of R/B Complex

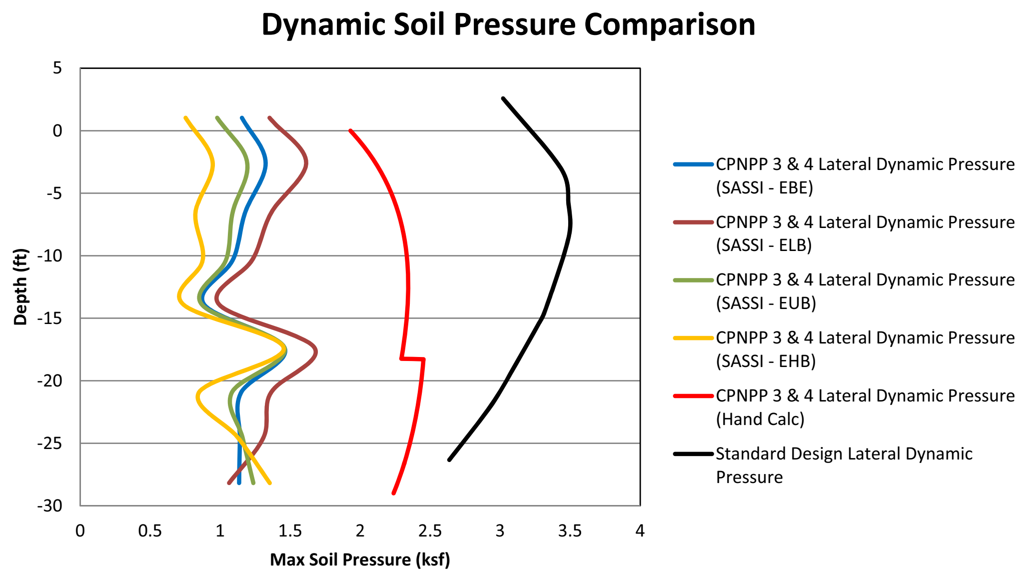

Figure 3NN-45 Lateral Dynamic Pressure Comparison – South Wall of ESWPC

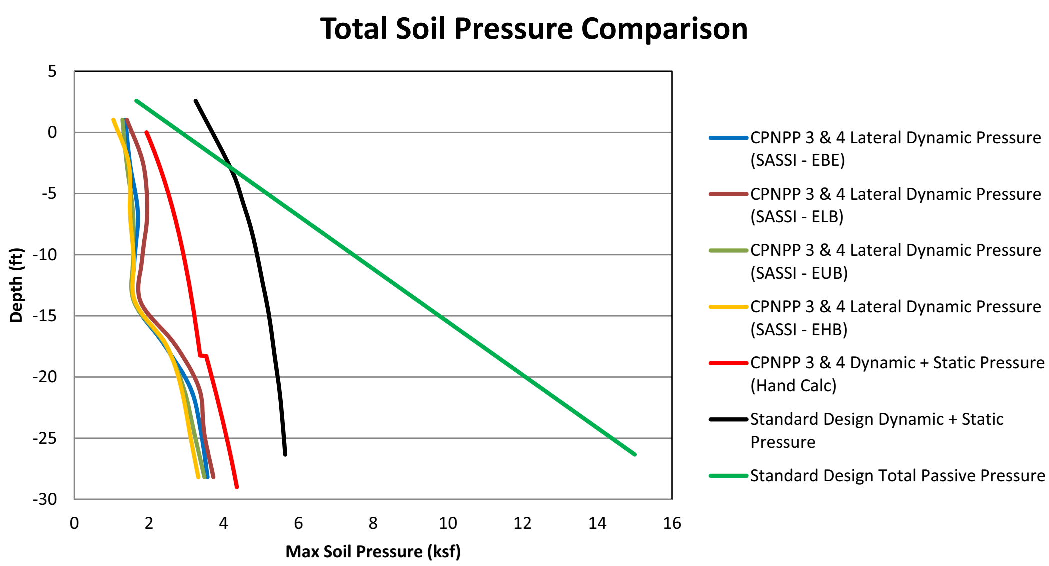

Figure 3NN-46 Total Lateral Earth Pressure Comparison – East Wall of East PS/B

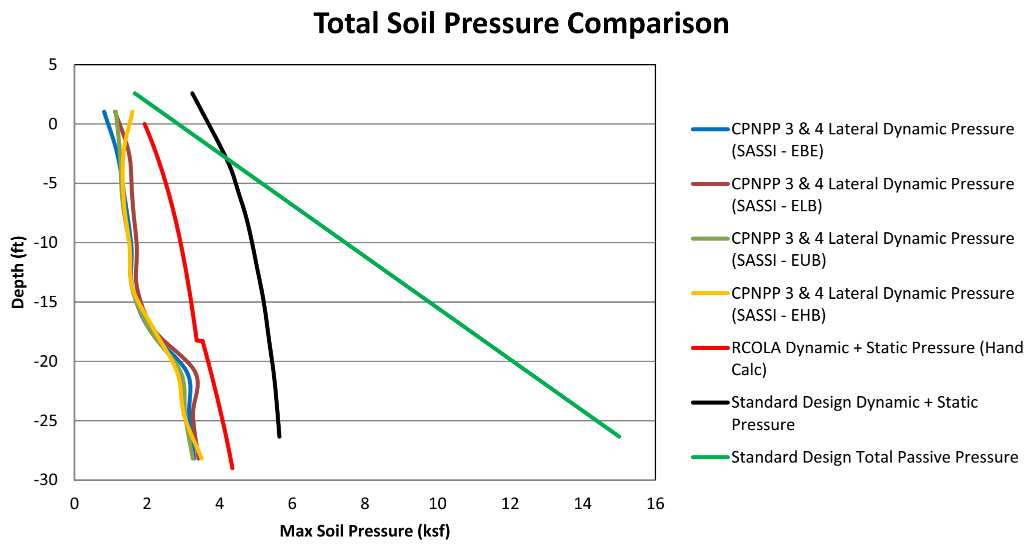

Figure 3NN-47 Total Lateral Earth Pressure Comparison – East Wall of Reactor Building

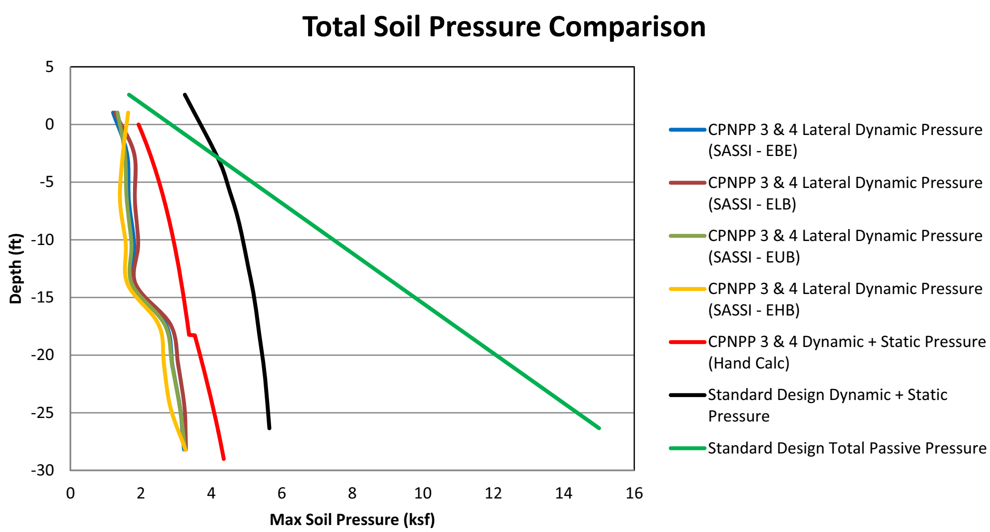

Figure 3NN-48 Total Lateral Earth Pressure Comparison – North Wall of Reactor Building

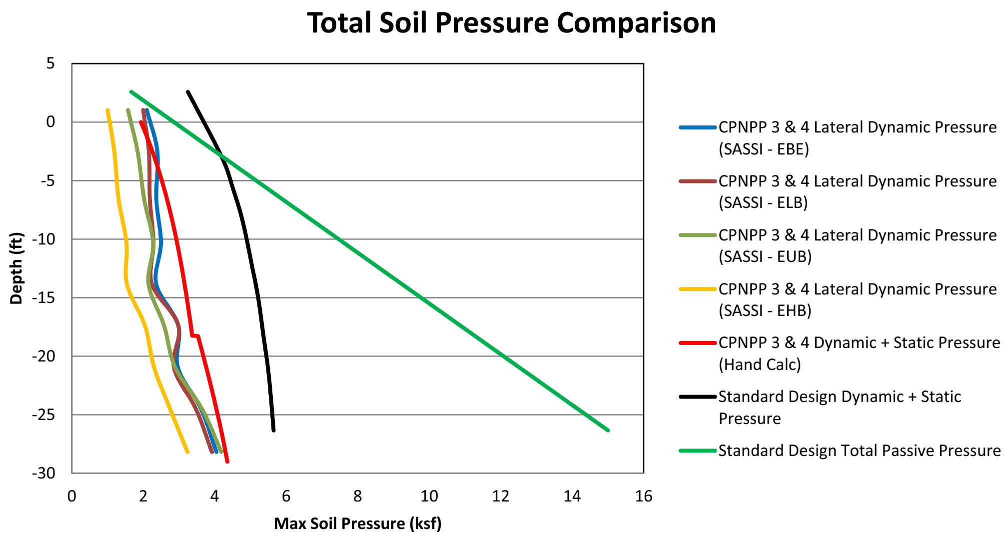

Figure 3NN-49 Total Lateral Earth Pressure Comparison – West Wall of R/B Complex

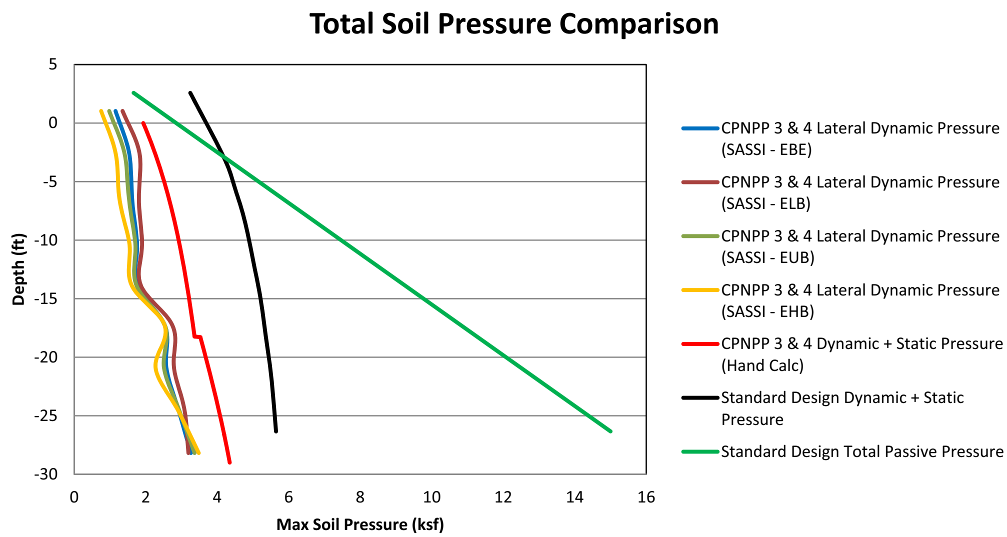

Figure 3NN-50 Total Lateral Earth Pressure Comparison – South Wall of ESWPC